

Université BLAISE PASCAL - Clermont II
École Doctorale Sciences pour l'Ingénieur

Rapport d'activité scientifique

présenté en vue de l'obtention de

l'Habilitation à Diriger des Recherches

par

Bruno SUDRET

Docteur de l'Ecole Nationale des Ponts et Chaussées

**Uncertainty propagation and sensitivity analysis
in mechanical models
Contributions to structural reliability
and stochastic spectral methods**

soutenue publiquement le 12 Octobre 2007 devant le jury composé de Messieurs :

PR. DIDIER CLOUTEAU	Ecole Centrale Paris	Président
PR. ARMEN DER KIUREGHIAN	University of California at Berkeley	Rapporteur
PR. MAURICE LEMAIRE	Institut Français de Mécanique Avancée	Rapporteur
PR. CHRISTIAN SOIZE	Université Paris-Est Marne-la-Vallée	Rapporteur
PR. STÉPHANE ANDRIEUX	Ecole Polytechnique	Examineur
DR. OLIVIER LE MAITRE	CNRS, Université Paris-Sud Orsay	Examineur
PR. JOHN SØRENSEN	University of Aalborg, Danemark	Examineur

Acknowledgements

Some years ago, as a fresh Ph.D from the *Ecole Nationale des Ponts et Chaussées* (ENPC, Paris), I decided to discover the New World, and more precisely, to spend one year as a visiting scholar at the University of California at Berkeley. Indeed, both ENPC and *Electricité de France* (now the EDF company) had awarded me a one-year grant to work on stochastic finite elements and finite element reliability analysis.

At that time, this field was entirely new and quite mysterious to me, since my Ph.D topic was completely different. Nevertheless, Pr. Armen Der Kiureghian kindly received me in his research group at the Department of Civil and Environmental Engineering, where he patiently taught me probabilistic engineering mechanics from the very basics. I would like to thank him very sincerely at first, both for his scientific advice and his kind support at that time and since then.

Back to France, I had the opportunity to be hired at the R&D Division of EDF, where I have been working as a research engineer in the Department for Materials and Mechanics of Components (MMC) since 2001. The existing partnership with the research group of Pr. Maurice Lemaire (Institut Français de Mécanique Avancée, Laboratoire Mécanique et Ingénieries (IFMA/LaMI)) in Clermont-Ferrand has allowed me to develop much of the research work gathered in this report. Both his strong implication in this partnership and his constant encouragements to prepare this thesis are gratefully acknowledged.

As a consequence, part of the results presented in the sequel have been obtained during the Ph.D thesis of students who were co-supervised by Pr. Lemaire. The successive Ph.D students who participated into these research projects are acknowledged for their contributions, namely Céline Andrieu-Renaud, Zakoua Guédé, Marc Berveiller, Frédéric Perrin and Géraud Blatman.

Three years ago, the collaboration with IFMA became tripartite by incorporating the consulting company Phimeca Engineering S.A. Part of the work reported in the following was carried out in collaboration with its C.E.O Dr. Maurice Pendola and Senior Engineer Gilles Defaux, who are gratefully acknowledged.

This work has been publicly defended on October 12th, 2007. In this respect I would like to thank very much the members of the jury, namely the chairman Pr. Didier Clouteau, the reporters Prs. Armen Der Kiureghian, Maurice Lemaire and Christian Soize and the examiners Prs. Stéphane Andrieux, John Sorensen and Dr. Olivier Le Maître.

Finally, I would like to thank sincerely the various reviewers of this manuscript, including Pr. Der Kiureghian, my colleagues Marc Berveiller, Géraud Blatman, Frédéric Perrin, Arsène Yaméogo and Mrs. Evelyne Donnizaux, English teacher in Abbeville (France).

Bruno Sudret, January 18th, 2008

To my beloved wife Valérie
and my three daughters
Louisiane, Salomé and Pénélope

Résumé

La mécanique probabiliste, à l'interface entre la modélisation des structures, la statistique et les probabilités permet de prendre en compte les incertitudes des paramètres des modèles mécaniques et d'étudier leur impact sur les prédictions. Au sens large, elle regroupe des domaines aussi variés que la dynamique stochastique, la fiabilité des structures, les éléments finis stochastiques, etc. Ce mémoire d'habilitation à diriger des recherches présente une approche méthodologique globale du traitement des incertitudes dans laquelle s'inscrivent différents développements originaux.

Le schéma général de traitement des incertitudes en mécanique proposé s'articule en trois étapes principales, rappelées dans le chapitre introductif : la définition du modèle mathématique décrivant le comportement physique du système considéré, la caractérisation probabiliste des incertitudes sur les paramètres de ce modèle, enfin la propagation de ces incertitudes à travers le modèle. Selon l'information recherchée (analyse des moments statistiques de la réponse, analyse de distribution, analyse de fiabilité, hiérarchisation des paramètres par leur importance), différentes méthodes de calcul peuvent être employées.

De façon à faciliter la lecture du mémoire, on rappelle tout d'abord les notions élémentaires de probabilités et statistique dans le chapitre 2. On présente les méthodes classiques de construction du modèle probabiliste des paramètres à partir de données disponibles : jugement d'expert, principe de maximum d'entropie, inférence statistique, approches bayésiennes. La modélisation de la variabilité spatiale des données par champs aléatoires est également abordée.

Un rapide état de l'art sur les méthodes de propagation des incertitudes est donné dans le chapitre 3. Pour le calcul des premiers moments statistiques de la réponse du modèle, on présente les méthodes de simulation de Monte Carlo, de perturbation et de quadrature. Les méthodes classiques de fiabilité (simulation de Monte Carlo, FORM/SORM, simulation d'importance, etc.) sont ensuite abordées. On introduit finalement différents outils permettant de hiérarchiser les paramètres d'entrée du modèle en fonction de leur importance (analyse de sensibilité) : facteurs d'importances, indices de Sobol'.

Les approches spectrales développées depuis une quinzaine d'années sous le nom d'*éléments finis stochastiques* sont abordées au chapitre 4. Elles sont fondées sur la représentation de la réponse aléatoire du modèle sur la base dite du *chaos polynomial*. On introduit dans un premier temps l'approche *intrusive*, bien adaptée à la résolution de problèmes stochastiques elliptiques. On présente ensuite de façon exhaustive les approches dites *non intrusives*, qui permettent d'obtenir les coefficients de la décomposition en chaos polynomial par une série d'évaluations de la réponse déterministe du modèle, pour des jeux de paramètres d'entrée judicieusement choisis. Les contributions de l'auteur au développement des méthodes de *projection* et *régression* sont soulignées. On montre également comment post-traiter de façon élémentaire les coefficients du chaos pour obtenir les moments statistiques ou la distribution de la réponse, résoudre un problème de fiabilité ou encore hiérarchiser les paramètres d'entrée. Une comparaison complète des différentes approches autour d'un problème linéaire de mécanique des structures permet de mesurer leurs performances respectives.

La propagation des incertitudes à travers un modèle mathématique s'appuie sur la caractérisation proba-

biliste de ses paramètres d'entrée. Celle-ci est parfois délicate à établir, alors que la qualité des prédictions probabilistes en dépend de façon importante. Dans le chapitre 5, on s'intéresse à des problèmes dans lesquels des informations relatives à la *réponse du système* peuvent être utilisées pour améliorer l'analyse. Lorsqu'on considère un système réel particulier, pour lequel on dispose de données d'auscultation, on peut utiliser les méthodes d'actualisation bayésienne des prédictions : on propose ici l'utilisation de la simulation de Monte Carlo par chaînes de Markov (méthode MCMC) et une méthode inspirée de la fiabilité des structures baptisée *FORM inverse bayésien*. Lorsqu'on s'intéresse à l'incertitude aléatoire de paramètres d'entrée du modèle non directement mesurables (telle qu'elle apparaît au travers de la dispersion observée dans la réponse de système identiques), on doit résoudre un *problème inverse probabiliste*. On propose alors de représenter ces paramètres de loi de probabilité inconnue à l'aide du chaos polynomial, dans un contexte d'inférence semi-paramétrique.

Le chapitre 6 aborde des développements spécifiques en fiabilité des structures lorsque le problème dépend du temps (*e.g.* chargement modélisé par des processus stochastiques, dégradation des propriétés des matériaux dans le temps, etc.). On introduit la notion de taux de franchissement pour le calcul de la probabilité de défaillance cumulée. Des bornes sur cette probabilité peuvent être calculées d'une part par une approche asymptotique, d'autre part par la méthode PHI2, dont l'auteur a contribué au développement. Les problèmes de fiabilité dépendant de l'espace sont finalement introduits, et notamment la notion d'*étendue de la défaillance*, qui définit la taille du sous-système mécanique pour lequel un critère de défaillance est ponctuellement atteint. Un exemple associé à la durabilité des poutres en béton armé soumises à la carbonation et à la corrosion des armatures illustre le propos.

Les développements originaux présentés dans ce mémoire sont en grande partie issus de problèmes concrets intéressant EDF. Le chapitre 7 permet de resituer ces travaux dans leur contexte applicatif : construction d'un référentiel probabiliste pour l'analyse des structures de tuyauterie de centrale nucléaire sollicitées en fatigue thermique, durabilité des coques d'aéro-réfrigérants, mécanique de la rupture non linéaire pour l'étude de la fissuration des tuyauteries.

Abstract

Probabilistic engineering mechanics aims at taking into account uncertainties on input parameters of mechanical models and studying their impact onto the model response. This field lies at the interface between mechanics, statistics and probability theory and encompasses various applications such as structural reliability, stochastic finite element analysis and random vibrations. This thesis introduces a global framework for dealing with uncertainties in mechanics and presents original results in this context.

The proposed global scheme for dealing with uncertainties relies upon three steps, namely the definition of the mathematical model of the physical system, the probabilistic characterization of the uncertainty on the input parameters and the propagation of the uncertainty through the model. Various computational schemes may be applied in practice according to the type of analysis of interest, namely statistical moment-, distribution, reliability and sensitivity analysis.

In order to make the reading easier, elementary notions of probability theory and statistics are recalled in Chapter 2. Methods for building the probabilistic model of the input parameters from the available data are reviewed, including expert judgment, principle of maximum entropy, classical and Bayesian inference. The modelling of spatially variable data using random fields is also addressed.

A short state-of-the-art on classical uncertainty propagation methods is given in Chapter 3. Second moment methods such as Monte Carlo simulation, perturbation and quadrature methods are reviewed, as well as structural reliability methods such as FORM/SORM and importance sampling. Various measures of sensitivity such as importance factors and Sobol' indices used for ranking the input parameters according to their importance are finally introduced.

Stochastic spectral methods are addressed in Chapter 4. They are based on the representation of the random model response in terms of *polynomial chaos expansions* (PCE). The principle of the so-called Galerkin *intrusive* solution scheme, which is well adapted to solve elliptic stochastic problems is first introduced. Then the *non intrusive* projection and regression schemes are detailed, which allow the analyst to compute the coefficients of the response PCE using a series of deterministic calculations based on a selected set of input parameters. The post-processing of the PCE coefficients in order to compute the response distribution and the statistical moments or to solve reliability and sensitivity problems is shown. An illustrative example dealing with a linear truss structure allows one to compare the relative efficiency of the various approaches.

The uncertainty propagation methods rely upon a probabilistic model of the input parameters, which may be difficult to build up in practice. In Chapter 5, problems in which information related to the *system response* is available are considered. When dealing with some particular real system, for which monitoring data is available, one may resort to Bayesian updating techniques in order to improve the model predictions: Markov chain Monte Carlo simulation (MCMC) is proposed in this context together with a *Bayesian inverse FORM* approach inspired by structural reliability methods. When the aleatoric uncertainty of some non measurable input parameters is of interest (whose uncertainty is caught through the very scattering of the measured model response), a *stochastic inverse problem* shall be solved. A method based on the polynomial chaos expansion of the input parameters is proposed in this context.

Chapter 6 addresses so-called *time-variant* reliability problems, in which time may appear in the modelling of loads (*e.g.* using random processes) or degrading materials. The outcrossing approach is introduced in order to compute bounds to the cumulative probability of failure by either an asymptotic approach or the so-called PHI2 method, which was partly developed by the author. Space-variant reliability problems are finally considered. The *extent of damage*, which is the volume of the subsystem in which some pointwise failure criterion is attained, is defined and studied. The durability of a RC beam submitted to concrete carbonation and rebars corrosion is finally addressed for the sake of illustration.

Most of the results gathered in this thesis have been obtained starting from real industrial problems that were of interest to EDF. Thus Chapter 7 presents three direct applications of this research, namely a probabilistic framework for thermal fatigue design of pipes in nuclear power plants, a study of the durability of cooling towers and the non linear fracture mechanics of cracked pipes.

Contents

1	Introduction	1
1	A brief history of modelling	1
2	Uncertainty propagation and sensitivity analysis	1
2.1	General framework	1
2.2	Models of physical systems (Step A)	3
2.3	Quantification of sources of uncertainty (Step B)	4
2.4	Uncertainty propagation (Step C)	5
2.5	Sensitivity analysis (Step C')	6
3	Outline	6
4	Reader's guide	7
2	Probabilistic model building	9
1	Introduction	9
2	Basics of probability theory	9
2.1	Probability space	9
2.1.1	Algebra of events and probability measure	9
2.1.2	Frequentist interpretation of probabilities	10
2.1.3	Conditional probability, Bayes' theorem and rule of total probability . . .	11
2.2	Random variables	11
2.2.1	Definition and basic properties	11
2.2.2	Examples	13
2.3	Random vectors	13
3	Quantification of sources of uncertainty	14
3.1	Introduction	14
3.2	Expert judgment and literature	14

3.3	Principle of maximum entropy	15
3.4	Statistics-based model building	15
3.4.1	Introduction	15
3.4.2	Method of moments and maximum likelihood estimation	16
3.5	Bayesian inference	16
3.6	Stochastic inverse methods	17
3.7	Conclusion	17
4	Modelling spatial variability	18
4.1	Introduction	18
4.2	Basics of random fields	18
4.2.1	Definition	18
4.2.2	Gaussian random fields	18
4.2.3	Principle of random field discretization	19
4.3	Series expansion methods	20
4.3.1	The Karhunen-Loève expansion	20
4.3.2	The orthogonal series expansion	21
4.3.3	The OLE/EOLE methods	22
4.3.4	Examples and recommendations	23
4.4	Non Gaussian fields	25
4.5	Conclusion	25
5	Conclusion	25
3	Methods for uncertainty propagation and sensitivity analysis	27
1	Introduction	27
2	Methods for second moment analysis	28
2.1	Introduction	28
2.2	Monte Carlo simulation	28
2.3	Perturbation method	29
2.3.1	Taylor series expansion of the model	29
2.3.2	Estimation of the variance of the response	30
2.3.3	Perturbation method in finite element analysis	30
2.3.4	Perturbation method in finite element analysis - random field input	31

2.4	Quadrature method	32
2.5	Weighted integral method	33
2.6	Conclusion	34
3	Methods for reliability analysis	35
3.1	Introduction	35
3.2	Problem statement	35
3.3	Monte Carlo simulation	35
3.4	First-order reliability method (FORM)	36
3.5	Second-order reliability method (SORM)	38
3.6	Importance sampling	38
3.7	Conclusion	40
4	Sensitivity analysis	41
4.1	Introduction	41
4.2	Sensitivity measures as a byproduct of uncertainty propagation	42
4.2.1	From the perturbation method	42
4.2.2	From FORM analysis	42
4.3	The Sobol' indices	42
4.3.1	Sobol' decomposition	42
4.3.2	Use in ANOVA	43
4.3.3	Computation by Monte Carlo simulation	44
4.4	Conclusion	45
5	Conclusion	45
4	Spectral methods	47
1	Introduction	47
2	Spectral representation of functions of random vectors	48
2.1	Introduction	48
2.2	Representation of scalar-valued models	49
2.2.1	Definition	49
2.2.2	Hilbertian basis of \mathcal{H} – Case of independent input random variables	49
2.2.3	Hilbertian basis of \mathcal{H} – Case of mutually dependent input random variables	50
2.2.4	Polynomial chaos representation of the model response	51

	2.2.5	Two strategies of application	51
	2.3	Representation of vector-valued models	52
	2.4	Practical implementation	53
	2.5	Conclusion	54
3		Galerkin solution schemes	54
	3.1	Brief history	54
	3.2	Deterministic elliptic problem	55
	3.2.1	Problem statement	55
	3.2.2	Galerkin method	55
	3.3	Stochastic elliptic problem	56
	3.3.1	Problem statement	56
	3.3.2	Two-step Galerkin method	56
	3.4	Computational issues	57
	3.5	Conclusion	58
4		Non intrusive methods	59
	4.1	Introduction	59
	4.2	Projection methods	60
	4.2.1	Introduction	60
	4.2.2	Simulation methods	60
	4.2.3	Quadrature methods	62
	4.3	Regression methods	63
	4.3.1	Introduction	63
	4.3.2	Problem statement	64
	4.3.3	Equivalence with the projection method	64
	4.3.4	Various discretized regression problems	65
	4.4	Conclusion	66
5		Post-processing of the PCE coefficients	67
	5.1	Response probability density function	67
	5.2	Statistical moments	68
	5.3	Reliability analysis	68
	5.4	Sensitivity analysis	68
	5.5	Conclusion	69

6	Application examples	70
6.1	Introduction	70
6.2	Geotechnical engineering	70
6.2.1	Example #1.1: Foundation problem – spatial variability	70
6.2.2	Example #1.2: Foundation problem – non Gaussian variables	73
6.2.3	Complementary applications	75
6.3	Structural mechanics	76
6.3.1	Deterministic problem statement	76
6.3.2	Probability density function of the midspan displacement	77
6.3.3	Statistical moments	78
6.3.4	Sensitivity analysis	80
6.3.5	Reliability analysis	81
6.3.6	Conclusion	82
7	Conclusion	83
5	Bayesian updating methods and stochastic inverse problems	85
1	Introduction	85
1.1	Bayesian updating techniques for real systems	85
1.2	Stochastic inverse methods	86
1.3	Measurement uncertainty and model error	86
1.3.1	Measurement uncertainty	87
1.3.2	Model error	87
1.3.3	Conclusion	88
2	Bayesian updating of model response	89
2.1	Introduction	89
2.2	Updating probabilities of failure	89
2.3	Computation of response quantiles by inverse FORM analysis	91
2.4	Computation of updated response quantiles by inverse FORM analysis	91
2.5	Conclusion	92
3	Bayesian updating of input parameters	92
3.1	Introduction	92
3.2	Problem statement	93

3.3	Markov chain Monte Carlo simulation	94
3.3.1	Metropolis-Hastings algorithm	94
3.3.2	Cascade Metropolis-Hastings algorithm	95
3.4	Conclusion	95
4	Stochastic inverse problems	96
4.1	Introduction	96
4.1.1	Problem statement	96
4.1.2	Outline	97
4.2	Identification using perfect measurements	97
4.2.1	Classical parametric approach	97
4.2.2	Polynomial chaos-based parametric approach	99
4.2.3	Conclusion	101
4.3	Identification with measurement/model error	101
4.3.1	Introduction	101
4.3.2	Parametric approach	102
4.3.3	PC-based parametric identification	102
4.4	Conclusion	103
5	Application examples	104
5.1	Bayesian updating in fatigue crack growth models	104
5.1.1	Introduction	104
5.1.2	Virkler's data base and deterministic fatigue crack growth model	104
5.1.3	Probabilistic model	105
5.1.4	Results	105
5.1.5	Conclusion	107
5.2	Stochastic identification of a Young's modulus	107
5.2.1	Problem statement	107
5.2.2	Pseudo-measurement data	109
5.2.3	Results in case of perfect measurements	110
5.2.4	Results in case of measurement error	111
5.2.5	Conclusion	112
6	Conclusions	113

6	Time and space-variant reliability methods	115
1	Introduction	115
1.1	Motivation	115
1.2	Outline	115
2	Random processes	116
2.1	Definition	116
2.2	Statistics of scalar random processes	117
2.3	Properties of random processes	117
2.3.1	Stationarity	117
2.3.2	Differentiability	118
2.3.3	Ergodic and mixing processes	120
2.3.4	Vector random processes	120
2.4	Poisson processes	120
2.5	Rectangular wave renewal processes	121
2.6	Gaussian processes	122
3	Time-variant reliability problems	123
3.1	Problem statement	123
3.2	Right-boundary problems	124
3.3	The outcrossing approach	125
3.3.1	Bounds to the probability of failure	126
3.3.2	Outcrossing rate	127
4	Analytical results for outcrossing rates	128
4.1	Rice's formula	128
4.2	Application of Rice's formula to Gaussian processes	129
4.3	Belayev's formula	130
4.4	Another estimation of the probability of failure	131
5	Asymptotic method	132
5.1	Introduction	132
5.2	Asymptotic Laplace integration	133
5.2.1	Introduction	133
5.2.2	"Boundary point" case	133
5.2.3	"Interior point" case	134

5.3	Application to scalar Gaussian differentiable processes	134
5.4	Outcrossing for general surfaces defined in the $R-Q-S$ -space	135
5.5	Conclusion	135
6	System reliability approach: the PHI2 method	135
6.1	Introduction	135
6.2	Analytical derivation of the outcrossing rate	136
6.3	Implementation of the PHI2 method using a time-invariant reliability code	137
7	Application examples	137
7.1	Analytical example	138
7.1.1	Problem statement	138
7.1.2	Closed-form solution	138
7.1.3	Numerical results	139
7.2	Durability of a corroded bending beam	140
7.2.1	Problem statement	140
7.2.2	Numerical results	141
7.3	General comparison between PHI2 and the asymptotic method	142
7.4	Conclusion	143
8	Space-variant reliability problems	143
8.1	Introduction	143
8.2	Space-variant probability of failure	144
8.3	Extent of damage for degrading structures	145
8.3.1	A class of degradation models	145
8.3.2	Space-variant reliability of damaged structures	146
8.3.3	Definition of the extent of damage	146
8.3.4	Statistical moments of the extent of damage	146
8.4	Application example	148
8.4.1	Point-in-space model of concrete carbonation	148
8.4.2	Probabilistic problem statement	149
8.4.3	Mean value and standard deviation of the extent of damage	150
8.4.4	Histogram of the extent of damage	152
8.5	Conclusion	153
9	Conclusion	153

7	Durability of industrial systems	155
1	Introduction	155
2	Thermal fatigue problems	155
2.1	Introduction	155
2.2	Deterministic framework for fatigue assessment	156
2.3	Probabilistic representation of the input data and the cumulated damage	157
2.3.1	Thermal loading	157
2.3.2	Mechanical model	158
2.3.3	Scatter of the fatigue test results	158
2.3.4	Specimen-to-structure passage factors	160
2.3.5	Random fatigue damage	160
2.4	Application example to a pipe	162
2.4.1	Problem statement	162
2.4.2	Mechanical model	162
2.4.3	Deterministic fatigue analysis	163
2.4.4	Probabilistic analysis	163
2.5	Conclusions	165
3	Cooling towers	166
3.1	Introduction	166
3.2	Exact response surface for linear structures	166
3.3	Deterministic model of the cooling tower	167
3.4	Limit state function and probabilistic model	167
3.4.1	Deterministic assessment of the structure	167
3.4.2	Limit state function	168
3.4.3	Probabilistic model of the input parameters	168
3.5	Point-in-space reliability analysis	169
3.5.1	Initial time-invariant analysis	169
3.5.2	Time-variant analysis	170
3.6	Space-variant reliability analysis	171
3.6.1	Problem statement	171
3.6.2	Results	172
3.7	Conclusion	172

4	Non linear fracture mechanics	173
4.1	Introduction and deterministic problem statement	173
4.2	Probabilistic description of the input parameters	174
4.3	Statistical moments of the crack driving force	175
4.4	Reliability analysis of the cracked pipe	176
4.5	Conclusion	178
5	Conclusion	178
8	Conclusion	181
A	Classical distributions and Monte Carlo simulation	183
1	Classical probability density functions	183
1.1	Normal distribution	183
1.2	Lognormal distribution	183
1.3	Uniform distribution	184
1.4	Gamma distribution	184
1.5	Beta distribution	185
1.6	Weibull distribution	185
2	Monte Carlo simulation	186
2.1	Introduction	186
2.2	Random number generators	186
2.3	Non uniform sampling	187
3	Nataf transform	188
B	Orthogonal polynomials and quadrature schemes	191
1	Orthogonal polynomials	191
1.1	Definition	191
1.2	Classical orthogonal polynomials	191
1.3	Hermite polynomials	192
1.4	Legendre polynomials	192
2	Gaussian quadrature rules	193

C	Academic achievements	195
1	Academic distinctions	195
1.1	Awards	195
1.2	Honors	195
1.3	Participation in Ph.D jury	195
1.3.1	Co-supervisor of the Ph.D	195
1.3.2	External examiner	196
1.4	Invited lectures and seminars	196
1.5	Organization of scientific events	196
1.6	Peer reviewing	197
2	Teaching	197
3	Supervising students	197
3.1	Ph.D students	197
3.2	MS students	198
4	List of publications	198
4.1	Thesis and monography	198
4.2	Book chapters	198
4.3	Peer-reviewed journal papers	199
4.4	International conference papers	200
4.5	National conference papers	203

Chapter 1

Introduction

1 A brief history of modelling

The birth of modern science is usually attributed to Descartes, Galileo and Newton who introduced the rigorous formalism of mathematics into physics. According to this vision, a *model* of a physical phenomenon may be defined as an idealized abstract representation of this phenomenon by a set of equations, whose solution reproduces the experimental observations.

Originally, models helped scientists decipher the laws of physics, *e.g.* gravitation, optics, electromagnetism, etc. During the 20th century, the original sense has evolved and modelling is nowadays the inescapable tool of engineers for the design, manufacturing, operating and monitoring of industrial systems or civil structures.

From this viewpoint, a major revolution has happened in the last four decades with the emergence of *computer simulation*. Basically the algorithms developed in the art of computing allow the analysts to solve the equations arising from their models of ever increasing complexity. Computing has become an everyday tool both in the academia and in the industry, where it is of irreplaceable use in the design of manufactured products (*e.g.* airplanes, cars, bridges, offshore structures, nuclear power plants, etc.) or in prospective predictions (*e.g.* meteorology, climate change, air pollution, etc.)

However, despite the increase in the accuracy of the representations and in the power of computers, models will never be able to catch comprehensively the complexity of the real world. Indeed, they always rely upon simplifying assumptions that are usually validated *a posteriori* by experimental evidence. Moreover, models should be fed by values of their input parameters, whose estimation may be difficult or inaccurate, *i.e.* uncertain. Dealing with these uncertainties is the main goal of this thesis.

2 Uncertainty propagation and sensitivity analysis

2.1 General framework

Probabilistic engineering aims at taking into account the uncertainties appearing in the modelling of physical systems and studying the impact of those uncertainties onto the system response. As a science, it emerged in civil and mechanical engineering in the 70's although pioneering contributions date back to the first half of the twentieth century (Mayer, 1926; Freudenthal, 1947; Lévi, 1949). This field lies at the

intersection of branches of physics on the one hand (*e.g.* civil, environmental and mechanical engineering) and applied mathematics on the other hand (*e.g.* statistics, probability theory and computer simulation).

In this thesis, methods for introducing uncertainty analysis in models of physical systems are considered. Although the models that will be investigated mostly resort to mechanics, these methods have a larger scope, *i.e.* they may be applied (and for some of them, have been already applied) to chemical engineering, electromagnetism, neutronics, etc.

The main steps for such kind of analysis are summarized in Figure 1.1. This sketch results from a multidisciplinary project carried out at EDF, R&D Division since 2003, in which the author took part (see a review in de Rocquigny (2006a,b)).

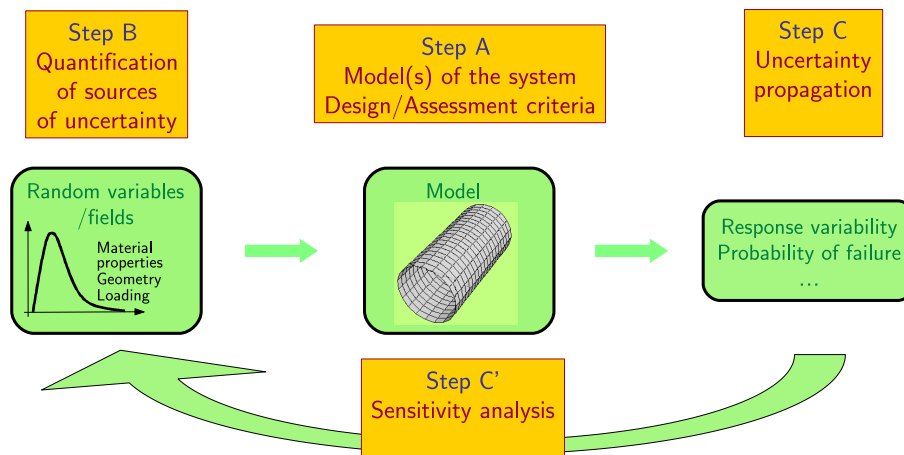


Figure 1.1: General sketch for uncertainty analysis

In the above figure, three steps are identified:

- Step A consists in *defining the model* or sequence of models and associated criteria (*e.g.* failure criteria) that should be used to assess the physical system under consideration. In case of complex systems and/or multiphysics approaches, it requires the clear identification of the input and output of each submodel. This step gathers all the ingredients used for a classical *deterministic* analysis of the physical system to be analyzed.
- Step B consists in *quantifying the sources of uncertainty*, *i.e.* identifying those input parameters that are not well known and modelling them in a probabilistic context. The end product of this step is a random vector of input parameters. In some cases, the description of the time (resp. spatial) variability of parameters requires the introduction of random processes (resp. random fields).
- Step C consists in *propagating the uncertainty* in the input through the model, *i.e.* characterizing the random response appropriately with respect to the assessment criteria defined in Step A. Numerous methods exist to carry out this task, as described below in Section 2.4.
- Uncertainty propagation methods usually provide information on the respective impact of the random input parameters on the response randomness. Such a hierarchization of the input parameters is known as *sensitivity analysis*. Note that this type of analysis (Step C' in Figure 1.1) may be sometimes the unique goal of the probabilistic mechanics study.

These main steps are now described in details.

2.2 Models of physical systems (Step A)

A *model* of a physical system will be considered throughout the report as a general function $\mathcal{M} : \mathbf{x} \mapsto \mathbf{y} = \mathcal{M}(\mathbf{x})$ with sufficient regularity conditions so that the subsequent derivations make sense. In this notation, the *input parameters* of the model are gathered into a vector $\mathbf{x} \in \mathcal{D} \subset \mathbb{R}^M$. The *model response* (also termed “response” or “vector of response quantities”) is a vector $\mathbf{y} = \mathcal{M}(\mathbf{x}) \in \mathbb{R}^N$.

In the elementary sense, the model may be a simple function defined by its mathematical expression. More generally, it may be a *black box* function such as a computer program (*e.g.* a finite element code) that takes input values and yields a result. In this case, the model \mathcal{M} is known only through pointwise evaluations $\mathbf{y}^{(i)} = \mathcal{M}(\mathbf{x}^{(i)})$ for each input vector $\mathbf{x}^{(i)}$ for which the computer program is run.

In the fields of civil and mechanical engineering that are more specifically of interest in this report, the input generally includes:

- parameters describing the geometry of the system, such as dimensions, length of structural members, cross-sections, etc.;
- parameters describing the material constitutive laws, such as Young’s moduli, Poisson’s ratios, yield stresses, hardening parameters, etc.;
- parameters describing the loading of the system, such as an applied pressure (wind, waves, etc.), a prestress state, a temperature-induced stress field, etc.
- parameters describing the boundary conditions such as imposed displacements, contact, etc.

In contrast, the response quantities usually include:

- displacements, *e.g.* vectors of nodal displacements in the context of finite element analysis;
- components of the elastic (resp. elastoplastic) strain tensor or invariants thereof, *e.g.* the cumulative equivalent plastic strain;
- components of the stress tensor, or derived quantities such as equivalent stresses, stress intensity factors, etc.;
- temperature, pore pressure, concentration of species, etc. in case of thermo-mechanical or multi-physics analysis.

In this thesis, a model as defined above includes both the equations describing the physics of the system and the algorithms used to solve them. It is implicitly assumed that the model is sufficiently accurate to predict the behaviour of the system, which means that the equations are relevant to describe the underlying physical phenomena and that the approximations introduced in the computational scheme, if any, are mastered.

If these assumptions do not hold strictly, it is always possible to introduce parameters describing the *model uncertainty*, *i.e.* correction factors that will be given a probabilistic description similar to the “physical” input parameters. Therefore, without any loss of generality, it will be assumed that the models used in the sequel (possibly including correction factors) faithfully predict the behaviour of the system, provided the input parameters are perfectly known. Unfortunately, this last statement does generally not hold.

2.3 Quantification of sources of uncertainty (Step B)

As observed by Soize (2005), distinction between *designed* and *real* systems should be made for the sake of clarity (see also Ditlevsen and Madsen (1996, chap. 3)). A designed system is an abstract object whose model and associated input parameters have been selected in such a way that design criteria (related with the purpose of the system) are fulfilled. In contrast, a real system is a physical object that has been built according to a given design. In practice, a real system never fully matches the initial design, at least for the following reasons:

- the true dimensions of the real system do not correspond exactly to the design due to the imperfections in the manufacturing process;
- the material properties of the real system may differ slightly from the codified properties of the class of material it is supposed to be made of;
- the loading (resp. boundary conditions) of the designed system are idealized so that they roughly represent the complexity of those of the real system.

For all these reasons, modelling the input parameters in a probabilistic context makes sense. The uncertainty that affects the input parameters may be of various kinds. They are usually classified as follows:

- *aleatoric uncertainty* refers to situations when there is a natural variability in the phenomenon under consideration. As an example, the number-of-cycles-to-failure of a sample specimen submitted to fatigue loading shows aleatoric uncertainty, since the very life-time of the specimens of the same material submitted to the same experimental conditions varies from one to the other.
- *epistemic uncertainty* refers to a lack of knowledge. As an example, the compressive strength of concrete of a given class shows scattering. On a building site though, measurements of the compressive strength of the very type of concrete that is used may show far less scattering. In this case, the initial lack of knowledge has been compensated for by gathering additional information. For this reason, epistemic uncertainty is qualified as reducible. In a sense, *measurement uncertainty* that appears in the fact that the same observation made by two different devices will not provide exactly the same value, is also epistemic.

In many cases, it is difficult to distinguish clearly between aleatoric and epistemic uncertainty, since both types may be present in the same system. In most of this report, no distinction is made between the two categories as far as their modelling is concerned: once the uncertainty in some input parameters has been recognized, a *probabilistic* model of the latter is built.

When data is available, establishing a probabilistic model that represents the scattering is merely a problem of statistics, whose comprehensive treatment is beyond the scope of this report. Note that it may happen in some cases (*e.g.* at the design stage of an innovative system) that no data is available. In this case, a probabilistic model should be prescribed from expert judgment. Finally, *Bayesian statistics* may be used to combine prior information (*e.g.* expert judgment) and scarce data. These various techniques will be briefly reviewed later on.

In any case, the end product of Step B is the description of the *random vector* of input parameters \mathbf{X} in terms of its joint probability density function (PDF) $f_{\mathbf{X}}(\mathbf{x})$. When spatial variability is modelled by introducing random fields, the discretization of the latter leads to the introduction of additional basic random variables that are gathered into the input random vector.

Remarks Note that other approaches may be used to model uncertainties in a non probabilistic paradigm. The Dempster-Shafer theory of evidence (Dempster, 1968; Shafer, 1976) is one possible approach and the possibility theory based on fuzzy sets (Zadeh, 1978) is another one. These approaches are beyond the scope of this report.

In the domain of stochastic dynamics and random vibrations (which is also not addressed in this report), a so-called *non parametric approach* has been recently proposed by Soize (2000) to take into account both model and parameter uncertainties in structural dynamics (see also Soize (2005) for a comprehensive overview of this approach). The uncertainties are introduced directly in the operators that mathematically describe the system dynamics, which leads to the formulation of random mass-, damping- and stiffness matrices. This approach has been applied to earthquake engineering (Desceliers et al., 2003; Cottereau et al., 2005), to the modelling of random field tensors of elastic properties (Soize, 2006), random impedance matrices (Cottereau, 2007; Cottereau et al., 2007), ground-borne vibrations in buildings (Arnst et al., 2006; Arnst, 2007).

2.4 Uncertainty propagation (Step C)

Let us consider a model $\mathbf{x} \mapsto \mathbf{y} = \mathcal{M}(\mathbf{x})$ and suppose that a probabilistic description of the input parameters is available in terms of a random vector \mathbf{X} . The *random response* is defined by:

$$\mathbf{Y} = \mathcal{M}(\mathbf{X}) \quad (1.1)$$

The main goal of probabilistic engineering mechanics is to study the probabilistic content of \mathbf{Y} , namely its joint probability density function $f_{\mathbf{Y}}(\mathbf{y})$. However, this function is not directly computable except in simple academic cases. Consequently, methods for *uncertainty propagation* have to be devised. These methods may be broadly classified into three categories, according to the specific information on the random response that is sought (see Figure 1.2).

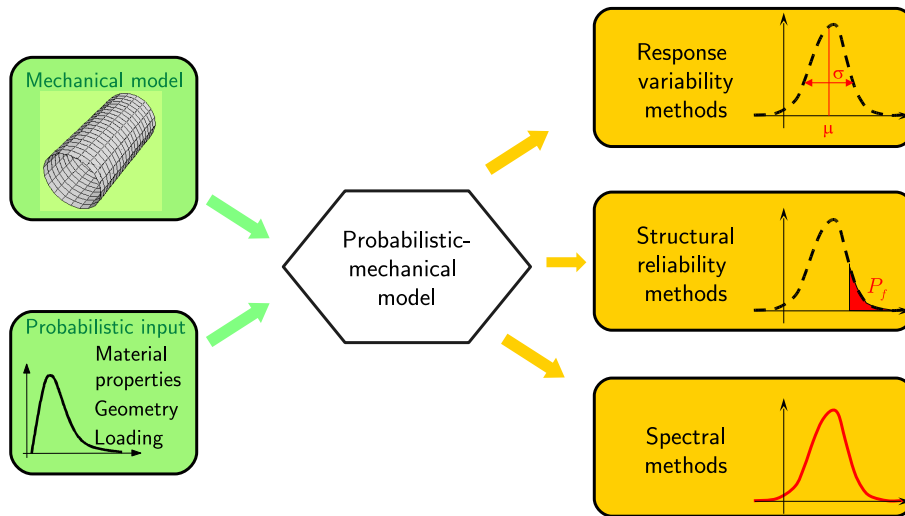


Figure 1.2: Classification of uncertainty propagation methods

- *second moment methods* deal with computing the mean value and variance of the model response. By extension, higher order moment methods may be envisaged. In other words, they merely give some information on the central part of the response PDF;
- *structural reliability methods* (Ditlevsen and Madsen, 1996; Melchers, 1999; Lemaire, 2005) essentially investigate the tails of the response PDF by computing the probability of exceeding a prescribed threshold (probability of failure);
- *spectral methods* represent the complete randomness of the response in an intrinsic way by using suitable tools of functional analysis. Also known as *stochastic finite element methods* in the context of computational mechanics (Ghanem and Spanos, 1991a), spectral methods have been fostering

an intense research effort for the last ten years. As explained later on, they allow the analyst to solve problems pertaining to second moment- or structural reliability analysis by a straightforward post-processing of their basic output, namely expansion coefficients on a suitable basis of functions.

2.5 Sensitivity analysis (Step C')

The modelling of complex systems usually requires a large number of input parameters. Defining a proper probabilistic model for these parameters may become a burden. However, in most real-world problems, only a limited number of input parameters happens to influence the response randomness significantly¹. In this context, sensitivity analysis aims at selecting the important parameters, usually by defining quantitative *importance measures* or *sensitivity indices* that allow the analyst to rank the latter.

As will be seen later on, most methods for uncertainty propagation provide sensitivity measures as a byproduct of their principal output.

3 Outline

From the general framework described in the previous section, the document is organized into seven chapters that are now presented.

Chapter 2 first introduces the basics of probability theory in order to set up the notation that will be used throughout the report. A not too mathematical (and hopefully sufficiently rigorous) formalism is chosen in order to facilitate the reading. Indeed, this work takes place in an engineering context and is in no way a thesis in statistics nor in probability theory. Then methods to build a probabilistic model of the input parameters from data are briefly reviewed. The representation of spatially varying quantities by random fields is finally addressed.

Chapter 3 presents the classical methods for uncertainty propagation and sensitivity analysis. This chapter should be considered as a survey of various topics of interest including second moment-, reliability- and global sensitivity analysis. Apart from introducing tools that are constantly used in the subsequent chapters, it also provides a unified presentation of well-known results and recent advances in this field.

Chapter 4 introduces the so-called spectral methods that have emerged in the late 80's in probabilistic engineering mechanics, and whose interest has dramatically grown up in the last five years. These cutting-edge approaches aim at representing the random model response as a series expansion onto a suitable basis. The coefficients of the expansion gather the whole probabilistic content of the random response. The so-called Galerkin (*i.e. intrusive*) and *non intrusive* computational schemes are presented in details, together with the post-processing techniques.

Chapter 5 introduces advanced methods to incorporate observation data into the uncertainty analysis. In case of designed systems, the so-called *stochastic inverse methods* allow the analyst to characterize the aleatoric uncertainty of some input parameters from measurements of output quantities carried out on a set of similar structures represented by the same model. In case of a single real structure that is monitored in time, Bayesian techniques help update both the probabilistic model of input data and the model predictions.

Chapter 6 addresses *time-variant reliability problems* in which time plays a particular role. The basic mathematics of random processes is first recalled and the time-variant reliability problem is posed. Various

¹It is always possible to devise mathematical models that are counter-examples to this statement, but they often do not have any physical meaning.

techniques to solve it are reviewed, with an emphasis onto the so-called PHI2 method. The space-variant reliability problems are finally introduced as an extension.

Chapter 7 finally presents different industrial applications which show the potential of the methods introduced in the previous chapters. A framework for fatigue assessment of nuclear components is first proposed. The application of structural reliability methods to cooling towers is then presented. Lastly, non intrusive stochastic finite element methods are applied to the fracture mechanics of a cracked pipe.

4 Reader's guide

This thesis presents the author's view on uncertainty propagation and sensitivity analysis in mathematical models of physical systems. It is a synthesis of seven years of research in this area. This research was initiated during the post-doctoral stay of the author at the University of California at Berkeley (Departement of Civil and Environmental Engineering) in 2000. It has been carried on at EDF, R&D Division, where the author has been working as a research engineer in the Department for Materials and Mechanics of Components (MMC) since 2001.

As a thesis submitted to graduate for the "*habilitation à diriger des recherches*", this document gathers contributions of the author to probabilistic engineering mechanics. Apart from presenting in a consistent way these contributions, the thesis also aims at establishing connections between fields that seldom communicate otherwise (*e.g.* spectral methods and reliability (resp. sensitivity) analysis). Hopefully it will bring an original overview of the field and foster future research.

Nonetheless, it is important to discriminate the contributions of the author from the rest of the document. In this respect, sections devoted to a review of the literature are clearly identified in each chapter, while sections presenting the original contributions of the author constantly refer to his own relevant publications.

Chapter 2

Probabilistic model building

1 Introduction

Following the general framework for uncertainty propagation in mathematical models of physical systems, the analyst has to build a probabilistic description of the data and more precisely, of the input parameters of the model (Figure 1.1, Step B).

In order to set up the scene, it is necessary to recall first the basics of probability theory. It is not intended here to fully cover this domain of mathematics, but rather to provide the minimal mathematical formalism required in the sequel. It includes in particular the notation that will be used throughout the report (Section 2). Should the reader be familiar with probabilistic methods, he or she can easily skip this section.

Once the mathematical background has been recalled, the techniques for building the probabilistic model of the data are summarized in Section 3.

The modelling of spatially varying random parameters requires the introduction of specific tools, namely random fields. The basic properties of random fields and a short review of discretization techniques are finally given in Section 4.

2 Basics of probability theory

2.1 Probability space

The following introduction to the basic concepts of probability theory is inspired from various textbooks including Lin (1967); Lacaze et al. (1997); Saporta (2006).

2.1.1 Algebra of events and probability measure

When a random phenomenon is observed, the set of all possible outcomes defines the sample space denoted by Ω . An event E is defined as a subset of Ω containing outcomes $\omega \in \Omega$. The classical notation used in set theory applies to events. The intersection (resp. the union) of two events A and B is denoted by $A \cap B$ (resp. $A \cup B$). Two events are called disjoint events when their intersection is the empty set \emptyset .

The complementary of an event A is denoted by \bar{A} and satisfies:

$$A \cap \bar{A} = \emptyset \quad A \cup \bar{A} = \Omega \quad (2.1)$$

The classical distributivity properties of union and intersection read:

$$\begin{aligned} (A \cup B) \cap C &= (A \cap C) \cup (B \cap C) \\ (A \cap B) \cup C &= (A \cup C) \cap (B \cup C) \end{aligned} \quad (2.2)$$

Any finite or numerable union (resp. intersection) of events is an event. The following inclusion / exclusion rules hold:

$$\begin{aligned} \overline{\bigcup_{i=1}^n A_i} &= \bigcap_{i=1}^n \bar{A}_i \\ \overline{\bigcap_{i=1}^n A_i} &= \bigcup_{i=1}^n \bar{A}_i \end{aligned} \quad (2.3)$$

A complete set of mutually exclusive events $\{A_1, \dots, A_n\}$ is defined as:

$$\begin{aligned} A_i &\neq \emptyset \quad i = 1, \dots, n \\ A_i \cap A_j &= \emptyset \quad 1 \leq i < j \leq n \\ \bigcup_{i=1}^n A_i &= \Omega \end{aligned} \quad (2.4)$$

The set of events defines the σ -algebra \mathcal{F} associated with Ω . A *probability measure* allows to associate numbers to events, *i.e.* their *probability of occurrence*. It is defined as an application $\mathbb{P} : \mathcal{F} \mapsto [0, 1]$ which follows the Kolmogorov axioms:

$$\mathbb{P}(A) \geq 0 \quad \forall A \in \mathcal{F} \quad (2.5)$$

$$\mathbb{P}(\Omega) = 1 \quad (2.6)$$

$$\mathbb{P}(A \cup B) = \mathbb{P}(A) + \mathbb{P}(B) \quad \forall A, B \in \mathcal{F}, A \cap B = \emptyset \quad (2.7)$$

From these axioms, the following elementary results hold:

$$\mathbb{P}(\emptyset) = 0 \quad (2.8)$$

$$\mathbb{P}(\bar{A}) = 1 - \mathbb{P}(A) \quad (2.9)$$

$$\mathbb{P}(A \cup B) = \mathbb{P}(A) + \mathbb{P}(B) - \mathbb{P}(A \cap B) \quad \forall A, B \in \mathcal{F} \quad (2.10)$$

The probability space constructed by means of these notions is denoted by $(\Omega, \mathcal{F}, \mathbb{P})$.

2.1.2 Frequentist interpretation of probabilities

The above construction of a probability space is purely mathematical. In practice, the probability of an event has to be given a clear significance. The so-called *frequentist* interpretation of probability theory consists in considering that the probability of an event is the limit of its empirical frequency of occurrence. Suppose that a random experiment is made n times, and that n_A denotes the number of times for which the event A is observed. The empirical frequency of occurrence of A is defined by:

$$\text{Freq}(A) = \frac{n_A}{n} \quad (2.11)$$

The probability of occurrence of A is considered as the limit of the empirical frequency of occurrence when the number of experiments tends to infinity:

$$\mathbb{P}(A) = \lim_{n \rightarrow \infty} \frac{n_A}{n} \quad (2.12)$$

2.1.3 Conditional probability, Bayes' theorem and rule of total probability

The conditional probability of an event A with respect to an event B is defined by:

$$\mathbb{P}(A|B) = \frac{\mathbb{P}(A \cap B)}{\mathbb{P}(B)} \quad (2.13)$$

Two events A and B are said *independent* events when the occurrence of B does not affect the probability of occurrence of A , *i.e.* when:

$$\mathbb{P}(A|B) = \mathbb{P}(A) \quad (2.14)$$

As a consequence, two events A and B are independent if and only if:

$$\mathbb{P}(A \cap B) = \mathbb{P}(A) \mathbb{P}(B) \quad (2.15)$$

Bayes' theorem is a straightforward application of the definition in Eq.(2.13). Given two events A and B , it states that:

$$\mathbb{P}(B|A) = \frac{\mathbb{P}(A|B) \mathbb{P}(B)}{\mathbb{P}(A)} \quad (2.16)$$

It is the foundation of the so-called Bayesian statistics which will be discussed later on. By considering a set of mutually exclusive and collectively exhaustive events $\{A_1, \dots, A_n\}$ (Eq.(2.4)) and another event B , the rule of total probability reads:

$$\mathbb{P}(B) = \sum_{i=1}^n \mathbb{P}(B|A_i) \mathbb{P}(A_i) \quad (2.17)$$

2.2 Random variables

2.2.1 Definition and basic properties

A real *random variable* X is a mapping $X : \Omega \mapsto \mathcal{D}_X \subset \mathbb{R}$. When \mathcal{D}_X is a discrete (possibly infinite) set, the random variable is said *discrete*, otherwise it is said *continuous*. A random variable is completely defined by its cumulative distribution function (CDF) denoted by $F_X(x)$:

$$F_X(x) = \mathbb{P}(X \leq x) \quad (2.18)$$

Examples of CDFs of discrete and continuous random variables are given in Figure 2.1. For a discrete random variable, the domain of definition may be represented as $\mathcal{D}_X = \{x^{(i)}, i \in \mathbb{N}\}$. The probability mass function is defined in this case as follows:

$$p_i = \mathbb{P}(X = x^{(i)}) \quad (2.19)$$

The CDF reads in this case:

$$F_X(x) = \sum_{i \in \mathbb{N}} p_i \mathbf{1}_{\{x \geq x^{(i)}\}}(x) \quad (2.20)$$

where $\mathbf{1}_{\{x \geq a\}}(x)$ is the indicator function of the set $\{x \in \mathbb{R} : x \geq a\}$ defined by:

$$\mathbf{1}_{\{x \geq a\}}(x) = \begin{cases} 1 & \text{if } x \geq a \\ 0 & \text{otherwise} \end{cases} \quad (2.21)$$

For a continuous random variable, the probability density function (PDF) is defined as:

$$f_X(x) = \lim_{h \rightarrow 0, h > 0} \mathbb{P}(x \leq X \leq x + h) / h \quad (2.22)$$

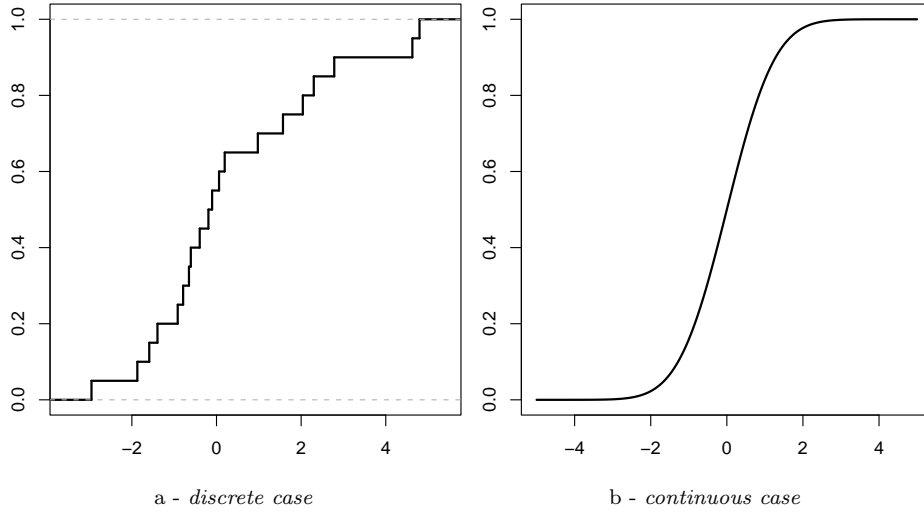


Figure 2.1: Examples of cumulative distribution functions

Hence:

$$f_X(x) = \frac{dF(x)}{dx} \quad (2.23)$$

The mathematical expectation will be denoted by $E[\cdot]$. The mean value (or expected value) of a random variable reads:

$$\mu_X \equiv E[X] = \int_{\mathcal{D}_X} x f_X(x) dx \quad (2.24)$$

The expectation of a function $g(X)$ is defined as (provided the integral exists):

$$E[g(X)] = \int_{\mathcal{D}_X} g(x) f_X(x) dx \quad (2.25)$$

The n -th moment (resp. centered moment) of X is defined as:

$$\mu'_n = E[X^n] = \int_{\mathcal{D}_X} x^n f_X(x) dx \quad (2.26)$$

$$\mu_n = E[(X - \mu_X)^n] = \int_{\mathcal{D}_X} (x - \mu_X)^n f_X(x) dx \quad (2.27)$$

The variance, standard deviation and coefficient of variation of X are defined as follows:

$$\text{Var}[X] = E[(X - \mu_X)^2] \quad (2.28)$$

$$\sigma_X = \sqrt{\text{Var}[X]} \quad (2.29)$$

$$CV_X = \frac{\sigma_X}{\mu_X} \quad (2.30)$$

The normalized third (resp. fourth) order centered moment is called the skewness (resp. kurtosis) coefficient and it will be denoted by δ_X (resp. κ_X):

$$\delta_X = \frac{1}{\sigma_X^3} E[(X - \mu_X)^3] \quad (2.31)$$

$$\kappa_X = \frac{1}{\sigma_X^4} E[(X - \mu_X)^4] \quad (2.32)$$

The covariance of two random variables X and Y is:

$$\text{Cov}[X, Y] = E[(X - \mu_X)(Y - \mu_Y)] \quad (2.33)$$

The correlation coefficient of two random variables is obtained by normalizing the covariance by the respective standard deviations:

$$\rho_{X,Y} = \frac{\text{Cov}[X, Y]}{\sigma_X \sigma_Y} \quad (2.34)$$

The vectorial space of real random variables with finite second moment ($E[X^2] < \infty$) is denoted by $\mathcal{L}^2(\Omega, \mathcal{F}, \mathbb{P})$. The expectation operator defines an inner product on this space:

$$\langle X, Y \rangle = E[XY] \quad (2.35)$$

When equipped with the above inner product, the space $\mathcal{L}^2(\Omega, \mathcal{F}, \mathbb{P})$ is a Hilbert space. In particular, two random variables X and Y are said *orthogonal* if and only if $E[XY] = 0$.

2.2.2 Examples

Gaussian random variables are of utmost importance in probability theory. In this report, they will be denoted by $X \sim \mathcal{N}(\mu, \sigma)$ where μ is the mean value and σ is the standard deviation. The notation ξ will be used for standard normal random variables, which correspond to $\mu = 0$, $\sigma = 1$. The standard normal PDF $\varphi(x)$ is defined by:

$$\varphi(x) = \frac{1}{\sqrt{2\pi}} e^{-x^2/2} \quad (2.36)$$

The standard normal CDF $\Phi(x)$ reads:

$$\Phi(x) = \int_{-\infty}^x \frac{1}{\sqrt{2\pi}} e^{-x^2/2} dx \quad (2.37)$$

Hence the PDF and CDF of a Gaussian random variable $X \sim \mathcal{N}(\mu, \sigma)$:

$$f_X(x) = \frac{1}{\sigma} \varphi\left(\frac{x-\mu}{\sigma}\right) \quad F_X(x) = \Phi\left(\frac{x-\mu}{\sigma}\right) \quad (2.38)$$

For the sake of completeness, the notation for the common distributions that will be used in this report is given in Appendix A.

2.3 Random vectors

A real *random vector* \mathbf{X} is a mapping $\mathbf{X} : \Omega \longrightarrow \mathcal{D}_{\mathbf{X}} \subset \mathbb{R}^q$, where q is the size of the vector ($q \geq 2$). It may be considered as a vector whose components are random variables: $\mathbf{X} \equiv \{X_1, \dots, X_q\}^\top$, where $(\cdot)^\top$ denotes the transposition. Its probabilistic description is contained in its joint PDF denoted by $f_{\mathbf{X}}(\mathbf{x})$. The marginal distribution of a given component X_i is obtained by integrating the joint PDF over all the remaining components (denoted by $d\mathbf{x}_{\sim i} = dx_1 \cdots dx_{i-1} dx_{i+1} \cdots dx_q$ throughout this report):

$$f_{X_i}(x_i) = \int_{\mathcal{D}_{\mathbf{X}}^{\sim i}} f_{\mathbf{X}}(\mathbf{x}) d\mathbf{x}_{\sim i} \quad (2.39)$$

where $\mathcal{D}_{\mathbf{X}}^{\sim i}$ is the subset of $\mathcal{D}_{\mathbf{X}}$ defined by $\{\mathbf{x} \in \mathcal{D}_{\mathbf{X}}, x_i \text{ fixed}\}$. Similarly, the joint distribution of two components (X_i, X_j) is given by:

$$f_{X_i, X_j}(x_i, x_j) = \int_{\mathcal{D}_{\mathbf{X}}^{\sim (i,j)}} f_{\mathbf{X}}(\mathbf{x}) d\mathbf{x}_{\sim ij} \quad (2.40)$$

The expectation of a random vector is the vector containing the expectation of each component:

$$\mu_{\mathbf{X}} = \{\mu_{X_1}, \dots, \mu_{X_q}\}^\top \quad (2.41)$$

The covariance matrix (resp. the correlation matrix) of \mathbf{X} is a square symmetric matrix \mathbf{C} (resp. \mathbf{R}) of size q , defined by the following entries:

$$\mathbf{C}_{i,j} = \text{Cov}[X_i, X_j] \quad (2.42)$$

$$\mathbf{R}_{i,j} = \rho_{X_i, X_j} \quad (2.43)$$

Introducing the diagonal matrix $\mathbf{\Lambda} = \text{Diag}(\sigma_{X_1}, \dots, \sigma_{X_q})$ containing the standard deviation of each component of \mathbf{X} , the covariance and correlation matrices satisfy:

$$\mathbf{C} = \mathbf{\Lambda} \mathbf{R} \mathbf{\Lambda} \quad (2.44)$$

Gaussian random vectors of size q , denoted by $\mathbf{X} \sim \mathcal{N}(\mu_{\mathbf{X}}, \mathbf{C})$, are completely defined by their mean value vector $\mu_{\mathbf{X}}$ and covariance matrix \mathbf{C} through the following joint PDF:

$$f_{\mathbf{X}}(\mathbf{x}) = \varphi_q(\mathbf{x} - \mu_{\mathbf{X}}; \mathbf{C}) \equiv (2\pi)^{-q/2} (\det \mathbf{C})^{-1/2} \exp \left[-\frac{1}{2} (\mathbf{x} - \mu_{\mathbf{X}})^{\top} \cdot \mathbf{C}^{-1} \cdot (\mathbf{x} - \mu_{\mathbf{X}}) \right] \quad (2.45)$$

Standard normal random vectors of size q are defined by $\mathbf{\Xi} \sim \mathcal{N}(0, \mathbf{I}_q)$ where \mathbf{I}_q is the identity matrix of size q . The associated multinormal PDF is then simply denoted by $\varphi_q(\mathbf{x})$:

$$\varphi_q(\mathbf{x}) = (2\pi)^{-q/2} \exp \left[-\frac{1}{2} (x_1^2 + \dots + x_q^2) \right] \quad (2.46)$$

3 Quantification of sources of uncertainty

3.1 Introduction

In order to quantify the sources of uncertainty, *i.e.* to build the probabilistic model of the input parameters of the system under consideration, data shall be gathered. Depending on the amount of available data, which may range from zero to thousands of observations, various techniques may be used:

- when no data is available to characterize the uncertainties in some input parameters, a probabilistic model may be prescribed by *expert judgment*, where physical consideration *e.g.* on the positiveness or physical bounds of the parameters may be argued. The principle of maximum entropy may help quantify the uncertainty in this case;
- when a large amount of data is available, the tools of *statistical inference* may be fully applied in order to set up a probabilistic model of the data;
- when both expert judgment and a minimum amount of observations is available, *Bayesian inference* may be resorted to;
- in some situations, gathering data on input parameters may be difficult, expensive and sometimes impossible, while other quantities can be more easily measured. In this case, *identification* techniques have to be used. This identification may be cast as a stochastic inverse problem or in a Bayesian context (when prior information is available). Specific techniques to solve these problems will be described in Chapter 5.

3.2 Expert judgment and literature

In the early stage of design of a system, the engineer often knows little about the uncertainties that should be taken into account to predict accurately the behaviour of the real system that will be built based on this design.

The choice of a specific probabilistic model for the input parameters may be prescribed in this case by *expert judgment*, *i.e.* from some general knowledge on similar systems and associated models previously dealt with or reported in the literature.

In order to allow the analyst to carry out uncertainty analysis at this early stage of design, the Joint Committee on Structural Safety (JCSS) has edited the *JCSS Probabilistic Model Code* (Vrouwenvelder, 1997; Joint Committee on Structural Safety, 2002), which reviews appropriate probabilistic models for loads (part II) and material properties (part III) that should be used when no other source of information is available. Note that a large amount of information on probabilistic models for loads and resistance is available in Melchers (1999, Chap. 7-8).

3.3 Principle of maximum entropy

The principle of maximum entropy (Jaynes, 1957; Kapur and Kesavan, 1992) states that the least biased probability density function $f_X(x) : \Omega \mapsto \mathcal{D}_X \subset \mathbb{R}$ that represents some information on a random variable X is the one that maximizes its *entropy* defined by:

$$H = - \int_{\mathcal{D}_X} f_X(x) \log f_X(x) dx \quad (2.47)$$

under the constraints imposed by the available information, *e.g.* positiveness, bounds, moments, etc. More precisely, let us consider the class of distributions with support $\mathcal{D}_X \subset \mathbb{R}$ such that the following constraints hold:

$$\mathbb{E}[g_j(X)] = \gamma_j \quad \forall j = 1, \dots, n_g \quad (2.48)$$

where $\{g_j, j = 1, \dots, n_g\}$ are sufficiently smooth functions such that the above constraint equations make sense. Boltzmann's theorem states that the probability density function of maximum entropy (ME) may be cast as:

$$f_X^{\text{ME}}(x) = c \exp \left(\sum_j^{n_g} \lambda_j g_j(x) \right) \quad (2.49)$$

where the constants $\{c, \lambda_j, j = 1, \dots, n_g\}$ have to be determined so that the integral of f_X^{ME} over \mathcal{D}_X is 1 and the constraints in Eq.(2.48) hold.

For instance, if only the mean value and standard deviation is known, the maximum entropy distribution is Gaussian. More generally, if the conditions in Eq.(2.48) correspond to statistical moments, the maximum entropy distribution is the exponential of a polynomial (Er, 1998; Puig and Akian, 2004). Note that the ME distribution of a bounded random variable such that $\mathcal{D}_X = [a, b]$ is the uniform distribution $\mathcal{U}[a, b]$.

3.4 Statistics-based model building

3.4.1 Introduction

In this section, we suppose that observations of certain input parameters are available and that the number of data points is large enough to apply statistical inference methods. Precisely, suppose that a sample set $\{x^{(1)}, \dots, x^{(n)}\}$ of input parameter X is available.

The basic assumption in statistics is that each data point $\{x^{(k)}, k = 1, \dots, n\}$ is the realization of a random variable X_k , and that the X_k 's are independent and identically distributed (i.i.d). The problem is to find out what is the common probability density function of these variables.

In order to define the best-fit probability density function (that will be used as the input data for uncertainty propagation), the following steps are usually necessary (Saporta, 2006).

- the tools of descriptive statistics are used to get a first feeling on the data. For instance, the sample mean, standard deviation, mode, range are computed and visualization tools such as box plots and histograms are used;
- a family (or several families) of distribution is chosen that could possibly fit the data (*e.g.* lognormal, Gaussian, Weibull, etc.);
- the parameters of the chosen distributions are estimated using *e.g.* the method of moments or the maximum likelihood method;
- goodness-of-fit tests are applied in order to validate the assumptions made for each distribution;
- from the results, *the* most appropriate distribution is selected and will be used for uncertainty propagation.

In case when a kind of dependence between some parameters is suspected, the above chart should be applied to the corresponding vector of parameters. In most practical cases, the full multi-dimensional inference is not feasible. On the contrary, the scalar parameters are studied one-by-one. Then the correlation structure between parameters is investigated. Note that non parametric statistical tools also exist, such as the kernel smoothing techniques, see Wand and Jones (1995).

3.4.2 Method of moments and maximum likelihood estimation

A key point in statistical inference is the estimation of the so-called *hyperparameters* of a distribution from a sample set of observations. The *method of moments* is probably the simplest way to infer parameters of the underlying distribution. It is based on the computation of the empirical moments of the sample set called *sample moments*. By equating these sample moments with the moments of the underlying random variable (see Eq.(2.26)) and by solving the resulting equations, the hyperparameters are determined.

The *maximum likelihood method* is known to be more robust than the method of moments and it is now briefly reviewed. Let us suppose that the joint PDF $f_{\mathbf{X}}(\mathbf{x}, \boldsymbol{\theta})$ of a random vector \mathbf{X} depends on a vector of hyperparameters $\boldsymbol{\theta}$ of size n_{θ} that is to be determined from a sample set of observations, say $\{\mathbf{x}^{(1)}, \dots, \mathbf{x}^{(n)}\}$. Provided that the observations are independent and identically distributed, the *likelihood function*, defined as a function of $\boldsymbol{\theta}$, reads:

$$L(\boldsymbol{\theta}; \mathbf{x}^{(1)}, \dots, \mathbf{x}^{(n)}) = \prod_{i=1}^n f_{\mathbf{X}}(\mathbf{x}^{(i)}, \boldsymbol{\theta}) \quad (2.50)$$

The principle of maximum likelihood states that the optimal vector of hyperparameters $\hat{\boldsymbol{\theta}}_{\text{ML}}$ is the one that maximizes $L(\boldsymbol{\theta}; \mathbf{x}^{(1)}, \dots, \mathbf{x}^{(n)})$ with respect to $\boldsymbol{\theta}$. In practice, one equivalently minimizes the opposite of the log-likelihood, namely:

$$\hat{\boldsymbol{\theta}}^{\text{ML}} = \arg \min_{\boldsymbol{\theta} \in \mathbb{R}^{n_{\theta}}} \left(- \sum_{i=1}^n \log f_{\mathbf{X}}(\mathbf{x}^{(i)}, \boldsymbol{\theta}) \right) \quad (2.51)$$

From a theoretical viewpoint, the maximum likelihood estimator $\hat{\boldsymbol{\theta}}^{\text{ML}}$ is asymptotically normal and efficient (it has the lowest possible variance among all the unbiased estimators) (Saporta, 2006, Chap. 13).

3.5 Bayesian inference

Broadly speaking, Bayesian statistics allows the analyst to combine *prior information* on the uncertainty in the parameters and experimental data to provide a *posterior* distribution for the random variables. A comprehensive description of this branch of statistics may be found in Robert (1992); O'Hagan and

Forster (2004). As far as the use of Bayesian statistics is concerned in this report, the following simplified formalism is sufficient.

Let us suppose again that the joint PDF $f_{\mathbf{X}}(\mathbf{x}, \boldsymbol{\theta})$ of random vector \mathbf{X} depends on a vector of hyperparameters $\boldsymbol{\theta}$ of size n_{θ} . In the Bayesian paradigm, a *prior distribution* $p_{\Theta}(\boldsymbol{\theta})$ is assigned to the vector of hyperparameters according to some prior information, *i.e.* some expert judgment available *before* any observation $\{\mathbf{x}^{(1)}, \dots, \mathbf{x}^{(n)}\}$ is collected. Then Bayes' theorem allows the analyst to define the *posterior distribution* of Θ denoted by $f''_{\Theta}(\boldsymbol{\theta})$:

$$f''_{\Theta}(\boldsymbol{\theta}) = \frac{1}{c} p_{\Theta}(\boldsymbol{\theta}) \mathsf{L}(\boldsymbol{\theta}; \mathbf{x}^{(1)}, \dots, \mathbf{x}^{(n)}) \quad (2.52)$$

where $\mathsf{L}(\boldsymbol{\theta}; \mathbf{x}^{(1)}, \dots, \mathbf{x}^{(n)})$ is the likelihood function defined in Eq.(2.50) and c is a normalizing constant defined by:

$$c = \int_{\mathcal{D}_{\Theta}} p_{\Theta}(\boldsymbol{\theta}) \mathsf{L}(\boldsymbol{\theta}; \mathbf{x}^{(1)}, \dots, \mathbf{x}^{(n)}) d\boldsymbol{\theta} \quad (2.53)$$

In the above equation, $\mathcal{D}_{\Theta} \subset \mathbb{R}^{n_{\theta}}$ is the support of p_{Θ} . From the posterior distribution $f''_{\Theta}(\boldsymbol{\theta})$, the *predictive* distribution of \mathbf{X} reads:

$$f''_{\mathbf{X}}(\mathbf{x}) = \int_{\mathcal{D}_{\Theta}} f_{\mathbf{X}}(\mathbf{x}, \boldsymbol{\theta}) f''_{\Theta}(\boldsymbol{\theta}) d\boldsymbol{\theta} \quad (2.54)$$

Alternatively, the analyst may avoid the latter integration by considering a point posterior distribution:

$$\hat{f}_{\mathbf{X}}(\mathbf{x}) \equiv f_{\mathbf{X}}(\mathbf{x}, \hat{\boldsymbol{\theta}}) \quad (2.55)$$

where $\hat{\boldsymbol{\theta}}$ is for instance the mode of f''_{Θ} . As will be shown in Chapter 5, the above framework may be extended to cases when the available data is not a sample set of \mathbf{X} but *e.g.* a sample set of response quantities $\mathbf{y}^{(q)} = \mathcal{M}(\mathbf{x}^{(q)})$, $q = 1, \dots, n_{obs}$.

3.6 Stochastic inverse methods

In many industrial problems, although there is experimental evidence of the scattering of some quantities that are used as input variables of the model under consideration, it is not always possible to measure these quantities directly. This may be due to the lack of adequate experimental devices or the excessive cost of data acquisition. In some cases, the model relies upon “non physical” parameters that can of course not be measured. Note that model correction factors may be classified into this category.

Conversely, data related to the model response may be sometimes easier to obtain. Methods that allow the analyst to characterize the aleatoric uncertainty of input variables by using measurement data related to output quantities will be called *stochastic inverse methods*. As can be guessed from this introduction, they make use of uncertainty propagation techniques such as those described in Chapters 3 and 4. Thus a specific part of this report will be devoted to these methods, namely Chapter 5.

3.7 Conclusion

Prescribing the probabilistic model of the input parameters is a key step in probabilistic engineering problems. It may require the use of expert judgment, statistical techniques or combination of both. It is not the aim of this report to address specifically the problem of probabilistic model building in the large. Thus only introductory notions have been recalled in this section.

4 Modelling spatial variability

4.1 Introduction

The mathematical tools presented in the above sections allow the analyst to build a probabilistic model that represents the uncertainty in the input variables of a physical model, *e.g.* geometrical characteristics, material properties, loading, etc. However, in case the physical system is mathematically described by a boundary value problem, this description may be insufficient. Indeed, some input parameters may exhibit spatial variability. The mathematical description of random spatially varying quantities requires the introduction of *random fields*. For computational purposes, the information contained in the random field description has to be reduced, *i.e.* represented (in an approximate manner though) using a finite number of random variables. This procedure is referred to as *random field discretization*. The author devoted quite a large amount of work to this aspect of probabilistic modelling in Sudret and Der Kiureghian (2000), from which selected results are reported in the sequel.

4.2 Basics of random fields

4.2.1 Definition

A scalar random field $H(\mathbf{x}, \omega)$ is a collection of random variables indexed by a continuous parameter $\mathbf{x} \in \mathcal{B}$, where \mathcal{B} is an open set of \mathbb{R}^d describing the geometry of the physical system ($d = 1, 2$ or 3 in practice). This means that for a given $\mathbf{x}_0 \in \mathcal{B}$, $H(\mathbf{x}_0, \omega)$ is a random variable. Conversely, for a given outcome $\omega_0 \in \Omega$, $H(\mathbf{x}, \omega_0)$ is a *realization* of the field. It is assumed to be an element of the Hilbert space $\mathcal{L}^2(\mathcal{B})$ of square integrable functions over \mathcal{B} .

A random field is said *unidimensional* or *multidimensional* according to the dimension d of \mathbf{x} , that is $d = 1$ or $d > 1$. A vector random field is defined when the quantity attached to point \mathbf{x} is a random vector. For the sake of simplicity, we consider only scalar random fields in the sequel.

4.2.2 Gaussian random fields

Gaussian random fields are of practical interest because they are completely described by a mean function $\mu(\mathbf{x})$ and an autocovariance function $C_{HH}(\mathbf{x}, \mathbf{x}')$:

$$C_{HH}(\mathbf{x}, \mathbf{x}') = \text{Cov}[H(\mathbf{x}), H(\mathbf{x}')] \quad (2.56)$$

Alternatively, the correlation structure of the field may be prescribed through the autocorrelation coefficient function $\rho(\mathbf{x}, \mathbf{x}')$ defined as:

$$\rho(\mathbf{x}, \mathbf{x}') = \frac{C_{HH}(\mathbf{x}, \mathbf{x}')}{\sigma(\mathbf{x})\sigma(\mathbf{x}')} \quad (2.57)$$

In this equation the variance function $\sigma^2(\mathbf{x})$ is defined by:

$$\sigma^2(\mathbf{x}) = C_{HH}(\mathbf{x}, \mathbf{x}) \quad (2.58)$$

The most common autocorrelation coefficient functions are reported below in case of unidimensional homogeneous fields (See Figure 2.2):

- Type A:

$$\rho_A(x_1, x_2) = \exp\left(-\frac{|x_1 - x_2|}{\ell_A}\right) \quad (2.59)$$

- Type B:

$$\rho_B(x_1, x_2) = \exp\left(-\left(\frac{x_1 - x_2}{\ell_B}\right)^2\right) \quad (2.60)$$

- Type C:

$$\rho_C(x_1, x_2) = \frac{\sin((x_1 - x_2)/\ell_C)}{(x_1 - x_2)/\ell_C} \quad (2.61)$$

In order to study the influence of the shape of the autocorrelation function, it is desirable to find an equivalence between the dimensional parameters ℓ_A, ℓ_B, ℓ_C . The *scale of fluctuation* proposed by Vanmarcke (1983) is usually used:

$$\vartheta = 2 \int_0^\infty \rho(0, x) dx \quad (2.62)$$

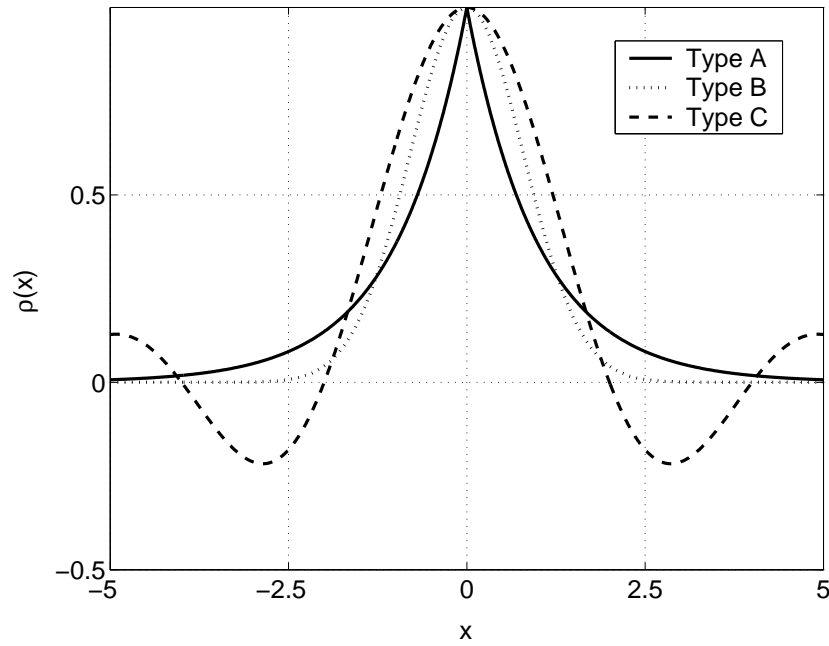


Figure 2.2: Autocorrelation coefficient functions (scale of fluctuation $\vartheta = 2$)

For the three types of autocorrelation coefficient functions given above, the scales of fluctuation read:

$$\begin{aligned} \vartheta_A &= 2 \ell_A \\ \vartheta_B &= \sqrt{\pi} \ell_B \\ \vartheta_C &= \pi \ell_C \end{aligned} \quad (2.63)$$

4.2.3 Principle of random field discretization

Random fields are non numerable infinite sets of correlated random variables, which is computationally intractable. Discretizing the random field $H(\mathbf{x})$ consists in approximating it by $\hat{H}(\mathbf{x})$, which is defined by means of a *finite set* of random variables $\{\chi_i, i = 1, \dots, n\}$, gathered into a random vector denoted by $\boldsymbol{\chi}$:

$$H(\mathbf{x}, \omega) \xrightarrow{\text{Discretization}} \hat{H}(\mathbf{x}, \omega) = \mathcal{G}[\mathbf{x}, \boldsymbol{\chi}(\omega)] \quad (2.64)$$

Several discretization methods have been developed since the 80's to carry out this task. They can be broadly divided into three groups:

- **point discretization methods**, where the random variables $\{\chi_i\}$ are *selected values* $\{H(\mathbf{x}_i), i = 1, \dots, N\}$ at some given points in the domain of discretization \mathcal{B} . In practice, a mesh of \mathcal{B} is first constructed. The *midpoint method* (Der Kiureghian and Ke, 1988) consists in associating a random variable to the centroid of each element of the mesh and representing the field in each point of the element by this very random variable. The *shape function method* (Liu et al., 1986a,b) interpolates the random variables associated to the nodes of the mesh using standard shape functions of the finite element method. The *optimal linear estimation* method (OLE), which is described below, makes use of “optimal” shape functions based on the autocorrelation function of the field.
- **average discretization methods**, where $\{\chi_i\}$ are *weighted integrals* of $H(\cdot)$ over a domain \mathcal{B}_i :

$$\chi_i = \int_{\mathcal{B}_i} H(\mathbf{x}) w(\mathbf{x}) d\mathbf{x} \quad (2.65)$$

These methods include the *spatial average* approach (Vanmarcke and Grigoriu, 1983; Vanmarcke, 1983) and, in a specific context, the *weighted integral* method (Deodatis, 1990, 1991; Deodatis and Shinozuka, 1991; Takada, 1990a,b).

- **series expansion methods**, where the field is exactly represented as a series involving random variables and deterministic spatial functions. The approximation is then obtained by a *truncation* of the series. The *Karhunen-Loève Expansion* (KL) (Loève, 1978; Ghanem and Spanos, 1991a), the *Expansion Optimal Linear Estimation* (EOLE) method (Li and Der Kiureghian, 1993) and the *Orthogonal Series Expansion* (OSE) (Zhang and Ellingwood, 1994) pertain to this category. They will be detailed in the next section.

A comprehensive review and comparison of these methods is presented in Li and Der Kiureghian (1993); Sudret and Der Kiureghian (2000). The early methods pertaining to the two first categories reveal relatively inefficient, in the sense that a large number of random variables is required to achieve a good approximation of the field. Surprisingly, they are still used in many recent papers addressing problems involving spatial variability.

4.3 Series expansion methods

4.3.1 The Karhunen-Loève expansion

Let us consider a random field $H(\mathbf{x}, \omega)$ whose mean value $\mu(\mathbf{x})$ and autocovariance function $C_{HH}(\mathbf{x}, \mathbf{x}') = \sigma(\mathbf{x})\sigma(\mathbf{x}')\rho(\mathbf{x}, \mathbf{x}')$ are prescribed. The Karhunen-Loève expansion of $H(\mathbf{x})$ reads:

$$H(\mathbf{x}, \omega) = \mu(\mathbf{x}) + \sum_{i=1}^{\infty} \sqrt{\lambda_i} \xi_i(\omega) \varphi_i(\mathbf{x}) \quad (2.66)$$

where $\{\xi_i, i \in \mathbb{N}^*\}$ are zero-mean orthogonal variables and $\{\lambda_i, \varphi_i(\mathbf{x})\}$ are solutions of the eigenvalue problem:

$$\int_{\mathcal{B}} C_{HH}(\mathbf{x}, \mathbf{x}') \varphi_i(\mathbf{x}') d\mathbf{x}' = \lambda_i \varphi_i(\mathbf{x}) \quad (2.67)$$

Eq.(2.67) is a Fredholm integral equation of second kind. The *kernel* $C_{HH}(\cdot, \cdot)$ being an autocovariance function, it is bounded, symmetric and positive definite. Thus the set of eigenfunctions $\{\varphi_i, i \in \mathbb{N}^*\}$ forms a *complete orthogonal basis*. The set of eigenvalues (spectrum) is moreover real, positive and numerable. The Karhunen-Loève expansion possesses other interesting properties (Ghanem and Spanos, 1991a):

- It is possible to order the eigenvalues λ_i in a descending series converging to zero. Truncating the ordered series (2.66) after the M -th term gives the KL approximated field:

$$\hat{H}(\mathbf{x}, \omega) = \mu(\mathbf{x}) + \sum_{i=1}^M \sqrt{\lambda_i} \xi_i(\omega) \varphi_i(\mathbf{x}) \quad (2.68)$$

- The covariance eigenfunction basis $\{\varphi_i(\mathbf{x})\}$ is optimal in the sense that the mean square error (integrated over \mathcal{B}) resulting from a truncation after the M -th term is minimized (with respect to the value it would take when any other basis is chosen).
- When the random field under consideration is Gaussian, the set of $\{\xi_i\}$ are *independent* standard normal variables. Furthermore, it can be shown that the Karhunen-Loève expansion of Gaussian fields is almost surely convergent (Loève, 1978). For non Gaussian fields, the KL expansion also exists, however the random variables appearing in the series are of unknown PDF and may not be independent (Phoon et al., 2002b, 2005; Li et al., 2007).
- From Eq.(2.68), the error variance obtained when truncating the expansion after M terms turns out to be, after basic algebra:

$$\text{Var} \left[H(\mathbf{x}) - \hat{H}(\mathbf{x}) \right] = \sigma^2(\mathbf{x}) - \sum_{i=1}^M \lambda_i \varphi_i^2(\mathbf{x}) = \text{Var} [H(\mathbf{x})] - \text{Var} \left[\hat{H}(\mathbf{x}) \right] \geq 0 \quad (2.69)$$

The righthand side of the above equation is always positive because it is the variance of some quantity. This means that the Karhunen-Loève expansion always *under-represents* the true variance of the field. The accuracy of the truncated expansion has been investigated in details in Huang et al. (2001).

Eq.(2.67) can be solved analytically only for few autocovariance functions and geometries of \mathcal{B} . Detailed closed form solutions for triangular and exponential covariance functions for one-dimensional homogeneous fields can be found in Ghanem and Spanos (1991a). Otherwise, a numerical solution to the eigenvalue problem (2.67) can be obtained (same reference, chap. 2). Wavelet techniques have been recently applied for this purpose in Phoon et al. (2002a), leading to a fairly efficient approximation scheme.

4.3.2 The orthogonal series expansion

The *orthogonal series expansion method* (OSE) was proposed by Zhang and Ellingwood (1994). Let $\{h_i(\mathbf{x})\}_{i=1}^{\infty}$ be a Hilbertian basis of $\mathcal{L}^2(\mathcal{B})$, *i.e.* a set of orthonormal functions, satisfying:

$$\int_{\mathcal{B}} h_i(\mathbf{x}) h_j(\mathbf{x}) d\mathbf{x} = \delta_{ij} \quad (\text{Kronecker symbol}) \quad (2.70)$$

Let $H(\mathbf{x}, \omega)$ be a random field with prescribed mean value function $\mu(\mathbf{x})$ and autocovariance function $C_{HH}(\mathbf{x}, \mathbf{x}')$. Any realization of the field is a function of $\mathcal{L}^2(\mathcal{B})$, which can be expanded by means of the orthogonal functions $\{h_i(\mathbf{x})\}_{i=1}^{\infty}$. Considering now all possible outcomes of the field, the coefficients in the expansion become random variables. Thus the following expansion holds:

$$H(\mathbf{x}, \omega) = \mu(\mathbf{x}) + \sum_{i=1}^{\infty} \chi_i(\omega) h_i(\mathbf{x}) \quad (2.71)$$

Using the orthogonality properties of the basis functions, it can be shown after some basic algebra that:

$$\chi_i(\omega) = \int_{\mathcal{B}} [H(\mathbf{x}, \omega) - \mu(\mathbf{x})] h_i(\mathbf{x}) d\mathbf{x} \quad (2.72)$$

$$(\boldsymbol{\Sigma}_{\chi\chi})_{kl} \equiv \text{E}[\chi_k \chi_l] = \int_{\mathcal{B}} \int_{\mathcal{B}} C_{HH}(\mathbf{x}, \mathbf{x}') h_k(\mathbf{x}) h_l(\mathbf{x}') d\mathbf{x} d\mathbf{x}' \quad (2.73)$$

If $H(\mathbf{x})$ is Gaussian, Eq.(2.72) proves that $\{\chi_i\}_{i=1}^{\infty}$ are zero-mean Gaussian random variables, possibly *correlated*. After selecting a finite set of functions of size M , it is possible to transform them into an uncorrelated standard normal vector $\boldsymbol{\Xi}$ by performing a spectral decomposition of the covariance matrix $\boldsymbol{\Sigma}_{\chi\chi}$:

$$\boldsymbol{\Sigma}_{\chi\chi} \cdot \boldsymbol{\Phi} = \boldsymbol{\Phi} \cdot \boldsymbol{\Lambda} \quad (2.74)$$

where $\mathbf{\Lambda}$ is the diagonal matrix containing the eigenvalues λ_i of $\mathbf{\Sigma}_{\chi\chi}$ and $\mathbf{\Phi}$ is a matrix whose columns are the corresponding eigenvectors. Random vector χ is related to Ξ by:

$$\chi = \mathbf{\Phi} \cdot \mathbf{\Lambda}^{1/2} \cdot \Xi \quad (2.75)$$

After some basic algebra, one gets:

$$\hat{H}(\mathbf{x}, \omega) = \mu(\mathbf{x}) + \sum_{k=1}^M \sqrt{\lambda_k} \xi_k(\omega) \varphi_k(\mathbf{x}) \quad (2.76)$$

The above equation is an approximate Karhunen-Loève expansion of the random field $H(\cdot)$, as seen by comparing with Eq.(2.66). As pointed out by Zhang and Ellingwood (1994), the OSE using a complete set of orthogonal functions $\{h_i(\mathbf{x})\}_{i=1}^{\infty}$ is strictly equivalent to the Karhunen-Loève expansion in case the eigenfunctions $\varphi_k(\mathbf{x})$ of the autocovariance function C_{HH} are approximated by using the same set of orthogonal functions $\{h_i(\mathbf{x})\}_{i=1}^{\infty}$.

4.3.3 The OLE/EOLE methods

The *expansion optimal linear estimation* method (EOLE) was proposed by Li and Der Kiureghian (1993). It is inspired by the *kriging method* (Matheron, 1962, 1967). It is a special case of the method of *regression on linear functionals*, see Ditlevsen (1996). It is based on the pointwise regression of the original random field with respect to selected values of the field, and a compaction of the data by spectral analysis.

Let us consider a Gaussian random field as defined above and a grid of points $\{\mathbf{x}_i \in \mathcal{B}, i = 1, \dots, N\}$. Let us denote by χ the random vector $\{H(\mathbf{x}_1), \dots, H(\mathbf{x}_N)\}^T$. By construction, χ is a Gaussian vector whose mean value μ_χ and covariance matrix $\mathbf{\Sigma}_{\chi\chi}$ read:

$$\mu_\chi^i = \mu(\mathbf{x}_i) \quad (2.77)$$

$$(\mathbf{\Sigma}_{\chi\chi})_{i,j} = \text{Cov}[H(\mathbf{x}_i), H(\mathbf{x}_j)] = \sigma(\mathbf{x}_i) \sigma(\mathbf{x}_j) \rho(\mathbf{x}_i, \mathbf{x}_j) \quad (2.78)$$

The *optimal linear estimation* (OLE) of random variable $H(\mathbf{x})$ onto the random vector χ reads:

$$H(\mathbf{x}) \approx \mu(\mathbf{x}) + \mathbf{\Sigma}_{H\chi}^T(\mathbf{x}) \cdot \mathbf{\Sigma}_{\chi\chi}^{-1} \cdot (\chi - \mu_\chi) \quad (2.79)$$

where $\mathbf{\Sigma}_{H\chi}(\mathbf{x})$ is a vector whose components are given by:

$$\mathbf{\Sigma}_{H\chi}^j(\mathbf{x}) = \text{Cov}[H(\mathbf{x}), \chi_j] = \text{Cov}[H(\mathbf{x}), H(\mathbf{x}_j)] \quad (2.80)$$

Let us now consider the spectral decomposition of the covariance matrix $\mathbf{\Sigma}_{\chi\chi}$:

$$\mathbf{\Sigma}_{\chi\chi} \phi_i = \lambda_i \phi_i \quad i = 1, \dots, N \quad (2.81)$$

This allows to transform linearly the original vector χ :

$$\chi = \mu_\chi + \sum_{i=1}^N \sqrt{\lambda_i} \xi_i(\omega) \phi_i \quad (2.82)$$

where $\{\xi_i, i = 1, \dots, N\}$ are *independent* standard normal variables. Substituting for (2.82) in (2.79) and using (2.81) yields the EOLE representation of the field:

$$\hat{H}(\mathbf{x}, \omega) = \mu(\mathbf{x}) + \sum_{i=1}^N \frac{\xi_i(\omega)}{\sqrt{\lambda_i}} \phi_i^T \mathbf{\Sigma}_{H(\mathbf{x})\chi} \quad (2.83)$$

As in the Karhunen-Loève expansion, the series may be further truncated after $r \leq N$ terms, the eigenvalues λ_i being sorted first in descending order. The variance of the error for EOLE is:

$$\text{Var}[H(\mathbf{x}) - \hat{H}(\mathbf{x})] = \sigma^2(\mathbf{x}) - \sum_{i=1}^r \frac{1}{\lambda_i} \left(\phi_i^T \mathbf{\Sigma}_{H(\mathbf{x})\chi} \right)^2 \quad (2.84)$$

As in the KL expansion, the second term in the above equation is identical to the variance of $\hat{H}(\mathbf{x})$. Thus EOLE also always *under-represents* the true variance. Due to the form of (2.84), the error monotonically decreases with r , the minimal error being obtained when no truncation is made ($r = N$). This allows one to define automatically the cut-off value r for a given tolerance in the variance error.

4.3.4 Examples and recommendations

The various series expansion techniques have been thoroughly compared in Sudret and Der Kiureghian (2000). As an example, consider a univariate unidimensional standard Gaussian field defined over $\mathcal{B} = [0, 10]$ with an autocorrelation coefficient function of type A ($\ell_A = 5$). The pointwise variance errors obtained for the various techniques and various orders of expansion are plotted in Figure 2.3. It is observed as expected that the KL expansion is always the most accurate approach, whereas EOLE is slightly better than OSE.

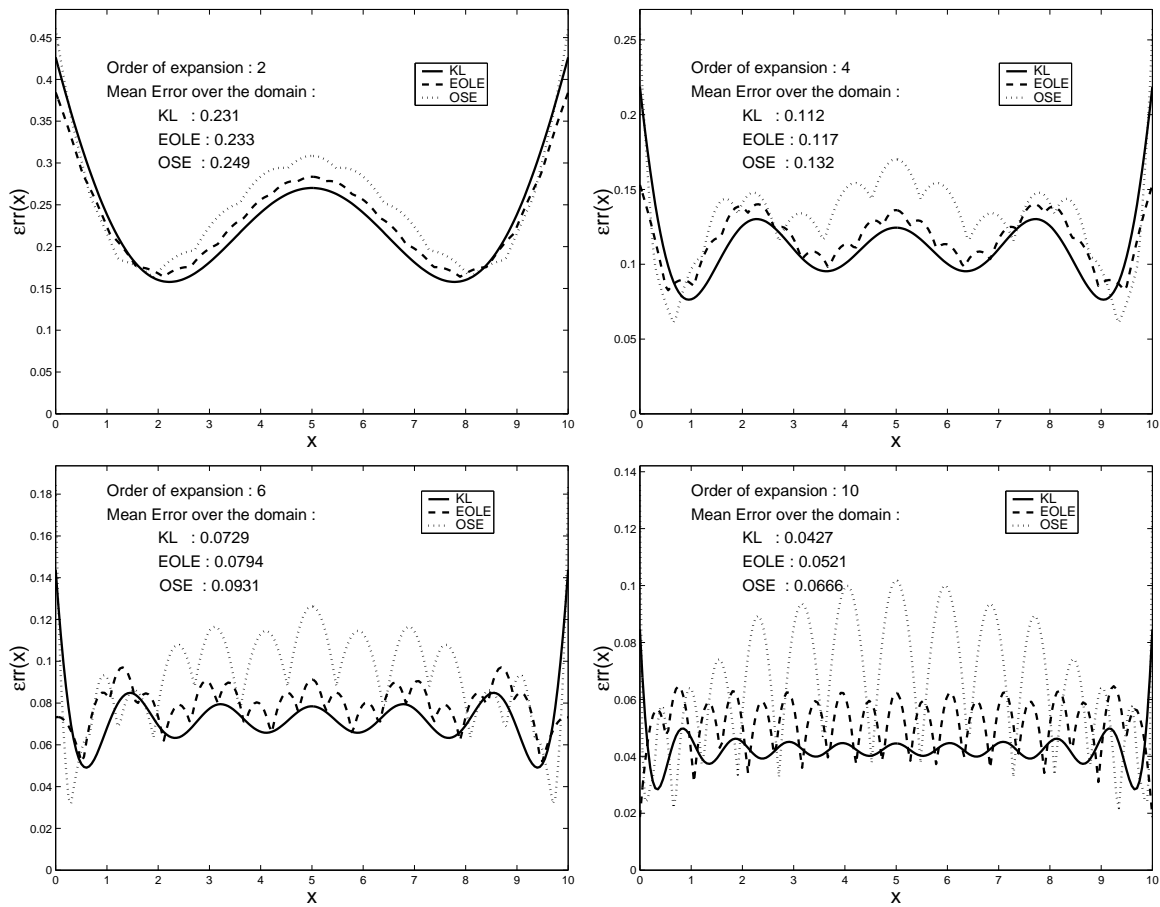


Figure 2.3: Point-wise estimate of the variance error for various discretization schemes and different orders of expansion (standard Gaussian field with autocorrelation coefficient functions of type A (Eq.(2.59)), $\ell_A = 5$)

It is also interesting to compare the expansions or random fields only differing from each other by the shape of their autocorrelation coefficient function. Let us consider a unidimensional standard Gaussian field defined over $\mathcal{B} = [0, 10]$, whose scale of fluctuation is $\vartheta = 2$ and whose autocorrelation coefficient function is either of type A, B or C (see Eqs.(2.59)-(2.61)). The EOLE method is applied using $N = 81$ points (regular grid with stepsize equal to $10/80 = 0.125$ and a number $r = 16$ terms is retained in the EOLE

expansion. Figure 2.4 presents the evolution of the variance error (Eq.(2.84)) as a function of $x \in [0, 10]$ for the three autocorrelation coefficient functions.

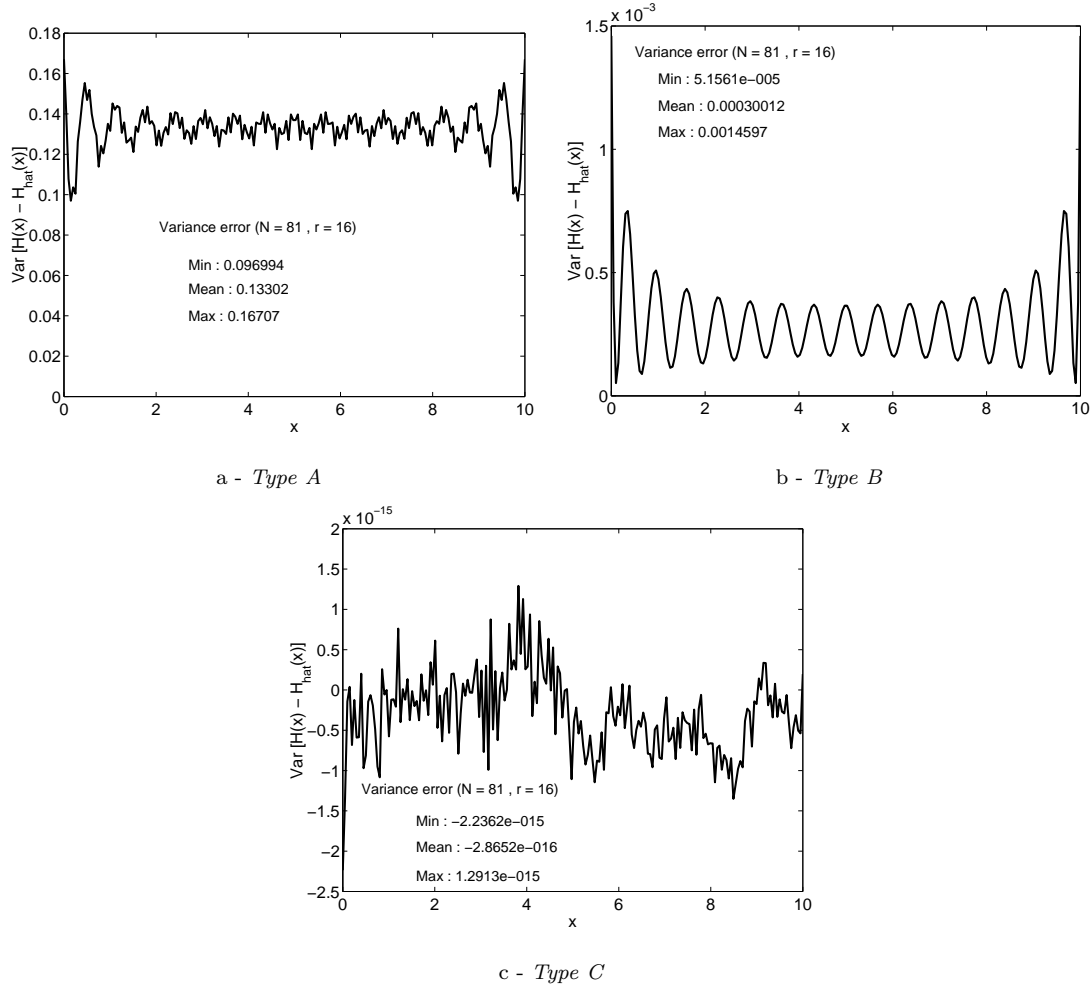


Figure 2.4: Variance of the error of discretization for various autocorrelation coefficient functions ($x \in [0, 10]$, $\vartheta = 2$, $N = 81$, $r = 16$)

It appears that the discretization scheme is not accurate enough for the type A correlation structure (maximal error of 16.7%), accurate enough for the type B (maximal error of 0.1%) and almost exact for the type C (maximal error of $10^{-13}\%$; the negative values in Figure 2.4-c are due to rounding errors). This is a general conclusion for such types of correlation structures: type A requires a large number of terms since the associated field is non differentiable, whereas type B requires few terms and type C even less. Recommendations for an optimal use of EOLE have been proposed in Sudret and Der Kiureghian (2000, Chap. 2).

As a consequence, one could expect that Type A Gaussian random fields would be avoided in practical applications due to their lack of smoothness. Surprisingly the exact opposite is observed in the literature: type A random fields are used in most (if not all) applications in stochastic finite element analysis (see Chapter 4) since there exists an analytical solution to their Karhunen-Loève expansion. This point should receive further attention in the future.

Furthermore, it would be of great interest to use methods such as OSE or EOLE in conjunction with other types of correlation functions, especially in the context of stochastic finite element analysis when the input parameters of interest smoothly vary in space.

4.4 Non Gaussian fields

The discretization of *non Gaussian fields* has been addressed by Li and Der Kiureghian (1993) in case they are defined as a non-linear transformation (also called *translation*) of a Gaussian field:

$$H_{\text{NG}}(\cdot) = \mathcal{NL}(H(\cdot)) \quad (2.85)$$

The discretized field is then simply obtained by:

$$\hat{H}_{\text{NG}}(\cdot) = \mathcal{NL}(\hat{H}(\cdot)) \quad (2.86)$$

Advanced methods for discretizing non Gaussian (and possibly non translation) fields have been recently proposed by Grigoriu (1998); Deodatis and Micaletti (2001); Phoon et al. (2002b, 2005); Li et al. (2007). They are beyond the scope of this report.

4.5 Conclusion

The modelling of the spatial variability of input parameters requires the introduction of random fields. For computational purpose, these random fields must be discretized, *i.e.* approximated by a finite set of random variables. Various discretization techniques have been reported and discussed. Note that discretization can be often dealt with independently from the uncertainty propagation to come. Therefore, without any loss of generality, it will be supposed in the sequel that the input random vector contains both the “physical” random variables and the basic variables used in the discretization of the input random fields, if any.

5 Conclusion

Once the mathematical model of the physical system under consideration has been set up (Step A in the general framework), a probabilistic model for the uncertain input parameters is to be built (Step B). After recalling the basics of probability theory, this chapter has briefly reviewed methods for building such a model, depending on the type and amount of available data, namely expert judgment and classical or Bayesian statistics. The particular issue of modelling spatially varying input quantities by random fields has been finally addressed. The next chapter now presents elementary methods for uncertainty propagation and sensitivity analysis (Steps C and C’).

Chapter 3

Classical methods for uncertainty propagation and sensitivity analysis

1 Introduction

As described in the introduction chapter, methods for propagating the uncertainty in the input parameters through a model may be classified according to the type of information that is investigated with respect to the (random) model output.

Suppose the response of a system is modelled by a mathematical function $\mathcal{M} : \mathbb{R}^M \mapsto \mathbb{R}$ that can be analytical or algorithmic (*e.g.* a computer code such as a finite element code), and \mathbf{x} is the vector of input parameters¹. The uncertainties in the input parameters are modelled by a random vector \mathbf{X} . Accordingly, the response becomes a random variable:

$$Y = \mathcal{M}(\mathbf{X}) \tag{3.1}$$

The full probabilistic content of the response Y is contained in its probability density function $f_Y(y)$, which depends on the probability density function of the input parameters $f_{\mathbf{X}}(\mathbf{x})$ and the model function \mathcal{M} . However, this quantity is not available analytically except in trivial cases.

The author proposed the following classification of methods for uncertainty propagation in Sudret and Der Kiureghian (2000):

- When the mean value μ_Y and standard deviation σ_Y of the response are of interest, *second moment analysis* methods are to be used. Methods such as the *perturbation method*, the *weighted integral method* or the *quadrature method* enter this category. They provide a first estimate on the response variability, which is limited to the first two statistical moments of the response.
- When the tail of the response PDF $f_Y(y)$ is of interest (*i.e.* the low quantiles), the problem may be recast as that of computing a probability of failure, where “failure” is defined in a broad sense as the event “ Y is exceeding a prescribed threshold”. Methods of *structural reliability analysis* such as FORM/SORM, importance sampling or directional simulation may be used in this case.
- When the whole PDF $f_Y(y)$ is of interest, methods of approximation thereof have to be considered. *Monte Carlo simulation* (MCS) is the basic approach to solve the problem. Note that this third

¹For the sake of simplicity in the notation, a scalar-valued model is considered. However the results presented in the sequel equally apply for vector-valued models.

category indirectly encompasses the two first kinds of problems, since the (possibly approximate) knowledge of $f_Y(y)$ may be post-processed in order to get statistical moments and quantiles. A new class of so-called *spectral methods* based on the expansion of the response quantity Y onto a suitable basis have emerged in the last fifteen years. They will be addressed in Chapter 4.

In this chapter, well-established methods used to solve the various kinds of problems are reviewed. Methods for second moment (resp. structural reliability) analysis will be detailed in Section 2 (resp. Section 3). They include in particular Monte Carlo simulation that may be applied indeed to solve each of the three kinds of problems described above. MCS is based on the simulation of pseudo-random numbers. Should the reader not be familiar with this technique, he or she can refer to Appendix A.

Global sensitivity analysis is another interesting aspect of probabilistic mechanics studies. Here, it is understood as the hierarchization of the input parameters of the model with respect to some output quantities. Second-moment and reliability analysis provide as a byproduct the so-called *importance factors* that allow such a hierarchization. They are introduced together with more advance sensitivity methods in Section 4.

2 Methods for second moment analysis

2.1 Introduction

In this section, methods for computing the mean value and standard deviation of a response quantity $Y = \mathcal{M}(\mathbf{X})$ are addressed. The specific use of Monte Carlo simulation (MCS) in this context is first presented. Confidence intervals on the results are derived. Then the perturbation method and the quadrature method are presented, together with applications in finite element analysis.

2.2 Monte Carlo simulation

Monte Carlo simulation can be used in order to estimate the mean value μ_Y and standard deviation σ_Y of a response quantity $Y = \mathcal{M}(\mathbf{X})$. Assume that a sample set of n input vectors has been generated, say $\{\mathbf{x}^{(1)}, \dots, \mathbf{x}^{(n)}\}$. The usual estimators of those quantities respectively read:

$$\hat{\mu}_Y = \frac{1}{n} \sum_{k=1}^n \mathcal{M}(\mathbf{x}^{(k)}) \quad (3.2)$$

$$\hat{\sigma}_Y^2 = \frac{1}{n-1} \sum_{k=1}^n \left(\mathcal{M}(\mathbf{x}^{(k)}) - \hat{\mu}_Y \right)^2 \quad (3.3)$$

The statistics computed on sample sets are random quantities in nature. In probabilistic engineering mechanics, it is common practice to run a single Monte Carlo simulation (possibly using a large size sample set), *i.e.* to provide a single realization of the estimator. A rigorous use of Monte Carlo simulation should provide confidence intervals on the results though. Suppose that the sample size n is fixed by the analyst. The estimator in Eq.(3.2) is asymptotically Gaussian due to the central limit theorem. Thus the $(1 - \alpha)$ confidence interval on μ_Y reads, provided n is sufficiently large:

$$\hat{\mu}_Y - u_{\alpha/2} \hat{\sigma}_Y / \sqrt{n-1} \leq \mu \leq \hat{\mu}_Y + u_{\alpha/2} \hat{\sigma}_Y / \sqrt{n-1} \quad (3.4)$$

where $u_{\alpha/2} = -\Phi^{-1}(1 - \alpha/2)$. Alternatively, the latter equation may be used together with a criterion on the width of the confidence interval. Suppose that the mean value is to be computed with a relative accuracy of $\pm \varepsilon_{\mu_Y}$ with $(1 - \alpha)$ confidence. Then the minimal sample size n_{min} is:

$$n_{min} = 1 + \text{ceil} \left[\left(u_{\alpha/2} \hat{C}V_Y / \varepsilon_{\mu_Y} \right)^2 \right] \quad (3.5)$$

where $\text{ceil}[x]$ rounds x upwards to the nearest integer and $\hat{C}V_Y = \hat{\sigma}_Y/\hat{\mu}_Y$ is the estimated coefficient of variation of Y . This minimal number of samples n_{min} is inversely proportional to the square of the relative accuracy ε_{μ_Y} and proportional to the square of $\hat{C}V_Y$.

Remarks

- Similar confidence intervals can be derived for the variance of the response (Saporta, 2006, Chap. 13).
- Monte Carlo simulation can also be used to compute higher order moments. However, the simulation does not converge as fast as for the mean and standard deviation, since the variance of the related estimators of higher moments is generally large.
- The application of Monte Carlo simulation to vector output models (*i.e.* $\mathbf{Y} = \mathcal{M}(\mathbf{X})$) is straightforward, since the estimators Eqs.(3.2)-(3.3) may be evaluated component by component.

2.3 Perturbation method

The perturbation method is based on the Taylor series expansion of the model response around the mean value of the input parameters. Its application in structural mechanics dates back to the early 80's (Handa and Andersson, 1981; Hisada and Nakagiri, 1981, 1985).

The basic formalism is first developed for a scalar response quantity. The application of the perturbation method in the context of finite element analysis is then presented.

2.3.1 Taylor series expansion of the model

The Taylor series expansion of the model $\mathcal{M}(\mathbf{x})$ around a prescribed value \mathbf{x}_0 reads:

$$\begin{aligned} \mathcal{M}(\mathbf{x}) = & \mathcal{M}(\mathbf{x}_0) + \sum_{i=1}^M \left. \frac{\partial \mathcal{M}}{\partial x_i} \right|_{\mathbf{x}=\mathbf{x}_0} (x_i - x_{0,i}) \\ & + \frac{1}{2} \sum_{i=1}^M \sum_{j=1}^M \left. \frac{\partial^2 \mathcal{M}}{\partial x_i \partial x_j} \right|_{\mathbf{x}=\mathbf{x}_0} (x_i - x_{0,i})(x_j - x_{0,j}) + o(\|\mathbf{x} - \mathbf{x}_0\|^2) \end{aligned} \quad (3.6)$$

In this expression, x_i (resp. $x_{0,i}$) denotes the i -th coordinate of vector \mathbf{x} (resp. \mathbf{x}_0) and $o(\cdot)$ means "negligible with respect to (\cdot) ".

Let us suppose now that the input is a random vector \mathbf{X} and that the expansion is carried out around its mean value $\mu_{\mathbf{X}} = \{\mu_{X_1}, \dots, \mu_{X_M}\}^T$. Due to linearity of the operator, the expectation of the response $Y = \mathcal{M}(\mathbf{X})$ reads:

$$\begin{aligned} \mathbb{E}[Y] = \mathbb{E}[\mathcal{M}(\mathbf{X})] \approx & \mathcal{M}(\mu_{\mathbf{X}}) + \sum_{i=1}^M \left. \frac{\partial \mathcal{M}}{\partial x_i} \right|_{\mathbf{x}=\mu_{\mathbf{X}}} \mathbb{E}[(X_i - \mu_{X_i})] \\ & + \frac{1}{2} \sum_{i=1}^M \sum_{j=1}^M \left. \frac{\partial^2 \mathcal{M}}{\partial x_i \partial x_j} \right|_{\mathbf{x}=\mu_{\mathbf{X}}} \mathbb{E}[(X_i - \mu_{X_i})(X_j - \mu_{X_j})] \end{aligned} \quad (3.7)$$

By definition, $\mathbb{E}[(\mathbf{X} - \mu_{\mathbf{X}})] = 0$ and $\mathbb{E}[(X_i - \mu_{X_i})(X_j - \mu_{X_j})] = \mathbf{C}_{ij}$ is the generic term of the covariance matrix of \mathbf{X} . Thus the approximation of the mean value:

$$\mathbb{E}[Y] \approx \mathcal{M}(\mu_{\mathbf{X}}) + \frac{1}{2} \sum_{i=1}^M \sum_{j=1}^M \mathbf{C}_{ij} \left. \frac{\partial^2 \mathcal{M}}{\partial x_i \partial x_j} \right|_{\mathbf{x}=\mu_{\mathbf{X}}} \quad (3.8)$$

In Eq.(3.8), the first term in the righthand side, namely $\mathcal{M}(\mu_{\mathbf{X}})$, is the first order approximation of $E[Y]$: it is obtained as the output of the model evaluated at the mean value of the input parameters. It is worth emphasizing that this result is exact if and only if the model \mathcal{M} is an affine function of the input parameters. Moreover, the second order correction term is depending on the covariance matrix \mathbf{C} and the Hessian matrix of the model computed at the mean value point.

The particular case of independent input parameters is worth to be mentioned. The covariance matrix \mathbf{C} is diagonal in this case and contains the variance of each input parameter, say $\sigma_{X_i}^2$. Eq.(3.7) reduces in this case to:

$$E[Y] \approx \mathcal{M}(\mu_{\mathbf{X}}) + \frac{1}{2} \sum_{i=1}^M \frac{\partial^2 \mathcal{M}}{\partial x_i^2} \Big|_{\mathbf{x}=\mu_{\mathbf{X}}} \sigma_{X_i}^2 \quad (3.9)$$

2.3.2 Estimation of the variance of the response

From Eq.(3.8), the variance of the response may be computed as follows:

$$\text{Var}[Y] = E[(Y - E[Y])^2] \approx E[(Y - \mathcal{M}(\mu_{\mathbf{X}}))^2] \quad (3.10)$$

From the first order expansion in Eq.(3.6) carried out at the mean value $\mu_{\mathbf{X}}$, the latter equation simplifies into:

$$\text{Var}[Y] \approx E \left[\left(\sum_{i=1}^M \frac{\partial \mathcal{M}}{\partial x_i} \Big|_{\mathbf{x}=\mu_{\mathbf{X}}} (X_i - \mu_{X_i}) \right)^2 \right] \quad (3.11)$$

Thus the first order expansion of the variance of the response:

$$\text{Var}[Y] \approx \sum_{i=1}^M \sum_{j=1}^M \mathbf{C}_{ij} \frac{\partial \mathcal{M}}{\partial x_i} \Big|_{\mathbf{x}=\mu_{\mathbf{X}}} \frac{\partial \mathcal{M}}{\partial x_j} \Big|_{\mathbf{x}=\mu_{\mathbf{X}}} \quad (3.12)$$

In case of independent input variables, Eq.(3.12) further simplifies into:

$$\text{Var}[Y] \approx \sum_{i=1}^M \left(\frac{\partial \mathcal{M}}{\partial x_i} \Big|_{\mathbf{x}=\mu_{\mathbf{X}}} \right)^2 \sigma_{X_i}^2 \quad (3.13)$$

The above result has the following interpretation: the variance of the response is the sum of contributions of each input parameter, each contribution being a mix of the variance of this input parameter and of the (deterministic) gradient of the response with respect to this parameter. This decomposition will allow to derive sensitivity measures, as shown in Section 4.

2.3.3 Perturbation method in finite element analysis

The above framework for second moment analysis has been applied to finite element models since the mid 80's by Handa and Andersson (1981) and Hisada and Nakagiri (1981, 1985) in structural mechanics, Baecher and Ingra (1981) and Phoon et al. (1990) for geotechnical problems, and Liu et al. (1986a,b) for non-linear dynamic problems, see also Kleiber and Hien (1992). Recent developments may be found in Kamiński and Hien (1999); Kamiński (2001). The review in Sudret and Der Kiureghian (2000, Chap. 3) is now summarized.

For linear elastic problems, the discretized balance equation reads:

$$\mathbf{K} \cdot \mathbf{U} = \mathbf{F} \quad (3.14)$$

where \mathbf{K} is the stiffness matrix, \mathbf{F} is the load vector and \mathbf{U} is the (unknown) vector of nodal displacements. The Taylor series expansions of the terms appearing in (3.14) around their mean values read, using the notation $\mathbf{X} = \mu_{\mathbf{X}} + \boldsymbol{\alpha}$:

$$\mathbf{K} = \mathbf{K}_o + \sum_{i=1}^M \mathbf{K}_i^I \alpha_i + \frac{1}{2} \sum_{i=1}^M \sum_{j=1}^M \mathbf{K}_{ij}^{II} \alpha_i \alpha_j + o(\|\boldsymbol{\alpha}\|^2) \quad (3.15)$$

$$\mathbf{U} = \mathbf{U}^o + \sum_{i=1}^M \mathbf{U}_i^I \alpha_i + \frac{1}{2} \sum_{i=1}^M \sum_{j=1}^M \mathbf{U}_{ij}^{II} \alpha_i \alpha_j + o(\|\boldsymbol{\alpha}\|^2) \quad (3.16)$$

$$\mathbf{F} = \mathbf{F}_o + \sum_{i=1}^M \mathbf{F}_i^I \alpha_i + \frac{1}{2} \sum_{i=1}^M \sum_{j=1}^M \mathbf{F}_{ij}^{II} \alpha_i \alpha_j + o(\|\boldsymbol{\alpha}\|^2) \quad (3.17)$$

The first (resp. second) order coefficients $(\cdot)_i^I$ (resp. $(\cdot)_{ij}^{II}$) are obtained from the first and second order derivatives of the corresponding quantities evaluated at $\boldsymbol{\alpha} = 0$, *e.g.*:

$$\mathbf{K}_i^I = \left. \frac{\partial \mathbf{K}}{\partial \alpha_i} \right|_{\boldsymbol{\alpha}=0} \quad (3.18)$$

$$\mathbf{K}_{ij}^{II} = \left. \frac{\partial^2 \mathbf{K}}{\partial \alpha_i \partial \alpha_j} \right|_{\boldsymbol{\alpha}=0} \quad (3.19)$$

These quantities shall be implemented directly in the finite element code. By substituting for (3.15)-(3.17) in (3.14) and identifying the coefficients of similar order on both sides of the equation, one successively obtains:

$$\mathbf{U}^o = \mathbf{K}_o^{-1} \cdot \mathbf{F}_o \quad (3.20)$$

$$\mathbf{U}_i^I = \mathbf{K}_o^{-1} \cdot \left(\mathbf{F}_i^I - \mathbf{K}_i^I \cdot \mathbf{U}^o \right) \quad (3.21)$$

$$\mathbf{U}_{ij}^{II} = \mathbf{K}_o^{-1} \cdot \left(\mathbf{F}_{ij}^{II} - \mathbf{K}_i^I \cdot \mathbf{U}_j^I - \mathbf{K}_j^I \cdot \mathbf{U}_i^I - \mathbf{K}_{ij}^{II} \cdot \mathbf{U}^o \right) \quad (3.22)$$

From these expressions, the statistics of \mathbf{U} are readily available from those of $\boldsymbol{\alpha}$ (note that, by definition, the mean value of $\boldsymbol{\alpha}$ is zero, and that its covariance matrix is identical to that of \mathbf{X} , namely \mathbf{C}). The second order estimate of the mean value is obtained from (3.16):

$$\mathbb{E}[\mathbf{U}] \approx \mathbf{U}^o + \frac{1}{2} \sum_{i=1}^M \sum_{j=1}^M \mathbf{C}_{ij} \mathbf{U}_{ij}^{II} \quad (3.23)$$

where the first term \mathbf{U}^o is the first-order approximation of the mean. The first order estimate of the covariance matrix reads:

$$\text{Cov}[\mathbf{U}, \mathbf{U}] \approx \sum_{i=1}^M \sum_{j=1}^M \mathbf{U}_i^I \cdot \left(\mathbf{U}_j^I \right)^{\top} \text{Cov}[\alpha_i, \alpha_j] = \sum_{i=1}^M \sum_{j=1}^M \mathbf{C}_{ij} \mathbf{U}_i^I \cdot \left(\mathbf{U}_j^I \right)^{\top} \quad (3.24)$$

Again, in case of independent input parameters, the latter expression simplifies into:

$$\text{Cov}[\mathbf{U}, \mathbf{U}] \approx \sum_{i=1}^M \sigma_{X_i}^2 \mathbf{U}_i^I \cdot \left(\mathbf{U}_i^I \right)^{\top} \quad (3.25)$$

The second-order approximation of the covariance matrix can also be derived. It involves the moments of $\boldsymbol{\alpha}$ up to the fourth order and is therefore more intricate to implement and computationally expensive to evaluate.

2.3.4 Perturbation method in finite element analysis - random field input

The perturbation method has been applied in the context of spatially variable input parameters by various authors, together with various methods for discretizing the fields:

- Using the spatial average (SA) method (see Chapter 2, Section 4.2.3), Baecher and Ingra (1981) obtained the second moment statistics of the settlement of a foundation over an elastic soil mass with random Young's modulus and compared the results with existing one-dimensional analysis.
- Vanmarcke and Grigoriu (1983) obtained the first and second order statistics of the nodal displacements of a cantilever beam.
- Extending the SA formalism to two-dimensional axisymmetric problems, Phoon et al. (1990) obtained the first order statistics of the settlement of a pile embedded in an elastic soil layer with random Young's modulus.
- Using the shape function discretization method (see Chapter 2, Section 4.2.3), Liu et al. (1986a,b) applied the perturbation method to static and dynamic non-linear problems.

In all these applications, the perturbation method yields rather accurate results provided the coefficient of variation of the input is small, say less than 20%. It seems to be the principal drawback of the method. Note that a higher perturbation method has been investigated recently in Kamiński (2007).

The author proposed an original application of the perturbation method together with the use of the EOLE discretization method (Chapter 2, Section 4.3.3) in Sudret (2002). It was shown that in some cases (*e.g.* the Young's modulus of the mechanical model is a random field), the second order terms \mathbf{K}_{ij}^{II} in Eq.(3.15) are simply equal to zero. The results compared well to those obtained by the spectral stochastic finite element method (presented later on in Chapter 4).

2.4 Quadrature method

Coming back to the very definition of the moments of a random variable (Eqs.(2.24),(2.27)), the mean and variance of the model response read:

$$\mu_Y = \text{E}[Y] = \int_{\mathcal{D}_{\mathbf{X}}} \mathcal{M}(\mathbf{x}) f_{\mathbf{X}}(\mathbf{x}) d\mathbf{x} \quad (3.26)$$

$$\sigma_Y^2 = \text{E}[(Y - \mu_Y)^2] = \int_{\mathcal{D}_{\mathbf{X}}} [\mathcal{M}(\mathbf{x}) - \mu_Y]^2 f_{\mathbf{X}}(\mathbf{x}) d\mathbf{x} \quad (3.27)$$

The integrals in the above equations may be evaluated by *quadrature formulae* (Abramowitz and Stegun, 1970). Evaluating an integral by quadrature consists in approximating it by a weighted sum of the integrand at selected points in $\mathcal{D}_{\mathbf{X}}$. The theory of Gaussian quadrature, which is closely related to the theory of orthogonal polynomials, is briefly reviewed in Appendix B for the sake of exhaustiveness.

It is sufficient to recall here the main results: a one-dimensional quadrature formula allows one to approximate a one-dimensional weighted integral I as follows:

$$I \equiv \int_{\mathcal{D}} h(x) w(x) dx \approx \sum_{k=1}^{\nu} \omega_k h(x_k) \quad (3.28)$$

In this expression, h is a square-integrable function with respect to the measure $\mu(dx) = w(x) dx$, ν is the order of the quadrature scheme and $\{(\omega_k, x_k), k = 1, \dots, \nu\}$ are the integration weights and points associated to the weight function $w : \mathcal{D} \rightarrow \mathbb{R}$, respectively.

Suppose now that \mathbf{X} is a random vector with independent components *i.e.* its PDF reads:

$$f_{\mathbf{X}}(\mathbf{x}) = f_{X_1}(x_1) \cdots f_{X_M}(x_M) \quad (3.29)$$

Quadrature formulæ may be derived for each probability measure $P(dx_i) = f_{X_i}(x_i) dx_i$, $i = 1, \dots, M$. Then the expectation of any function of \mathbf{X} can be evaluated using a so-called *tensorized* quadrature scheme :

$$\begin{aligned} \mathbb{E}[h(\mathbf{X})] &= \int_{\mathcal{D}_{\mathbf{X}}} h(\mathbf{x}) f_{\mathbf{X}}(\mathbf{x}) d\mathbf{x} \\ &\approx \sum_{k_1=1}^{\nu_1} \cdots \sum_{k_M=1}^{\nu_M} \omega_{k_1} \cdots \omega_{k_M} h(x_{k_1}, \dots, x_{k_M}) \end{aligned} \quad (3.30)$$

This tensorized quadrature scheme can be straightforwardly applied to compute the mean value (resp. the variance) of the model response by setting $h(\mathbf{x}) \equiv \mathcal{M}(\mathbf{x})$ (resp. $h(\mathbf{x}) = (\mathcal{M}(\mathbf{x}) - \mu_Y)^2$). If the input random vector has dependent components, an isoprobabilistic transform should be first applied, see Appendix A. Applications of the quadrature approach to second moment analysis can be found in Baldeweck (1999).

The main drawback of the tensorized scheme is the so-called *curse of dimensionality*. Suppose indeed a ν -th order scheme is retained for each dimension. Then the nested sum in Eq.(3.30) has ν^M terms, which exponentially increases with respect to M . An approximate strategy based on the selection of the greatest products of weights has been successfully applied in Sudret and Cherradi (2003). However the computational cost is not dramatically reduced.

In the context of spectral methods developed in the next chapter, *sparse* quadrature schemes (also known as Smolyak quadrature) have been introduced to bypass the curse of dimensionality. This technique could be equally applied in the context of second moment analysis. It seems however that no specific work in this direction has been published so far.

2.5 Weighted integral method

This method was developed by Deodatis (1990, 1991), Deodatis and Shinozuka (1991) and also investigated by Takada (1990a,b) in the context of stochastic finite elements. Recent developments can be found in Wall and Deodatis (1994); Graham and Deodatis (1998, 2001). It is basically intended to linear elastic structures. The main idea is to consider the *element stiffness matrices* as basic random quantities. More precisely, using standard finite element notations, the stiffness matrix associated with a given element occupying a volume \mathcal{V}_e reads (Zienkiewicz and Taylor, 2000):

$$\mathbf{k}^e = \int_{\mathcal{V}_e} \mathbf{B}^T \cdot \mathbf{D} \cdot \mathbf{B} d\mathcal{V}_e \quad (3.31)$$

where \mathbf{D} denotes the elasticity matrix, and \mathbf{B} is a matrix that relates the components of strains to the nodal displacements. Consider now the elasticity matrix obtained as a product of a deterministic matrix by a univariate random field (*e.g.* Young's modulus):

$$\mathbf{D}(\mathbf{x}, \omega) = \mathbf{D}_o [1 + H(\mathbf{x}, \omega)] \quad (3.32)$$

where \mathbf{D}_o is the mean value and $H(\mathbf{x}, \omega)$ is a zero-mean process². Thus Eq.(3.31) can be rewritten as:

$$\mathbf{k}^e(\omega) = \mathbf{k}_o^e + \Delta \mathbf{k}^e(\omega) \quad , \quad \Delta \mathbf{k}^e(\omega) = \int_{\mathcal{V}_e} H(\mathbf{x}, \omega) \mathbf{B}^T \cdot \mathbf{D}_o \cdot \mathbf{B} d\mathcal{V}_e \quad (3.33)$$

The elements in matrix \mathbf{B} are obtained by derivation of the element shape functions with respect to the coordinates. Hence they are polynomials in the latter, say (x, y, z) . A given entry of $\Delta \mathbf{k}^e$ is thus obtained after matrix product (3.33) as:

$$\Delta k_{ij}^e(\omega) = \int_{\mathcal{V}_e} P_{ij}(x, y, z) H(\mathbf{x}, \omega) d\mathcal{V}_e \quad (3.34)$$

²For the sake of clarity, the dependency of random variables on outcomes ω is given in this section.

where the coefficients of polynomial P_{ij} are obtained from those of \mathbf{B} and \mathbf{D}_o . Let us write P_{ij} as:

$$P_{ij}(x, y, z) = \sum_{l=1}^{\text{NWI}} a_{ij}^l x^{\alpha_l} y^{\beta_l} z^{\gamma_l} \quad (3.35)$$

where NWI is the number of monomials in P_{ij} , each of them corresponding to a set of exponents $\{\alpha_l, \beta_l, \gamma_l\}$. Substituting for (3.35) in (3.34) and introducing the following *weighted integrals* of random field $H(\cdot)$:

$$\chi_l^e(\omega) = \int_{\mathcal{V}_e} x^{\alpha_l} y^{\beta_l} z^{\gamma_l} H(\mathbf{x}, \omega) d\mathcal{V}_e \quad (3.36)$$

it follows that:

$$\Delta \mathbf{k}_{ij}^e(\omega) = \sum_{l=1}^{\text{NWI}} a_{ij}^l \chi_l^e(\omega) \quad (3.37)$$

Collecting now the coefficients a_{ij}^l in a matrix $\Delta \mathbf{k}_i^e$, the (stochastic) element stiffness matrix can finally be written as:

$$\mathbf{k}^e = \mathbf{k}_o^e + \sum_{l=1}^{\text{NWI}} \Delta \mathbf{k}_l^e \chi_l^e \quad (3.38)$$

By assembling these contributions over the N elements of the system, a global stochastic stiffness matrix involving $\text{NWI} \times N$ random variables is obtained.

The vector of nodal displacements is then given by a first order Taylor expansion with respect to the variables χ_l^e as in Eq.(3.16). Applying the perturbation scheme (Eqs.(3.20)-(3.22)), it is possible to obtain the coefficients $\{\mathbf{U}^0, \mathbf{U}^I\}$ of this expansion and then the second order statistics of the response, which depend on the covariance matrix of the χ_l^e 's. Introducing *variability response functions*, one can bound the variance of each nodal displacement by some quantity that is independent of the correlation structure of the input field, see details in the original papers.

As already observed in Sudret and Der Kiureghian (2000, Chap. 3), the weighted integral method has some limitations. First of all, as pointed out by Matthies et al. (1997), it is actually *mesh-dependent* as it can be seen from Eq.(3.36). If the correlation length of the random field is small compared to the size of integration domain \mathcal{V}_e , the accuracy of the method is questionable. The computation of the bound of the response variance may be delicate to implement. Finally, the weighted integral method and the related variability response functions seems limited to linear elastic problems. It is observed that the method has not received much attention in the recent years.

2.6 Conclusion

In this section, various second moment methods have been reviewed. Some of them are quite general, *i.e.* they can be applied to either analytical or finite element models, possibly including spatial variability represented by random fields.

The quadrature method allows one to compute higher order moments. However, it is in nature limited to problems with few random variables due to the exponential growth of the computation time with the number of input parameters. As a consequence, it is not adapted to problems involving discretized random fields.

The perturbation method appears quite general and may be applied at a low computational cost, especially if the gradients of the model response are available. This is often the case when analytical models are used. This may also be the case for finite element models, when the finite element code itself implement response gradients, *e.g.* eDF's own finite element code Code_Aster (<http://www.code-aster.org>) or OpenSees (<http://opensees.berkeley.edu>). If such gradients are not directly available, their computation may always be carried out by a finite difference scheme, with a loss of accuracy and an increased computational cost though.

3 Methods for reliability analysis

3.1 Introduction

Structural reliability analysis aims at computing the probability of failure of a mechanical system with respect to a prescribed failure criterion by accounting for uncertainties arising in the model description (geometry, material properties) or the environment (loading). It is a general theory whose development started in the early 70's. The research in this field is still quite active. The reader is referred to classical textbooks for a comprehensive presentation (*e.g.* Ditlevsen and Madsen (1996); Melchers (1999); Lemaire (2005) among others). This section summarizes some well-established methods to solve reliability problems. It is intended to facilitate the reading of the following chapters.

3.2 Problem statement

Let us denote by \mathbf{X} the vector of basic random variables. When considering models of mechanical systems, these variables usually describe the randomness in the geometry, material properties and loading. They can also represent model uncertainties. This set also includes the variables used in the discretization of random fields, if any. The model of the system yields a vector of response quantities $\mathbf{Y} = \mathcal{M}(\mathbf{X})$. In a mechanical context, these response quantities are *e.g.* displacements, strain or stress components, or quantities computed from the latter.

The mechanical system is supposed to fail when some requirements of safety or serviceability are not fulfilled. For each failure mode, a failure criterion is set up. It is mathematically represented by a *limit state function* $g(\mathbf{X}, \mathcal{M}(\mathbf{X}), \mathbf{X}')$. As shown in this expression, the limit state function may depend on input parameters, response quantities that are obtained from the model and possibly additional random variables and parameters gathered in \mathbf{X}' . For the sake of simplicity, the sole notation \mathbf{X} is used in the sequel to refer to all random variables involved in the analysis. Let M be the size of \mathbf{X} .

Conventionally, the limit state function g is formulated in such a way that:

- $\mathcal{D}_s = \{\mathbf{x} : g(\mathbf{x}) > 0\}$ is the *safe domain* in the space of parameters;
- $\mathcal{D}_f = \{\mathbf{x} : g(\mathbf{x}) \leq 0\}$ is the *failure domain*.

The set of points $\{\mathbf{x} : g(\mathbf{x}) = 0\}$ defines the *limit state surface*. Denoting by $f_{\mathbf{X}}(\mathbf{x})$ the joint probability density function of random vector \mathbf{X} , the probability of failure of the system is:

$$P_f = \int_{\mathcal{D}_f} f_{\mathbf{X}}(\mathbf{x}) d\mathbf{x} \quad (3.39)$$

In all but academic cases, this integral cannot be computed analytically. Indeed, the failure domain depends on response quantities (*e.g.* displacements, strains, stresses, etc.), which are usually computed by means of computer codes (*e.g.* finite element code). In other words, the failure domain is *implicitly* defined as a function of \mathbf{X} . Thus numerical methods have to be employed.

3.3 Monte Carlo simulation

Monte Carlo simulation is a universal method for evaluating integrals such as in Eq.(3.39). Denoting by $1_{\mathcal{D}_f}(x)$ the indicator function of the failure domain (*i.e.* the function that takes the value 0 in the safe

domain and 1 in the failure domain), Eq.(3.39) rewrites:

$$P_f = \int_{\mathbb{R}^M} 1_{\mathcal{D}_f}(\mathbf{x}) f_{\mathbf{X}}(\mathbf{x}) d\mathbf{x} = \mathbb{E} [1_{\mathcal{D}_f}(x)] \quad (3.40)$$

where $\mathbb{E}[\cdot]$ denotes the mathematical expectation. Practically, Eq.(3.40) can be evaluated by simulating n realizations of the random vector \mathbf{X} , say $\{\mathbf{x}^{(1)}, \dots, \mathbf{x}^{(n)}\}$. For each sample, $g(\mathbf{x}^{(k)})$ is evaluated. An estimate of P_f is given by the empirical mean:

$$P_{f,\text{MCS}} = \frac{1}{n} \sum_{k=1}^n 1_{\mathcal{D}_f}(\mathbf{x}^{(k)}) = \frac{n_{fail}}{n} \quad (3.41)$$

where n_{fail} denotes the number of samples that are in the failure domain. Using a more formal setup, the estimator of the probability of failure is defined by:

$$\hat{P}_{f,\text{MCS}} = \frac{1}{n} \sum_{k=1}^n 1_{\mathcal{D}_f}(\mathbf{X}^k) \quad (3.42)$$

where $\{\mathbf{X}^k, k = 1, \dots, n\}$ are i.i.d random vectors having the same joint PDF as \mathbf{X} . This estimator is unbiased ($\mathbb{E}[\hat{P}_{f,\text{MCS}}] = P_f$) and its variance reads:

$$\text{Var} [\hat{P}_{f,\text{MCS}}] = P_f(1 - P_f)/n \quad (3.43)$$

For common values of the probability of failure ($P_f \ll 1$), the above equation allows one to derive the coefficient of variation of the estimator, namely:

$$CV_{\hat{P}_{f,\text{MCS}}} = \sqrt{\text{Var} [\hat{P}_{f,\text{MCS}}] / P_f} \approx 1/\sqrt{n P_f} \quad (3.44)$$

Suppose that the magnitude of P_f is 10^{-k} and a coefficient of variation of 5% is required in its computation. The above equation shows that a number of samples $n > 4.10^{k+2}$ should be used, which is clearly big when small values of P_f are sought.

As a summary, crude Monte Carlo simulation as described above is theoretically applicable whatever the complexity of the deterministic model. However its computational cost makes it rather impracticable when the computational cost of each run of the model is non negligible and when the probability of failure of interest is small.

3.4 First-order reliability method (FORM)

The First Order Reliability Method has been introduced to get an approximation of the probability of failure at a low cost compared to Monte Carlo simulation, where the cost is measured in terms of the number of evaluations of the limit state function.

The first step consists in recasting the problem in the standard normal space by using an isoprobabilistic transform $\mathbf{X} \mapsto \boldsymbol{\Xi} = T(\mathbf{X})$. Two types of transforms have been mainly used (see Ditlevsen and Madsen (1996, Chap. 7)):

- the Rosenblatt transform (Rosenblatt, 1952) was introduced in the context of structural reliability by Hohenbichler and Rackwitz (1981);
- the Nataf transform (Nataf, 1962) was introduced in this context by Der Kiureghian and Liu (1986); Liu and Der Kiureghian (1986)

Using one of these transforms (that are recalled in Appendix A), Eq.(3.40) rewrites:

$$P_f = \int_{\mathcal{D}_f} f_{\mathbf{X}}(\mathbf{x}) d\mathbf{x} = \int_{\{g(T^{-1}(\boldsymbol{\xi})) \leq 0\}} \varphi_M(\boldsymbol{\xi}) d\boldsymbol{\xi} \quad (3.45)$$

where $\varphi_M(\boldsymbol{\xi})$ is the standard multinormal PDF (see Eq.(2.46)). This PDF is maximal at the origin and decreases exponentially with $\|\boldsymbol{\xi}\|^2$. Thus the points that contribute at most to the integral in Eq.(3.45) are those of the failure domain that are closest to the origin of the space.

Thus the second step in FORM consists in determining the so-called design point, *i.e.* the point of the failure domain closest to the origin in the standard normal space. This point P^* is obtained by solving an optimization problem:

$$P^* = \boldsymbol{\xi}^* \equiv \arg \min_{\boldsymbol{\xi} \in \mathbb{R}^M} \left\{ \|\boldsymbol{\xi}\|^2 : g(T^{-1}(\boldsymbol{\xi})) \leq 0 \right\} \quad (3.46)$$

Several algorithms are available to solve the above optimization problem, *e.g.* the Rackwitz-Fiessler algorithm (Rackwitz and Fiessler, 1978), the Abdo-Rackwitz algorithm (Abdo and Rackwitz, 1990), the iHLRF algorithm (Zhang and Der Kiureghian, 1995, 1997) or the Polak-He algorithm (Haukaas and Der Kiureghian, 2006), see also Liu and Der Kiureghian (1991) for the comparison of the efficiency of other algorithms.

Once the design point has been found, the corresponding reliability index is defined as:

$$\beta = \text{sign} [g(T^{-1}(0))] \cdot \|\boldsymbol{\xi}^*\| \quad (3.47)$$

It corresponds to the algebraic distance of the design point to the origin, counted as positive if the origin is in the safe domain, or negative in the other case.

The third step of FORM then consists in replacing the failure domain by the half space $HS(P^*)$ defined by means of the hyperplane which is tangent to the limit state surface at the design point (see Figure 3.1).

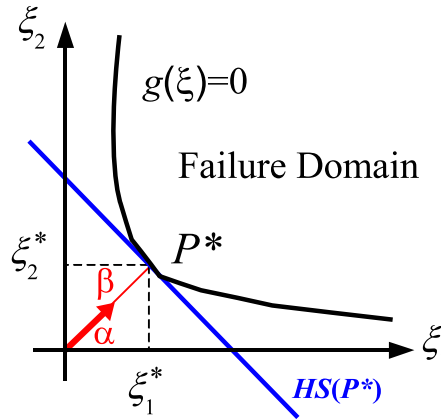


Figure 3.1: Principle of the First Order Reliability Method (FORM)

The equation of this hyperplane may be cast as:

$$\beta - \boldsymbol{\alpha} \cdot \boldsymbol{\xi} = 0 \quad (3.48)$$

where the unit vector $\boldsymbol{\alpha} = \boldsymbol{\xi}^*/\beta$ is also normal to the limit state surface at the design point:

$$\boldsymbol{\alpha} = - \frac{\nabla g(T^{-1}(\boldsymbol{\xi}^*))}{\|\nabla g(T^{-1}(\boldsymbol{\xi}^*))\|} \quad (3.49)$$

This leads to:

$$P_f = \int_{\{g(T^{-1}(\boldsymbol{\xi})) \leq 0\}} \varphi_M(\boldsymbol{\xi}) d\boldsymbol{\xi} \approx \int_{HS(P^*)} \varphi_M(\boldsymbol{\xi}) d\boldsymbol{\xi} \quad (3.50)$$

The latter integral can be evaluated in a closed form and gives the first order approximation of the probability of failure:

$$P_f \approx P_{f,\text{FORM}} = \Phi(-\beta) \quad (3.51)$$

where $\Phi(x)$ denotes the standard normal CDF.

3.5 Second-order reliability method (SORM)

The First Order Reliability Method relies upon the linearization of the limit state function around the design point. Once a FORM result is available, it is natural to look after a *second order* approximation of the probability of failure. This is essentially what the various types of Second Order Reliability Methods (SORM) do.

The so-called *curvature-fitting* SORM consists in establishing a second order Taylor series expansion of the limit state function around the design point. This requires the computation of the Hessian of the limit state function at this point. Using a suitable rotation of the coordinate system in the standard normal space, say $\mathbf{u} = \mathfrak{R} \cdot \boldsymbol{\xi}$, the limit state function may be recast as:

$$g(T^{-1}(\boldsymbol{\xi})) \approx \beta - u_M + \sum_{j=1}^{M-1} \frac{1}{2} \kappa_j u_j^2 \quad (3.52)$$

where $\{\kappa_j, j = 1, \dots, M-1\}$ denote the curvature of the approximate paraboloid whose axis is set along the design point direction $\boldsymbol{\alpha}$. An asymptotic formula for the probabilistic content of such paraboloid has been derived by Breitung (1984):

$$P_{f,\text{SORM}} \approx \Phi(-\beta) \prod_{j=1}^{M-1} (1 - \beta \kappa_j)^{-1/2} \quad (3.53)$$

It clearly appears in this expression that the SORM approximation of P_f is obtained by a correction of $P_{f,\text{FORM}} = \Phi(-\beta)$. Note that the asymptotic expression Eq.(3.53) becomes singular when $\beta \kappa_j \rightarrow 1$. An exact integral expression of the probabilistic content of a paraboloid has been proposed by Tvedt (1990) and can be used in case the asymptotic expression fails.

Other methods for constructing an approximate paraboloid have been proposed by Der Kiureghian et al. (1987) (point-fitting SORM). An original algorithm to compute the curvatures can be found in Der Kiureghian and de Stefano (1991). The theory behind SORM may also be cast as asymptotic expansions of multidimensional integrals that can be formally applied either in the standard normal space or in the original space of basic variables, see *e.g.* Breitung (1989); Rackwitz (2004) for details.

3.6 Importance sampling

The FORM/SORM methods presented in the above paragraphs allow the analyst to compute estimates of the probability of failure at a relative low computational cost compared to Monte Carlo simulation. An important property of FORM is that the computational burden is *not* related to the magnitude of the probability of failure, in contrast to Monte Carlo simulation. The counterpart of this noticeable feature is that FORM/SORM estimates come without any indication of accuracy. For sure FORM will be all the more accurate since the probability of failure is low (due to the asymptotic properties) and the limit state function is close to linear in the standard normal space. However, in complex problems, there is no guarantee of any kind that:

- a FORM algorithm will converge to a design point;
- if so, that the obtained design point is unique (other local minima of the constrained optimization problem Eq.(3.46) may exist, see Der Kiureghian and Dakessian (1998) for a possible solving strategy);
- that the estimates in Eqs.(3.51),(3.53) are sufficiently accurate.

In order to bypass these possible difficulties, a complementary approach called *importance sampling* was proposed in the mid 80's (Harbitz, 1983; Shinozuka, 1983). The basic idea is to recast the definition of P_f in Eq.(3.40) as follows:

$$P_f = \int_{\mathbb{R}^M} 1_{\mathcal{D}_f}(\mathbf{x}) \frac{f_{\mathbf{X}}(\mathbf{x})}{\Psi(\mathbf{x})} \Psi(\mathbf{x}) d\mathbf{x} = E_{\Psi} \left[1_{\mathcal{D}_f}(\mathbf{X}) \frac{f_{\mathbf{X}}(\mathbf{X})}{\Psi(\mathbf{X})} \right] \quad (3.54)$$

where Ψ is a M -dimensional *sampling distribution* to be selected, and $E_{\Psi}[\cdot]$ denotes the expectation with respect to this distribution.

An estimate of P_f by importance sampling is then given by the empirical mean:

$$P_{f,IS} = \frac{1}{n} \sum_{k=1}^n 1_{\mathcal{D}_f}(\mathbf{x}^{(k)}) \frac{f_{\mathbf{X}}(\mathbf{x}^{(k)})}{\Psi(\mathbf{x}^{(k)})} \quad (3.55)$$

where the sample set $\{\mathbf{x}^{(k)}, k = 1, \dots, n\}$ is drawn according to the sample density Ψ .

The general formulation in Eqs.(3.54)-(3.55) reveals rather efficient when the sampling density Ψ is selected according to the results of a previous FORM analysis. Using the isoprobabilistic transform, Eq.(3.54) may be recast in the standard normal space as:

$$P_f = E_{\Psi} \left[1_{\mathcal{D}_f}(T^{-1}(\boldsymbol{\xi})) \frac{\varphi_M(\boldsymbol{\xi})}{\Psi(\boldsymbol{\xi})} \right] \quad (3.56)$$

Suppose now that FORM has yielded a design point $\boldsymbol{\xi}^*$ in the standard normal space and choose the following multinormal sampling density:

$$\Psi(\boldsymbol{\xi}) = \varphi_M(\boldsymbol{\xi} - \boldsymbol{\xi}^*) \quad (3.57)$$

The estimate of the probability of failure in Eq.(3.55) reduces in this case to:

$$P_{f,IS} = \frac{\exp[\beta^2/2]}{n} \sum_{k=1}^n 1_{\mathcal{D}_f} \left(T^{-1}(\boldsymbol{\xi}^{(k)}) \right) \exp \left[-\boldsymbol{\xi}^{(k)} \cdot \boldsymbol{\xi}^* \right] \quad (3.58)$$

As any sampling method, IS comes with confidence intervals on the result. In practice, this allows one to monitor the simulation according to the coefficient of variation of the estimate. Note that if FORM does not converge, the sequence of points computed by the optimization algorithm may help select a relevant sampling density in most cases. For instance, if the non convergence is due to oscillations between several design points, a sampling density obtained by the mixing of Gaussian distributions centered on these points may be efficient.

Various improvements of importance sampling have been proposed, such as the *axis-orthogonal importance sampling* (Hohenbichler and Rackwitz, 1988), *adaptive importance sampling* (Bucher, 1988; Au and Beck, 1999), *radial importance sampling* (Melchers, 1990) and others (Maes et al., 1993; Cambier et al., 2002; Au and Beck, 2001b, 2003a).

3.7 Conclusion

A rapid survey of reliability methods has been presented in this section. Even if FORM/ SORM methods remain the best efficiency vs. accuracy compromise to solve reliability problems associated with industrial applications, it is important to be able to resort to other techniques such as importance sampling when the former fail. For the sake of completeness, other methods such as *Latin Hypercube sampling* (LHS) (McKay et al., 1979; Olsson et al., 2003) and *directional simulation* (e.g. Ditlevsen et al. (1987); Bjerager (1988); Melchers (1990), see also Ditlevsen and Madsen (1996, Chap. 9) and Waarts (2000)) should be mentioned. Note that the increasing power of the computers has renewed the interest in computationally costly methods such as the various simulation-based methods.

The approaches reviewed in this section can be used whatever the nature of the model under consideration. Although originally developed together with analytical models, they have been coupled to finite element codes quite early as in the pioneering work by Der Kiureghian and Taylor (1983); Der Kiureghian and Ke (1988) and more recently by Flores Macias (1994); Flores Macias and Lemaire (1997); Lemaire (1998); Lemaire and Mohamed (2000). So-called finite element reliability methods are now commonly used in the industry.

It is worth mentioning that the research for new methods to solve more efficiently structural reliability problems is quite active. Not to mention the spectral methods developed in the next chapter, new tracks have been proposed in the recent years, including:

- the *subset simulation* method (Au and Beck, 2001a), which relies upon the decomposition of the probability of failure into a product of conditional probabilities that are estimated by Markov chain Monte Carlo simulation (MCMC), an algorithm originally proposed by Metropolis et al. (1953). Variants of the method have been proposed such as the subset simulation with splitting (Ching et al., 2005b), the hybrid subset simulation (Ching et al., 2005a) or the spherical subset simulation (Katafygiotis and Cheung, 2007). Applications can be found in Au and Beck (2003b); Au et al. (2007).
- the *line sampling* technique (Schuëller et al., 2004; Koutsourelakis et al., 2004; Schuëller and Pradlwarter, 2007), which consists in determining first an important direction \mathbf{a} that points towards the failure domain (e.g. parallel to the gradient of the limit state function at the origin of the standard normal space). Then points are sampled in the hyperplane orthogonal to \mathbf{a} , and a line parallel to \mathbf{a} is defined from each of them. The intersection of this line with the limit state surface is approximately found by some interpolation technique, and the information obtained from all the lines is gathered in an estimator of the probability of failure whose variance is much smaller than that obtained by crude Monte Carlo simulation. Applications of this technique can be found in Pradlwarter et al. (2005, 2007). Note that this technique is very similar to the *axis orthogonal sampling* proposed by Hohenbichler and Rackwitz (1988): the important direction \mathbf{a} in this case is the direction to the design point obtained by FORM.

As a conclusion, it is important to remark that the various methods summarized in this section can be almost unlimitedly combined with each other to solve specific problems. In other words, it is likely that no universal technique will ever show up to solve reliability problems. It is more the confrontation and combination of several methods that helps the analyst be confident in the numbers he or she eventually obtains.

4 Sensitivity analysis

4.1 Introduction

Broadly speaking, sensitivity analysis (SA) aims at quantifying the relative importance of each input parameter of a model. Methods of sensitivity analysis are usually classified into two categories:

- *local* sensitivity analysis concentrates on the local impact of input parameters on the model. It is based on the computation of the gradient of the response with respect to its parameters around a nominal value. Numerous techniques have been developed to compute the gradient efficiently, including finite-difference schemes, direct differentiation or adjoint differentiation methods (Cacuci, 2003).
- *global* sensitivity analysis tries to quantify the output uncertainty due to the uncertainty in the input parameters, which are taken singly or in combination with others.

Many papers have been devoted to the latter topic in the last twenty years. A good state-of-the-art of the techniques is available in Saltelli et al. (2000), who gather the methods into two groups:

- *regression-based methods*: the standardized regression coefficients (SRC) are based on a linear regression of the output on the input vector. The input/output Pearson correlation coefficients measure the effect of each input variable by the correlation it has with the model output. The partial correlation coefficients (PCC) are based on results of regressions of the model on all input variables except one. These coefficients are useful to measure the effect of the input variables if the model is linear, *i.e.* if the coefficient of determination R^2 of the regression is close to one. In case of nonlinearity, they fail to represent properly the response sensitivities. However, in case of monotonicity of the model with respect to the input parameters, the rank transform can be used, leading to the so-called SRRC (standardized rank regression-) and PRCC (partial rank correlation-) coefficients. As a whole, in case of general non linear non monotonic models, these approaches fail to produce satisfactory sensitivity measures (Saltelli and Sobol', 1995).
- *variance-based methods*: these methods aim at decomposing the variance of the output as a sum of contributions of each input variable, or combinations thereof. They are sometimes called *ANOVA techniques* for "ANalysis Of VAriance". The *correlation ratios* proposed in McKay (1995) enter this category. They are formulated as conditional variances and usually evaluated by crude Monte Carlo simulation or Latin Hypercube Sampling. The Fourier amplitude sensitivity test (FAST) indices (Cukier et al., 1978; Saltelli et al., 1999) and the Sobol' indices (Sobol', 1993; Saltelli and Sobol', 1995; Archer et al., 1997), see also the review in Sobol' and Kucherenko (2005), are intended to represent the sensitivities for general models. The Sobol' indices are practically computed using Monte Carlo simulation, which makes them hardly applicable for computationally demanding models, *e.g.* finite element models in engineering mechanics.

In this section, emphasis is put first on sensitivity measures that are obtained as a byproduct of uncertainty propagation. Then the theory of Sobol' indices is presented.

4.2 Sensitivity measures as a byproduct of uncertainty propagation

4.2.1 From the perturbation method

The perturbation method presented in Section 2 allows to derive an approximate expression of the response variance, which, in case of independent input random variables, reduces to:

$$\text{Var}[Y] \equiv \sigma_Y^2 \approx \sum_{i=1}^M \left(\left. \frac{\partial \mathcal{M}}{\partial x_i} \right|_{\mathbf{x}=\boldsymbol{\mu}_{\mathbf{X}}} \right)^2 \sigma_{X_i}^2 \quad (3.59)$$

It is clear from this expression that the response variance is a sum of contributions related to each input random variables. By normalizing Eq.(3.59), one defines the *relative importance* of each input parameter:

$$\eta_i^2 = \left(\left. \frac{\partial \mathcal{M}}{\partial x_i} \right|_{\mathbf{x}=\boldsymbol{\mu}_{\mathbf{X}}} \right)^2 \left(\frac{\sigma_{X_i}}{\sigma_Y} \right)^2 \quad (3.60)$$

whose sum adds up to one. This so-called decomposition of the response variance is carried out here in a linearized context since Eq.(3.59) is based on the Taylor series expansion of the response. The general formulation of variance decomposition techniques is described below in Section 4.4.

If the input random variables are correlated, no such importance measure can be derived for a single variable. Nonetheless, the relative importance of a group of correlated variables that is independent of all the remaining variables can be straightforwardly derived. Note that Eq.(3.60) may still be used, although the sum of the importance measures will not add up to unity.

4.2.2 From FORM analysis

As shown in Section 3.4, FORM leads to the computation of a linearized limit state function g_{FORM} whose equation may be cast as:

$$g_{\text{FORM}}(\boldsymbol{\xi}) = \beta - \boldsymbol{\alpha} \cdot \boldsymbol{\xi} \quad (3.61)$$

where β is the reliability index and $\boldsymbol{\alpha}$ is the unit vector to the design point (see Eq.(3.48)).

This linearized limit state function can be considered as a margin function which quantifies the “distance” between a realization $\boldsymbol{\xi}$ of the (transformed) input random vector and the failure surface. Its variance straightforwardly reads:

$$\text{Var}[g_{\text{FORM}}(\boldsymbol{\xi})] = \sum_{i=1}^M \alpha_i^2 = 1 \quad (3.62)$$

since the components of $\boldsymbol{\xi}$ are independent and since $\boldsymbol{\alpha}$ is a unit vector.

Thus the coefficients $\{\alpha_i^2, i = 1, \dots, M\}$, known as *FORM importance factors* (Ditlevsen and Madsen, 1996) correspond to the portion of the variance of the linearized margin which is due to each ξ_i . When the input random variables \mathbf{X} are independent, there is a one-to-one mapping between X_i and ξ_i , $i = 1, \dots, M$. Thus α_i^2 is interpreted as the importance of the i -th input parameter in the failure event. When the input random variable are correlated, other measures of importance should be used such as the γ -factors defined in Der Kiureghian (1999); Haukaas and Der Kiureghian (2005).

4.3 The Sobol’ indices

4.3.1 Sobol’ decomposition

Let us consider a scalar model having M input parameters gathered in an input vector \mathbf{x} , and a scalar output y :

$$y = \mathcal{M}(\mathbf{x}), \quad \mathbf{x} \in [0, 1]^M \quad (3.63)$$

where the input parameters are defined on the M -dimensional unit cube $[0, 1]^M$. The Sobol' decomposition of $\mathcal{M}(\mathbf{x})$ into summands of increasing dimension reads (Sobol', 1993):

$$\mathcal{M}(\mathbf{x}) = \mathcal{M}_0 + \sum_{i=1}^M \mathcal{M}_i(x_i) + \sum_{1 \leq i < j \leq M} \mathcal{M}_{ij}(x_i, x_j) + \cdots + \mathcal{M}_{12\dots M}(\mathbf{x}) \quad (3.64)$$

where \mathcal{M}_0 is a constant and where it is imposed that the integral of each summand $\mathcal{M}_{i_1\dots i_s}(x_{i_1}, \dots, x_{i_s})$ over any of its arguments is zero, *i.e.* :

$$\int_0^1 \mathcal{M}_{i_1\dots i_s}(x_{i_1}, \dots, x_{i_s}) dx_{i_k} = 0 \quad \text{for } 1 \leq k \leq s \quad (3.65)$$

The classical properties of this decomposition are the following (Homma and Saltelli, 1996):

- The sum in Eq.(3.64) contains a number of summands equal to:

$$\sum_{i=1}^M \binom{M}{i} = 2^M - 1 \quad (3.66)$$

- The constant \mathcal{M}_0 is the mean value of the function:

$$\mathcal{M}_0 = \int_{[0,1]^M} \mathcal{M}(\mathbf{x}) d\mathbf{x} \quad (3.67)$$

where $d\mathbf{x}$ stands for $dx_1 \dots dx_M$ for the sake of simplicity.

- Due to Eq.(3.65), the summands are orthogonal to each other in the following sense:

$$\int_{[0,1]^M} \mathcal{M}_{i_1\dots i_s}(x_{i_1}, \dots, x_{i_s}) \mathcal{M}_{j_1\dots j_t}(x_{j_1}, \dots, x_{j_t}) d\mathbf{x} = 0 \quad \text{for } \{i_1, \dots, i_s\} \neq \{j_1, \dots, j_t\} \quad (3.68)$$

With the above assumptions, the decomposition in Eq.(3.64) is *unique* whenever $\mathcal{M}(\mathbf{x})$ is integrable over $[0, 1]^M$. Moreover, the terms in the decomposition may be derived analytically. Indeed, the univariate terms read:

$$\mathcal{M}_i(x_i) = \int_{[0,1]^{M-1}} \mathcal{M}(\mathbf{x}) d\mathbf{x}_{\sim i} - \mathcal{M}_0 \quad (3.69)$$

In this expression, $\int_{[0,1]^{M-1}} d\mathbf{x}_{\sim i}$ denotes the integration over all variables except x_i . Similarly, the bivariate terms read:

$$\mathcal{M}_{ij}(x_i, x_j) = \int_{[0,1]^{M-2}} \mathcal{M}(\mathbf{x}) d\mathbf{x}_{\sim \{ij\}} - \mathcal{M}_i(x_i) - \mathcal{M}_j(x_j) - \mathcal{M}_0 \quad (3.70)$$

Here again, $\int_{[0,1]^{M-2}} d\mathbf{x}_{\sim \{ij\}}$ denotes the integration over all parameters except x_i and x_j . More generally, the symbol “ \sim ” means “complementary of” in the sequel. Following this construction, any summand $\mathcal{M}_{i_1\dots i_s}(x_{i_1}, \dots, x_{i_s})$ may be written as the difference of a multidimensional integral and summands of lower order. However, these functions need not be explicitly computed to carry out sensitivity analysis, as explained below.

4.3.2 Use in ANOVA

Consider now that the input parameters are independent random variables uniformly distributed over $[0, 1]$:

$$\mathbf{X} = \{X_1, \dots, X_M\}^\top, \quad X_i \sim \mathcal{U}(0, 1), \quad i = 1, \dots, M \quad (3.71)$$

As a consequence, the model response $Y = \mathcal{M}(\mathbf{X})$ is a random variable, whose variance D (also called *total variance* in the literature on global sensitivity) reads:

$$D = \text{Var} [\mathcal{M}(\mathbf{X})] = \int_{[0,1]^M} \mathcal{M}^2(\mathbf{x}) d\mathbf{x} - \mathcal{M}_0^2 \quad (3.72)$$

By integrating the square of Eq.(3.64) and by using (3.68), it is possible to decompose the total variance (3.72) as follows:

$$D = \sum_{i=1}^M D_i + \sum_{1 \leq i < j \leq M} D_{ij} + \dots + D_{12\dots M} \quad (3.73)$$

where the *partial variances* appearing in the above expansion read:

$$D_{i_1\dots i_s} = \int_{[0,1]^s} \mathcal{M}_{i_1\dots i_s}^2(x_{i_1}, \dots, x_{i_s}) dx_{i_1} \dots dx_{i_s} \quad 1 \leq i_1 < \dots < i_s \leq M, s = 1, \dots, M \quad (3.74)$$

The Sobol' indices are defined as follows :

$$S_{i_1\dots i_s} = D_{i_1\dots i_s} / D \quad (3.75)$$

By definition, according to Eqs.(3.73),(3.75), they satisfy:

$$\sum_{i=1}^M S_i + \sum_{1 \leq i < j \leq M} S_{ij} + \dots + S_{12\dots M} = 1 \quad (3.76)$$

Thus each index $S_{i_1\dots i_s}$ is a sensitivity measure describing which amount of the total variance is due to the uncertainties in the set of input parameters $\{i_1 \dots i_s\}$. The first order indices S_i give the influence of each parameter taken alone whereas the higher order indices account for possible mixed influence of various parameters.

The *total sensitivity indices* S_{T_i} have been defined in order to evaluate the total effect of an input parameter (Homma and Saltelli, 1996). They are defined from the sum of all partial sensitivity indices $D_{i_1\dots i_s}$ involving parameter i :

$$S_{T_i} = \sum_{\mathcal{I}_i} D_{i_1\dots i_s} / D \quad \mathcal{I}_i = \{\{i_1, \dots, i_s\} \supset \{i\}\} \quad (3.77)$$

It is easy to show that:

$$S_{T_i} = 1 - S_{\sim i} \quad (3.78)$$

where $S_{\sim i}$ is the sum of all $S_{i_1\dots i_s}$ that do *not* include index i .

4.3.3 Computation by Monte Carlo simulation

The Sobol' indices are usually computed using Monte Carlo simulation. From Eqs.(3.67),(3.72), the following estimates of the mean value, total and partial variance can be derived using n samples (Saltelli et al., 2000):

$$\hat{\mathcal{M}}_0 = \frac{1}{n} \sum_{k=1}^n \mathcal{M}(\mathbf{x}^{(k)}) \quad (3.79)$$

$$\hat{D} = \frac{1}{n} \sum_{k=1}^n \mathcal{M}^2(\mathbf{x}^{(k)}) - \hat{\mathcal{M}}_0^2 \quad (3.80)$$

$$\hat{D}_i = \frac{1}{n} \sum_{k=1}^n \mathcal{M}(\mathbf{x}_{(\sim i)}^{(k),1}, x_i^{(k),1}) \mathcal{M}(\mathbf{x}_{(\sim i)}^{(k),2}, x_i^{(k),1}) - \hat{\mathcal{M}}_0^2 \quad (3.81)$$

In the latter equations, $\mathbf{x}^{(k)} = (x_1^k, x_2^k, \dots, x_M^k)$ denotes the k -th sample point and:

$$\mathbf{x}_{(\sim i)}^{(k)} = (x_1^{(k)}, x_2^{(k)}, \dots, x_{(i-1)}^{(k)}, x_{(i+1)}^{(k)}, \dots, x_M^{(k)}) \quad (3.82)$$

Moreover the superscripts ¹ and ² in Eq.(3.81) indicate that two different samples are generated and their components mixed. A similar expression allows to estimate in a single shot the total sensitivity index S_{T_i} :

$$\hat{D}_{\sim i} = \frac{1}{n} \sum_{k=1}^n \mathcal{M}(\mathbf{x}_{(\sim i)}^{(k),1}, x_i^{(k),1}) \mathcal{M}(\mathbf{x}_{(\sim i)}^{(k),1}, x_i^{(k),2}) - \hat{\mathcal{M}}_0^2 \quad \hat{S}_{T_i} = 1 - \hat{D}_{\sim i} / \hat{D} \quad (3.83)$$

The Sobol' indices are known to be good descriptors of the sensitivity of the model to its input parameters, since they do not suppose any kind of linearity or monotonicity in the model. However, the full description requires the evaluation of 2^M Monte Carlo integrals, which is not practically feasible unless M is low. In practice, the analyst often computes the first-order and total sensitivity indices, sometimes the second order ones. Note that the first-order indices are equivalent to the sensitivity indices obtained by the FAST method (Cukier et al., 1978; Saltelli and Bolado, 1998), whose computation may be more efficient. Moreover, recent work has been devoted to further reduce the computational cost in evaluating the Sobol' indices (Saltelli, 2002) and obtain "for free" additional indices, see also the accelerated estimation procedure for variance-based measures in Oakley and O'Hagan (2004).

4.4 Conclusion

In this section, various sensitivity measures available in the literature have been reviewed and discussed. The importance factors derived from the perturbation method (resp. FORM) are obtained almost for free once the propagation of the uncertainties through the model has been carried out. This is the reason why they are popular.

However, the formalism of Sobol' indices appears more robust and versatile, since it does not rely upon any linearization of the model. The usual technique to compute these Sobol' indices is Monte Carlo simulation, which reveals inappropriate when each evaluation of the model is costly. Moreover, the convergence of the estimators of the Sobol' indices is rather low, see a discussion in Homma and Saltelli (1996). It will be shown in the next chapter that the Sobol' approach to sensitivity analysis is particularly interesting when combined with spectral methods.

5 Conclusion

Well-known methods for uncertainty propagation and sensitivity analysis have been reviewed in this chapter. As far as second moment analysis is concerned, the perturbation method remains the best compromise between accuracy and efficiency, especially in case the coefficient of variation of the input random variables is not too large and the model is not too non linear. It may be particularly efficient when used with modern finite element codes that implement the gradients of the response quantities, *e.g.* OpenSees (Pacific Earthquake Engineering and Research Center, 2004) or Code-Aster (eDF, R&D Division, 2006). Note that the quadrature approach using sparse schemes could be an interesting alternative in cases when the size of the input random vector is not too large. The advantage of this approach leads in the fact that higher order moments may be estimated in the same shot.

As far as reliability analysis is concerned, FORM/SORM methods complemented by importance sampling are robust tools that allow the analyst to solve the problem in most cases. Recent techniques such as subset simulation and line sampling seem attractive when the complexity of the limit state function makes the classical methods fail.

Chapter 4

Spectral methods

1 Introduction

The classical methods for moment and reliability analysis presented in chapter 3 have been devised to solve specific problems of probabilistic mechanics. Precisely, methods such as the perturbation method for second moment analysis, or FORM /SORM for reliability analysis introduce relevant assumptions and approximations to attain their goal. Should the analyst be interested first in the mean and the standard deviation of the model response, and then in some failure event, he or she should perform independently both types of analysis.

From a heuristic point of view, it is clear though that the probabilistic content of a response quantity is contained in its probability density function (PDF). If the PDF were accurately predicted both in its central part and in the tails, second moment- as well as reliability analysis could be easily performed as a post-processing. In a sense, Monte Carlo simulation (MCS) provides such a complete representation: samples of the parameters are drawn according to the input probabilistic model and the corresponding response values can be gathered in a histogram or an empirical cumulative distribution function (CDF). However, the efficiency of such a procedure is low, meaning that the number of samples has to be large to get accurate results. For instance, it was observed in Chapter 3 that the number of samples required to evaluate a probability of failure of magnitude 10^{-k} is about $4 \cdot 10^{k+2}$, when a relative accuracy of 5% is prescribed.

From a more mathematical point of view, the random response obtained by propagating the input probabilistic model through the mathematical model of the physical system is a member of a suitable space of random vectors. In this respect, MCS can be viewed as a collocation-type method which allows the *pointwise* characterization of this random response.

In order to understand the philosophy (and related poor efficiency) of MCS better, a comparison with a classical deterministic continuum mechanics problem may be fruitful. Consider an elastic problem posed on a domain $\mathcal{B} \subset \mathbb{R}^d$, $d = 1, 2, 3$ where the displacement field $\mathbf{u}(\mathbf{x})$, $\mathbf{x} \in \mathcal{B}$ is the main unknown. The counterpart of Monte Carlo simulation to solve this deterministic problem would be a method that provides, for any $\mathbf{x}_0 \in \mathcal{B}$ the sole response quantity $\mathbf{u}(\mathbf{x}_0)$. To get a flavor of the complete displacement field would then require applying this (obviously not efficient) method to a large set of sample points in \mathcal{B} .

Of course, deterministic problems in continuum mechanics are not solved this way. In contrast, when the finite element method is considered, the displacement field, which is a member of a suitable functional space \mathcal{H} (introduced in the weak formulation of the governing equations) is approximated onto a finite

N -dimensional subspace $\mathcal{H}^{(N)} \subset \mathcal{H}$. The basis functions spanning this subspace are in practice associated with a mesh of domain \mathcal{B} and known as *shape functions*. Then the boundary value problem is reduced to finding the *nodal displacements*, which are the coordinates of the approximate displacement field in this basis.

The so-called *spectral methods* presented in this chapter are nothing but a transcription of the above well known ideas to the probabilistic space: instead of apprehending the (say, scalar) random response $Y(\omega) = \mathcal{M}(\mathbf{X}(\omega))$ by a set of realizations $\{y^{(i)} = \mathcal{M}(\mathbf{x}^{(i)})\}$, as MCS does, it will rather be expanded onto a suitable basis of the space of second-order random variables and represented by its “coordinates” $\{y_j, j \in \mathbb{N}\}$:

$$Y(\omega) = \sum_{j \in \mathbb{N}} y_j \phi_j(\omega) \quad (4.1)$$

In this equation, the notation ω has been kept in order to show that the response Y as well as the basis functions are random variables. It will be used in the sequel anytime it is necessary for the sake of clarity, and omitted otherwise.

The mathematical setting for the representation of models having random input is first described in Section 2. Two categories of methods to compute the expansion coefficients in Eq.(4.1) are then reviewed, namely:

- the *Galerkin* or *intrusive* approach, which will be presented from its historical perspective (Section 3).
- the *non intrusive* approaches, namely the projection and regression methods, which have been more specifically investigated by the author (Section 4).

The post-processing of the coefficients $\{y_j, j \in \mathbb{N}\}$ for moment, reliability and global sensitivity analyses is then detailed in Section 5. Application examples are presented in Section 6.

2 Spectral representation of functions of random vectors

This section is inspired by the presentation proposed by Soize and Ghanem (2004) for introducing the *polynomial chaos representation*. It is related to the use of Hilbertian algebra to characterize square integrable functions of random vectors.

2.1 Introduction

Of interest is a physical system described by a mathematical model \mathcal{M} having M input parameters and N output quantities. Suppose that the uncertainties in the system are modelled in a probabilistic framework by an input random vector \mathbf{X} . Let us denote by $f_{\mathbf{X}}(\mathbf{x})$ its joint PDF, and by $P_{\mathbf{X}}$ the associated probability measure such that $P_{\mathbf{X}}(d\mathbf{x}) = f_{\mathbf{X}}(\mathbf{x}) d\mathbf{x}$.

The model response is cast as a random vector \mathbf{Y} of size N such that:

$$\mathbf{Y} = \mathcal{M}(\mathbf{X}) \quad (4.2)$$

In order to properly characterize the random properties of \mathbf{Y} , suitable functional spaces have to be defined. The case of scalar models ($N = 1$) is first addressed for the sake of simplicity. Then the extension to the vector case is presented.

2.2 Representation of scalar-valued models

2.2.1 Definition

In this section, a scalar-valued model $\mathcal{M} : \mathbb{R}^M \mapsto \mathbb{R}$ is considered. Let us suppose that its random response $Y = \mathcal{M}(\mathbf{X})$ is a second-order random variable:

$$\mathbb{E} [Y^2] < +\infty \quad (4.3)$$

Let us denote by $\mathcal{H} = \mathcal{L}_{P_{\mathbf{X}}}^2(\mathbb{R}^M, \mathbb{R})$ the Hilbert space of $P_{\mathbf{X}}$ -square integrable real-valued functions of $\mathbf{x} \in \mathbb{R}^M$ equipped with the inner product:

$$\langle u, v \rangle_{\mathcal{H}} \equiv \int_{\mathbb{R}^M} u(\mathbf{x}) v(\mathbf{x}) f_{\mathbf{X}}(\mathbf{x}) d\mathbf{x} \quad (4.4)$$

Eq.(4.3) is equivalent to:

$$\mathbb{E} [\mathcal{M}^2(\mathbf{X})] = \langle \mathcal{M}, \mathcal{M} \rangle_{\mathcal{H}} < +\infty \quad (4.5)$$

Consequently, considering model responses that are second-moment random variables is equivalent to considering models that belong to the Hilbert space \mathcal{H} .

2.2.2 Hilbertian basis of \mathcal{H} – Case of independent input random variables

In this paragraph, it is supposed that the random vector \mathbf{X} has independent components, say $\{X_i, i = 1, \dots, M\}$ with associated marginal PDF $f_{X_i}(x_i)$. It follows that the PDF of \mathbf{X} reads:

$$f_{\mathbf{X}}(\mathbf{x}) = \prod_{k=1}^M f_{X_k}(x_k) \quad (4.6)$$

Let $\mathcal{H}_i = \mathcal{L}_{P_{X_i}}^2(\mathbb{R}, \mathbb{R})$ be the real Hilbert space associated with the probability measure P_{X_i} such that $P_{X_i}(dx_i) = f_{X_i}(x_i) dx_i$ and equipped with the inner product:

$$\langle u, v \rangle_{\mathcal{H}_i} \equiv \int_{\mathbb{R}} u(x) v(x) f_{X_i}(x) dx \quad (4.7)$$

Let $\{\psi_k^i, k \in \mathbb{N}\}$ be a Hilbertian basis of \mathcal{H}_i , *i.e.* a complete orthonormal family of functions satisfying:

$$\langle \psi_k^i, \psi_l^i \rangle_{\mathcal{H}_i} = \delta_{kl} \quad (\text{Kronecker symbol}) \quad (4.8)$$

Let $\tilde{\mathcal{H}}$ be the real Hilbert space defined by the following tensor product:

$$\tilde{\mathcal{H}} \equiv \bigotimes_{i=1}^M \mathcal{H}_i \quad (4.9)$$

equipped with the inner product:

$$\langle u, v \rangle_{\tilde{\mathcal{H}}} \equiv \int_{\mathbb{R}} \dots \int_{\mathbb{R}} u(x_1, \dots, x_M) v(x_1, \dots, x_M) f_{X_1}(x_1) \dots f_{X_M}(x_M) dx_1 \dots dx_M \quad (4.10)$$

From Eqs.(4.8),(4.9), one can define the following Hilbertian basis of $\tilde{\mathcal{H}}$:

$$\{\psi_{k_1}^1 \otimes \dots \otimes \psi_{k_M}^M, (k_1, \dots, k_M) \in \mathbb{N}^M\} \quad (4.11)$$

By substituting for Eq.(4.6) in Eq.(4.10) and comparing with Eq.(4.4), it is clear that:

$$\langle u, v \rangle_{\tilde{\mathcal{H}}} = \int_{\mathbb{R}^M} u(\mathbf{x}) v(\mathbf{x}) f_{\mathbf{X}}(\mathbf{x}) d\mathbf{x} = \langle u, v \rangle_{\mathcal{H}} \quad (4.12)$$

showing that \mathcal{H} and $\tilde{\mathcal{H}}$ are isomorphic. Thus any function belonging to \mathcal{H} may be uniquely represented as its series expansion onto the basis defined in Eq.(4.11):

$$\forall h \in \mathcal{H}, \quad h(x_1, \dots, x_M) = \sum_{\alpha_1 \in \mathbb{N}} \cdots \sum_{\alpha_M \in \mathbb{N}} h_{\alpha_1 \dots \alpha_M} \psi_{\alpha_1}^1(x_1) \cdots \psi_{\alpha_M}^M(x_M) \quad (4.13)$$

For convenience in the notation, the above equation may be rewritten as:

$$h(\mathbf{x}) = \sum_{\alpha \in \mathbb{N}^M} h_{\alpha} \Psi_{\alpha}(\mathbf{x}) \quad (4.14)$$

where α denotes all the possible M -uplets $(\alpha_1, \dots, \alpha_M) \in \mathbb{N}^M$ and $\Psi_{\alpha}(\mathbf{x})$ is defined by:

$$\Psi_{\alpha}(\mathbf{x}) \equiv \prod_{i=1}^M \psi_{\alpha_i}^i(x_i) \quad (4.15)$$

2.2.3 Hilbertian basis of \mathcal{H} – Case of mutually dependent input random variables

In the general case, the input vector \mathbf{X} may have mutually dependent components. Nevertheless, it is possible to derive a Hilbertian basis of \mathcal{H} based on the above construction.

Let us introduce for this purpose the marginal PDFs $\{f_{X_i}(x_i), i = 1, \dots, M\}$ of the random variables $\{X_i, i = 1, \dots, M\}$ (see Eq.(2.39)). Soize and Ghanem (2004) show that the following set of functions is a Hilbertian basis of \mathcal{H} :

$$\phi_{\alpha}(\mathbf{x}) = \left[\frac{\prod_{i=1}^M f_{X_i}(x_i)}{f_{\mathbf{X}}(\mathbf{x})} \right]^{1/2} \Psi_{\alpha}(\mathbf{x}) \quad (4.16)$$

where $\Psi_{\alpha}(\mathbf{x})$ has been defined in Eq.(4.15).

The above equation can be further elaborated by introducing the formalism of *copula theory* (Nelsen, 1999). This theory is a tool for the representation of multivariate CDFs, which is of common use in financial engineering whereas rather unused in probabilistic engineering mechanics. Copula theory allows to clearly separate the description of a random vector \mathbf{X} into two parts:

- the marginal distribution (or margin) of each component, denoted by $\{F_{X_i}(x_i), i = 1, \dots, M\}$;
- the structure of dependence between these components, contained in a so-called *copula function* $C : [0, 1]^M \mapsto [0, 1]$, which is nothing but a M -dimensional CDF with standard uniform margins.

According to Sklar's theorem (Sklar, 1959), a continuous joint CDF $F_{\mathbf{X}}(\mathbf{x})$ has a *unique* representation in terms of its margins and its copula function $C(u_1, \dots, u_M)$:

$$F_{\mathbf{X}}(\mathbf{x}) = C(F_{X_1}(x_1), \dots, F_{X_M}(x_M)) \quad (4.17)$$

The practical feature of this approach appears when the probabilistic model of \mathbf{X} is to be built from data: the models for the margins is first inferred, then suitable methods for determining the appropriate copula function are applied. Introducing the density of the copula:

$$c(u_1, \dots, u_M) = \frac{\partial^M C(u_1, \dots, u_M)}{\partial u_1 \dots \partial u_M} \quad (4.18)$$

it comes from Eq.(4.17):

$$f_{\mathbf{X}}(\mathbf{x}) = c(F_{X_1}(x_1), \dots, F_{X_M}(x_M)) f_{X_1}(x_1) \dots f_{X_M}(x_M) \quad (4.19)$$

Thus the basis functions in Eq.(4.16) finally reduce to:

$$\phi_{\alpha}(\mathbf{x}) = \frac{\Psi_{\alpha}(\mathbf{x})}{[c(F_{X_1}(x_1), \dots, F_{X_M}(x_M))]^{1/2}} \quad (4.20)$$

Note that the above basis functions reduce to those in Eq.(4.15) when the components of the input random vector \mathbf{X} are mutually independent: in this case indeed, the copula in Eq.(4.17) (called *product* or *independent copula*) and its density respectively read:

$$C^{ind}(u_1, \dots, u_M) = u_1 u_2 \dots u_M \quad c^{ind}(u_1, \dots, u_M) = 1 \quad (4.21)$$

2.2.4 Polynomial chaos representation of the model response

One can observe that the tensor structure in Eq.(4.11) eventually reduces the problem to specifying the Hilbertian basis of $\mathcal{H}_i = \mathcal{L}_{P_{X_i}}^2(\mathbb{R}, \mathbb{R})$, which is the space of univariate scalar functions which are square-integrable with respect to P_{X_i} . As seen in Eqs.(4.7)-(4.8), such a basis $\{\psi_k^i, k \in \mathbb{N}\}$ satisfies:

$$\int_{\mathbb{R}} \psi_k^i(x) \psi_l^i(x) f_{X_i}(x) dx = \delta_{kl} \quad (4.22)$$

From the above equation, the link between this Hilbertian basis and the theory of orthogonal polynomials is obvious. As the marginal PDF f_{X_i} is a suitable weight function, a family of orthogonal polynomials denoted by $\{P_k^{f_{X_i}}, k \in \mathbb{N}\}$ can be built accordingly (see Appendix B for details). After proper normalization, one finally gets an orthonormal polynomial basis of \mathcal{H}_i :

$$\psi_k^i(x) = \frac{P_k^{f_{X_i}}(x)}{\|P_k^{f_{X_i}}\|_{\mathcal{H}_i}} \quad (4.23)$$

where $\|P_k^{f_{X_i}}\|_{\mathcal{H}_i} = \sqrt{\langle P_k^{f_{X_i}}, P_k^{f_{X_i}} \rangle_{\mathcal{H}_i}}$.

Should the basic random variables be independent standard normal ($\mathbf{X} \equiv \boldsymbol{\xi}$), then the obtained polynomials are the Hermite polynomials $H_{e_k}(x), k \in \mathbb{N}$. In this case, any random variable Y defined as the random response of a model (*i.e.* obtained by the propagation of the uncertainties contained in $\boldsymbol{\xi}$ through the model) may be cast as the following series expansion called Wiener-Hermite *polynomial chaos expansion*:

$$Y = \sum_{\alpha \in \mathbb{N}^M} y_{\alpha} \Psi_{\alpha}(\boldsymbol{\xi}) \quad (4.24)$$

The first generalization to other kinds of basic random variables has been proposed by Xiu and Karniadakis (2002) under the name *generalized* polynomial chaos. By a heuristic generalization of the above equation, and using the so-called Askey scheme of orthogonal polynomials (Askey and Wilson, 1985), the authors could represent functions of any kind of *independent* basic variables. The paper by Soize and Ghanem (2004), which serves as a basis for the current chapter, is an extension of this construction that poses a more rigorous framework and relaxes the assumption of independence.

2.2.5 Two strategies of application

Practically speaking, the polynomial chaos representation may be used in one or the other of the following forms:

- for a given input random vector \mathbf{X} defined by its joint PDF $f_{\mathbf{X}}(\mathbf{x})$ (or equivalently its margins and its copula, see Eq.(4.19)), gathering Eqs.(4.11),(4.20),(4.23) yields the following basis of \mathcal{H} :

$$\phi_{\alpha}(\mathbf{x}) = \frac{1}{d_{\alpha}} \frac{\prod_{i=1}^M P_{\alpha_i}^{f_{X_i}}(x_i)}{[c(F_{X_1}(x_1), \dots, F_{X_M}(x_M))]^{1/2}}, \quad \alpha \in \mathbb{N}^M \quad (4.25)$$

where d_{α} is a normalizing coefficient such that $\|\phi_{\alpha}\|_{\mathcal{H}} = 1$. Any second-order response quantity is thus expanded as follows:

$$Y = \sum_{\alpha \in \mathbb{N}^M} y_{\alpha} \phi_{\alpha}(\mathbf{X}) \quad (4.26)$$

This representation will be called *generalized polynomial chaos expansion* in the sequel (as it is usual in the literature). Strictly speaking, the above basis functions are polynomials only when the input variables are independent, but the original name is kept for the sake of clarity.

Similarly, if these normalizing coefficients are easily obtained when the basic variables are independent, this may not be the case in general. The following alternative strategy may then be used.

- The input random vector \mathbf{X} is first transformed into a basic random vector denoted by \mathbf{U} (*e.g.* a standard normal random vector) using an isoprobabilistic transform $\mathbf{X} = T^{-1}(\mathbf{U})$. Then the compound model $\mathcal{M} \circ T^{-1}$ is represented onto the polynomial chaos basis associated with \mathbf{U} :

$$Y \equiv \mathcal{M}(T^{-1}(\mathbf{U})) = \sum_{\alpha \in \mathbb{N}^M} y_{\alpha} \Psi_{\alpha}(\mathbf{U}) \quad (4.27)$$

2.3 Representation of vector-valued models

The construction made in Section 2.2 is now easily extended to vector-valued models. For this purpose, let us introduce the canonical basis of \mathbb{R}^N , say $\{\mathbf{b}^1, \dots, \mathbf{b}^N\}$, and let us denote the canonical inner product in \mathbb{R}^N by:

$$\mathbf{u}^{\top} \mathbf{v} \equiv \langle \mathbf{u}, \mathbf{v} \rangle_{\mathbb{R}^N} = \sum_{k=1}^N u_k v_k \quad (4.28)$$

where:

$$\mathbf{u} = \sum_{k=1}^N u_k \mathbf{b}^k \quad \mathbf{v} = \sum_{k=1}^N v_k \mathbf{b}^k \quad (4.29)$$

Let us finally denote by $\|\mathbf{u}\|$ the Euclidean norm:

$$\|\mathbf{u}\|^2 = \sum_{k=1}^N u_k^2 \quad (4.30)$$

Suppose now that the random response $\mathbf{Y} = \mathcal{M}(\mathbf{X})$ is a second-order random vector satisfying:

$$\mathbb{E} [\|\mathbf{Y}\|^2] < +\infty \quad (4.31)$$

Let us denote by $\mathcal{H}^{(N)} = \mathcal{L}_{P_{\mathbf{X}}}^2(\mathbb{R}^M, \mathbb{R}^N)$ the space of N -dimensional vector functions whose components are members of \mathcal{H} , *i.e.* :

$$\mathcal{H}^{(N)} = \mathcal{H} \otimes \mathbb{R}^N \quad (4.32)$$

and let it be equipped with the following inner product:

$$\langle \mathbf{u}, \mathbf{v} \rangle_{\mathcal{H}^{(N)}} = \sum_{k=1}^N \langle u_k, v_k \rangle_{\mathcal{H}} \quad (4.33)$$

where $\{u_k(\mathbf{x}), k = 1, \dots, N\}$ (resp. $\{v_k(\mathbf{x}), k = 1, \dots, N\}$) are the component functions of \mathbf{u} (resp. \mathbf{v}). Since:

$$\mathbb{E} [\|\mathbf{Y}\|^2] = \mathbb{E} [\|\mathcal{M}(\mathbf{X})\|^2] \equiv \langle \mathcal{M}(\mathbf{X}), \mathcal{M}(\mathbf{X}) \rangle_{\mathcal{H}^{(N)}} \quad (4.34)$$

assuming this is a finite quantity is equivalent to require that the vector-valued model \mathcal{M} is a member of $\mathcal{H}^{(N)}$.

In case \mathbf{X} has independent components, the following basis tensor product is a possible Hilbertian basis of $\mathcal{H}^{(N)}$ due to Eqs.(4.14),(4.32):

$$\left\{ \Psi_{\alpha} \otimes \mathbf{b}^k, \quad \alpha \in \mathbb{N}^M, k = 1, \dots, N \right\} \quad (4.35)$$

Thus the representation of any function $\mathbf{h} \in \mathcal{H}^{(N)}$ reads:

$$\mathbf{h}(\mathbf{x}) = \sum_{\alpha \in \mathbb{N}^M} \sum_{k=1}^N h_{k,\alpha} \Psi_{\alpha}(\mathbf{x}) \mathbf{b}^k \quad (4.36)$$

Introducing the notation $\mathbf{h}_{\alpha} = \sum_{k=1}^N h_{k,\alpha} \mathbf{b}^k$, one gets the following representation of any member of $\mathcal{H}^{(N)}$:

$$\mathbf{h}(\mathbf{x}) = \sum_{\alpha \in \mathbb{N}^M} \mathbf{h}_{\alpha} \Psi_{\alpha}(\mathbf{x}) \quad , \quad \mathbf{h}_{\alpha} \in \mathbb{R}^N \quad (4.37)$$

As a consequence, the random model response $\mathbf{Y} = \mathcal{M}(\mathbf{X})$ has a unique chaos representation:

$$\mathbf{Y} = \sum_{\alpha \in \mathbb{N}^M} \mathbf{y}_{\alpha} \Psi_{\alpha}(\mathbf{X}) \quad (4.38)$$

where the vector coefficients $\{\mathbf{y}_{\alpha}, \alpha \in \mathbb{N}^M\}$ have to be computed.

2.4 Practical implementation

For practical implementation, *finite dimensional* polynomial chaoses have to be built. The usual choice consists in selecting those multivariate polynomials that have a total degree $q = |\alpha| \equiv \sum_{i=1}^M \alpha_i$ less than a maximal degree p . The size of this finite-dimensional basis is denoted by P :

$$P = \binom{M+p}{p} \quad (4.39)$$

The full procedure requires the following steps:

- the construction of the sets of univariate orthogonal polynomials associated with each marginal PDF of the components of \mathbf{X} ;
- the computation of the associated norm of these polynomials, in order to make the basis orthonormal (see Eq.(4.25));
- an algorithm that builds the set of multi-indices α which correspond to the P multivariate polynomials based on M variables, whose degree is less than or equal to p . Ghanem and Spanos (1991a) proposed a strategy based on symbolic computing in case of Hermite chaos. A completely different algorithm, which is applicable to general chaoses, was proposed by the author in Sudret and Der Kiureghian (2000), see also Sudret et al. (2006).

2.5 Conclusion

The name *polynomial chaos* has been originally introduced together with an infinite numerable family of independent standard normal random variables $\{\xi_j, j \geq 0\}$ by Wiener (1938), in order to represent functions of Gaussian random processes. This representation was introduced in the late 80's by Ghanem and Spanos (1990, 1991a) in order to solve boundary value problems with stochastic coefficients. The Cameron-Martin theorem states that the obtained series expansion is L_2 -convergent (Cameron and Martin, 1947). The practical computation of the series expansion coefficients requires to truncate both the set of basic variables and the polynomial chaos expansion. The finite-dimensional approach then results in the same formalism as that developed in Section 2.3, although the starting point of the representation is conceptually different. However, it is believed that the formalism developed above is more fruitful, especially for generalizing to problems with input random vectors of arbitrary probability measure (see Soize and Ghanem (2004) for a detailed discussion).

3 Galerkin solution schemes

3.1 Brief history

The Spectral Stochastic Finite Element Method (SSFEM) was proposed by Ghanem and Spanos (1990, 1991b) in the early 90's to solve boundary value problems in mechanics with stochastic coefficients. The approach was presented in details in a book by the authors (Ghanem and Spanos, 1991a).

In the original presentation, the input quantities are represented by Gaussian random fields that are discretized by the Karhunen-Loève (KL) expansion (Eq.(2.66)). The model response, *i.e.* the vector of nodal displacements, is expanded onto the polynomial chaos. The solution to the problem is obtained by a Galerkin procedure in the random dimension.

This SSFEM was applied to various problems including geotechnical problems (Ghanem and Brzkala, 1996), transport in random media (Ghanem and Dham, 1998; Ghanem, 1998), non linear random vibrations (Li and Ghanem, 1998) and heat conduction (Ghanem, 1999c), in which non Gaussian fields were introduced (see also Ghanem (1999b)). A general framework that summarizes the various developments can be found in Ghanem (1999a).

In the last five years, a mathematical approach to stochastic elliptic problems has emerged, which complements the original SSFEM approach. Deb et al. (2001); Babuska and Chatzipantelidis (2002); Babuska et al. (2004); Frauenfelder et al. (2005) give a sound mathematical description of the variational form of the elliptic stochastic differential equations and discuss various strategies of resolution and error estimates, which are outside the scope of this document. The spectral approaches have also benefited much from advances in computational fluid mechanics, see *e.g.* Le Maître et al. (2001, 2002); Debusschere et al. (2003); Reagan et al. (2003) and a recent review by Knio and Le Maître (2006).

The Galerkin approach to solve partial differential equations is now summarized.

3.2 Deterministic elliptic problem

3.2.1 Problem statement

Let us consider a bounded set $\mathcal{B} \in \mathbb{R}^d$, $d = 1, 2, 3$ and a boundary value problem of the form:

$$\begin{aligned} \operatorname{div}(\mathbf{k}(\mathbf{x}) \cdot \nabla u(\mathbf{x})) + f(\mathbf{x}) &= 0 \quad \forall \mathbf{x} \in \mathcal{B} \\ u(\mathbf{x}) \Big|_{\Gamma_0} &= 0 \quad \nabla u(\mathbf{x}) \Big|_{\Gamma_1} = \bar{f}(\mathbf{x}) \quad \Gamma_0 \cup \Gamma_1 = \partial \mathcal{B} \end{aligned} \quad (4.40)$$

where the input $\mathbf{k}(\mathbf{x}), \bar{f}(\mathbf{x})$ satisfies sufficient conditions of regularity so that the problem has a unique solution. The variational form of this problem reads:

$$\text{Find } u \in \mathcal{V} : \quad \mathbf{a}(u, v) = \mathbf{b}(v) \quad \forall v \in \mathcal{V} \quad (4.41)$$

where \mathcal{V} is a suitable Hilbert space of functions that are zero on Γ_0 (e.g. $H_0^1(\mathcal{B})$) and where the bilinear (resp. linear) form $\mathbf{a}(\cdot, \cdot)$ (resp. $\mathbf{b}(\cdot)$) reads:

$$\begin{aligned} \mathbf{a}(u, v) &= \int_{\mathcal{B}} \nabla v(\mathbf{x})^\top \cdot \mathbf{k}(\mathbf{x}) \cdot \nabla u(\mathbf{x}) \, d\mathbf{x} \\ \mathbf{b}(v) &= \int_{\mathcal{B}} f(\mathbf{x}) v(\mathbf{x}) \, d\mathbf{x} + \int_{\Gamma_1} \bar{f}(\mathbf{x}) v(\mathbf{x}) \, d\mathbf{x} \end{aligned} \quad (4.42)$$

3.2.2 Galerkin method

The Galerkin solution to this problem consists in considering a series of discretized problems that are posed on subspaces of \mathcal{V} . Let \mathcal{V}^N be such a N -dimensional subspace, e.g. the subspace spanned by the shape functions associated with a mesh of domain \mathcal{B} in the finite element context. The discretized problem reads:

$$\text{Find } u^{(N)} \in \mathcal{V}^N : \quad \mathbf{a}(u^{(N)}, v^{(N)}) = \mathbf{b}(v^{(N)}) \quad \forall v^{(N)} \in \mathcal{V}^N \quad (4.43)$$

A basis of the subspace \mathcal{V}^N is chosen, say $\mathbf{b}(\mathbf{x}) \equiv \{b_1(\mathbf{x}), \dots, b_N(\mathbf{x})\}$, which allows one to introduce the coordinates of any function $u^{(N)}(\mathbf{x})$ of \mathcal{V}^N (resp. any function $v^{(N)}(\mathbf{x})$) in this basis:

$$u^{(N)}(\mathbf{x}) \equiv \sum_{i=1}^N u_i b_i(\mathbf{x}) \quad v^{(N)}(\mathbf{x}) \equiv \sum_{i=1}^N v_i b_i(\mathbf{x}) \quad (4.44)$$

For the sake of simplicity, these coordinates are gathered into a vector \mathbf{U} (resp. \mathbf{V}) and the following notation is used:

$$u^{(N)}(\mathbf{x}) = \mathbf{b}(\mathbf{x}) \cdot \mathbf{U} \quad v^{(N)}(\mathbf{x}) = \mathbf{b}(\mathbf{x}) \cdot \mathbf{V} \quad (4.45)$$

Substituting for Eqs.(4.44),(4.45) in Eqs.(4.42),(4.43), one gets:

$$\begin{aligned} \mathbf{a}(u^{(N)}, v^{(N)}) &= \mathbf{V}^\top \left(\int_{\mathcal{B}} \nabla \mathbf{b}(\mathbf{x})^\top \cdot \mathbf{k}(\mathbf{x}) \cdot \nabla \mathbf{b}(\mathbf{x}) \, d\mathbf{x} \right) \mathbf{U} \equiv \mathbf{V}^\top \mathbf{K} \mathbf{U} \\ \mathbf{b}(v) &= \mathbf{V}^\top \left(\int_{\mathcal{B}} f(\mathbf{x}) \mathbf{b}^\top(\mathbf{x}) \, d\mathbf{x} + \int_{\Gamma_1} \bar{f}(\mathbf{x}) \mathbf{b}^\top(\mathbf{x}) \, d\mathbf{x} \right) \equiv \mathbf{V}^\top \mathbf{F} \end{aligned} \quad (4.46)$$

The discretized problem in Eq.(4.43) rewrites:

$$\text{Find } \mathbf{U} \in \mathbb{R}^N : \quad \mathbf{V}^\top \mathbf{K} \mathbf{U} = \mathbf{V}^\top \mathbf{F} \quad \forall \mathbf{V} \in \mathbb{R}^N \quad (4.47)$$

which leads to the linear system:

$$\mathbf{K} \mathbf{U} = \mathbf{F} \quad (4.48)$$

When dealing with elastic mechanical problems, \mathbf{U} is the vector of nodal displacements (also called vector of primary unknowns), \mathbf{K} is the stiffness matrix and \mathbf{F} is the load vector. This well known formalism is now extended to address stochastic boundary value problems.

3.3 Stochastic elliptic problem

3.3.1 Problem statement

Let us now consider an elliptic stochastic boundary value problem, *i.e.* a partial differential equation whose coefficients are random fields. The “random” counterpart of Eq.(4.40) reads:

$$\begin{aligned} \operatorname{div}(\mathbf{k}(\mathbf{x}, \omega) \cdot \nabla u(\mathbf{x}, \omega)) + f(\mathbf{x}, \omega) &= 0 \quad \text{almost surely} \quad \forall \mathbf{x} \in \mathcal{B} \\ u(\mathbf{x}, \omega) \Big|_{\Gamma_0} &= 0 \quad \nabla u(\mathbf{x}, \omega) \Big|_{\Gamma_1} = \bar{f}(\mathbf{x}, \omega) \quad \text{almost surely} \end{aligned} \quad (4.49)$$

where $\mathbf{k}(\mathbf{x}, \omega)$, $f(\mathbf{x}, \omega)$ and $\bar{f}(\mathbf{x}, \omega)$ are random fields with suitable properties of regularity. Note that neither the domain of definition \mathcal{B} nor the portions Γ_0 and Γ_1 of its boundary are random in this formulation (see Clément et al. (2007) for problems with a random geometry).

The variational formulation of the problem leads to the introduction of a suitable functional space for the solution $u(\mathbf{x}, \omega)$. The natural tensor structure of the problem leads to select $\mathcal{V} \otimes \mathcal{W}$, where $\mathcal{W} = \mathcal{L}^2(\Omega, \mathcal{F}, \mathbb{P})$ is a reasonable choice. The variational form of the above problem then reads:

$$\text{Find } u \in \mathcal{V} \otimes \mathcal{W} : \quad \mathfrak{A}(u, v) = \mathfrak{B}(v) \quad \forall v \in \mathcal{V} \otimes \mathcal{W} \quad (4.50)$$

where the bilinear (resp. linear) form $\mathfrak{A}(\cdot, \cdot)$ (resp. $\mathfrak{B}(\cdot)$) reads:

$$\begin{aligned} \mathfrak{A}(u, v) &= \mathbb{E}[\mathfrak{a}(u, v)] = \int_{\Omega} \mathfrak{a}(u(\mathbf{x}, \omega), v(\mathbf{x}, \omega)) dP(\omega) \\ \mathfrak{B}(v) &= \mathbb{E}[\mathfrak{b}(v)] = \int_{\Omega} \mathfrak{b}(v(\mathbf{x}, \omega)) dP(\omega) \end{aligned} \quad (4.51)$$

3.3.2 Two-step Galerkin method

In order to solve the above problem by a Galerkin approach, suitable subspaces of $\mathcal{V} \otimes \mathcal{W}$ shall be selected. As in the deterministic finite element analysis, $\mathcal{V}^N \subset \mathcal{V}$ may be chosen as the subspace spanned by shape functions associated with a mesh of domain \mathcal{B} .

The Galerkin approximation *in the random dimension* requires the introduction of finite-dimensional subspaces $\mathcal{W}^P \subset \mathcal{W}$. In the literature, various approaches have been proposed:

- *polynomial chaos bases*: this is the original choice in SSFEM (where a Wiener-Hermite chaos was used), as well in the generalized chaos approach (Xiu and Karniadakis, 2003a,b; Keese and Matthies, 2005; Matthies and Keese, 2005). This corresponds to a spectral representation in the random dimension;
- bounded support functions such as *wavelets* (Le Maître et al., 2004a,b) or finite element-like basis functions (Deb et al., 2001);
- combinations of both types (Wan and Karniadakis, 2005).

In the sequel, we will focus on polynomial chaos representations. For this purpose, it is supposed that the input random fields in Eq.(4.49) are discretized using a set of M random variables $\{X_i, i = 1, \dots, M\}$ gathered in a random vector $\mathbf{Z}(\omega)$ of known PDF (*e.g.* using the Karhunen-Loève expansion, see Chapter 2, Section 4). As shown in Section 2, it is possible to represent any random variable of second order as an expansion onto a generalized polynomial chaos $\{\Psi_{\alpha}(\mathbf{Z}(\omega)), \alpha \in \mathbb{N}^M\}$, whose basis elements will be simply denoted by Ψ_{α} from now on for the sake of clarity.

Let \mathcal{W}^P be the subspace of \mathcal{W} defined by:

$$\mathcal{W}^P = \text{span}\{\Psi_{\alpha}, 0 \leq |\alpha| \leq p\} \quad , \quad P = \binom{M+p}{p} \quad (4.52)$$

The Galerkin approximation of the problem defined in Eqs.(4.50),(4.51) reads:

$$\text{Find } u^{(N,P)} \in \mathcal{V}^N \otimes \mathcal{W}^P : \quad \mathfrak{A}(u^{(N,P)}, v^{(N,P)}) = \mathfrak{B}(v^{(N,P)}) \quad \forall v^{(N,P)} \in \mathcal{V}^N \otimes \mathcal{W}^P \quad (4.53)$$

Again, a vector notation is introduced to represent any random field $u^{(N,P)}$ (resp. $v^{(N,P)}$) by its coordinates onto the tensor product basis $\{b_i(\mathbf{x}) \otimes \Psi_{\alpha}, i = 1, \dots, N, 0 \leq |\alpha| \leq p\}$:

$$u^{(N,P)}(\mathbf{x}, \omega) \equiv \sum_{0 \leq |\alpha| \leq p} \mathbf{b}(\mathbf{x}) \cdot \mathbf{U}_{\alpha} \Psi_{\alpha} \quad (4.54)$$

$$v^{(N,P)}(\mathbf{x}, \omega) \equiv \sum_{0 \leq |\alpha| \leq p} \mathbf{b}(\mathbf{x}) \cdot \mathbf{V}_{\alpha} \Psi_{\alpha} \quad (4.55)$$

Gathering the vectors $\{\mathbf{U}_{\alpha}, 0 \leq |\alpha| \leq p\}$ (resp. $\{\mathbf{V}_{\alpha}, 0 \leq |\alpha| \leq p\}$) into a block vector \mathbf{U} (resp. \mathbf{V}) of size $N \times P$, the problem in Eq.(4.53) rewrites:

$$\text{Find } \mathbf{U} \in \mathbb{R}^{N \times P} : \quad \sum_{0 \leq |\alpha| \leq p} \sum_{0 \leq |\beta| \leq p} \mathbf{V}_{\alpha}^T \mathbb{E}[\mathbf{K}(\omega) \Psi_{\alpha} \Psi_{\beta}] \mathbf{U}_{\beta} = \mathbf{V}_{\alpha}^T \mathbb{E}[\mathbf{F}(\omega) \Psi_{\alpha}] \quad \forall \mathbf{V} \in \mathbb{R}^{N \times P} \quad (4.56)$$

which reduces to a set of linear equations:

$$\sum_{0 \leq |\beta| \leq p} \mathbb{E}[\mathbf{K}(\omega) \Psi_{\alpha} \Psi_{\beta}] \mathbf{U}_{\beta} = \mathbb{E}[\mathbf{F}(\omega) \Psi_{\alpha}] \quad \forall \alpha : \quad 0 \leq |\alpha| \leq p \quad (4.57)$$

These equations are usually arranged in a unique linear system:

$$\mathbf{K} \mathbf{U} = \mathbf{F} \quad (4.58)$$

where \mathbf{F} is the block vector whose α -th block is $\mathbf{F}_{\alpha} = \mathbb{E}[\mathbf{F}(\omega) \Psi_{\alpha}]$, and \mathbf{K} is a block matrix whose (α, β) -block is $\mathbf{K}_{\alpha\beta} = \mathbb{E}[\mathbf{K}(\omega) \Psi_{\alpha} \Psi_{\beta}]$.

3.4 Computational issues

The linear system in Eq.(4.58) is of size $N \times P$ and usually very sparse, as seen in Figure 4.1 where the non zero terms of \mathbf{K} have been plotted for various order of expansion M of the input random field (resp. various PC maximal degree p). This sparsity is twofold:

- first, each block matrix $\mathbf{K}_{\alpha\beta}$ has the same (sparse) structure as the stiffness matrix associated to the deterministic problem;
- second, if the stochastic stiffness matrix is itself represented by a spectral representation, say $\mathbf{K}(\omega) = \sum_{0 \leq |\gamma| \leq p_K} \mathbf{K}_{\gamma} \Psi_{\gamma}$, the blocks in \mathbf{K} read:

$$\mathbf{K}_{\alpha\beta} = \sum_{0 \leq |\gamma| \leq p_K} \mathbb{E}[\Psi_{\alpha} \Psi_{\beta} \Psi_{\gamma}] \mathbf{K}_{\gamma} \quad (4.59)$$

in which many spectral products $\mathbb{E}[\Psi_{\alpha} \Psi_{\beta} \Psi_{\gamma}]$ and consequently many blocks $\mathbf{K}_{\alpha\beta}$ vanish.

Consequently, due to the large size and sparsity of \mathbf{K} , the system in Eq.(4.58) is not solved by direct resolution techniques. Indeed, the memory requirements and computational cost when assembling this matrix would be prohibitive. Krylov-type iterative solvers are thus preferred, namely preconditioned conjugate gradient techniques, see Ghanem and Kruger (1996); Pellissetti and Ghanem (2000); Chung et al. (2005). The preconditioner is classically taken as a block diagonal matrix corresponding to the mean stiffness matrix.

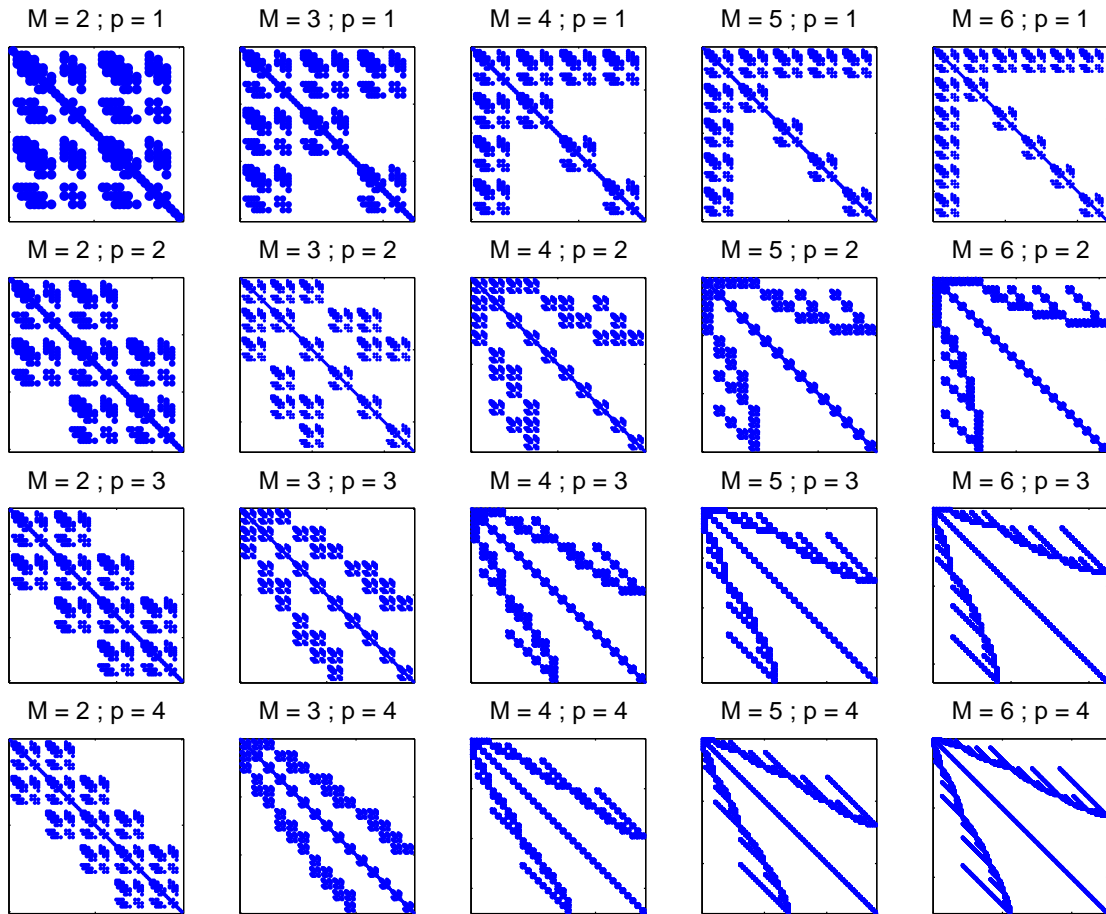


Figure 4.1: Non zero entries in a linear system resulting from the Galerkin solution to an elliptic stochastic differentiable equation

3.5 Conclusion

The Spectral Stochastic Finite Element Method has been presented as a strategy to solve elliptic stochastic partial differential equations. A variational form of these equations is given first. Then the problem is solved by a Galerkin strategy in a tensor product Hilbert space $\mathcal{V} \otimes \mathcal{W}$, where \mathcal{V} is the approximation space in deterministic finite element analysis and \mathcal{W} is the space of random variables with finite second moments.

In the linear case, the original problem reduces to a linear system of size $N \times P$, where N is the number of degrees of freedom of the discretized deterministic problem, and P is the number of terms in the polynomial chaos expansion of the solution. This Galerkin strategy has been called “intrusive” in the sense that it requires a specific implementation for each problem under consideration.

The intrusive approach to solve stochastic finite element problems has focused much of the attention devoted by the researchers to this topic since the early 90’s (not only for elliptic problems). Indeed:

- it is a natural extension of the classical finite element method “in the random dimension”. Thus theoretical results on convergence, error estimates, etc. can be proven (Deb et al., 2001; Frauenfelder et al., 2005);
- adaptive strategies can be developed from well known results in deterministic finite element analysis

(Le Maître et al., 2004a,b; Wan and Karniadakis, 2005).

On the other hand, various drawbacks of the intrusive approaches have been observed, namely:

- the Galerkin-like discretization of the equations both in the physical and in the random space leads to a complex system of equations of large size. Although specific solvers that are suited to large sparse systems have been proposed, the computational time and memory requirements remain an issue when dealing with complex systems. Note that a generalized spectral decomposition has been recently proposed by Nouy (2005, 2007), where the terms in the expansion are computed step-by-step as solutions of generalized eigenvalue problems. This method appears promising for a drastic reduction of the computational burden.
- the stochastic problem has to be solved in terms of *all* the primal unknowns *e.g.* nodal displacements, temperature, etc. at once. If the analyst is interested only in the random description of a specific part of the response, he or she should solve the full coupled system anyway.
- if the analyst is interested in *derived* quantities (such as strain or stress components, stress intensity factors, etc.), the projection of these quantities onto the PC basis requires additional effort. This can be a hard task in itself when non linear functions of the primal unknowns are of interest (see Debusschere et al. (2003) for possible strategies). In practice, non linear problems involving *e.g.* plasticity, contact, large strains, etc. have not been given generic solutions so far, although attempts can be found in Li and Ghanem (1998); Anders and Hori (2001); Acharjee and Zabaras (2006).
- From an industrial point of view, the intrusive approach reveals inappropriate in the sense that it requires specific developments and subsequent implementation for each new class of problems. This means that legacy codes cannot be used without deep modifications of the source code.

In order to bypass most of these difficulties, non intrusive solution schemes have emerged in the last five years. They are now presented from the author's personal viewpoint.

4 Non intrusive methods

4.1 Introduction

The term *non intrusive spectral methods* denotes a class of computational schemes that allow the analyst to compute the polynomial chaos coefficients from a series of calls to the deterministic model, instead of a Galerkin-type computation. In contrast to that approach, no specific modification of the deterministic code is necessary (it is used "as is" for selected values of the input vector). Two different approaches have been recently proposed in the literature, namely projection and regression.

The *projection* method has been introduced in Ghanem and Ghiocel (1998); Ghiocel and Ghanem (2002) in the context of seismic soil-structure interaction, Ghanem et al. (2000) for the study of the eigenmodes of a spatial frame structure and Field et al. (2000); Field (2002) in a non linear shock and vibration analysis. Le Maître et al. (2002) makes use of the same so-called *non intrusive spectral projection* (NISP) to solve a natural convection problem in a square cavity.

The *regression* method has been introduced by Choi et al. (2004b); Berveiller (2005) based on early results in ocean engineering by Tatang (1995); Tatang et al. (1997) and Isukapalli (1999) under the name "probabilistic collocation methods".

Both approaches are now reviewed in a unified presentation and discussed.

4.2 Projection methods

4.2.1 Introduction

Let us assume that the random response of a model, say $Y = \mathcal{M}(\mathbf{X})$, is represented onto a generalized PC expansion:

$$Y = \sum_{\alpha \in \mathbb{N}^M} y_{\alpha} \Psi_{\alpha}(\mathbf{X}) \quad (4.60)$$

Due to the orthogonality of the PC expansion, each coefficient is nothing but the projection of the response Y onto the α -th dimension. Indeed, by premultiplying (4.60) by Ψ_{β} and by taking the expectation, one gets:

$$\mathbb{E}[Y \Psi_{\alpha}(\mathbf{X})] = \sum_{\beta \in \mathbb{N}^M} y_{\beta} \mathbb{E}[\Psi_{\alpha}(\mathbf{X}) \Psi_{\beta}(\mathbf{X})] \quad (4.61)$$

where the expectation in the summation is equal to one if $\alpha = \beta$ and zero otherwise. Hence:

$$y_{\alpha} = \mathbb{E}[Y \Psi_{\alpha}(\mathbf{X})] \quad (4.62)$$

Reminding that the expectation is related to the underlying probability measure $P_{\mathbf{X}}$, one gets:

$$y_{\alpha} = \mathbb{E}[\mathcal{M}(\mathbf{X}) \Psi_{\alpha}(\mathbf{X})] = \int_{\mathcal{D}_{\mathbf{X}}} \mathcal{M}(\mathbf{x}) \Psi_{\alpha}(\mathbf{x}) f_{\mathbf{X}}(\mathbf{x}) d\mathbf{x} \quad (4.63)$$

The two different expressions for y_{α} in the above equation lead to two classes of projection schemes:

- *simulation methods*, which correspond to evaluating the expectation as the empirical mean of the expression within the brackets;
- *quadrature methods*, which corresponds to evaluating numerically the integral in (4.63) by multidimensional quadrature schemes.

4.2.2 Simulation methods

Monte Carlo simulation This approach is the crudest technique to compute $y_{\alpha} = \mathbb{E}[\mathcal{M}(\mathbf{X}) \Psi_{\alpha}(\mathbf{X})]$. A sample set of input vectors $\{\mathbf{x}^{(i)}, i = 1, \dots, n\}$ is drawn according to the distribution $f_{\mathbf{X}}$ (see Appendix A). Then the empirical mean is evaluated:

$$\hat{y}_{\alpha}^n = \frac{1}{n} \sum_{i=1}^n \mathcal{M}(\mathbf{x}^{(i)}) \Psi_{\alpha}(\mathbf{x}^{(i)}) \quad (4.64)$$

From a statistical point of view, the variance of this estimator denoted by \hat{Y}_{α}^n reads:

$$\text{Var}[\hat{Y}_{\alpha}^n] = \text{Var}[\mathcal{M}(\mathbf{X}) \Psi_{\alpha}(\mathbf{X})] / n \quad (4.65)$$

This shows the well-known $\mathcal{O}(1/\sqrt{n})$ convergence rate of Monte Carlo simulation. Such a crude MCS scheme has been originally applied in Field et al. (2000); Ghiocel and Ghanem (2002) in the context of stochastic finite element analysis.

Latin Hypercube Sampling Latin Hypercube Sampling(LHS) was first proposed by McKay et al. (1979). It is a stratified sampling technique, which aims at yielding samples that are better distributed in the sample space than those obtained by MCS.

Suppose a n -sample set is to be drawn and the input random variables are independent. The PDF of each input variable is divided into n bins (or stratas) having the same weight $1/n$. Exactly one sample is

drawn in each bin and each dimension. Then the samples in each dimension are paired using an algorithm that allows to have a satisfying space-filling. The convergence of LHS is usually faster than that of crude MCS. Due to the correlation of the samples, no direct estimation of the accuracy is available though. When the input variables are correlated, specific modifications of the sampling scheme have to be done. LHS has been used in the context of stochastic finite element analysis by Le Maître et al. (2002).

Quasi-random numbers Quasi-random numbers, also known as *low discrepancy sequences*, are deterministic sequences that allow one to fill uniformly a unit hypercube $[0, 1]^M$ (Niederreiter, 1992; Morokoff and Caffisch, 1995). Several types of sequences have been proposed, namely the Halton, Faure and Sobol' sequences. As an illustration, the latter is briefly described in the sequel.

Let us consider the binary expansion of a natural integer n :

$$n \equiv (q_m \cdots q_0)_2 \quad (4.66)$$

The n -th term of the Sobol' sequence reads:

$$u^{(n)} = \sum_{i=0}^m \frac{q_i}{2^{i+1}} \quad (4.67)$$

Figure 4.2 shows the space-filling process of $[0,1]$ using this technique.

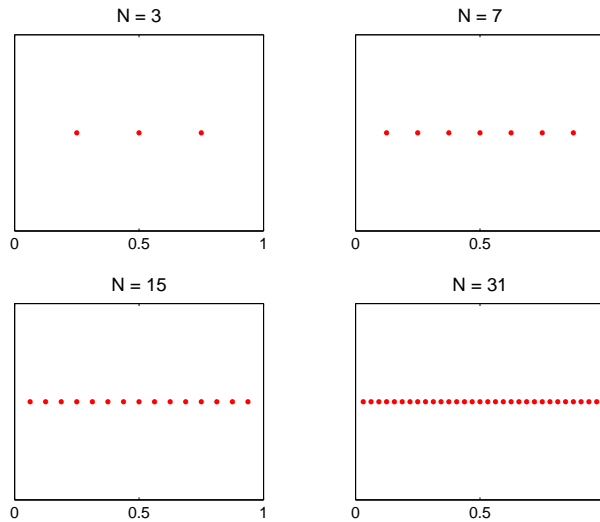


Figure 4.2: Space-filling process of $[0,1]$ using a unidimensional Sobol' sequence

The M -dimensional sequences are built by pairing M permutations of the unidimensional sequences. Figure 4.3 shows the space-filling process of $[0,1]^2$ using a two-dimensional Sobol' sequence. Figure 4.4 compares the filling obtained by MCS, LHS and the Sobol' sequence for $n = 512$ points. The better uniformity of the latter is obvious in this figure.

The use of quasi-random numbers in the context of stochastic finite element has been originally mentioned in Keese (2004). Upon introducing a mapping from $\mathcal{D}_{\mathbf{X}}$ to $[0,1]^M$, the integral in Eq.(4.63) reads:

$$y_{\alpha} = \int_{[0,1]^M} \mathcal{M}(T^{-1}(\mathbf{u})) \Psi_{\alpha}(T^{-1}(\mathbf{u})) d\mathbf{u} \quad (4.68)$$

where $T : \mathbf{X} \mapsto \mathbf{U}$ is the isoprobabilistic transform that maps each component of \mathbf{X} into a uniform random variable $\mathcal{U}[0,1]$. Let $\{\mathbf{u}^{(1)}, \dots, \mathbf{u}^{(n)}\}$ be a set of n quasi-random numbers. The *quasi-Monte*

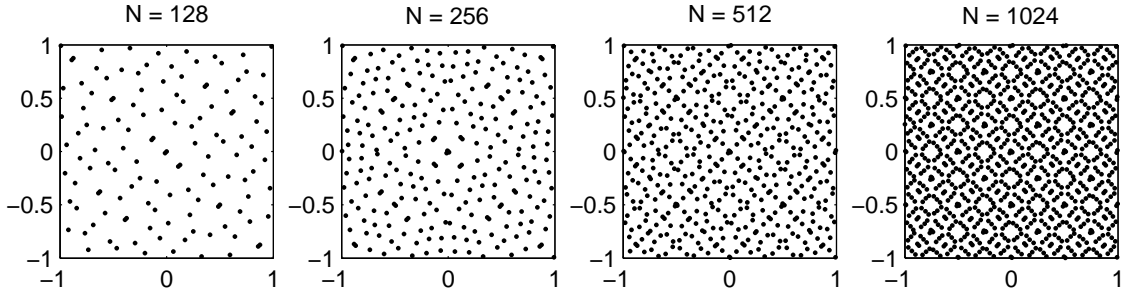


Figure 4.3: Space-filling process of $[0,1]^2$ using a two-dimensional Sobol' sequence

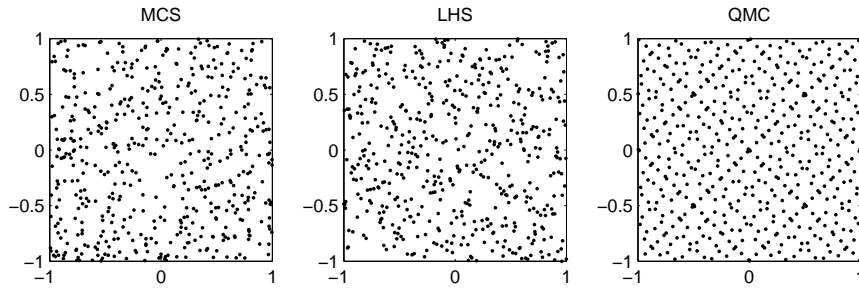


Figure 4.4: Space-filling process of $[0,1]^2$: comparison of MCS, LHS and QMC sampling schemes ($n = 512$ points)

Carlo (QMC) estimate of y_α is given by:

$$\hat{y}_\alpha^{n,QMC} = \frac{1}{n} \sum_{i=1}^n \mathcal{M} \left(T^{-1}(\mathbf{u}^{(i)}) \right) \Psi_\alpha \left(T^{-1}(\mathbf{u}^{(i)}) \right) \quad (4.69)$$

The Koksma-Hlawka inequality (Morokoff and Caflisch, 1995) provides an upper bound of the absolute error:

$$|y_\alpha - \hat{y}_\alpha^{n,QMC}| \leq V(\mathcal{M}(T^{-1})\psi_\alpha(T^{-1})) D_n(\mathbf{u}^{(1)}, \dots, \mathbf{u}^{(n)}) \quad (4.70)$$

where $V(f)$ denotes the so-called *total variation* of a function f , which depends on the mixed derivatives of this function, and D_n represents the *star discrepancy* of the quasi-random sample, which measures its uniformity. The Sobol' sequence presented above has a star discrepancy D_n which converges at the rate $\mathcal{O}(n^{-1} \log^M(n))$, *i.e.* faster than MCS.

Conclusion From the experience of the author, it clearly appears that the quasi-random numbers outperform the classical simulation methods such as MCS and LHS. The different quasi-random sequences mentioned above (namely the Halton, Faure and Sobol' sequences) have been used to compute the PCE coefficients of analytical models in Sudret et al. (2007) and compared. In the average, the Sobol' sequence appears more efficient than the other two. The relative efficiency of MCS, LHS and the Sobol' sequence has been compared on the example of a truss structure in Blatman et al. (2007a,b).

4.2.3 Quadrature methods

Tensorized quadrature The use of quadrature schemes to compute multidimensional integrals has been already mentioned in Chapter 3, Section 2.4 in the context of second moment analysis. To elaborate

on this method, let us first introduce the following notation for the quadrature of a multivariate function $h : \mathbb{R}^M \mapsto \mathbb{R}$

$$\mathcal{Q}^\nu(h) \equiv \mathcal{Q}^{(\nu_1, \dots, \nu_M)}(h) \equiv \sum_{i_1=1}^{\nu_1} \dots \sum_{i_M=1}^{\nu_M} \omega_{i_1} \dots \omega_{i_M} h(x_{i_1} \dots i_M) \quad (4.71)$$

The application of the latter equation to the integral in Eq.(4.63) leads to:

$$\hat{y}_\alpha^\nu = \mathcal{Q}^\nu(\mathcal{M} \Psi_\alpha) \quad (4.72)$$

where $\nu = (\nu_1, \dots, \nu_M)$ is a M -uplet containing the order of the quadrature scheme along each dimension (the notation \hat{y}_α^ν recalls what type of integration scheme has been used for the estimation of y_α).

To select the multidimensional quadrature scheme, the following heuristic arguments can be referred to. Suppose first that the model \mathcal{M} is polynomial of order p and consider its p -th order PC expansion (which shall be exact). The integrand in Eq.(4.63) is polynomial of degree less or equal than $2p$. In case of a single input variable ($M = 1$), a quadrature scheme corresponding to $\nu = p + 1$ would give the exact result. As an extension, a quadrature scheme $\nu = (p + 1, \dots, p + 1)$ is suited to the multivariate case $M > 1$.

Consider now a general (*i.e.* non polynomial) model. When selecting a p -th order PC expansion, it is believed that the remaining terms in the series are negligible. Thus the quadrature scheme $\nu = (p + 1, \dots, p + 1)$ is usually used again. This scheme requires $(p + 1)^M$ evaluations of the model. This number obviously blows up when M increases: this problem is known as the *curse of dimensionality* and shall be solved using alternative quadrature schemes.

Smolyak quadrature scheme Let us first observe that the full tensorized scheme is somehow too accurate, even for polynomial models \mathcal{M} . Indeed, when a p -th degree PCE is considered, the integrand in Eq.(4.63) is a multivariate polynomial of *total* degree less than or equal to $2p$. In contrast, the quadrature scheme \mathcal{Q}^ν exactly integrates multivariate polynomials obtained as products of univariate polynomials up to degree p , *i.e.* having a total degree of $M \times p$.

An alternative so-called *sparse quadrature* scheme originally introduced by Smolyak (1963) has been proposed to solve the curse of dimensionality (Novak and Ritter, 1996; Gerstner and Griebel, 1998). Using the notation in Eq.(4.71), Smolyak's formula reads:

$$\mathcal{Q}_{Smolyak}^{M,l} \equiv \sum_{l \leq |\mathbf{k}| \leq l+M-1} (-1)^{l+M-|\mathbf{k}|+1} \binom{M-1}{|\mathbf{k}|-l} \mathcal{Q}^{\mathbf{k}} \quad (4.73)$$

It allows to integrate exactly multivariate polynomials of total degree p , which is exactly what is required in Eq.(4.63).

The use of Smolyak cubature in non intrusive spectral projection has been mentioned by Keese (2004) and applied by Le Maître et al. (2004a). Recently, the mathematical aspects of the use of sparse grids (*e.g.* convergence and error estimators) in stochastic collocation methods have been studied in Babuska et al. (2007); Xiu (2007).

4.3 Regression methods

4.3.1 Introduction

Linear regression techniques have been used for decades in order to build functional relationships between variables from which data sets are available (Saporta, 2006). In various domains of engineering, response surfaces are built from experiences that are carried out according to an *experimental design*.

The coefficients of these response surfaces are obtained by regression. Finding an optimal experimental design has focused much attention in this context (Atkinson and Donev, 1992; Gauchi, 1997; Myers and Montgomery, 2002).

In the context of uncertainty propagation, the idea of building a surrogate model in the *probabilistic space* emerged in the pioneering work by Tatang (1995); Pan et al. (1997); Tatang et al. (1997) who proposed a *probabilistic collocation method*. In this work, Gaussian input random variables were used and it was proposed to use an experimental design based on the roots of the Hermite polynomials, the size of the latter being exactly that of the set of unknown coefficients.

Due to poor results when using the collocation scheme in large dimensions, Isukapalli (1999) introduced a *stochastic response surface method*. In this approach, the size of the experimental design is larger than the number of unknown coefficients (*e.g.* $n = 2P$) and the points are selected by a rule of thumb.

The application of these ideas in the context of stochastic finite element analysis has been thoroughly studied in Berveiller (2005), where various experimental designs are investigated. An original overview of these results is now presented.

4.3.2 Problem statement

The generalized PC expansion in Eq.(4.60) is truncated in practice for computational purpose. The series expansion can thus be viewed as the sum of a truncated series and a residual:

$$Y = \mathcal{M}(\mathbf{X}) = \sum_{j=0}^{P-1} y_j \Psi_j(\mathbf{X}) + \varepsilon_P \quad (4.74)$$

where $P = \binom{M+p}{p}$ if all the multivariate polynomials $\Psi_{\alpha}(\mathbf{X})$ such that $0 \leq |\alpha| \leq p$ are considered (and numbered from 0 to $P-1$). Introducing the vector notation:

$$\mathbf{Y} = \{y_0, \dots, y_{P-1}\}^T \quad (4.75)$$

$$\Psi(\mathbf{x}) = \{\Psi_0(\mathbf{x}), \dots, \Psi_{P-1}(\mathbf{x})\}^T \quad (4.76)$$

Eq.(4.74) rewrites:

$$Y = \mathbf{Y}^T \Psi(\mathbf{X}) + \varepsilon_P \quad (4.77)$$

A natural way of computing the unknown response coefficients \mathbf{Y} is to consider Eq.(4.77) as a regression problem. Minimizing the mean-square error of the residual leads to the following problem:

$$(P1) : \quad \hat{\mathbf{Y}} = \arg \min_{\mathbf{Y} \in \mathbb{R}^P} \mathbb{E} \left[\left(\mathcal{M}(\mathbf{X}) - \mathbf{Y}^T \Psi(\mathbf{X}) \right)^2 \right] \quad (4.78)$$

4.3.3 Equivalence with the projection method

The solution to this optimization problem is straightforward. Expanding the terms in the brackets in Eq.(4.78) yields:

$$\hat{\mathbf{Y}} = \arg \min_{\mathbf{Y} \in \mathbb{R}^P} \mathbb{E} \left[\mathcal{M}^2(\mathbf{X}) - 2\mathbf{Y}^T \Psi(\mathbf{X}) + \mathbf{Y}^T \Psi(\mathbf{X}) \Psi(\mathbf{X})^T \mathbf{Y} \right] \quad (4.79)$$

The last term reduces to $\mathbf{Y}^T \mathbf{Y}$ since $\mathbb{E} [\Psi(\mathbf{X}) \Psi(\mathbf{X})^T] = \mathbf{I}_P$ is the identity matrix due to the orthonormality of the PC basis. Hence:

$$\hat{\mathbf{Y}} = \arg \min_{\mathbf{Y} \in \mathbb{R}^P} \mathbb{E} \left[\mathbf{Y}^T \mathbf{Y} - 2\mathbf{Y}^T \Psi(\mathbf{X}) + \mathcal{M}^2(\mathbf{X}) \right] \quad (4.80)$$

The expression within the brackets attains its minimum when its derivative with respect to \mathbf{Y} is zero, which yields:

$$\mathbf{Y} = \mathbb{E}[\mathcal{M}(\mathbf{X})\Psi(\mathbf{X})] \quad (4.81)$$

This means that the exact solution to the regression problem is the projection result (see Eq.(4.62)), which proves the theoretical equivalence between the regression and projection approaches. This statement was originally pointed out in Sudret (2005b) in the context of stochastic finite element analysis.

However, recasting the problem as in Eq.(4.78) paves the path to other resolution techniques. In practice, the mean-square minimization in that equation is replaced by a *computational* mean-square minimization problem defined as follows:

$$(P1): \quad \hat{\mathbf{Y}} = \arg \min_{\mathbf{Y} \in \mathbb{R}^P} \hat{\mathbb{E}} \left[\left(\mathcal{M}(\mathbf{X}) - \mathbf{Y}^\top \Psi(\mathbf{X}) \right)^2 \right] \quad (4.82)$$

where $\hat{\mathbb{E}}[\cdot]$ is a deterministic or statistical estimation of the mean-square error evaluated from a set of realizations of the residual ε_P .

In the sequel, the set of realizations of the input random vector that is used for this estimation is called *experimental design* and denoted by $\{\mathbf{x}^{(1)}, \dots, \mathbf{x}^{(n)}\}$.

4.3.4 Various discretized regression problems

Random or quasi-random design The expectation in Eq.(4.82) can be evaluated using one of the simulation techniques presented in Section 4.2.2, namely MCS, LHS, QMC. Suppose n samples of the input random vector are drawn according to its distribution $f_{\mathbf{X}}$. The minimization problem is approximated by:

$$(P2): \quad \hat{\mathbf{Y}} = \arg \min_{\mathbf{Y} \in \mathbb{R}^P} \frac{1}{n} \sum_{i=1}^n \left[\mathcal{M}(\mathbf{x}^{(i)}) - \mathbf{Y}^\top \Psi(\mathbf{x}^{(i)}) \right]^2 \quad (4.83)$$

Problem (P2) is nothing but a least-square minimization problem. Introducing the notation $\mathfrak{M} = \{\mathcal{M}(\mathbf{x}^{(1)}), \dots, \mathcal{M}(\mathbf{x}^{(n)})\}^\top$ and denoting by \mathbf{A} the matrix whose entries read:

$$\mathbf{A}_{ij} = \Psi_j(\mathbf{x}^{(i)}) \quad (4.84)$$

the solution to (P2) reads:

$$\hat{\mathbf{Y}} = (\mathbf{A}^\top \mathbf{A})^{-1} \mathbf{A}^\top \mathfrak{M} \quad (4.85)$$

Such an approach has been applied using a LHS experimental design by Choi et al. (2004b,a); Choi et al. (2006).

Roots of orthogonal polynomials Isukapalli (1999) proposed to build an experimental design based on the roots of orthogonal polynomials. This idea comes from results on optimal experimental designs in classical response surface methods using polynomial regressors (Fedorov, 1972; Villadsen and Michelsen, 1978; Gauchi, 1997). Following this idea, Berveiller (2005) studied in details the accuracy of various schemes in the context of Hermite polynomial chaos. The optimal resulting procedure eventually obtained is now summarized:

- Suppose a PC expansion of maximal degree p is selected. The roots of the Hermite polynomial of next order He_{p+1} are computed, say $\{r_1, \dots, r_{p+1}\}$.
- All the possible M -uplets $\{\mathbf{r}_k, k = 1, \dots, (p+1)^M\}$ are built from these roots:

$$\mathbf{r}_k = (r_{i_1}, \dots, r_{i_M}) \quad 1 \leq i_1 \leq \dots \leq i_M \leq p+1 \quad (4.86)$$

- These M -uplets are sorted according to their increasing norm $\|\mathbf{r}\|$ in ascending order and the n M -uplets with smallest norm are retained. In case of Hermite chaos, these M -uplets correspond to the largest values of the joint PDF of the basic random vector $\boldsymbol{\xi}$.

From a comprehensive parametric study on various problems, Berveiller (2005) shows that $n \approx (M-1)P$ is an optimal size for the experimental design, since additional points do not change much the obtained PCE coefficients. Sudret (2008a) shows that the accuracy of the results is related to the conditioning of the information matrix $\mathbf{A}^\top \mathbf{A}$ (see Eq.(4.85)) and proposes an iterative construction of the latter. Such an approach has been applied in Berveiller et al. (2004a,b, 2005a, 2006) and recently in Huang et al. (2007) for problems involving random fields.

Weighted regression The expectation in Eq.(4.78) may be considered as an integral which may be evaluated by quadrature. Thus the minimization problem:

$$(P3) : \quad \hat{\mathbf{Y}} = \arg \min_{\mathbf{Y} \in \mathbb{R}^P} \mathcal{Q}^\nu \left(\left[\mathcal{M}(\mathbf{x}) - \mathbf{Y}^\top \boldsymbol{\Psi}(\mathbf{x}) \right]^2 \right) \quad (4.87)$$

(P3) can be interpreted as a weighted least-square minimization problem, whose solution reads:

$$\hat{\mathbf{Y}} = (\mathbf{A}^\top \mathbf{W} \mathbf{A})^{-1} \mathbf{W} \mathbf{A}^\top \mathfrak{M} \quad (4.88)$$

where \mathbf{A} has been defined in Eq.(4.84) and $\mathbf{W} = \text{diag}(\omega_1, \dots, \omega_n)$ is the diagonal matrix containing the integration weights of the quadrature scheme \mathcal{Q}^ν . This weighted regression scheme could be applied together with a sparse grid design or full tensorized design.

4.4 Conclusion

The various non intrusive methods presented in this section allow the analyst to compute the PCE coefficients based on a series of calls to the model function \mathcal{M} . The input vectors for which the model is run are known in advance. Thus these model evaluations can be easily parallelized over a cluster of processors. Moreover, the computational machinery may be implemented once and for all, in contrast to the intrusive Galerkin approach. Any model with uncertain input may be dealt with without any limitation on its physical content. The knowledge accumulated in legacy codes is thus fully taken advantage of. As already observed, the non intrusive approaches are of course not limited to finite element models.

Problems involving random fields may be solved using any of the non intrusive methods provided the input random field(s) have been previously discretized. Any of the discretization methods reviewed in Chapter 2, Section 4 may be used, meaning that it is not necessary to resort to Karhunen-Loève expansions.

In contrast to the Galerkin approach, the computational cost does not blow up when the size N of the response vector increases. Indeed, the computational cost simply increases along with the unit cost of a deterministic finite element analysis. Note that in case of finite element models, only the response quantities of interest (*e.g.* selected nodal displacements, stress components or post-processed quantities thereof) may be considered. Provided the full response vector of each finite element analysis has been stored in a database, the cost of the PC expansion of an additional response quantity (which would have been disregarded in a first step) reduces to a matrix-vector product.

When using projection techniques, and assuming that the computational cost of each model evaluation (*i.e.* $y^{(i)} = \mathcal{M}(\mathbf{x}^{(i)})$) is the main issue, it seems obvious that evaluating a large number of coefficients at once (*i.e.* selecting a rather large value of p and associated number of coefficients P) may be a good strategy. This is not the case though. Indeed, the accuracy of the estimates of the PC coefficients deteriorates with the order of the coefficients in the expansion. This may be explained as follows:

- if a sampling method such as Monte Carlo simulation is used, the variance of the estimator of the coefficients increases with the order of the coefficient in the expansion. Thus, for a fixed number of samples, the low order coefficients are better estimated than the higher order ones. The inaccuracy in the latter may then pollute the post-processed quantities (see next section).
- if a quadrature method of a fixed order is used, the lower order coefficients are again estimated more accurately than the higher order ones, since they correspond to lower degree polynomial functions.

As a conclusion, the order of expansion should be carefully selected together with the computational projection scheme.

When regression techniques are considered, the truncation of the series is selected *ab initio*, which introduces a first potential error. Then an experimental design is built according to this choice. If it is poorly chosen, the obtained coefficients may be quite far away from their true value, even if the selected truncated expansion was in principle accurate enough. Consequently, there are two potential sources of inaccuracy that should be taken care of simultaneously.

In all cases, it is important in the future to develop adaptive strategies that could jointly yield the optimal PC expansion together with the optimal computational scheme for its evaluation. This work is currently in progress (Blatman, 2007).

5 Post-processing of the PCE coefficients

The spectral methods described in the previous sections yield an intrinsic representation of the random response of a model in terms of its polynomial chaos expansion:

$$Y = \sum_{j=0}^{P-1} y_j \Psi_j(\mathbf{X}) \quad (4.89)$$

For practical interpretation, the coefficients of this expansion should be post-processed to derive quantities of interest. In this section, the computation of the probability density function of the response and its statistical moments is successively presented. Then the use of PC expansion in structural reliability and sensitivity analysis is described.

5.1 Response probability density function

In order to obtain a graphical representation of the response PDF, the series expansion in Eq.(4.89) may be simulated using MCS. This yields a sample set of response quantities, say $\{y^{(i)}, i = 1, \dots, n\}$. From this set, an histogram may be built. Smoother representations may be obtained using *kernel smoothing* techniques, see *e.g.* Wand and Jones (1995).

Broadly speaking, the *kernel density approximation* of the response PDF is given by:

$$\hat{f}_Y(y) = \frac{1}{n h_K} \sum_{i=1}^n K\left(\frac{y - y^{(i)}}{h_K}\right) \quad (4.90)$$

In this expression, $K(x)$ is a suitable positive function called kernel, and h_K is the bandwidth parameter. Well-known kernels are the Gaussian kernel (which is the standard normal PDF) and the Epanechnikov kernel $K_E(x) = \frac{3}{4}(1 - x^2) \mathbf{1}_{|x| \leq 1}$. The bandwidth parameter is selected according to the choice of the kernel and the sample size n . In the present case, the MC simulation of the PC expansion (which is analytical and polynomial) is rather inexpensive and usually negligible with respect to the model runs

that were previously required to obtain the PC coefficients. Thus a large sample may be used for the kernel approximation, *e.g.* $n = 1,000-10,000$. In case of such large samples, the obtained kernel density is independent of the choice of the kernel function.

5.2 Statistical moments

The statistical moments could be obtained at any order from the empirical moments of the samples of the response $\{y^{(i)}, i = 1, \dots, n\}$ mentioned earlier. However, due to the orthogonality of the PC expansion coefficients, they can be given analytical expressions which avoids the sampling. The mean value and variance of Y indeed read:

$$\mu_Y^{\text{PC}} \equiv \text{E}[Y] = y_0 \quad (4.91)$$

$$\sigma_Y^{2,\text{PC}} \equiv \text{Var}[Y] = \sum_{j=1}^{P-1} y_j^2 \quad (4.92)$$

The higher order moments may also be straightforwardly computed. For instance, the skewness and kurtosis coefficients read:

$$\delta_Y^{\text{PC}} = \frac{1}{\sigma_Y^{3,\text{PC}}} \text{E}[(Y - y_0)^3] = \frac{1}{\sigma_Y^{3,\text{PC}}} \sum_{i=1}^{P-1} \sum_{j=1}^{P-1} \sum_{k=1}^{P-1} d_{ijk} y_i y_j y_k \quad (4.93)$$

$$\kappa_Y^{\text{PC}} = \frac{1}{\sigma_Y^{4,\text{PC}}} \text{E}[(Y - y_0)^4] = \frac{1}{\sigma_Y^{4,\text{PC}}} \sum_{i=1}^{P-1} \sum_{j=1}^{P-1} \sum_{k=1}^{P-1} \sum_{l=1}^{P-1} d_{ijkl} y_i y_j y_k y_l \quad (4.94)$$

where $d_{ijk} = \text{E}[\Psi_i(\mathbf{X})\Psi_j(\mathbf{X})\Psi_k(\mathbf{X})]$ (resp. $d_{ijkl} = \text{E}[\Psi_i(\mathbf{X})\Psi_j(\mathbf{X})\Psi_k(\mathbf{X})\Psi_l(\mathbf{X})]$). In case of Hermite chaos, these coefficients may be computed analytically (see *e.g.* Sudret et al. (2006)). The set of these so-called spectral products has a sparse structure, in the sense that many of them are zero. As a consequence, they could be computed and stored once and for all.

From the author's experience and the application examples found in the literature, second-order PC expansion are usually sufficiently accurate to compute the mean and variance of the response, whereas at least third order expansions should be used to capture properly the higher order moments.

5.3 Reliability analysis

The use of spectral methods for reliability analysis was illustrated for the first time in Sudret and Der Kiureghian (2002). Since then, many applications have been proposed by the author and colleagues (Sudret et al., 2003a, 2004; Berveiller et al., 2005a,b) and others (Choi et al., 2004b,a).

The main idea is to approximate first the response quantities that enter the limit state function using a PC expansion, then to solve the approximate reliability problem. As illustrated in Sudret et al. (2003a), the PC approach may be extremely efficient for parametric reliability studies.

From the author's experience, third order expansion should be used in general, although second order expansion may be sufficiently accurate in specific cases.

5.4 Sensitivity analysis

In this section, the fruitful link between PC expansions and the formalism of Sobol' indices (Chapter 3, Section 4.3) is established. This work was originally published in Sudret (2006a, 2008a).

Let us suppose the model response is represented by a truncated PC expansion:

$$\mathcal{M}(\mathbf{x}) \approx \mathcal{M}^{\text{PC}}(\mathbf{x}) = \sum_{|\alpha| \leq p} y_{\alpha} \Psi_{\alpha}(\mathbf{x}) \quad (4.95)$$

where the multi-index notation is used, see Eq.(4.15). Let us define by $\mathcal{I}_{i_1, \dots, i_s}$ the set of multi-indices so that only the indices (i_1, \dots, i_s) are non zero:

$$\mathcal{I}_{i_1, \dots, i_s} = \left\{ \alpha : \begin{array}{ll} \alpha_k > 0 & \forall k = 1, \dots, M, \quad k \in (i_1, \dots, i_s) \\ \alpha_k = 0 & \forall k = 1, \dots, M, \quad k \notin (i_1, \dots, i_s) \end{array} \right\} \quad (4.96)$$

Note that \mathcal{I}_i corresponds to the polynomials depending only on parameter x_i . Using this notation, the terms in Eq.(4.95) may now be gathered according to the parameters they really depend on:

$$\begin{aligned} \mathcal{M}^{\text{PC}}(\mathbf{x}) = & y_0 + \sum_{i=1}^n \sum_{\alpha \in \mathcal{I}_i} y_{\alpha} \Psi_{\alpha}(x_i) + \sum_{1 \leq i_1 < i_2 \leq n} \sum_{\alpha \in \mathcal{I}_{i_1, i_2}} y_{\alpha} \Psi_{\alpha}(x_{i_1}, x_{i_2}) + \dots \\ & + \sum_{1 \leq i_1 < \dots < i_s \leq n} \sum_{\alpha \in \mathcal{I}_{i_1, \dots, i_s}} y_{\alpha} \Psi_{\alpha}(x_{i_1}, \dots, x_{i_s}) + \dots + \sum_{\alpha \in \mathcal{I}_{1, 2, \dots, n}} y_{\alpha} \Psi_{\alpha}(x_1, \dots, x_n) \end{aligned} \quad (4.97)$$

In the above equation, the true dependence of each polynomial basis function to each subset of input parameters has been given for the sake of clarity. Each term of the form $\sum_{\alpha \in \mathcal{I}_{i_1, \dots, i_s}} y_{\alpha} \Psi_{\alpha}(x_{i_1}, \dots, x_{i_s})$ in the right hand side is a polynomial function depending on *all* the input parameters (i_1, \dots, i_s) and *only* on them. Thus the summands in the Sobol' decomposition of $\mathcal{M}(\mathbf{x})$ (see Eq.(3.64)) straightforwardly read:

$$\mathcal{M}_{i_1 \dots i_s}(x_{i_1}, \dots, x_{i_s}) = \sum_{\alpha \in \mathcal{I}_{i_1, \dots, i_s}} y_{\alpha} \Psi_{\alpha}(x_{i_1}, \dots, x_{i_s}) \quad (4.98)$$

Due to the property of uniqueness, it may be concluded that Eq.(4.97) is *the* Sobol' decomposition of $\mathcal{M}^{\text{PC}}(\mathbf{x})$.

It is now easy to derive sensitivity indices from the above representation. These indices, called *polynomial chaos based Sobol' indices* and denoted by $SU_{i_1 \dots i_s}$ are defined as:

$$SU_{i_1 \dots i_s} = \frac{1}{\sigma_Y^2} \sum_{\alpha \in \mathcal{I}_{i_1, \dots, i_s}} y_{\alpha}^2 = \sum_{\alpha \in \mathcal{I}_{i_1, \dots, i_s}} y_{\alpha}^2 / \sum_{0 < |\alpha| \leq p} y_{\alpha}^2 \quad (4.99)$$

Although the above mathematical presentation is quite a burden, the idea behind is simple: once the polynomial chaos coefficients are computed, they are simply gathered according to the dependency of each basis polynomial, square-summed and normalized as shown in Eq.(4.99).

The *total PC-based sensitivity indices* are also easy to compute:

$$SU_{j_1, \dots, j_t}^T = \sum_{(i_1, \dots, i_s) \subset (j_1, \dots, j_t)} SU_{i_1, \dots, i_s} \quad (4.100)$$

As the terms in the summation are the PC-based Sobol indices, whose analytical expression has been given above, the total sensitivity indices may be computed at almost no additional cost.

5.5 Conclusion

The spectral methods provide a representation of the random response in terms of its PCE coefficients in a specific basis. In this section, it has been shown that the coefficients may be easily post-processed in order to compute the response PDF and the statistical moments. Reliability and sensitivity analysis may be equally carried out for free, *i.e.* at a computational cost which is usually negligible compared to a single run of the model \mathcal{M} . The various post-processing techniques are sketched in Figure 4.5.

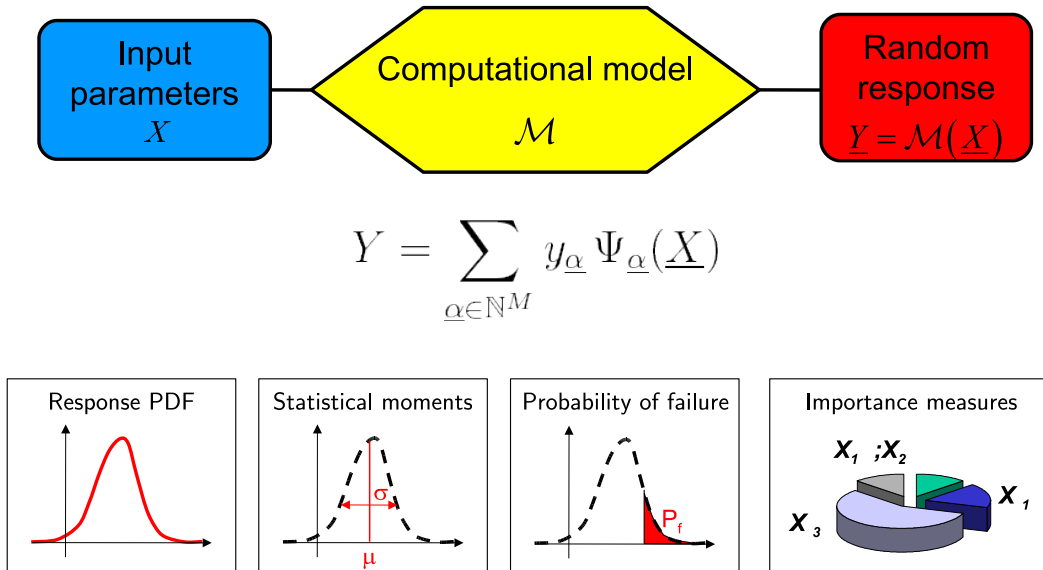


Figure 4.5: Post-processing of the polynomial chaos expansion of the random response

6 Application examples

6.1 Introduction

In this section various application examples in stochastic finite element analysis are proposed for the sake of illustration. The first example deals with geotechnical engineering and more specifically with the reliability of a foundation over an elastic soil mass with respect to a maximal admissible settlement.

Two sub-problems are considered. First the Young's modulus of the soil layer is supposed to be spatially variable (Sudret and Der Kiureghian, 2000). Second, the soil mass is made of two homogeneous layers, whose elastic properties are random and non Gaussian (Berveiller et al., 2006).

The second example deals with an elastic truss structure whose member properties and loading are random (Blatman et al., 2007a). This quite simple mechanical system allows one to compare comprehensively the various non intrusive schemes presented in Section 4.

6.2 Geotechnical engineering

6.2.1 Example #1.1: Foundation problem – spatial variability

Description of the deterministic problem Let us consider an elastic soil layer of thickness t lying on a rigid substratum. A superstructure to be founded on this soil mass is idealized as a uniform pressure P applied over a length $2B$ of the free surface (see Figure 4.6). The soil is modeled as an elastic linear isotropic material. A plane strain analysis is carried out.

Due to the symmetry, half of the structure is modeled by finite elements. Strictly speaking, there is no symmetry in the system when random fields of material properties are introduced. However, it is believed that this simplification does not significantly influence the results. The parameters selected for the deterministic model are listed in Table 4.1.

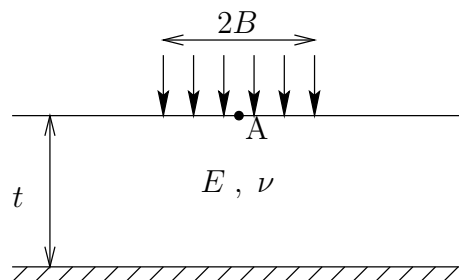


Figure 4.6: Example #1.1 – Settlement of a foundation – problem definition

Table 4.1: Example #1.1 – Foundation – Parameters of the deterministic model

Parameter	Symbol	Value
Soil layer thickness	t	30 m
Foundation width	$2B$	10 m
Applied pressure	P	0.2 MPa
Soil Young's modulus	E	50 MPa
Soil Poisson's ratio	ν	0.3
Mesh width	L	60 m

A refined mesh was first used to obtain the “exact” maximum displacement under the foundation (point A in Figure 4.6). Less refined meshes were then tried in order to design a mesh with as few elements as possible that yielded no more than 1% error in the computed maximum settlement. The mesh displayed in Figure 4.7-a was eventually chosen. It contains 99 nodes and 80 elements. The maximum settlement computed with this mesh is equal to 5.42 cm.

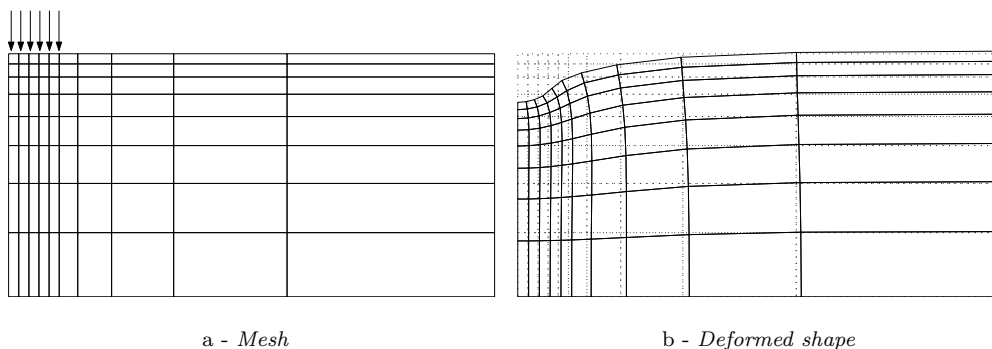


Figure 4.7: Example #1.1 – Foundation – Finite element mesh and deformed shape for mean values of the parameters by a deterministic analysis

Description of the probabilistic data The assessment of the serviceability of the foundation described in the above paragraph is now investigated under the assumption that the Young's modulus of the soil mass is spatially varying.

The Young's modulus of the soil is considered to vary only in the vertical direction, so that it is modeled as a one-dimensional homogeneous random field along the depth z . This is a reasonable model for a layered soil medium. The field is assumed to be lognormal and homogeneous. Its second-moment properties are considered to be the mean $\mu_E = 50$ MPa, the coefficient of variation $\delta_E = \sigma_E/\mu_E = 0.2$. The

autocorrelation coefficient function of the underlying Gaussian field $N(\mathbf{x}, \omega)$ is of type A (Eq.(2.59)), *i.e.* $\rho(z, z') = \exp(-|z - z'|/\ell_A)$, where z is the depth coordinate and $\ell_A = 30$ m is the correlation length.

The underlying Gaussian field $N(\mathbf{x}, \omega)$ is discretized using the Karhunen-Loève expansion, see Eq.(2.66). The accuracy of the discretization is measured by the following error estimate:

$$\bar{\varepsilon} = \frac{1}{|\mathcal{B}|} \int_{\mathcal{B}} \frac{\text{Var} [N(\mathbf{x}) - \hat{N}(\mathbf{x})]}{\text{Var} [N(\mathbf{x})]} d\mathcal{B} \quad (4.101)$$

A relative accuracy in the variance of 12% (resp. 8%, 6%) is obtained when using $M = 2$ (resp. $M = 3, 4$) terms in the KL expansion of $N(\mathbf{x})$. Of course these values are closely related to the parameters defining the random field, particularly the correlation length ℓ_A . As ℓ_A is comparable here to the size of the domain \mathcal{B} , an accurate discretization is obtained using few terms. Many more terms would be required to get a satisfactory accuracy when $\ell_A \ll |\mathcal{B}|$.

Reliability analysis The limit state function is defined in terms of the maximum settlement u_A at the center of the foundation:

$$g(\Xi) = u_{max} - u_A(\Xi) \quad (4.102)$$

where u_{max} is an admissible threshold initially set equal to 10 cm and Ξ is the vector of basic random variables used for the random field discretization.

Table 4.2 reports the results of the reliability analysis carried out either by direct coupling between the finite element model and the FORM algorithm (column #2), or by the application of FORM after solving the SFE problem (column #6, for various values of p). Both results have been validated using importance sampling (columns #3 and #7 respectively). In the direct coupling approach, 1,000 samples (corresponding to 1,000 deterministic FE runs) were used, leading to a coefficient of variation of the simulation less than 6%. In the SFE approach, the polynomial chaos expansion of the response is used for importance sampling around the design point obtained by FORM (*i.e.* no additional finite element run is required), and thus 50,000 samples can be used, leading to a coefficient of variation of the simulation less than 1%.

Table 4.2: Example #1.1 – Foundation – Reliability index β : Influence of the orders of expansion M and p ($u_{max} = 10$ cm)

M	β_{direct}^{FORM}	β_{direct}^{IS}	p	P	β_{SFE}^{FORM}	β_{SFE}^{IS}
2	3.452	3.433	2	6	3.617	3.613
			3	10	3.474	3.467
3	3.447	3.421	2	10	3.606	3.597
			3	20	3.461	3.461
4	3.447	3.449	2	15	3.603	3.592
			3	35	3.458	3.459

It appears that the solution is not much sensitive to the order of expansion of the input field (when comparing the results for $M = 2$ with respect to those obtained for $M = 4$). This can be easily understood by the fact that the maximum settlement of the foundation is related to the global (*i.e.* homogenized) behaviour of the soil mass. Modeling in a refined manner the spatial variability of the stiffness of the soil mass by adding terms in the KL expansion does not significantly influence the results.

In contrast, it appears that a PC expansion of third degree ($p = 3$) is required in order to get a satisfactory accuracy on the reliability index. Note that the accuracy of FORM in both approaches (*i.e.* direct coupling or after SSFEM) is satisfactory since the relative discrepancy with the IS results is less than 1%.

Parametric study A comprehensive comparison of the two approaches is presented in Sudret and Der Kiureghian (2000), where the influences of various parameters are investigated. Selected results are reported in this section. More precisely, the accuracy of the SFE method combined with FORM is investigated when varying the value of the admissible settlement from 6 to 20 cm, which leads to an increasing reliability index. A two-term ($M = 2$) KL expansion of the underlying Gaussian field is used. The results are reported in Table 4.3. Column #2 shows the values obtained by direct coupling between FORM and the deterministic finite element model. Column #4 shows the values obtained using FORM after the SFE solution of the problem using an intrusive approach (IS results are not reported since they are very close to the FORM results, as in Table 4.2).

Table 4.3: Example #1.1 – Foundation – Influence of the threshold in the limit state function

u_{max} (cm)	β_{direct}	p	β_{SFE}
6	0.473	2	0.477
		3	0.488
		4	0.488
8	2.152	2	2.195
		3	2.165
		4	2.166
10	3.452	2	3.617
		3	3.474
		4	3.467
12	4.514	2	4.858
		3	4.559
		4	4.534
15	5.810	2	6.494
		3	5.918
		4	5.846
20	7.480	2	8.830
		3	7.737
		4	7.561

The results in Table 4.3 show that the “SFE+FORM” procedure obviously converges to the direct coupling results when p is increased. It appears that a third-order expansion is accurate enough to predict reliability indices up to 5, *i.e.* $P_f \approx 10^{-7}$. For larger values of β , a higher order expansion should be used.

Note that a *single* SFE analysis is carried out to get the reliability indices associated with the various values of the threshold u_{max} (once p is chosen). In contrast, a FORM analysis has to be restarted for each value of u_{max} when a direct coupling is used. As a conclusion, if a single value of β (and related $P_f \approx \Phi(-\beta)$) is of interest, the direct coupling using FORM is probably the most efficient method. When the evolution of β with respect to a threshold is investigated, the “SFE+FORM” approach may become more appealing.

6.2.2 Example #1.2: Foundation problem – non Gaussian variables

Deterministic problem statement Let us consider now an elastic soil mass made of two layers of different isotropic linear elastic materials lying on a rigid substratum. A foundation on this soil mass is modeled by a uniform pressure P_1 applied over a length $2B_1 = 10$ m of the free surface. An additional load P_2 is applied over a length $2B_2 = 5$ m (Figure 4.8).

Due to the symmetry, half of the structure is modeled by finite elements. The mesh comprises 80 QUAD4 elements as in the previous section. The finite element code used in this analysis is the open source

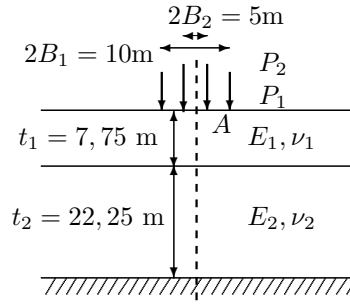


Figure 4.8: Example #1.2 – Foundation on a two-layer soil mass

code Code_Aster (eDF, R&D Division, 2006). The geometry is considered as deterministic. The elastic material properties of both layers and the applied loads are modelled by random variables, whose PDF are specified in Table 4.4. All six random variables are supposed to be independent.

Table 4.4: Example #1.2 – Foundation on a two-layer soil mass – Parameters of the model

Parameter	Notation	Type of PDF	Mean value	Coef. of variation
Upper layer soil thickness	t_1	Deterministic	7.75 m	-
Lower layer soil thickness	t_2	Deterministic	22.25 m	-
Upper layer Young's modulus	E_1	Lognormal	50 MPa	20 %
Lower layer Young's modulus	E_2	Lognormal	100 MPa	20 %
Upper layer Poisson ratio	ν_1	Uniform	0.3	15 %
Lower layer Poisson ratio	ν_2	Uniform	0.3	15 %
Load #1	P_1	Gamma	0.2 MPa	20 %
Load #2	P_2	Weibull	0.4 MPa	20 %

Again the model response under consideration is the maximum vertical displacement at point A, say u_A (figure 4.8), considered as a function of the six input parameters:

$$u_A = \mathcal{M}(E_1, E_2, \nu_1, \nu_2, P_1, P_2) \quad (4.103)$$

Reliability analysis The serviceability of this foundation on a layered soil mass vis-à-vis an admissible settlement is studied. Again, two strategies are compared:

- a direct coupling between the finite element model and the probabilistic code PROBAN (Det Norske Veritas, 2000). The limit state function given in Eq.(4.102) is rewritten in this case as:

$$g(\mathbf{X}) = u_{max} - \mathcal{M}(E_1, E_2, \nu_1, \nu_2, P_1, P_2) \quad (4.104)$$

where u_{max} is the admissible settlement. The failure probability is computed using FORM analysis followed by importance sampling. 1,000 samples are used in IS allowing a coefficient of variation of the simulation less than 5%.

- a SFE analysis using the regression method is carried out, leading to an approximation of the maximal vertical settlement:

$$u_A^{PC} = \sum_{j=0}^{P-1} u_j \Psi_j(\boldsymbol{\xi}) \quad (4.105)$$

For this purpose, the six input variables $\{E_1, E_2, \nu_1, \nu_2, P_1, P_2\}$ are first transformed into a six-dimensional standard normal gaussian vector $\boldsymbol{\Xi}$. Then a third order ($p = 3$) PC expansion of

the response is performed which requires the computation of $P = \binom{6+3}{3} = 84$ coefficients. The following approximate limit state function is then considered:

$$g^{\text{PC}}(\mathbf{X}) = u_{\max} - \sum_{j=0}^{P-1} u_j \Psi_j(\boldsymbol{\xi}) \quad (4.106)$$

Then FORM analysis followed by importance sampling is applied (1,000 samples, coefficient of variation less than 1% for the simulation). Note that in this case, FORM as well as IS are performed using the *analytical* limit state function Eq.(4.106). This computation is almost costless compared to the computation of the PC expansion coefficients $\{u_j\}_{j=0}^{P-1}$ in Eq.(4.105) .

Table 4.5 shows the probability of failure obtained by direct coupling and by SFE/regression using various numbers of points in the experimental design (see Section 4.3.4). Figure 4.9 shows the evolution of the ratio between the logarithm of the probability of failure (divided by the logarithm of the converged probability of failure) vs. the number of regression points for several values of the maximum admissible settlement u_{\max} . Accurate results are obtained when using 420 regression points or more for different values of the failure probability (from 10^{-1} to 10^{-4}). When taking less than 420 points, results are inaccurate. When taking more than 420 points, the accuracy is not improved. Thus this number seems to be the best compromise between accuracy and efficiency. Note that it corresponds to $(M-1)P = 5 \times 84$ points, as observed in other application examples (Berveiller, 2005).

Table 4.5: Example #1.2 – Foundation on a two-layer soil mass - probability of failure P_f

Threshold u_{\max} (cm)	Direct	Non intrusive SFE/regression approach				
	Coupling	84 pts	168 pts	336 pts	420 pts	4096 pts
12	$3.09 \cdot 10^{-1}$	$1.62 \cdot 10^{-1}$	$2.71 \cdot 10^{-1}$	$3.31 \cdot 10^{-1}$	$3.23 \cdot 10^{-1}$	$3.32 \cdot 10^{-1}$
15	$6.83 \cdot 10^{-2}$	$6.77 \cdot 10^{-2}$	$6.90 \cdot 10^{-2}$	$8.43 \cdot 10^{-2}$	$6.73 \cdot 10^{-2}$	$6.93 \cdot 10^{-2}$
20	$2.13 \cdot 10^{-3}$	-	$9.95 \cdot 10^{-5}$	$8.22 \cdot 10^{-4}$	$2.01 \cdot 10^{-3}$	$1.98 \cdot 10^{-3}$
22	$4.61 \cdot 10^{-4}$	-	$7.47 \cdot 10^{-7}$	$1.31 \cdot 10^{-4}$	$3.80 \cdot 10^{-4}$	$4.24 \cdot 10^{-4}$
Number of FE runs required		84	168	336	420	4096

6.2.3 Complementary applications

Examples in geotechnical engineering have constantly supported the development of spectral methods by the author and colleagues.

Application example #1.1 was originally addressed in Sudret and Der Kiureghian (2000) and reported in Sudret (2001); Sudret and Der Kiureghian (2002). It has been recently benchmarked in Sachdeva et al. (2006). The first application of an intrusive approach in order to solve a reliability problem involving non Gaussian random variables was presented in Sudret et al. (2003b, 2004). A similar example including the computation of fragility curves is presented in Sudret et al. (2003a). A comprehensive presentation of the intrusive computational scheme and various additional application examples can be found in Berveiller et al. (2006). The regression method was applied to this problem in Sudret et al. (2006). A survey paper is available in Sudret and Berveiller (2007).

The non intrusive methods were first applied to the study of the convergence of a tunnel submitted to earth pressure in Berveiller et al. (2004a,b).

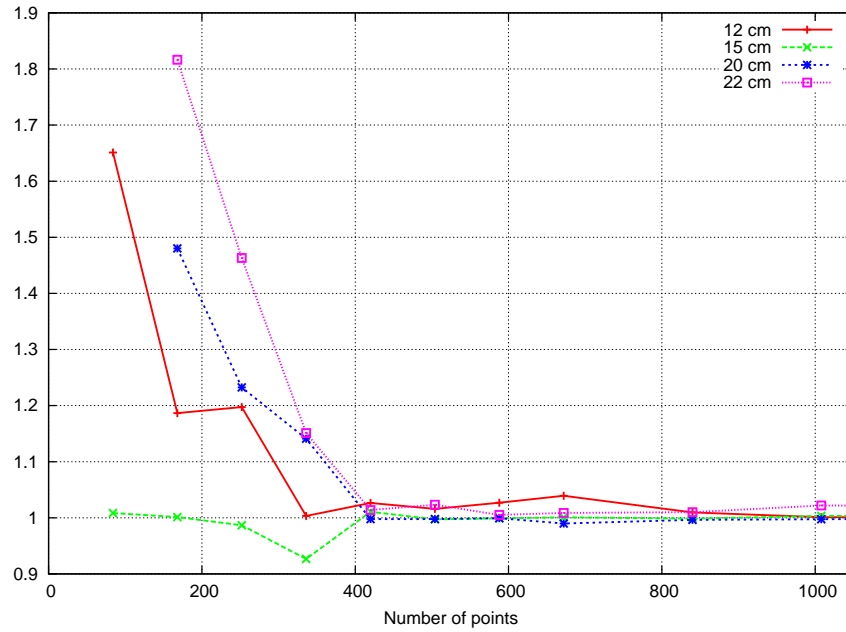


Figure 4.9: Example #1.2: – Foundation on a two-layer soil mass - evolution of the logarithm of the failure probability divided by the converged value vs. the number of regression points

6.3 Structural mechanics

6.3.1 Deterministic problem statement

Let us consider the simply supported truss structure sketched in Figure 4.10. It is made of 23 elastic bars, whose Young's modulus and cross sections are uncertain. The truss is loaded by six vertical loads $P_1 - P_6$.

This quite simple structure allows us to compare the various non intrusive stochastic finite element methods described in Section 4. Different problems are successively considered, namely the estimation of probability density function and statistical moments of the midspan vertical displacement, the associated sensitivity analysis and the reliability of the truss with respect to a maximal admissible displacement.

Ten *independent* input random variables are considered, whose distribution, mean and standard deviation are reported in Table 4.6

Table 4.6: Example #2 – Truss structure – Input random variables

Description	Name	Distribution	Mean	Standard Deviation
Young's modulus	E_1, E_2 (Pa)	Lognormal	2.10×10^{11}	2.10×10^{10}
Cross section of the horizontal bars	A_1 (m ²)	Lognormal	2.0×10^{-3}	2.0×10^{-4}
Cross section of the vertical bars	A_2 (m ²)	Lognormal	1.0×10^{-3}	1.0×10^{-4}
Loads	$P_1 - P_6$ (N)	Gumbel	5.0×10^4	7.5×10^3

Of interest is the midspan deflection v (counted positively downwards). The model of the structure is the algorithmic (finite element-based) function that yields this quantity for any value of the input parameters:

$$v = \mathcal{M}(E_1, E_2, A_1, A_2, P_1, \dots, P_6) \quad (4.107)$$

The different problems are addressed using a second-order ($p = 2$) Hermite polynomial chaos expansion.

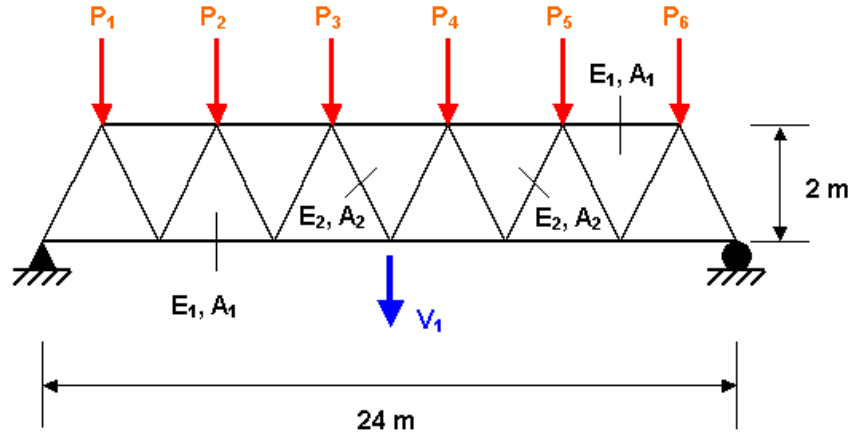


Figure 4.10: Example #2 – Elastic truss structure with 23 members

In this respect, it is necessary to transform the input random vector $\mathbf{X} = \{E_1, E_2, A_1, A_2, P_1, \dots, P_6\}^T$ into a standardized Gaussian vector:

$$\xi_i = F_{X_i}^{-1}(\Phi(X_i)) \quad , \quad i = 1, \dots, 10 \quad (4.108)$$

where F_{X_i} is the CDF of the i -th component of \mathbf{X} and Φ is the standard normal CDF. This leads to:

$$v^{\text{PC}}(\boldsymbol{\xi}) = \sum_{0 \leq |\boldsymbol{\alpha}| \leq 2} v_{\boldsymbol{\alpha}} \Psi_{\boldsymbol{\alpha}}(\boldsymbol{\xi}) \quad (4.109)$$

where $v_{\boldsymbol{\alpha}}$ are the unknown coefficients to be computed (there are $P = \binom{10+2}{2} = 66$ such coefficients).

The non intrusive methods used for this computation and compared in the sequel include:

- three simulation methods, namely Monte Carlo simulation (MCS), Latin Hypercube Sampling (LHS) and Sobol' quasi-random sequence (QMC); 10,000 samples are used in each case.
- two quadrature schemes, namely the full tensorized quadrature scheme using $3^{10} = 59051$ points and Smolyak quadrature scheme (266 points);
- regression applied together with random experimental designs (namely MCS, LHS and QMC) and designs based on the roots of Hermite polynomials respectively. In the latter case, two experimental designs are successively considered, namely the one proposed by Berveiller (2005) ($(M - 1) \times P = 594$ points) and the minimal design by Sudret (2008a) (66 points).

Some of the results have been originally presented in Blatman et al. (2007a).

6.3.2 Probability density function of the midspan displacement

The reference solution is obtained by crude Monte Carlo simulation using 1,000,000 runs of the finite element model. The PCE-based solution corresponds to 1,000,000 samples of the PC expansion. In both cases, a kernel density representation of the sample set is used (Figure 4.11).

It appears that the PDF obtained from the QMC approach is much closer to the reference solution (*i.e.* almost identical) than that derived from the MCS and LHS computation, both in the central part and in the tails (see the plot with logarithmic scale in Figure 4.11-b).

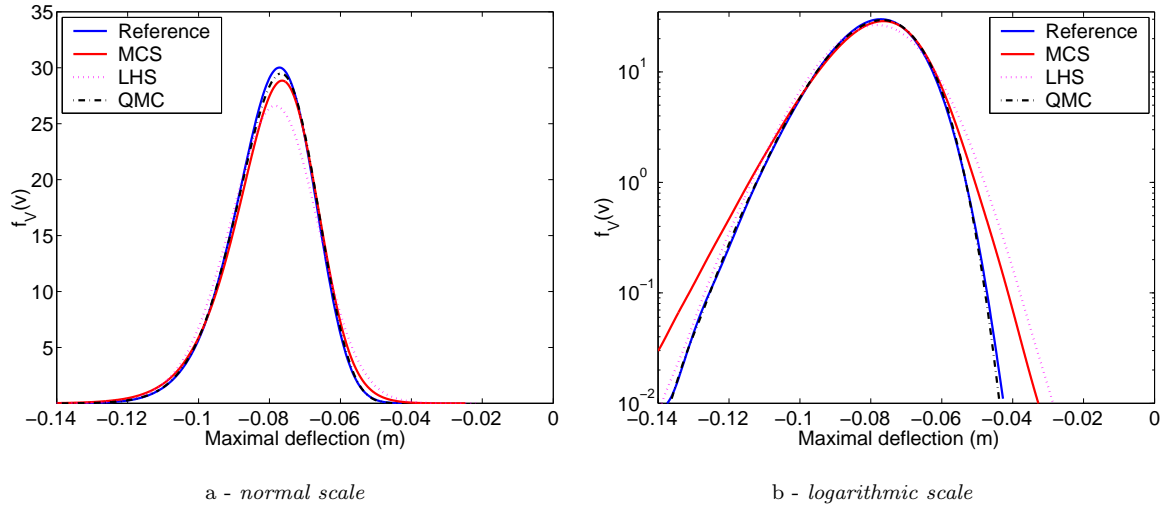


Figure 4.11: Example #2 – Truss example – probability density function of the maximal deflection obtained by projection methods

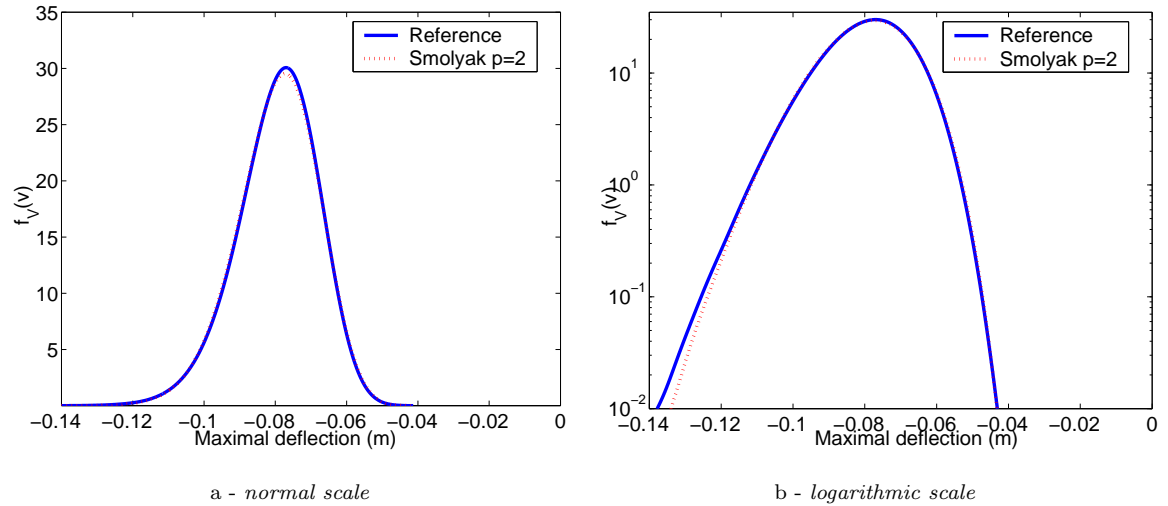


Figure 4.12: Example #2 – Truss structure – probability density function of the maximal deflection obtained by Smolyak quadrature

The PDF obtained from the PC coefficients computed by Smolyak quadrature (Figure 4.12) is rather accurate both in the central part and in the tails, with a better accuracy in the upper tail. The same results hold for the PDF obtained from the PC coefficients computed by regression (Figure 4.13). Note that there is little difference between the PDF obtained from the minimal experimental design compared to the design proposed by Berveiller (2005) (also in the tails), whereas the computational cost is divided by 9.

6.3.3 Statistical moments

The statistical moments of the response v are now considered. Reference results are obtained using crude Monte Carlo simulation of the problem with 1,000,000 samples to estimate the moments of the midspan vertical displacement up to order 4. On the other hand, estimates of the PCE coefficients are post-processed using Eqs.(4.91)-(4.94). The results obtained by projection techniques are reported in

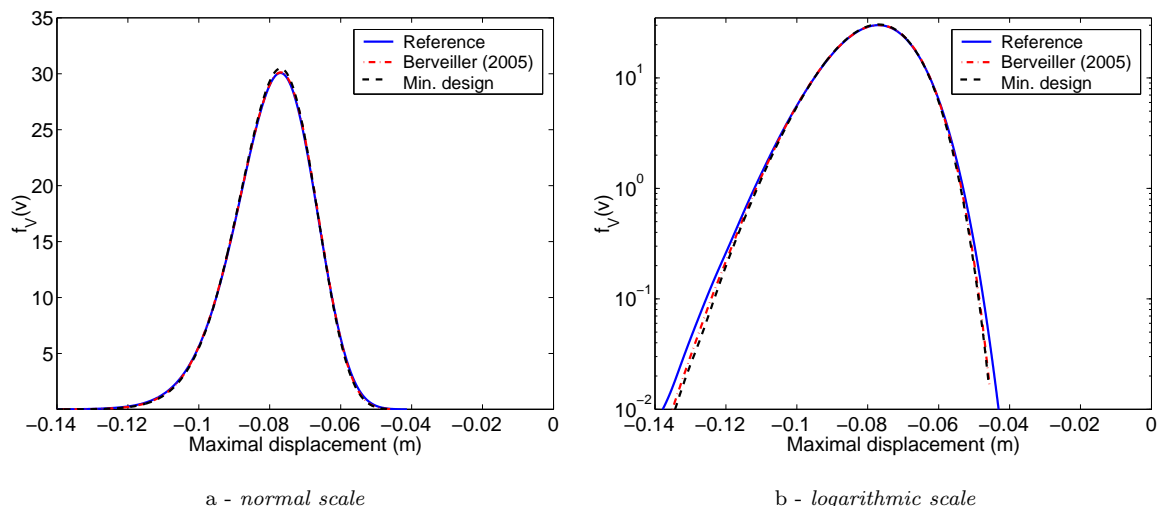


Figure 4.13: Example #2 – Truss structure – probability density function of the maximal deflection obtained by regression

Table 4.7 together with the reference values.

Table 4.7: Example #2 – Truss structure – Estimates of the first four statistical moments of the midspan displacement by projection

Moment	Ref. solution	Simulation			Quadrature	
		MCS	LHS	QMC	Full	Smolyak
Mean value	0.0794	0.0792	0.0794	0.0794	0.0794	0.0794
Std. deviation	0.0111	0.0120	0.0124	0.0112	0.0111	0.0111
Skewness	-0.4920	-0.5605	-0.2052	-0.4959	-0.4638	-0.4332
Kurtosis	3.4555	3.9667	3.2944	3.3676	3.2961	3.2535
Number of FE runs	1,000,000	10,000	10,000	10,000	59,049	231

Accurate estimates of the mean value are obtained when using LHS and QMC, whereas the MCS scheme also yields a rather insignificant relative error $\varepsilon = 0.3\%$ with respect to the reference value.

However, QMC provides by far the best estimates of the higher order moments, with a relative error of $\varepsilon = 0.9\%$ on the standard deviation, $\varepsilon = 0.8\%$ on the skewness coefficient and $\varepsilon = 2.5\%$ on the kurtosis coefficients. The relative errors on these moments are indeed equal to 8.1%, 13.7%, 14.8% respectively when using MCS. They are equal to 11.7%, 58.3%, 4.7% respectively when using LHS.

Table 4.8: Example #2 – Truss structure – Estimates of the first four statistical moments of the midspan displacement by regression

Moment	Ref. solution	Random ED			Deterministic ED	
		MCS	LHS	QMC	Berveiller (2005)	Min. design
Mean value	0.0794	0.0793	0.0795	0.0794	0.0794	0.0794
Std. deviation	0.0111	0.0110	0.0110	0.0111	0.0109	0.0108
Skewness	0.4920	0.4672	0.4876	0.4344	0.4824	0.4724
Kurtosis	3.4555	3.2968	3.3329	3.2676	3.3273	3.3031
# FE runs	1,000,000	100	100	100	594	66

The results obtained by regression techniques are reported in Table 4.8 together with the reference values. Regression with random experimental design (columns #2-4) has been carried out using MCS, LHS and

QMC samples (100 samples were used in each case). Regression with a design based on roots of the Hermite polynomials has been also carried out. Column #5 corresponds to the design proposed in Berveiller (2005). Column #6 corresponds to a “minimal design” as presented in Sudret (2008a). It can be observed that all the designs lead to accurate predictions of mean and standard deviation. However, the designs based on the roots of the Hermite polynomials give slightly better results for the skewness and kurtosis coefficients. It is not clear from this example whether one of the random designs is more efficient than the others.

6.3.4 Sensitivity analysis

Sensitivity analysis of the midspan vertical displacement is now carried out. The total Sobol’ indices are considered. The reference values are obtained by Monte Carlo simulation using $n = 500,000$ samples for each index. This leads to perform $n(M + 1) = 5,500,000$ deterministic finite element runs. These reference results and the results obtained by projection methods are reported in Table 4.9.

Table 4.9: Example #2 – Truss structure – Total Sobol’ indices obtained by projection

Variable	Ref. solution	Simulation			Quadrature	
		MCS	LHS	QMC	Full	Smolyak
A_1	0.388	0.320	0.344	0.366	0.371	0.372
E_1	0.367	0.356	0.331	0.373	0.371	0.372
P_3	0.075	0.067	0.095	0.077	0.077	0.077
P_4	0.079	0.124	0.080	0.077	0.077	0.077
P_5	0.035	0.086	0.068	0.046	0.037	0.037
P_2	0.031	0.079	0.067	0.039	0.037	0.037
A_2	0.014	0.074	0.052	0.014	0.013	0.013
E_2	0.010	0.088	0.115	0.013	0.013	0.013
P_6	0.005	0.067	0.013	0.014	0.005	0.005
P_1	0.004	0.037	0.063	0.005	0.005	0.005
# FE runs	5,500,000		10,000		59,049	231

It is observed from the results in Table 4.9 that the variability of the deflection v is mainly due to the variables E_1 and A_1 , then E_2 and A_2 . This makes sense from a physical point of view since the properties of the horizontal bars are more influential on the midspan vertical displacement than the oblique ones. It can be also observed that the Sobol’ indices associated with E_1 and A_1 (resp. E_2 and A_2) are similar. This is due to the fact that these variables have the same type of PDF and same coefficient of variation, and that the displacement v only depends on them through the products E_1A_1 and E_2A_2 .

Strictly speaking, an exact symmetry should be observed in the reference results (*i.e.* $S_{T_{A_1}} = S_{T_{E_1}}$ and $S_{T_{A_2}} = S_{T_{E_2}}$). Note that the Sobol’ indices should also reflect the symmetry of the problem, giving similar importances to the loads that are symmetrically applied (*e.g.* P_3 and P_4). Moreover, greater sensitivity indices are logically attributed to the forces that are close to the midspan than those located at the ends.

Considering first the PC simulation results, it is worth emphasizing that the symmetry properties that are commented above are not exactly recovered. The QMC results appear more accurate than those obtained by MCS and LHS. In contrast, very accurate results perfectly reflecting the symmetries mentioned above are obtained using either of the quadrature schemes.

The total Sobol’ indices obtained from regression-based PC coefficients are reported in Table 4.10. Again the results obtained from deterministic experimental designs reflect the expected symmetries while those obtained from random designs do not. The minimum design in column #7 provides rather accurate results using only 66 model runs.

Table 4.10: Example #2 – Truss structure – Total Sobol' indices obtained by regression

Variable	Ref. solution	Random ED			Deterministic ED	
		MCS	LHS	QMC	Berveiller (2005)	Min. design
A_1	0.388	0.372	0.371	0.373	0.370	0.367
E_1	0.367	0.375	0.368	0.369	0.368	0.367
P_3	0.075	0.074	0.079	0.078	0.079	0.080
P_4	0.079	0.077	0.077	0.077	0.079	0.080
P_5	0.035	0.039	0.041	0.036	0.038	0.039
P_2	0.031	0.036	0.035	0.037	0.038	0.039
A_2	0.014	0.013	0.017	0.014	0.013	0.012
E_2	0.010	0.014	0.014	0.014	0.013	0.012
P_6	0.005	0.007	0.007	0.008	0.005	0.005
P_1	0.004	0.014	0.005	0.007	0.005	0.005
# FE runs	10,000,000	100	100	100	594	66

6.3.5 Reliability analysis

The serviceability of the structure with respect to an admissible maximal deflection is studied. The associated limit state function reads:

$$g(\mathbf{x}) = v_{max} - |v(\mathbf{x})| \leq 0 \quad , \quad v_{max} = 0.11 \text{ m} \quad (4.110)$$

The reference value of the probability of failure has been obtained by crude Monte Carlo simulation:

$$P_f^{\text{MCS}} = \frac{N_{fail}}{N} \quad (4.111)$$

where $N = 1,000,000$ samples and N_{fail} is the number of samples corresponding to a negative value of the limit state function in Eq.(4.110). The result is $P_f^{\text{MCS}} = 8.7 \cdot 10^{-3}$, and the coefficient of variation of the underlying estimator is 1.1%. The corresponding *reliability index* is given by $\beta^{\text{MCS}} \equiv -\Phi^{-1}(P_f^{\text{MCS}}) = 2.378$.

The reliability analysis is then performed using the PC expansion of the maximal vertical displacement obtained by various non intrusive methods. The associated limit state function reads:

$$g^{\text{PC}}(\mathbf{x}(\boldsymbol{\xi})) = v_{max} - |v^{\text{PC}}(\boldsymbol{\xi})| \quad (4.112)$$

The probability of failure is then computed from Eq.(4.112) (which is a polynomial function almost costless to evaluate) using 1,000,000 Monte Carlo samples.

Table 4.11: Example #2 – Truss structure – Estimates of the probability of failure and the reliability index obtained by projection

	Reference	MCS	LHS	QMC	Smolyak
Number of FE runs	1,000,000	10,000	10,000	10,000	231
P_f	$8.70 \cdot 10^{-3}$ (CV = 1.1%)	$1.51 \cdot 10^{-2}$	$1.12 \cdot 10^{-2}$	$9.06 \cdot 10^{-3}$	$7.63 \cdot 10^{-3}$
β	2.378	2.167	2.284	2.363	2.426
Relative error on β	-	8.8%	3.9%	0.8%	2.0%

Results obtained by projection methods are reported in Table 4.11. QMC provides the most accurate estimate with a relative error of 0.8% on β , whereas relative errors of 8.8% and 3.8% are respectively associated to MCS and LHS. The Smolyak quadrature scheme provides a 2% accuracy using only 231 runs

of the finite element model. This method appears to be the best compromise between efficiency and accuracy in this case.

Finally, a parametric study is carried out to assess the accuracy of the QMC and Smolyak estimates of P_f and β when the threshold v_{max} is varied. The QMC estimates are obtained using $N = 10,000$ samples. Results are reported in Table 4.12 together with the reference values. Due to the magnitude of the probabilities of failure, the latter have been obtained by applying FORM followed by importance sampling to the original finite element model.

Table 4.12: Example #2 – Truss structure – Reliability results obtained by projection (parametric study) using $p = 2$

Threshold (cm)	Ref. solution		QMC Simulation		Smolyak Quadrature	
	P_f	β	P_f	β	P_f	β
10	$4.31 \cdot 10^{-2}$	1.715	$4.40 \cdot 10^{-2}$	1.706	$4.07 \cdot 10^{-2}$	1.730
11	$8.70 \cdot 10^{-3}$	2.378	$9.06 \cdot 10^{-3}$	2.363	$7.63 \cdot 10^{-3}$	2.426
12	$1.50 \cdot 10^{-3}$	2.967	$1.42 \cdot 10^{-3}$	2.983	$1.06 \cdot 10^{-3}$	3.074
14	$3.49 \cdot 10^{-5}$	3.977	$2.15 \cdot 10^{-5}$	4.091	$1.04 \cdot 10^{-5}$	4.256
16	$6.03 \cdot 10^{-7}$	4.855	$1.84 \cdot 10^{-7}$	5.085	$5.16 \cdot 10^{-8}$	5.321

As mentioned earlier, the PC expansion of the response is less accurate in the far tail of the response PDF. Thus the relative error increases together with the reliability index β , *i.e.* when the threshold value increases. This indicates that a second order PC expansion is not sufficiently accurate to describe the far tails of the response PDF.

Table 4.13: Example #2 – Truss structure – Reliability results obtained by Smolyak projection (parametric study) using a third order polynomial chaos expansion ($p = 3$)

Threshold (cm)	Ref. solution		Smolyak Quadrature	
	P_f	β	P_f	β
10	$4.31 \cdot 10^{-2}$	1.715	$4.29 \cdot 10^{-2}$	1.718
11	$8.70 \cdot 10^{-3}$	2.378	$8.70 \cdot 10^{-3}$	2.377
12	$1.50 \cdot 10^{-3}$	2.967	$1.50 \cdot 10^{-3}$	2.974
14	$3.49 \cdot 10^{-5}$	3.977	$2.83 \cdot 10^{-5}$	4.026
16	$6.03 \cdot 10^{-7}$	4.855	$4.01 \cdot 10^{-7}$	4.935

This statement is confirmed by the results in Table 4.13, where a third order ($p = 3$) PC expansion is considered. The PC coefficients have been computed by the Smolyak quadrature scheme using 1771 points. This leads to a 2%-accuracy on the reliability index for values ranging from 1 to 5.

6.3.6 Conclusion

The simple truss structure studied in this section has allowed us to benchmark the various non intrusive methods for different problems ranging from the representation of the response PDF, the computation of moments and the hierarchization of input random variables to reliability analysis.

From these results, and other benchmark problems investigated elsewhere (Blatman, 2007), the following conclusions may be drawn:

- when dealing with moment and sensitivity analysis, second order PC expansions usually provide sufficiently accurate results. When dealing with reliability analysis, third order PC expansions may be required, in particular when small probabilities of failure are sought;

- the most efficient projection/simulation method is QMC, *i.e.* the method related to the use of Sobol' quasi-random sequences. It should be preferred to MCS and LHS. Note that parametric studies with respect to the number of samples have shown that convergence is attained from 1,000 QMC samples in the case of the truss structure, whereas it is not attained for 10,000 MCS or LHS samples (Blatman et al., 2007a);
- Smolyak quadrature provide accurate results at a relative low cost when the number of variable is small, say less than 20.
- Regression techniques also provide accurate results provided the size of the experimental design is large enough compared to the number of unknown coefficients. The minimal experimental design proposed in Sudret (2008a) provides rather accurate results at a low cost (66 finite element runs in the present example). However, the size of this design still increases much with the number of input random variables. Thus random designs may be more efficient for large size problems.

7 Conclusion

In this chapter, spectral methods that have emerged in the early 90's have been reviewed. Two classes of methods respectively called the Galerkin (*i.e.* intrusive) and non intrusive approach, have been presented. Emphasis has been put on the second class to which the author specifically contributed.

The appealing characteristics of the spectral methods lie in the fact that any random response quantity may be represented by a set of coefficients in a suitable basis, which contains the complete probabilistic information. The non intrusive methods allow the analyst to compute these coefficients by a series of runs of the model at hand, which may be launched in a fully parallel computational environment. The post-processing of the result is shown to be straightforward, whatever the information of interest (*e.g.* moment, reliability or sensitivity analysis).

The spectral methods may be considered as a breakthrough in probabilistic engineering mechanics. It is the belief of the author that they will become an everyday tool of the engineer in the near future, exactly as finite element analysis pioneered in the 60's is nowadays inescapable in every industrial context. The non intrusive methods appear most interesting since they provide generic tools that can be applied together with any deterministic models and legacy codes. Note that the author has recently contributed to the spreading of these methods in electromagnetism (Gaignaire et al., 2006a,b,c, 2007a,b).

The stochastic response surfaces that are eventually obtained from the spectral methods are a particular meta-model in the probabilistic space. In this respect, the polynomial chaos may be outperformed by other approaches that have proven efficient in functional approximation. The wavelets used by Le Maître et al. (2004a,b) seem to be suitable to problems with discontinuities. More generally, the kriging methods (Sacks et al., 1989), the support vector regression (Schölkopf and Smola, 2002; Smola and Schölkopf, 2006) and the use of reproducing kernel Hilbert spaces (Vazquez, 2005) constitute promising alternatives to polynomial chaos expansions in the context of uncertainty propagation, which are being investigated in Blatman (2007).

Chapter 5

Bayesian updating methods and stochastic inverse problems

1 Introduction

The construction of a probabilistic model for the input parameters of a mathematical model that is consistent with the available data is a key step in probabilistic engineering mechanics. Several methods including classical and Bayesian statistics have been reviewed in Chapter 2, Section 3. They have been called “direct” methods since they rely upon the existence of sample sets of input parameters.

In real applications though, it may happen that no data is available for some input parameters, *e.g.* when the cost of data acquisition is too important or when these parameters are not directly measurable (*e.g.* parameters of a complex constitutive law). In contrast, data related to the model output (*e.g.* displacements, strains, temperature, etc.) may be easily collected in these situations. Thus specific so called *inverse* methods have to be devised so as to incorporate this data into the general framework of uncertainty propagation described in Chapter 1.

Two classes of problems are considered in this chapter, for which specific methods are proposed that allow the analyst to deal with the data at hand.

1.1 Bayesian updating techniques for real systems

When a *real* or *existing* system (as opposed to designed systems, see the discussion in Chapter 1, Section 2.3) is monitored in time, response quantities are measured, which can be compared to the model predictions. Due to model uncertainty and measurement error, the two quantities usually do not exactly match.

The measurement data may be used in two ways:

- The analyst may be mainly interested in improving the *model predictions*. In this case, he or she can resort to methods that *update* the model response by incorporating the monitoring data. These techniques have been much developed in structural reliability analysis (see *e.g.* Madsen (1987), Ditlevsen and Madsen (1996, Chap. 13)). They correspond to computing the probability of failure *conditionally* to the observations.

- The analyst may be interested in improving the knowledge on the *input parameters* of the model of the real system, *e.g.* in order to use this information in the design of similar systems. In this case, the probabilistic description of the input parameters is *updated* conditionally to the observations. Note that the methods developed by Tarantola (1987, 2005), which have inspired some of the developments presented later on, belong to this category.

Bayesian statistics is the natural tool to incorporate the measurement data into the computational schemes in both situations. Applications of these techniques are encountered in the assessment of real structures that are monitored all along their life time, such as:

- civil engineering structures for which displacements and strains are regularly measured, *e.g.* the maximal deflection of a bridge span, the delayed strains of a concrete containment vessel of a nuclear powerplant, the downwards displacement of the crest of a concrete dam, etc.;
- damaging structures, for which some indicator is monitored through regular inspections, *e.g.* the length of cracks in steel structures (pipes, offshore structures, etc.), the depth of concrete carbonation in concrete structures, the corrosion depth in rebars, etc.

The traditional approach to the reliability analysis of existing systems is described in Section 2. An original algorithm that provides *updated confidence intervals* on the model predictions is more specifically introduced. The updating of the input parameters describing the real system is then presented in Section 3, where Markov chain Monte Carlo simulation is introduced.

Note that the techniques of *data assimilation* broadly used in ocean engineering (Bennett, 1992), meteorology (Talagrand, 1997) and atmospheric pollution (Sportisse, 2004; Bocquet, 2006) are applied to solve similar, although different types of problems: a dynamic real system is considered for which it is not possible to determine the initial conditions of the associated model. Thus a probabilistic framework is used in order to model the discrepancy between predictions and observations at each time instant and update the input accordingly. Techniques such as Kalman filters and their extensions are used for this purpose. Attempts to use these techniques in civil engineering may be found in Ching et al. (2006a,b).

1.2 Stochastic inverse methods

When the analyst wants to characterize the aleatoric uncertainty of some physical parameter which is an input variable of a system model, and for which no direct measuring is possible, he or she has to resort to stochastic inverse methods.

Precisely, a *set of real systems* that derive from a unique designed system is considered (*e.g.* a set of identical testing samples used to characterize some material property). These real systems are consequently represented by the same mathematical model. The scattering observed in measuring some response quantity on all of these systems mainly reflects the aleatoric uncertainty in the input parameters, provided the model is correct and the measurement uncertainty is negligible (both sources of additional uncertainty may be however present and should be taken care of in a consistent way). Original methods are proposed in Section 4 to deal with these so-called *stochastic inverse problems*.

1.3 Measurement uncertainty and model error

The various methods presented in the following sections make assumptions on the accuracy of both model predictions and measurement procedures. Before proceeding, it is important to clarify what is meant by *measurement uncertainty* and *model error*.

1.3.1 Measurement uncertainty

Let us consider a real system and a supposedly perfect model of its physical behaviour $\mathbf{y} = \mathcal{M}(\mathbf{x})$. Let $\tilde{\mathbf{y}}$ be the true value of the model response, *i.e.* the value that would be obtained from infinitely accurate measurement devices. Let $\tilde{\mathbf{x}}$ be the corresponding true value of the input parameters. As the model is supposed to be perfect, the following relationship holds:

$$\tilde{\mathbf{y}} = \mathcal{M}(\tilde{\mathbf{x}}) \quad (5.1)$$

In practice, the measured response \mathbf{y}_{obs} may differ from the true value of the response:

$$\mathbf{y}_{obs} = \tilde{\mathbf{y}} + \mathbf{e} = \mathcal{M}(\tilde{\mathbf{x}}) + \mathbf{e} \quad (5.2)$$

It is common practice to consider that the measurement error \mathbf{e} is a realization of a Gaussian random vector \mathbf{E} with zero mean (if the measurements are unbiased) and covariance matrix \mathbf{C}_{meas} , the latter being known from the calibration of the measurement devices. When considering now that the true value of the input parameters $\tilde{\mathbf{x}}$ is a particular realization of the input random vector \mathbf{X} , Eq.(5.2) simply states that the conditional distribution of the measured response \mathbf{Y}_{obs} reads:

$$\mathbf{Y}_{obs} | \mathbf{X} = \tilde{\mathbf{x}} \sim \mathcal{N}(\mathcal{M}(\tilde{\mathbf{x}}); \mathbf{C}_{meas}) \quad (5.3)$$

which rewrites as follows in terms of conditional probability density function:

$$f_{\mathbf{Y}_{obs} | \mathbf{X}}(\mathbf{y} | \mathbf{X} = \mathbf{x}) = (2\pi)^{-N/2} (\det \mathbf{C}_{meas})^{-1/2} \exp \left[-\frac{1}{2} (\mathbf{y} - \mathcal{M}(\mathbf{x}))^T \cdot \mathbf{C}_{meas}^{-1} \cdot (\mathbf{y} - \mathcal{M}(\mathbf{x})) \right] \quad (5.4)$$

In this equation N is the size of the response vector \mathbf{y} . This expression will be taken advantage of in the sequel. Note that the measurement error \mathbf{E} is in nature independent of \mathbf{X} .

1.3.2 Model error

As already observed in Chapter 1, models are abstract representations of real systems that always simplify the complexity of the underlying physics. Even when there is no measurement uncertainty (or when it is negligible), there may be some discrepancy between the predicted and the observed values in most situations. This is called *model error* in the sequel. Note that model error has been disregarded in the first four chapters of this thesis: a perfect model was assumed since the interest was in the probabilistic modelling of the input uncertainty and its subsequent propagation. However, when dealing with inverse problems, this assumption becomes too restrictive.

Experimental model calibration When considering a model $\mathbf{y} = \mathcal{M}(\mathbf{x})$ of a physical system, the model uncertainty may be of two kinds, as discussed by Gardoni (2002); Gardoni et al. (2002):

- there may be some error in the form of the model, *e.g.* a linear model is proposed whereas the actual system response depends non linearly on the input. The same type of error occurs when the model at hand is deliberately biased in order to be conservative, such as simplified models of structural capacity codified in standards;
- there may be missing variables that have been neglected (for the sake of parcimony in the model) or that are not even known (*i.e.* hidden variables).

Consequently, the true response of a real system may be cast as:

$$\tilde{\mathbf{y}} = \mathcal{M}(\mathbf{x}) + \gamma(\mathbf{x}, \boldsymbol{\theta}_\gamma) + \mathbf{e} \quad (5.5)$$

In this expression, $\gamma(\mathbf{x}, \boldsymbol{\theta}_\gamma)$ denotes a function that models the bias observed between predicted and true responses and e represents the influence of the missing variables.

Gardoni (2002) proposes to represent the *bias correction term* $\gamma(\mathbf{x}, \boldsymbol{\theta}_\gamma)$ by explanatory functions $\theta_\gamma^l h_l(\mathbf{x})$ depending on a set of parameters $\boldsymbol{\theta}_\gamma$:

$$\gamma(\mathbf{x}, \boldsymbol{\theta}_\gamma) \equiv \sum_{l=1}^{n_\gamma} \theta_\gamma^l h_l(\mathbf{x}) \quad (5.6)$$

The explanatory functions are chosen by the analyst with respect to physical considerations. The residual error is modelled by a centered Gaussian distribution, *e.g.* with variance σ_e^2 in the scalar case. Using a set of experimental data obtained for prescribed values of the input parameters, one is able to estimate $\boldsymbol{\theta}_\gamma$ as well as the residual variance error. The latter may be eventually used to compare various bias correction terms with each other and select the best model accordingly.

This approach is similar to the *experimental model calibration* presented in Ditlevsen and Madsen (1996, Chap. 11). It basically assumes that the observation data is obtained in a controlled environment, *i.e.* that the values of the input corresponding to each observation are *known*. Such approaches cannot be applied to the stochastic inverse problems addressed in this chapter, since the realizations of the input vectors are supposed *not to be known* in the present case.

Proposed formulation of the model error From the above paragraph, it is intuitively clear that the experimental model calibration and the stochastic inverse problem are different in nature and that they cannot be solved simultaneously. As this chapter focuses on the latter problem, the following representation of model error will be retained in the sequel.

- the model at hand is considered as *unbiased*;
- the model error due to missing variables and/or inexact model form is taken into account exactly as the measurement uncertainty, *i.e.* the discrepancy between the model response and the observation vector is supposed to be a realization \mathbf{e} of a random vector \mathbf{E} :

$$\mathbf{y}_{obs} = \mathcal{M}(\tilde{\mathbf{x}}) + \mathbf{e} \quad (5.7)$$

- it is further assumed that the conditional distribution of the model error is Gaussian, which leads to the following expression similar to Eq.(5.3):

$$\mathbf{Y}_{obs} | \mathbf{X} = \tilde{\mathbf{x}} \sim \mathcal{N}(\mathcal{M}(\tilde{\mathbf{x}}); \mathbf{C}_{mod}) \quad (5.8)$$

where \mathbf{C}_{mod} is the covariance matrix of the model error.

1.3.3 Conclusion

In the context of stochastic inverse problems developed in this chapter, model uncertainty cannot be calibrated independently from measurement uncertainty. Indeed, the realizations of the input parameters corresponding to a set of observations \mathbf{Y}_{obs} are not known, since the very scattering of the input vector is to be inferred from \mathbf{Y}_{obs} .

In practice, a single error term called *measurement/model error* is introduced in the analysis. Each observation \mathbf{y}_{obs} is considered as a realization of the (random) observation vector \mathbf{Y}_{obs} whose conditional joint PDF is assigned:

$$\mathbf{Y}_{obs} | \mathbf{X} = \mathbf{x} \sim \mathcal{N}(\mathcal{M}(\mathbf{x}); \mathbf{C}_{obs}) \quad (5.9)$$

where \mathbf{C}_{obs} is the covariance matrix of the measurement/model error. As already observed by Tarantola (2005, Chap. 1) using a slightly different formulation, if both the measurement uncertainty and model error are additive and Gaussian (with respective covariance matrix \mathbf{C}_{meas} and \mathbf{C}_{mod}) then the measurement/model error is Gaussian with covariance matrix

$$\mathbf{C}_{obs} = \mathbf{C}_{meas} + \mathbf{C}_{mod} \quad (5.10)$$

Remark It is worth emphasizing that all the developments presented in this chapter remain valid if a non Gaussian distribution is assumed in Eq.(5.9).

2 Bayesian updating of model response

2.1 Introduction

The large-scale structures encountered in civil engineering (*e.g.* bridges, dams, etc.), nuclear engineering (*e.g.* concrete containment vessels, reactor vessels, etc.) or offshore engineering (*e.g.* steel jacket structures) are designed so as to fulfill some service requirements for a prescribed lifetime. Often the models used to design such components or structures are elementary (*e.g.* elastic models) in order to comply with the design rules codified in standards. Moreover, these models are usually intended to be *conservative*, *i.e.* they are supposed to make the system work “on the safe side”.

Due to the uniqueness of such complex systems, monitoring devices are usually installed during the construction so as to allow the manager of the facility to check that the behaviour of the system is satisfactory all along its service life. The monitoring data is often used *per se* and scarcely confronted to the structural models that were used at the design stage¹.

In the context of structural reliability, methods have been proposed back in the mid 80’s to update the probability of failure of a system from monitoring data (Madsen (1987). Applications of such Bayesian updating schemes can be found in fatigue crack growth (Zhao and Haldar, 1996; Zhang and Mahadevan, 2000; Baker and Stanley, 2002; Ayala-Uraga and Moan, 2002), fracture mechanics of offshore tubular joints (Rajansankar et al., 2003), modal analysis (López de Lacalle et al., 1996) or chloride ingress in concrete bridges (Rafiq et al., 2004). In all these applications, a Bayesian framework is used in order to update probabilities of failure by incorporating destructive or non destructive inspection data.

From a practical point of view, the analyst may be more interested in updating *model predictions* though. In a probabilistic context, this corresponds to computing the probability density function of response quantities conditionally to the monitoring data. This problem is closely related to that of computing updated probabilities of failure.

The traditional Bayesian updating of a probability of failure is first recalled. Then the problem of computing quantiles of response quantities is cast as an inverse reliability problem. Finally an original algorithm to compute updated quantiles is proposed. This method was originally presented in Sudret et al. (2006).

2.2 Updating probabilities of failure

Let us consider a scalar time-dependent model of a system $y = \mathcal{M}(\mathbf{x}, t)$ and let us assume that the input variables are modelled by a random vector \mathbf{X} with joint PDF $f_{\mathbf{X}}(\mathbf{x})$ ². Let us suppose that the reliability

¹There may be practical reasons for this: the owner of the facility has not always access to the detailed design of the system he manages, since this information may remain the property of the consultancy firms that carried out the design.

²In this paragraph, the model response is supposed to be scalar for the sake of simplicity in the notation. A generalization to vector models is however straightforward.

of the system with respect to some failure criterion is of interest, where the time-dependent limit state function reads:

$$g(\mathbf{X}, t) \equiv \tilde{g}(\mathbf{X}, \mathcal{M}(\mathbf{X}, t), t) \quad (5.11)$$

The point-in-time probability of failure at time instant t is defined by³:

$$P_f(t) = \mathbb{P}(g(\mathbf{X}, t) \leq 0) \quad (5.12)$$

Let us suppose now that measurements of the model response are carried out at various time instants $t_j, j = 1, \dots, n_{obs}$:

$$\mathbf{Y}_{obs} = \{y_{obs}^{(j)}, j = 1, \dots, n_{obs}\} \quad (5.13)$$

Due to measurement uncertainty, there is some discrepancy between the j -th observation and the model prediction at $t = t_j$ (see Eq.(5.2) in the scalar case):

$$e_j = y_{obs}^{(j)} - \mathcal{M}(\tilde{\mathbf{x}}, t_j) \quad (5.14)$$

where $\tilde{\mathbf{x}}$ is the best estimate value of the input parameters used in the prediction. According to the discussion in Section 1.3, it is further assumed that $\{e_j, j = 1, \dots, n_{obs}\}$ are realizations of independent normal variables E_j of variance σ_j^2 . Following Ditlevsen and Madsen (1996, Chap. 13), one defines the j -th *measurement event* by $\{H_j = 0\}$, where H_j reads:

$$H_j = y_{obs}^{(j)} + E_j - \mathcal{M}(\mathbf{X}, t_j) \quad (5.15)$$

The *updated probability of failure* is defined as the probability that the limit state function takes negative values *conditionally* to the measurement events:

$$P_f^{\text{upd}}(t) \equiv \mathbb{P} \left(g(\mathbf{X}, t) \leq 0 \mid \bigcap_{j=1}^{n_{obs}} \{H_j = 0\} \right) \quad (5.16)$$

Since the conditioning events $\{H_j = 0\}$ have a zero probability of occurrence, the updated probability of failure has to be more precisely defined for mathematical well-posedness, namely:

$$P_f^{\text{upd}}(t) \equiv \lim_{\theta \rightarrow 0^+} \frac{\mathbb{P}(g(\mathbf{X}, t) \leq 0 \cap \{-\theta \leq H_1 \leq 0\} \cap \dots \cap \{-\theta \leq H_{n_{obs}} \leq 0\})}{\mathbb{P} \left(\bigcap_{j=1}^{n_{obs}} \{-\theta \leq H_j \leq 0\} \right)} \quad (5.17)$$

In the context of first order reliability analysis, the reliability index associated with the above probability of failure reads:

$$\beta^{\text{upd}}(t) = \frac{\beta_0(t) - \mathbf{R}_0^\top \cdot \mathbf{R} \cdot \boldsymbol{\beta}}{\sqrt{1 - (\mathbf{R}_0^\top \cdot \mathbf{R} \cdot \mathbf{R}_0)^2}} \quad (5.18)$$

where $\beta_0(t)$ is the unconditional reliability index associated with $\{g(\mathbf{X}, t) \leq 0\}$ at time t , $\boldsymbol{\beta}$ is the vector of the reliability indices associated to the events $\{\{H_j \leq 0\}, j = 1, \dots, n_{obs}\}$, \mathbf{R} is the matrix whose entries read $\mathbf{R}_{ij} = \boldsymbol{\alpha}_i \cdot \boldsymbol{\alpha}_j$ and \mathbf{R}_0 is a vector such that $R_{0,j} = \boldsymbol{\alpha}_0 \cdot \boldsymbol{\alpha}_j$. In the latter equations, the $\boldsymbol{\alpha}$ -vectors correspond to the usual unit normal vector to the limit state surface at the design point (see Eq.(3.49)), the subscript “0” referring to the limit state function $\{g(\mathbf{X}, t) \leq 0\}$, and the subscript j referring to the limit states $\{\{H_j \leq 0\}, j = 1, \dots, n_{obs}\}$.

³A comprehensive introduction to time-variant reliability problems is given in Chapter 6.

2.3 Computation of response quantiles by inverse FORM analysis

As mentioned in the introduction, the analyst may want to compute confidence intervals (*i.e.* quantiles) of the time-dependent response for a robust prediction of the system behaviour. Theoretically speaking, the methods presented in Chapter 3 and 4 may be used for this purpose. However, these methods do not allow one to include easily monitoring data. In contrast, the Bayesian updating techniques straightforwardly apply in the context of reliability analysis, as shown in the above paragraph. Thus it appears interesting to transform the problem of computing response quantiles into reliability problems.

Accordingly, let us consider the evolution in time of the yet-to-be-determined response PDF $f_Y(y, t)$ of $Y(t)$, and more precisely α -quantiles of the latter, which are denoted by $y_\alpha(t)$. In practice, one is often interested in establishing a 95% confidence interval. This means that the 2.5% and 97.5% quantiles are of interest in this particular case. Introducing the response CDF:

$$F_Y(y, t) = \mathbb{P}(Y(t) \leq y) \quad (5.19)$$

the α -quantiles of the response can be obtained as the solution of the following problem:

$$\text{Find } y_\alpha(t) : F_Y(y_\alpha(t), t) = \alpha \quad (5.20)$$

The above equation is now interpreted as an *inverse reliability problem*. Generally speaking, suppose that a limit state function $g(\mathbf{X}, \theta)$ depends on a parameter θ and suppose that a target probability of failure P_f^c is prescribed. The inverse reliability problem reads:

$$\text{Find } \theta : \mathbb{P}(g(\mathbf{X}, \theta) \leq 0) = P_f^c \quad (5.21)$$

In the context of first order reliability analysis, a target reliability index β^c is prescribed and Eq.(5.21) is recast as:

$$\text{Find } \theta : \mathbb{P}_{\text{FORM}}(g(\mathbf{X}, \theta) \leq 0) = \Phi(-\beta^c) \quad (5.22)$$

where $\mathbb{P}_{\text{FORM}}(\cdot)$ means that the probability of failure is computing using FORM analysis. Various algorithms have been proposed to carry out this so-called *inverse FORM analysis*, see Der Kiureghian et al. (1994) and more recently Li and Foschi (1998); Minguéz et al. (2005).

Combining Eqs.(5.19),(5.20),(5.22), the α -quantiles of the response quantity may be obtained by applying the inverse FORM algorithm using an appropriate limit state function and a target reliability index $\beta^c = -\Phi^{-1}(\alpha)$. More precisely, Eq.(5.20) is recast as:

$$\text{Find } y_\alpha(t) : \mathbb{P}_{\text{FORM}}(\mathcal{M}(\mathbf{X}, t) - y_\alpha(t) \leq 0) = \alpha \quad (5.23)$$

As FORM analysis is all the more accurate since the obtained probability of failure is small, Eq.(5.23) should be used for lower quantiles, *e.g.* 2.5%. For upper quantiles (*e.g.* $\alpha = 97.5\%$), the *opposite* limit state function should be preferred, together with a target reliability index $\beta^c = \Phi^{-1}(1 - \alpha)$.

2.4 Computation of updated response quantiles by inverse FORM analysis

The Bayesian updating formulæ Eqs.(5.17)-(5.18) are now combined with the inverse FORM method to compute *updated quantiles of the response*, which are denoted by $y_\alpha^{\text{upd}}(t)$. The “updated” counterpart of Eq.(5.20) reads:

$$\text{Find } y_\alpha^{\text{upd}}(t) : F_Y^{\text{upd}}(y_\alpha^{\text{upd}}(t), t) = \alpha \quad (5.24)$$

where the function in the righthand side of Eq.(5.24) reads:

$$\begin{aligned}
 F_Y^{\text{upd}}(y, t) &\equiv \mathbb{P} \left(\mathcal{M}(\mathbf{X}, t) - y \leq 0 \mid \bigcap_{j=1}^{n_{\text{obs}}} \{H_j = 0\} \right) \\
 &\equiv \lim_{\theta \rightarrow 0^+} \frac{\mathbb{P}(\mathcal{M}(\mathbf{X}, t) - y \leq 0 \cap \{-\theta \leq H_1 \leq 0\} \cap \dots \cap \{-\theta \leq H_{n_{\text{obs}}} \leq 0\})}{\mathbb{P} \left(\bigcap_{j=1}^{n_{\text{obs}}} \{-\theta \leq H_j \leq 0\} \right)} \quad (5.25)
 \end{aligned}$$

The problem in Eq.(5.24) may be solved by adapting the inverse FORM algorithm proposed by Der Kiureghian et al. (1994). This corresponds to solving the “updated” counterpart of Eq.(5.23):

$$\text{Find } y_\alpha^{\text{upd}}(t) : \quad \mathbb{P}_{\text{FORM}}(\mathcal{M}(\mathbf{X}, t) - y_\alpha^{\text{upd}}(t) \leq 0 \mid H_1 = 0 \cap \dots \cap H_N = 0) = \alpha \quad (5.26)$$

At each time instant, the inverse FORM algorithm is applied together with the limit state $\{g(\mathbf{X}, t, y_\alpha^{\text{upd}}(t)) \equiv \mathcal{M}(\mathbf{X}, t) - y_\alpha^{\text{upd}}(t) \leq 0\}$, except that the target reliability index β^c changes from iteration k to the next:

$$\beta^{c,(k+1)} = -\Phi^{-1}(\alpha) \sqrt{1 - \left(\mathbf{R}_0^{(k)\top} \cdot \mathbf{R} \cdot \mathbf{R}_0^{(k)} \right)^2} + \mathbf{R}_0^{(k)\top} \cdot \mathbf{R} \cdot \boldsymbol{\beta}^{(k)} \quad (5.27)$$

In this equation, matrix \mathbf{R} does not change from one iteration to the next (it may be computed and stored once and for all), in contrast to vectors \mathbf{R}_0 and $\boldsymbol{\beta}$. Note that no formal proof of the convergence of such an algorithm has been given. However, it has been applied successfully in various contexts.

2.5 Conclusion

The method presented in this section allows the analyst to compute updated quantiles of the time-dependent response of a model by incorporating monitoring data that is obtained at various time instants. It is based on the transformation of the original problem into an inverse reliability problem. The latter is solved by an inverse FORM algorithm adapted to the Bayesian updating context.

An application example in fracture mechanics will be given in Section 5, see also Perrin et al. (2007a). The application to the updated prediction of concrete delayed stresses in a containment vessel has been shown in Sudret et al. (2006), where an analytical model \mathcal{M} was used. A similar application in which a finite element model of the containment vessel is introduced, is presented in Berveiller et al. (2007). Due to the computational burden, a polynomial chaos expansion of the finite element model response is used in the latter case.

To conclude, it is worth emphasizing that the proposed method does update model predictions (in terms of a conditional distribution) *without* yielding any information about the input variables. A Bayesian updating technique for the input parameters of a model based on data related to response quantities is now proposed.

3 Bayesian updating of input parameters

3.1 Introduction

In the previous section, the data gathered on a real system by monitoring was used to update the model predictions, in the specific context of a time-dependent response. However, the proposed method does not bring any additional information on the input parameters of the model.

Updating the probabilistic description of the input parameters may be of interest though. Various techniques have been proposed for this purpose, especially in structural dynamics. A large amount of literature addresses the problem of identifying (in a Bayesian context) the best value of the input parameter from dynamic test responses together with their uncertainty, see *e.g.* Katafygiotis et al. (1998); Beck and Katafygiotis (2001); Katafygiotis and Beck (1998); Papadimitriou et al. (2001); Yuen and Katafygiotis (2001, 2002); Beck and Au (2002). Similar Bayesian techniques have been introduced in structural health monitoring in which the monitoring data is used to infer the changes in the stiffness of the structure due to damage, see *e.g.* Johnson et al. (2004); Lam et al. (2004); Ching and Beck (2004); Yuen et al. (2004).

A Bayesian framework to update the joint PDF of model input parameters that is consistent with the assumptions in Section 1 is now presented.

3.2 Problem statement

Let us consider a real system and its (possibly time-dependent) model $\mathbf{y} = \mathcal{M}(\mathbf{x}, t)$. The input is modelled by a random vector \mathbf{X} with prescribed distribution $p_{\mathbf{X}}(\mathbf{x})$. Let us assume that a set of measured response quantities is available:

$$\mathcal{Y}_{obs} = \{\mathbf{y}_{obs}^{(j)}, j = 1, \dots, n_{obs}\} \quad (5.28)$$

From Section 1.3, it is supposed that the conditional distribution of each observation reads (Eq.(5.9)):

$$\mathbf{Y}_{obs} | \mathbf{X} = \tilde{\mathbf{x}} \sim \mathcal{N}(\mathcal{M}(\tilde{\mathbf{x}}); \mathbf{C}_{obs}) \quad (5.29)$$

where $\tilde{\mathbf{x}}$ is the (unknown) realization of the input random vector that corresponds to the very system under consideration. In other words, the conditional PDF of the j -th observation \mathbf{Y}_j carried out at $t = t_j$ reads:

$$\begin{aligned} f_{\mathbf{Y}_j | \mathbf{X}}(\mathbf{y} | \mathbf{X} = \tilde{\mathbf{x}}) &= \varphi_N(\mathbf{y} - \mathcal{M}(\tilde{\mathbf{x}}, t_j); \mathbf{C}_{obs}) \\ &\equiv (2\pi)^{-N/2} (\det \mathbf{C}_{obs})^{-1/2} \exp \left[-\frac{1}{2} (\mathbf{y} - \mathcal{M}(\tilde{\mathbf{x}}, t_j))^T \cdot \mathbf{C}_{obs}^{-1} \cdot (\mathbf{y} - \mathcal{M}(\tilde{\mathbf{x}}, t_j)) \right] \end{aligned} \quad (5.30)$$

In the Bayesian paradigm, the above equation is interpreted as follows: vector \mathbf{X} plays the role of the ‘‘hyperparameters’’ of the distribution of \mathbf{Y}_j , $j = 1, \dots, n_{obs}$. The Bayes’ theorem allows to derive the posterior distribution of \mathbf{X} based on realizations of \mathbf{Y}_j ’s, namely \mathcal{Y}_{obs} . This posterior distribution reads:

$$f_{\mathbf{X}}(\mathbf{x} | \mathcal{Y}_{obs}) = c p_{\mathbf{X}}(\mathbf{x}) \mathsf{L}(\mathbf{x}; \mathcal{Y}_{obs}) \quad (5.31)$$

where c is a normalizing constant and $\mathsf{L}(\mathbf{x}; \mathcal{Y}_{obs})$ is the likelihood function of the observations:

$$\mathsf{L}(\mathbf{x}; \mathcal{Y}_{obs}) = \prod_{j=1}^{n_{obs}} \varphi_N(\mathbf{y}_{obs}^{(j)} - \mathcal{M}(\mathbf{x}, t_j); \mathbf{C}_{obs}) \quad (5.32)$$

Note that, in contrast to classical Bayesian analysis, the end product here is the posterior distribution of \mathbf{X} , and not the predictive distribution of the \mathbf{Y}_j ’s.

In order to completely characterize the posterior distribution $f_{\mathbf{X}}(\mathbf{x} | \mathcal{Y}_{obs})$, the normalizing constant c in Eq.(5.31) shall be computed, namely:

$$\frac{1}{c} = \int_{\mathbb{R}^M} p_{\mathbf{X}}(\mathbf{x}) \prod_{j=1}^{n_{obs}} \varphi_N(\mathbf{y}_{obs}^{(j)} - \mathcal{M}(\mathbf{x}, t_j); \mathbf{C}_{obs}) d\mathbf{x} \quad (5.33)$$

This so-called *Bayesian integral* may be computed by simulation techniques (*e.g.* Monte-Carlo simulation, Latin Hypercube sampling, etc.) or quadrature methods (Geyskens et al., 1993, 1998). Tensorized Gaussian quadrature may be used when the dimension M of \mathbf{X} is not too large. Note that sparse

quadrature schemes as those used in Chapter 4, Section 4.2 in the context of spectral methods may be used in larger dimensions (Perrin, 2008).

Alternatively, specific methods have been proposed recently that are especially suited to simulating probability density functions resulting from Bayes' theorem. These so-called *Markov chain Monte Carlo methods* are now presented.

3.3 Markov chain Monte Carlo simulation

Markov chain Monte Carlo (MCMC) methods are a class of algorithms that allow one to sample from probability distributions based on the construction of a Markov chain. Various methods known as the random walk, the Gibbs sampler or the Metropolis-Hastings algorithm pertain to these methods. The idea is to generate iteratively samples of a Markov chain, which asymptotically behaves as the PDF which is to be sampled.

3.3.1 Metropolis-Hastings algorithm

The Metropolis-Hastings algorithm (Metropolis et al., 1953; Hastings, 1970) is a rejection sampling algorithm that works as follows. A starting point $\mathbf{x}^{(0)}$ is selected. Then in each step, the transition between the states $\mathbf{x}^{(k)}$ and $\mathbf{x}^{(k+1)}$ reads:

$$\mathbf{x}^{(k+1)} = \begin{cases} \tilde{\mathbf{x}} \sim q(\mathbf{x} | \mathbf{x}^{(k)}) & \text{with probability } \alpha(\mathbf{x}^{(k)}, \tilde{\mathbf{x}}) \\ \mathbf{x}^{(k)} & \text{else} \end{cases} \quad (5.34)$$

In this equation, $q(\mathbf{x} | \mathbf{x}^{(k)})$ is the so-called *transition* or *proposal* distribution, and the *acceptance probability* $\alpha(\mathbf{x}^{(k)}, \tilde{\mathbf{x}})$ reads:

$$\alpha(\mathbf{x}^{(k)}, \tilde{\mathbf{x}}) = \min \left\{ 1, \frac{f_{\mathbf{X}}(\tilde{\mathbf{x}}) q(\mathbf{x}^{(k)} | \tilde{\mathbf{x}})}{f_{\mathbf{X}}(\mathbf{x}^{(k)}) q(\tilde{\mathbf{x}} | \mathbf{x}^{(k)})} \right\} \quad (5.35)$$

A common transition is obtained by generating the candidate $\tilde{\mathbf{x}}$ by adding a random disturbance $\boldsymbol{\xi}$ to $\mathbf{x}^{(k)}$ *i.e.* $\tilde{\mathbf{x}} = \mathbf{x}^{(k)} + \boldsymbol{\xi}$. This random vector $\boldsymbol{\xi}$ is often built by means of independent zero-mean Gaussian or uniform components. This implementation is referred to as a *random walk algorithm* and this was the original version of the method suggested by Metropolis et al. (1953). In this case, the transition distribution (*e.g.* uniform or Gaussian in practice) reads: $q(\tilde{\mathbf{x}} | \mathbf{x}^{(k)}) = q(\tilde{\mathbf{x}} - \mathbf{x}^{(k)})$. Due to the symmetry, the acceptance probability defined in Eq.(5.35) reduces to:

$$\alpha(\mathbf{x}^{(k)}, \tilde{\mathbf{x}}) = \min \left\{ 1, \frac{f_{\mathbf{X}}(\tilde{\mathbf{x}})}{f_{\mathbf{X}}(\mathbf{x}^{(k)})} \right\} \quad (5.36)$$

In order to select $\tilde{\mathbf{x}}$ with probability $\alpha(\mathbf{x}^{(k)}, \tilde{\mathbf{x}})$ (Eq.(5.34)), a sample $u^{(k)}$ is drawn from a uniform distribution $\mathcal{U}([0, 1])$. Then $\tilde{\mathbf{x}}$ is accepted if $u^{(k)} < \alpha(\mathbf{x}^{(k)}, \tilde{\mathbf{x}})$ and rejected otherwise.

Thus Eqs.(5.34),(5.36) allow one to draw samples of any distribution provided an algorithmic expression (*i.e.* not necessarily analytical) for $f_{\mathbf{X}}(\mathbf{x})$ is available. It is important to make sure that the simulated Markov chain obtained by the Metropolis-Hastings algorithm is likely to be generated by the PDF $f_{\mathbf{X}}(\mathbf{x})$ of interest. Several monitoring methods ensure the control of convergence, see details in Raftery and Lewis (1992); Cowles and Carlin (1996); Brooks and Roberts (1998) and a review in El Adlouni et al. (2006). In particular, a number of samples generated first, which correspond to the so-called *burn-in period*, are eventually discarded from the sample set.

3.3.2 Cascade Metropolis-Hastings algorithm

In order to simulate posterior densities such as that obtained in Eq.(5.31), the Metropolis-Hastings algorithm is used in a two-step *cascade* version, as proposed by Tarantola (2005). Broadly speaking, the candidate $\tilde{\mathbf{x}}$ should be accepted first with respect to the prior distribution as in Eq.(5.34). Then it is accepted or rejected with respect to the likelihood function. The full algorithm is now summarized.

1. $k = 0$, initialize the Markov chain $\mathbf{x}^{(0)}$ in a deterministic or random way;

While $k \leq n_{MCMC}$

2. generate a random increment $\boldsymbol{\xi}^{(k)}$, compute the candidate $\tilde{\mathbf{x}} = \mathbf{x}^{(k)} + \boldsymbol{\xi}^{(k)}$
3. evaluate the “prior” acceptance probability: $\alpha_p(\mathbf{x}^{(k)}, \tilde{\mathbf{x}}) = \min \left\{ 1, \frac{p_{\mathbf{X}}(\tilde{\mathbf{x}})}{p_{\mathbf{X}}(\mathbf{x}^{(k)})} \right\}$
4. compute a sample $u_p \sim \mathcal{U}([0, 1])$:
 - (a) if $u_p < \alpha_p(\mathbf{x}^{(k)}, \tilde{\mathbf{x}})$ then go to 5. (acceptation)
 - (b) else go to 2. (rejection)
5. evaluate the “likelihood” acceptance probability: $\alpha_L(\mathbf{x}^{(k)}, \tilde{\mathbf{x}}) = \min \left\{ 1, \frac{\mathbf{L}(\tilde{\mathbf{x}}; \mathcal{Y}_{obs})}{\mathbf{L}(\mathbf{x}^{(k)}; \mathcal{Y}_{obs})} \right\}$ where $\mathbf{L}(\cdot)$ is the likelihood function in Eq.(5.32). Note that this requires a call to the model function.
6. compute a sample $u_L \sim \mathcal{U}([0, 1])$
 - (a) if $u_L < \alpha_L(\mathbf{x}^{(k)}, \tilde{\mathbf{x}})$ then $\mathbf{x}^{(k+1)} \leftarrow \tilde{\mathbf{x}}$ and $k \leftarrow k + 1$ (acceptation)
 - (b) else go to 2. (rejection)

Once the required number of states of the Markov chain n_{MCMC} has been computed, the first n_{burn} terms are discarded, as explained above.

3.4 Conclusion

In this section, the use of Markov chain Monte Carlo simulation for simulating the posterior PDF of the input parameters has been introduced. This method allows the analyst to obtain samples of the posterior PDF $f_{\mathbf{X}}(\mathbf{x})$. These samples may be post-processed by kernel smoothing for graphical representation or in order to compute quantiles or moments.

Each evaluation of the likelihood function requires an evaluation of the model (Eq.(5.32)). Thus it is clear that the method is computationally expensive in terms of number of calls to the model, especially since the candidate $\tilde{\mathbf{x}}$ may be rejected by the test in step 6 of the cascade algorithm. Practically, it may be applied using either analytical models or surrogate models (*e.g.* polynomial chaos expansions) of complex models.

Once the samples of the posterior distribution have been computed, samples of the response vector are available without any additional effort. Thus the cascade MCMC method also provides for free the updated distribution of the response quantities. This means that the method developed in this section may be applied to solve the same problems as those addressed in Section 2, at a greater computational cost though. In particular, the Bayesian inverse FORM approach should be preferred when low quantiles of the updated response are of interest. Indeed, obtaining an accurate description of the tails of the posterior density of the response by MCMC is simply intractable.

Various application examples of Bayesian updating of input parameters may be found in Tarantola (2005, Chap. 7). Applications to the identification of parameters in structural dynamics may be found in Pillet et al. (2006); Arnst (2007). Marzouk et al. (2007) make use of polynomial chaos expansions together with the Bayesian framework in order to identify the sources in an inverse diffusion problem. A comparison of the Bayesian inverse FORM and MCMC approaches in fracture mechanics will be given in Section 5 for the sake of illustration.

4 Stochastic inverse problems

4.1 Introduction

4.1.1 Problem statement

Let us consider again a mathematical model of a physical system $\mathbf{y} = \mathcal{M}(\mathbf{x})$ that is possibly time-dependent, although this dependency is not explicitly shown in the sequel for the sake of simplicity. In a probabilistic context, the input is modelled by a random vector \mathbf{X} , which is split here into two parts as follows:

$$\mathbf{X} = \{\mathbf{X}_1, \mathbf{X}_2\}^\top \quad (5.37)$$

In this equation, random vector \mathbf{X}_2 gathers the input variables whose joint probability density function (PDF) $f_{\mathbf{X}_2}(\mathbf{x}_2)$ can be determined by either of the direct methods presented in Chapter 2, Section 3. By simplicity, it will be referred to as the “known” input vector, meaning the vector of input variables with known PDF.

Random vector \mathbf{X}_1 gathers the input variables whose joint PDF shall be obtained by an inverse method, *i.e.* using data related to model response quantities. By simplicity, it will be referred to as the “unknown” input vector, meaning the vector of input variables with yet-to-be-identified PDF. It is supposed throughout this section that both vectors are independent (the notation \mathbf{x} and $(\mathbf{x}_1, \mathbf{x}_2)$ is used equivalently in the sequel). Hence:

$$f_{\mathbf{X}}(\mathbf{x}) \equiv f_{\mathbf{X}}(\mathbf{x}_1, \mathbf{x}_2) = f_{\mathbf{X}_1}(\mathbf{x}_1) f_{\mathbf{X}_2}(\mathbf{x}_2) \quad (5.38)$$

The size of \mathbf{X}_1 and \mathbf{X}_2 will be denoted by M_1 and M_2 respectively ($M_1 + M_2 = M$).

In order to identify the unknown PDF $f_{\mathbf{X}_1}(\mathbf{x}_1)$, a set of observations of response quantities is available:

$$\mathcal{Y}_{obs} = \{\mathbf{y}_{obs}^{(1)}, \dots, \mathbf{y}_{obs}^{(n_{obs})}\} \quad (5.39)$$

where n_{obs} is the number of observations. Practically speaking, this means that n_{obs} different real systems have been observed, which are all modelled by the same function \mathcal{M} , whereas the true value (*i.e.* realization) of the input variables may differ from one real system to the other. This is the case when a set of theoretically identical samples are tested in the same experimental conditions.

Remark It is worth emphasizing the difference between this section and Sections 2 and 3 again. In those sections the realizations were related to a *single* real system, whereas each observation in this section corresponds to a different real system. It is indeed the aleatoric uncertainty of the input parameters \mathbf{X}_1 within these real systems that is sought.

The literature addressing stochastic inverse problems as defined above is rather rare. In the context of pure statistical approaches (*i.e.* where the input/output relationship is a mere linear or non linear regression model), these problems shall be related to the so-called *EM algorithm* (which stands for Expectation - Maximization) (Dempster et al., 1977) and its “stochastic” variants (Celeux and Diebolt, 1992; Celeux et al., 1996) and “stochastic approximation EM” (SAEM) (Delyon et al., 1999; Kuhn, 2003).

The same kind of inverse problems as those presented in this section is posed by Du et al. (2006); Cooke et al. (2006) in the case when the available information is given in terms of quantiles of the response quantities (instead of samples). Ratier et al. (2005) apply a stochastic inverse framework in order to identify a single dispersion parameter used in a non parametric model of mistuned bladed disks. Arnst (2007, Chap. 5) identifies the spatially varying Young's modulus in a collection of bars from dynamical tests.

4.1.2 Outline

The aim of this section is to present computational schemes that allow to estimate the unknown PDF $f_{\mathbf{X}_1}(\mathbf{x}_1)$ from $f_{\mathbf{X}_2}(\mathbf{x}_2)$, \mathcal{M} , \mathcal{Y}_{obs} . Various approaches are proposed depending on the following assumptions:

- the observations are supposed to be exact or not, *i.e.* the measurement error can be neglected or not.
- the joint PDF $f_{\mathbf{X}_1}(\mathbf{x}_1)$ is either cast in a parametric or non parametric representation.

4.2 Identification using perfect measurements

Let us suppose first that the observations of response quantities are perfect (in practice, this means that the measurement uncertainty is considered as negligible) and that the model is perfect. Note that an imperfect model can always be considered as perfect by introducing an additive or multiplicative correction factor, which is an additional random variable to be identified in \mathbf{X}_1 . Under these assumptions, the observations are considered as *realizations* of the random response vector:

$$\mathcal{Y}_{obs} = \{\mathbf{y}_{obs}^{(q)} = \mathcal{M}(\mathbf{x}_1^{(q)}, \mathbf{x}_2^{(q)}), q = 1, \dots, n_{obs}\} \quad (5.40)$$

Moreover, it is supposed that the observations are *independent*. Strictly speaking, this means that $\{\mathbf{x}_1^{(q)}, q = 1, \dots, n_{obs}\}$ (resp. $\{\mathbf{x}_2^{(q)}, q = 1, \dots, n_{obs}\}$) are realizations of independent identically distributed random vectors $\{\mathbf{X}_1^q, q = 1, \dots, n_{obs}\}$ (resp. $\{\mathbf{X}_2^q, q = 1, \dots, n_{obs}\}$) which have the same distribution $f_{\mathbf{X}_1}(\mathbf{x}_1)$ (resp. $f_{\mathbf{X}_2}(\mathbf{x}_2)$). However, for the sake of simplicity, the above sample sets are simply called “realizations of \mathbf{X}_1 ” (resp. \mathbf{X}_2).

4.2.1 Classical parametric approach

Kernel density approximation of the response PDF In this paragraph, the unknown PDF $f_{\mathbf{X}_1}(\mathbf{x}_1)$ is supposed to belong to a family of distributions which depend on a vector of hyperparameters $\boldsymbol{\theta}$:

$$f_{\mathbf{X}_1}(\mathbf{x}_1) \equiv p(\mathbf{x}_1; \boldsymbol{\theta}) \quad (5.41)$$

This situation occurs when there are some physical arguments that explain the variability of the input variables in \mathbf{X}_1 . The choice may also be imposed by expert judgment. The identification problem then reduces to estimating the vector of hyperparameters $\boldsymbol{\theta} \in \mathcal{D}_{\boldsymbol{\theta}} \subset \mathbb{R}^{n_{\boldsymbol{\theta}}}$ that best fits the observations. The maximum likelihood method may be applied for this purpose.

Let us denote by $f_{\mathbf{Y}}(\mathbf{y}; \boldsymbol{\theta})$ the joint PDF of the response vector $\mathbf{Y} = \mathcal{M}(\mathbf{X}_1, \mathbf{X}_2)$ in the case when the joint PDF of \mathbf{X}_1 is $p(\mathbf{x}_1; \boldsymbol{\theta})$. The joint PDF $f_{\mathbf{Y}}(\mathbf{y}; \boldsymbol{\theta})$ is of course not known analytically, however it may be estimated by a kernel density approximation (Chapter 4, Section 5.1) as follows, for any prescribed value of $\boldsymbol{\theta}$:

- samples of \mathbf{X}_1 are drawn according to $p(\mathbf{x}_1; \boldsymbol{\theta})$, say $\{\mathbf{x}_{1,\boldsymbol{\theta}}^{(k)}, k = 1, \dots, n_K\}$;
- samples of \mathbf{X}_2 are drawn according to $f_{\mathbf{X}_2}(\mathbf{x}_2)$, say $\{\mathbf{x}_2^{(k)}, k = 1, \dots, n_K\}$;
- realizations of \mathbf{Y} are computed:

$$\mathbf{y}^{(k)} = \mathcal{M}(\mathbf{x}_{1,\boldsymbol{\theta}}^{(k)}, \mathbf{x}_2^{(k)}) \quad k = 1, \dots, n_K \quad (5.42)$$

Then the PDF of \mathbf{Y} is approximated by:

$$\hat{f}_{\mathbf{Y}}(\mathbf{y}; \boldsymbol{\theta}) = \frac{1}{n_K} \sum_{k=1}^{n_K} K_h(\mathbf{y} - \mathcal{M}(\mathbf{x}_{1,\boldsymbol{\theta}}^{(k)}, \mathbf{x}_2^{(k)})) \quad (5.43)$$

where $K_h(\cdot)$ is a suitable multidimensional kernel (see Wand and Jones (1995) for details).

Maximum likelihood estimation From the above equation, the likelihood function of the observations is estimated by:

$$\begin{aligned} \mathsf{L}(\boldsymbol{\theta}; \mathcal{Y}_{obs}) &= \prod_{q=1}^{n_{obs}} \hat{f}_{\mathbf{Y}}(\mathbf{y}_{obs}^{(q)}; \boldsymbol{\theta}) \\ &= \prod_{q=1}^{n_{obs}} \left[\frac{1}{n_K} \sum_{k=1}^{n_K} K_h(\mathbf{y}_{obs}^{(q)} - \mathcal{M}(\mathbf{x}_{1,\boldsymbol{\theta}}^{(k)}, \mathbf{x}_2^{(k)})) \right] \end{aligned} \quad (5.44)$$

The maximum likelihood estimator of $\boldsymbol{\theta}$ is solution to the following maximization problem:

$$\hat{\boldsymbol{\theta}}^{\text{ML}} = \arg \max_{\boldsymbol{\theta} \in \mathcal{D}_{\boldsymbol{\theta}}} \mathsf{L}(\boldsymbol{\theta}; \mathcal{Y}_{obs}) = \arg \max_{\boldsymbol{\theta} \in \mathcal{D}_{\boldsymbol{\theta}}} \prod_{q=1}^{n_{obs}} \left[\frac{1}{n_K} \sum_{k=1}^{n_K} K_h(\mathbf{y}_{obs}^{(q)} - \mathcal{M}(\mathbf{x}_{1,\boldsymbol{\theta}}^{(k)}, \mathbf{x}_2^{(k)})) \right] \quad (5.45)$$

Note that the domain of optimization $\mathcal{D}_{\boldsymbol{\theta}}$ may be either the natural domain of definition of the hyperparameters of $p(\mathbf{x}_1; \boldsymbol{\theta})$ or some restrained (*e.g.* bounded) domain inferred by expert judgment.

The joint PDF $f_{\mathbf{X}_1}(\mathbf{x}_1)$ identified by this parametric approach eventually reads:

$$\hat{f}_{\mathbf{X}_1}^{\text{ML}}(\mathbf{x}_1) = p(\mathbf{x}_1; \hat{\boldsymbol{\theta}}^{\text{ML}}) \quad (5.46)$$

Computational issues The maximum likelihood estimator in Eq.(5.45) is independent of the choice of the kernel K_h provided the number of samples n_K used in the representation is large enough (*e.g.* 1,000 – 10,000 in the applications). This means that n_K runs of the model are used for each evaluation of the likelihood function, which is itself evaluated many times in the optimization algorithm. This is computationally tractable only when \mathcal{M} is an analytical model or when surrogate models such as polynomial chaos expansions are considered.

Moreover, the approximate expression for the likelihood function is usually not smooth and may present local maxima (this problem is to be related to the identifiability of the parameters). Thus gradient-based optimization algorithms often fail. The CONDOR algorithm (Vanden Berghen, 2004; Vanden Berghen and Bersini, 2004), which is a trust-region algorithm, revealed remarkably efficient in this context.

In order to get a smoother approximation of $\mathsf{L}(\boldsymbol{\theta}; \mathcal{Y}_{obs})$ when $\boldsymbol{\theta}$ varies (*e.g.* throughout the maximization process), the following strategy may be adopted when \mathbf{X}_1 can be cast as a $\boldsymbol{\theta}$ -dependent transform of a unique random vector $\boldsymbol{\chi}$, say $\mathbf{X}_1 = T(\boldsymbol{\chi}, \boldsymbol{\theta})$. In this case, a single sample set of realizations of $\boldsymbol{\chi}$ (of size n_K) should be drawn at the beginning of the procedure, whereas the sample set $\{\mathbf{x}_{1,\boldsymbol{\theta}}^{(k)} = T(\boldsymbol{\chi}^{(k)}, \boldsymbol{\theta}), k = 1, \dots, n_K\}$ is used when evaluating Eq.(5.44) for various values of $\boldsymbol{\theta}$.

4.2.2 Polynomial chaos-based parametric approach

In most situations, the analyst does not know the form of the joint PDF of the unknown random vector \mathbf{X}_1 . The framework proposed in the above paragraph may be generalized to a *semi-parametric* identification using polynomial chaos expansions. The term “semi-parametric” means in this context that the PDF $f_{\mathbf{X}_1}(\mathbf{x}_1)$ is not sought in a prescribed family of distributions. In order to avoid any confusion, the term *PC-based parametric approach* is used in the sequel.

Polynomial chaos representation By assuming that random vector \mathbf{X}_1 is of second order, one can represent it as its Wiener-Hermite expansion (Ghanem and Spanos, 1991a):

$$\mathbf{X}_1 = \sum_{\boldsymbol{\alpha} \in \mathbb{N}^{\mathbb{N}}} \mathbf{a}_{\boldsymbol{\alpha}} \Psi_{\boldsymbol{\alpha}}(\{\xi_j\}_{j \geq 1}) \quad (5.47)$$

where $\{\xi_j\}_{j \geq 1}$ is an infinite sequence of independent standard normal random variables and $\boldsymbol{\alpha}$ are integer sequences with a finite number of non zero terms. By selecting a finite dimensional chaos using R_1 basic variables and polynomials up to order p_1 , the random vector may be given the following truncated PC expansion:

$$\mathbf{X}_1^{\text{PC}} = \sum_{\boldsymbol{\alpha} \in \mathbb{N}^{R_1}, 0 \leq |\boldsymbol{\alpha}| \leq p_1} \mathbf{a}_{\boldsymbol{\alpha}} \Psi_{\boldsymbol{\alpha}}(\boldsymbol{\Xi}) \quad , \quad \boldsymbol{\Xi} = \{\xi_1, \dots, \xi_{R_1}\}^{\text{T}} \quad (5.48)$$

Note that the number of basic random variables R_1 is not necessarily equal to M_1 , although this is often a suitable choice. In particular, when the components of \mathbf{X}_1 are supposed to be independent, it is efficient to associate one single basic variable ξ_i to each component $X_{1,i}$ and expand the latter using univariate Hermite polynomials in ξ_i :

$$X_{1,i} = \sum_{j=0}^{p_1} a_j^i \text{He}_j(\xi_i), \quad i = 1, \dots, M_1 \quad (5.49)$$

From Eq.(5.48), it is seen that the unknown random vector \mathbf{X}_1 may be approximately represented by a finite set of coefficients:

$$\mathfrak{A} = \{a_{\boldsymbol{\alpha}}^k : \boldsymbol{\alpha} \in \mathbb{N}^{R_1}, 0 \leq |\boldsymbol{\alpha}| \leq p_1, \quad k = 1, \dots, M_1\} \quad (5.50)$$

To identify $f_{\mathbf{X}_1}(\mathbf{x}_1)$ reduces in some sense to determining the optimal set \mathfrak{A} , which plays the role of the hyperparameters $\boldsymbol{\theta}$ in the parametric approach presented in Section 4.2.1. The difference lies in the fact that the number of hyperparameters in the parametric case is usually much smaller than the number of PC coefficients in the PC-based parametric case, at a price of far less flexibility though.

From the above notation, the joint PDF $f_{\mathbf{X}_1}(\mathbf{x}_1)$ of interest is now approximated by:

$$f_{\mathbf{X}_1}(\mathbf{x}_1) \approx f_{\mathbf{X}_1^{\text{PC}}}(\mathbf{x}_1; \mathfrak{A}) \quad (5.51)$$

which is the PC-based parametric counterpart of Eq.(5.41). The only difference is that the above equation is not an explicit expression, which is however not a problem for the identification, as will be shown in the sequel.

Kernel density approximation of the response PDF In order to estimate the PC coefficients gathered in \mathfrak{A} by the maximum likelihood method, it is again necessary to derive an expression of the response PDF conditioned on these coefficients. In the parametric approach developed in Section 4.2.1, this PDF was obtained by kernel density approximation (Eq.(5.43)), *i.e.* through realizations of \mathbf{X}_1 . In the present context, kernel density approximation may be equally used, provided the realizations of

\mathbf{X}_1 are now conditioned on \mathfrak{A} . These realizations may be straightforwardly obtained from realizations of standard normal vector Ξ from Eq.(5.48). This leads to:

$$\hat{f}_{\mathbf{Y}}(\mathbf{y}; \mathfrak{A}) = \frac{1}{n_K} \sum_{k=1}^{n_K} K_h \left(\mathbf{y} - \mathcal{M} \left(\sum_{\alpha \in \mathbb{N}^{R_1}, 0 \leq |\alpha| \leq p_1} \mathbf{a}_\alpha \Psi_\alpha(\xi^{(k)}, \mathbf{x}_2^{(k)}) \right) \right) \quad (5.52)$$

As mentioned above, it is better to use the same set of realizations $\{\xi^{(k)}, k = 1, \dots, n_K\}$ for all the evaluations of the above PDF. The likelihood function of the observations \mathbf{y}_{obs} is computed as in Eq.(5.44):

$$L(\mathfrak{A}; \mathbf{y}_{obs}) = \prod_{q=1}^{n_{obs}} \hat{f}_{\mathbf{Y}}(\mathbf{y}_{obs}^{(q)}; \mathfrak{A}) \quad (5.53)$$

Thus the maximum likelihood estimator of \mathfrak{A} is solution to the following problem:

$$\hat{\mathfrak{A}}^{ML} = \arg \max_{\mathfrak{A} \in \mathcal{D}_{\mathfrak{A}}} \prod_{q=1}^{n_{obs}} \left[\frac{1}{n_K} \sum_{k=1}^{n_K} K_h \left(\mathbf{y}_{obs}^{(q)} - \mathcal{M} \left(\sum_{\alpha \in \mathbb{N}^{R_1}, 0 \leq |\alpha| \leq p_1} \mathbf{a}_\alpha \Psi_\alpha(\xi^{(k)}, \mathbf{x}_2^{(k)}) \right) \right) \right] \quad (5.54)$$

The domain of optimization $\mathcal{D}_{\mathfrak{A}}$ may be constrained to improve the convergence of the optimization algorithm. For instance, bounds to the components of the mean value of \mathbf{X}_1 (which is \mathbf{a}_0 in the PC representation) may be imposed by the constraints:

$$a_{0,k}^- \leq a_{0,k} \leq a_{0,k}^+, \quad k = 1, \dots, M_1 \quad (5.55)$$

Bounds to the variance of each component of \mathbf{X}_1 may be imposed as well:

$$\sum_{\alpha \in \mathbb{N}^{R_1}, 0 < |\alpha| \leq p_1} (a_{\alpha,k})^2 \leq (\sigma_k^+)^2, \quad k = 1, \dots, M_1 \quad (5.56)$$

Such bounds may be easily included in the CONDOR optimizer mentioned earlier. The joint PDF $f_{\mathbf{X}_1}(\mathbf{x}_1)$ identified by the above PC-based parametric approach eventually reads:

$$f_{\mathbf{X}_1}(\mathbf{x}_1) \approx f_{\mathbf{X}_1^{PC}}(\mathbf{x}_1; \hat{\mathfrak{A}}^{ML}) \quad (5.57)$$

which is not explicit. Note however that Eq.(5.48) may be used to draw samples according to the above joint PDF, from which representations of the joint or marginal PDFs may be derived again by kernel density approximation.

PC-based parametric “direct” statistical inference The formalism developed in this section may be straightforwardly applied to the polynomial chaos representation of a set of measurements of input parameters, *i.e.* to the *direct* PC-based parametric statistical inference problem. Suppose that a sample set $\{\mathbf{x}^{(q)}, q = 1, \dots, n_{obs}\}$ of a random vector \mathbf{X} is available. This random vector may be approximated by a PC expansion as in Eq.(5.48). Then the maximum likelihood estimator of the PC coefficients $\mathfrak{A}_{\mathbf{X}}$ reads (see Eq.(5.54) using the trivial model $\mathbf{y} = \mathbf{x}$):

$$\hat{\mathfrak{A}}_{\mathbf{X}}^{ML} = \arg \max_{\mathfrak{A} \in \mathcal{D}_{\mathfrak{A}}} \prod_{q=1}^{n_{obs}} \left[\frac{1}{n_K} \sum_{k=1}^{n_K} K_h \left(\mathbf{x}^{(q)} - \sum_{\alpha \in \mathbb{N}^{R_1}, 0 \leq |\alpha| \leq p_1} \mathbf{a}_\alpha \Psi_\alpha(\xi^{(k)}) \right) \right] \quad (5.58)$$

This kind of direct representation of the input data onto the polynomial chaos is of utmost interest in the context of spectral stochastic finite element methods developed in Chapter 4, as already remarked by Doostan and Ghanem (2005); Ghanem and Doostan (2006) who developed such polynomial chaos-based identification methods for random fields.

4.2.3 Conclusion

In this section, two methods have been proposed to identify “unknown” joint PDFs from observations of response quantities in case the measurement error is negligible. This led to the introduction of kernel density approximations in order to approximate the joint PDF of the response quantities, from which the observations are realizations. Then the maximum likelihood method has been used to identify the hyperparameters of the joint PDF $f_{\mathbf{X}_1}(\mathbf{x}_1)$.

In a parametric paradigm, $f_{\mathbf{X}_1}(\mathbf{x}_1)$ is selected within a family of distributions. A PC-based parametric version of the method has also been proposed using a polynomial chaos representation. In both cases, the “known” input vector \mathbf{x}_2 is modelled by a random vector \mathbf{X}_2 with prescribed joint PDF.

In certain situations, it may happen that the observation data is gathered in a controlled experimental environment, *i.e.* components of the input vector \mathbf{x}_2 may be considered as *deterministic* for each observation (possibly with different values). This is for instance the case when considering laboratory experiments. Consequently, the term $\mathbf{x}_2^{(q)}$ in Eq.(5.40) is supposed to be known, say $\tilde{\mathbf{x}}_2^{(q)}$ (it may be different for each observation). The derivations in the two previous sections remain valid, provided $\mathbf{x}_2^{(k)}$ (which was related to the sampling of \mathbf{X}_2 in the kernel density representations) is replaced by $\tilde{\mathbf{x}}_2^{(q)}$ in Eqs.(5.45),(5.54).

Remark One possible way of identifying the joint PDF $f_{\mathbf{X}_1}(\mathbf{x}_1)$ would be:

- to solve the *deterministic inverse problem* for each observation, *e.g.* by least-square minimization:

$$\{\mathbf{x}_1^{(q)}, \mathbf{x}_2^{(q)}\} = \underset{\mathbf{x} \in \mathbb{R}^M}{\text{Argmin}} \|\mathbf{y}_{obs}^{(q)} - \mathcal{M}(\mathbf{x})\|^2 \quad (5.59)$$

where $\|\cdot\|$ is the Euclidean norm;

- to study the statistics of the obtained samples.

Such an approach has been used in Desceliers et al. (2006, 2007) in order to identify the spatially varying Young’s modulus in an elastic structure. An approximation is obviously introduced when the minimal value obtained in Eq.(5.59) is not zero, *i.e.* when there is no exact solution to the inverse problem. This situation is likely to happen in real-world problems in which measurement and model errors cannot be neglected. An identification technique accounting for measurement/model error is now proposed to deal with these cases, which does not resort to the solution of deterministic inverse problems.

4.3 Identification with measurement/model error

4.3.1 Introduction

The ideal case of negligible measurement error is scarcely encountered in practice. Moreover, even if the model is unbiased in the mean, there may be some discrepancy between its output and the true value of the system response for specific realizations of the input variables. As explained in Section 1.3, it is possible to introduce a single measurement/model error term (simply qualified as error term in the sequel). According to the discussion in that section, assuming the error term has a centered Gaussian distribution (with covariance matrix \mathbf{C}_{obs}) leads to introduce the conditional joint PDF of the observation vector \mathbf{Y}_{obs} (Eq.(5.30)). From this equation, the *unconditional* PDF of the observations reads:

$$f_{\mathbf{Y}_{obs}}(\mathbf{y}) = \mathbb{E}_{\mathbf{X}} [f_{\mathbf{Y}_{obs}|\mathbf{X}}(\mathbf{y}|\mathbf{X})] = \mathbb{E}_{\mathbf{X}} [\varphi_N(\mathbf{y} - \mathcal{M}(\mathbf{X}); \mathbf{C}_{obs})] \quad (5.60)$$

4.3.2 Parametric approach

In this paragraph, the unknown PDF $f_{\mathbf{X}_1}(\mathbf{x}_1)$ is such cast as $f_{\mathbf{X}_1}(\mathbf{x}_1) \equiv p(\mathbf{x}_1; \boldsymbol{\theta})$ where the vector of hyperparameters $\boldsymbol{\theta}$ is to be computed. Eq.(5.60) rewrites in this case:

$$f_{\mathbf{Y}_{obs}}(\mathbf{y}; \boldsymbol{\theta}) = \int_{\mathbb{R}^{M_1}} \int_{\mathbb{R}^{M_2}} \varphi_N(\mathbf{y} - \mathcal{M}(\mathbf{x}_1, \mathbf{x}_2); \mathbf{C}_{obs}) p(\mathbf{x}_1; \boldsymbol{\theta}) f_{\mathbf{X}_2}(\mathbf{x}_2) d\mathbf{x}_1 d\mathbf{x}_2 \quad (5.61)$$

where the dependence in $\boldsymbol{\theta}$ has been shown for the sake of clarity. Thus the likelihood function of the observations \mathbf{Y}_{obs} reads:

$$\mathcal{L}(\boldsymbol{\theta}; \mathbf{Y}_{obs}) = \prod_{q=1}^{n_{obs}} f_{\mathbf{Y}_{obs}}(\mathbf{y}_{obs}^{(q)}; \boldsymbol{\theta}) \quad (5.62)$$

The maximum likelihood estimate $\hat{\boldsymbol{\theta}}^{ML}$ is obtained as the solution of the following maximization problem:

$$\hat{\boldsymbol{\theta}}^{ML} = \arg \max_{\boldsymbol{\theta} \in \mathcal{D}_{\boldsymbol{\theta}}} \prod_{q=1}^{n_{obs}} \int_{\mathbb{R}^{M_1}} \int_{\mathbb{R}^{M_2}} \varphi_N(\mathbf{y}_{obs}^{(q)} - \mathcal{M}(\mathbf{x}_1, \mathbf{x}_2); \mathbf{C}_{obs}) p(\mathbf{x}_1; \boldsymbol{\theta}) f_{\mathbf{X}_2}(\mathbf{x}_2) d\mathbf{x}_1 d\mathbf{x}_2 \quad (5.63)$$

Then the identified joint PDF reads $\hat{f}_{\mathbf{X}_1}^{ML}(\mathbf{x}_1) = p(\mathbf{x}_1; \hat{\boldsymbol{\theta}}^{ML})$.

From a computational point of view, the double integral in Eq.(5.63) may be evaluated by one of the methods presented in Chapter 4 for the evaluation of polynomial chaos coefficients:

- simulation methods, *e.g.* crude Monte Carlo simulation, Latin Hypercube sampling. Note that quasi-random sequences may be used as well, provided the double integral is first mapped onto $[0, 1]^{M_1+M_2}$;
- full or sparse quadrature methods.

Depending on the value of M , one or the other class of methods may be more efficient.

As observed by Cambier⁴, Eq.(5.63) may be ill-conditioned if the variance of the measurement error \mathbf{C}_{obs} is small compared to the scattering of the response that results from the aleatoric uncertainty of \mathbf{X} . An alternative expression for the likelihood may be obtained again by kernel density estimation. Realizations of \mathbf{Y} shall be computed as in Section 4.2.1, except that realizations of the error term are now added to the realizations of the model response in Eq.(5.42). Then the PDF of \mathbf{Y} is obtained by a kernel density approximation as in Eq.(5.43) and used to compute the likelihood function. This strategy was successfully used in Ratier et al. (2005), where a single parameter was identified. The two computational strategies have been recently benchmarked in Perrin (2008).

4.3.3 PC-based parametric identification

When the analyst does not want to prescribe a particular shape for the joint PDF $f_{\mathbf{X}_1}(\mathbf{x}_1)$, he or she may represent \mathbf{X}_1 by a suitable polynomial chaos expansion. Using the same notation as in Section 4.2.2, the joint PDF of an observation reads:

$$f_{\mathbf{Y}_{obs}}(\mathbf{y}; \mathfrak{A}) = \mathbb{E}_{\Xi, \mathbf{X}_2} \left[\varphi_N \left(\mathbf{y} - \mathcal{M} \left(\sum_{\alpha \in \mathbb{N}^{R_1}, 0 \leq |\alpha| \leq p_1} \mathbf{a}_{\alpha} \Psi_{\alpha}(\Xi), \mathbf{X}_2 \right); \mathbf{C}_{obs} \right) \right] \quad (5.64)$$

⁴Private communication.

Consequently the likelihood function reads:

$$\mathsf{L}(\mathfrak{A}; \mathcal{Y}_{obs}) = \prod_{q=1}^{n_{obs}} f_{\mathcal{Y}_{obs}}(\mathbf{y}_{obs}^{(q)}; \mathfrak{A}) \quad (5.65)$$

and the maximum likelihood estimator reads:

$$\hat{\mathfrak{A}}^{\text{ML}} = \arg \max_{\mathfrak{A} \in \mathcal{D}_{\mathfrak{A}}} \prod_{q=1}^{n_{obs}} \left\{ \int_{\mathbb{R}^{R_1}} \int_{\mathbb{R}^{M_2}} \varphi_N \left(\mathbf{y}_{obs}^{(q)} - \mathcal{M} \left(\sum_{\alpha \in \mathbb{N}^{R_1}, 0 \leq |\alpha| \leq p_1} \mathbf{a}_{\alpha} \Psi_{\alpha}(\boldsymbol{\xi}), \mathbf{X}_2 \right); \mathbf{C}_{obs} \right) \dots \right. \\ \left. \dots \varphi_{R_1}(\boldsymbol{\xi}) f_{\mathbf{X}_2}(\mathbf{x}_2) d\boldsymbol{\xi} d\mathbf{x}_2 \right\} \quad (5.66)$$

where $\varphi_{R_1}(\boldsymbol{\xi})$ is the R_1 -dimensional standard normal PDF.

From a computational point of view, the PC-based likelihood function in Eq.(5.66) is similar to (*i.e.* not more complex than) the parametric one in Eq.(5.63), provided the simulation or quadrature methods used for its evaluation are applied with respect to $\varphi_{R_1}(\boldsymbol{\xi}) f_{\mathbf{X}_2}(\mathbf{x}_2)$ instead of $p(\mathbf{x}_1; \boldsymbol{\theta}) f_{\mathbf{X}_2}(\mathbf{x}_2)$.

4.4 Conclusion

This section has addressed so-called stochastic inverse problems which consist in inferring the joint PDF of input parameters from observations of response quantities on a set of real systems that are represented by the same model \mathcal{M} .

In contrast to other approaches presented recently, the methods proposed here do not rely upon the preliminary solution of deterministic inverse problems. They may be applied in the context of perfect measurements or in case of measurement/model error. In each case, a parametric and a non parametric solution is proposed, the latter being based on the polynomial chaos representation of the unknown vector \mathbf{X}_1 .

All the variants of the method have in common the fact that they require a large number of model evaluations. Practically speaking, analytical or semi-analytical models may be treated. For complex systems, surrogate models should be envisaged.

Finally, it is worth remarking that as in classical statistics, the maximum likelihood method provides accurate results if there is a sufficient number of observations (*e.g.* 30-50). The same kind of restriction applies in the context of inverse problems: the need for a large sample set is usually even more crucial here, due to problems of identifiability. In particular, a unique solution cannot be expected if the size of \mathbf{X}_1 is greater than that of \mathbf{y}_{obs} . In case of fewer observations, Bayesian approaches are to be resorted to: the joint PDF $f_{\mathbf{X}_1}(\mathbf{x}_1)$ is given a prior density $p_{\mathbf{X}_1}(\mathbf{x}_1)$. Determining the posterior density exactly reduces to the formalism described in Section 3. Thus the solving strategy developed in that section fully applies in this context.

To conclude, one can observe that the identification “with an error term” (Section 4.3) tends to the identification “without error” (Section 4.2) when the variance of the observation error \mathbf{C}_{obs} tends to zero. The proof may be sketched (without any mathematical rigour) as follows. When considering the parametric approach, the likelihood in Eq.(5.62) has the following limit when $\mathbf{C}_{obs} \rightarrow 0$:

$$\lim_{\|\mathbf{C}_{obs}\| \rightarrow 0} \mathsf{L}(\boldsymbol{\theta}; \mathcal{Y}_{obs}) = \prod_{q=1}^{n_{obs}} \mathbb{E}_{\mathbf{X}_1, \boldsymbol{\theta}, \mathbf{X}_2} \left[\delta(\mathbf{y}_{obs}^{(q)} - \mathcal{M}(\mathbf{X})) \right] \quad (5.67)$$

where δ is the Dirac function. The kernel density approximation in Eq.(5.44) tends to the same expression when the number of samples n_K tends to ∞ and the bandwidth h to zero simultaneously. The same reasoning applies in the PC-based parametric case (Eqs.(5.64),(5.65) vs. (5.52),(5.53)).

5 Application examples

5.1 Bayesian updating in fatigue crack growth models

5.1.1 Introduction

Fatigue crack growth under homogeneous cycling conditions shows scattering as experimentally observed by Virkler et al. (1979). These experimental results have been used later on in several statistical analyses, see *e.g.* Ditlevsen and Olesen (1986); Kotulski (1998)⁵. Fatigue crack growth is commonly modelled by the Paris-Erdogan equation, whose parameters should be given a probabilistic description in order to reproduce the observations, *i.e.* the evolution of the crack length vs. the number of cycles. As will be shown below, this *prior* estimation may be quite inaccurate.

The present example aims at demonstrating that measurements of the crack length at early stages of crack propagation may be used to update the predictions and reduce the uncertainty accordingly. The approaches respectively presented in Sections 2 and 3 are applied and compared.

5.1.2 Virkler's data base and deterministic fatigue crack growth model

Virkler et al. (1979) experimentally studied the scattering of fatigue crack growth by testing a set of 68 specimens made of 2024-T3 aluminium alloy with identical geometry (length $L = 558.8$ mm, width $w = 152.4$ mm and thickness $d = 2.54$ mm). Each trajectory of crack propagation consists in 164 points. The applied stress range is equal to $\Delta\sigma = 48.28$ MPa and the stress ratio is $R = 0.2$. As shown in Figure 5.1, fatigue crack growth shows scattering, since the limit crack size $a_{lim} = 49.8$ mm is attained between 215,000 and 310,000 cycles depending on the sample.

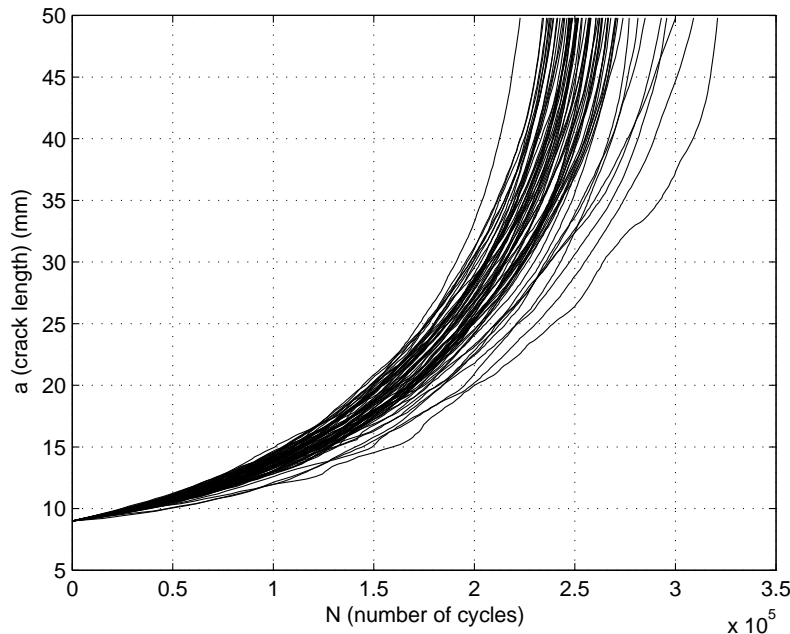


Figure 5.1: Fatigue crack growth – experimental curves obtained by Virkler et al. (1979)

⁵The original data was provided to the authors by Dr Jean-Marc Bourinet, Institut Français de Mécanique Avancée, who is gratefully acknowledged.

In the sequel, fatigue crack growth is modelled by the Paris-Erdogan equation (Paris and Erdogan, 1963):

$$\frac{da}{dN} = C (\Delta K)^m \quad (5.68)$$

In this expression, a is the crack length, ΔK is the variation of the stress intensity factor in one cycle of amplitude $\Delta\sigma$ and (C, m) are material parameters. The variation of the stress intensity factor ΔK reads:

$$\Delta K = \Delta\sigma F\left(\frac{a}{w}\right) \sqrt{\pi a} \quad (5.69)$$

where w is the specimen width and where the so-called Feddersen correction factor is given by:

$$F\left(\frac{a}{w}\right) = \frac{1}{\sqrt{\cos\left(\pi\frac{a}{w}\right)}} \quad \text{for} \quad \frac{a}{w} < 0.7 \quad (5.70)$$

This correction factor is valid for cracks embedded in finite-width plates as those used by Virkler et al. Eqs.(5.68)-(5.70) are solved by numerical integration using Matlab in this application example.

5.1.3 Probabilistic model

For each experimental curve in Figure 5.1, the best-fit values of $(m, \log C)$ in Eq.(5.68) may be identified. The statistics of the obtained parameters $(m, \log C)$ have been computed by Kotulski (1998). They are reported in Table 5.1. The correlation coefficient is equal to 0.997, meaning that there is a strong linear dependency between the two parameters.

Table 5.1: Probabilistic input data for the Paris-Erdogan law (Kotulski, 1998)

Parameter	Type of distribution	Bounds	Mean	Coef. of variation
m	Truncated normal	$[-\infty, 3.2]$	2.874	5.7%
$\log C$	Truncated normal	$[-28, +\infty]$	-26.155	3.7 %

The point of this example application is to show that the use of crack length measurements in the early stage of the crack propagation allows one to predict accurately the remaining part of the curve. For this purpose, a particular experimental curve (among the 68 available) is considered: it corresponds to the slowest crack propagation (the critical crack length $\bar{a} = 49.8$ mm is attained in about 310,000 cycles).

5.1.4 Results

Prior prediction When considering the input PDFs reported in Table 5.1, *prior* confidence intervals on the crack propagation curve may be computed by inverse FORM analysis (see Section 2.3) and validated by Monte Carlo simulation. The 2.5% and 97.5% quantiles have been plotted in Figure 5.2 together with the “slowest” experimental crack propagation curve. It clearly appears that the latter departs much from the 95% confidence interval. Indeed the predicted median (28.3 mm) overestimates by 40% the observed crack length at 200,000 cycles (19.9 mm). Moreover the bandwidth of the 95% confidence interval is equal to 12.2 mm which makes the prediction rather loose.

Updated prediction by Bayesian inverse FORM The updating scheme presented in Section 2 has been applied using 5 measured values of crack length, as reported in Table 5.2 (see the squares in Figure 5.3). For each value, the standard deviation of the measurement/model error is equal to 0.2 mm.

The posterior confidence interval in Figure 5.3 encompasses the experimental curve. The error in the median prediction at 200,000 cycles is about 7% whereas the bandwidth of the 95% confidence interval is 2.4 mm.

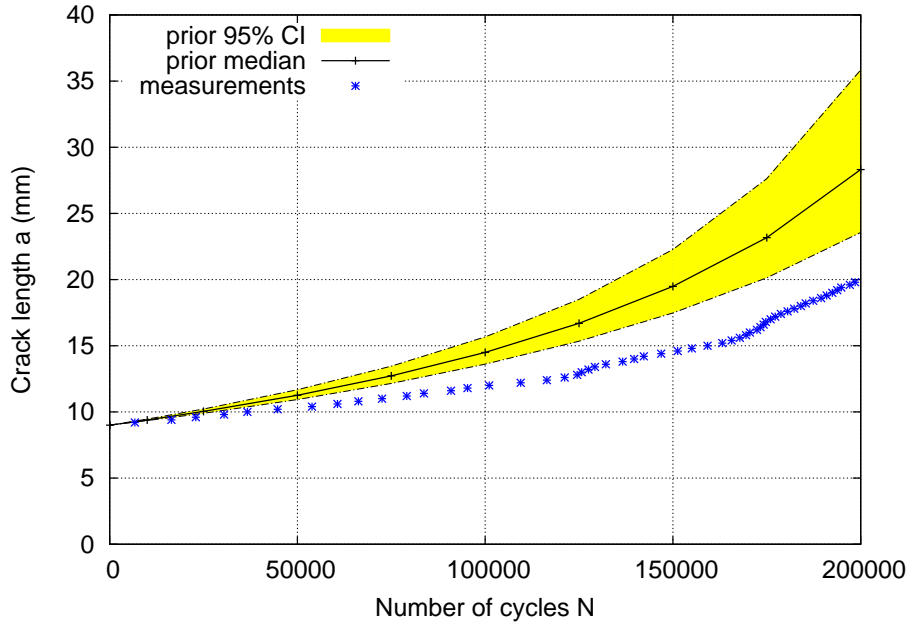


Figure 5.2: Fatigue crack growth – prior prediction of the 95% confidence interval and experimental “slow” crack propagation curve

Table 5.2: Fatigue crack growth – data used for updating the predictions

Crack length (mm)	Number of cycles
9.4	16,345
10.0	36,673
10.4	53,883
11.0	72,556
12.0	101,080

Updated prediction by MCMC simulation The updating scheme presented in Section 3 is now applied. The cascade Metropolis-Hastings algorithm is used to obtain a 10,000-sample Markov chain (the burn-in period is automatically adjusted and corresponds in practice to the 200-300 first samples). Plots of the prior and posterior PDFs of the model input parameters ($\log C$, m) are shown in Figure 5.4 for two values of the standard deviation of the measurement/model error, namely $\sigma_{obs} = 0.1$ mm and $\sigma_{obs} = 0.2$ mm. As expected, the posterior distributions show less scattering than the prior. Moreover the difference between the posterior PDFs is rather insignificant (especially the mode ($\log C = -26.7$, $m = 2.9$) is almost identical in both cases). This is an interesting result since the standard deviation of the measurement/model error will be often prescribed by expert judgment in practice.

By propagating the samples of the posterior distributions obtained by MCMC simulation through the crack growth model, it is possible to obtain *posterior* confidence intervals. Results are plotted in Figure 5.5 for $\sigma_{obs} = 0.1$ mm and $\sigma_{obs} = 0.2$ mm.

It is first observed that the updated confidence interval is again much narrower than that obtained from the prior analysis. Moreover, it satisfactorily encompasses the experimental curve up to $N=175,000$ cycles. It is observed that the experimental curve eventually deviates from the prediction, as if there was a secondary crack propagation kinetics after 175,000 cycles different from the early stage. Of course this cannot be predicted by the Paris law with constant coefficients. Note however that the updated results can be improved when selecting a larger model error, as seen from Figure 5.5-b.

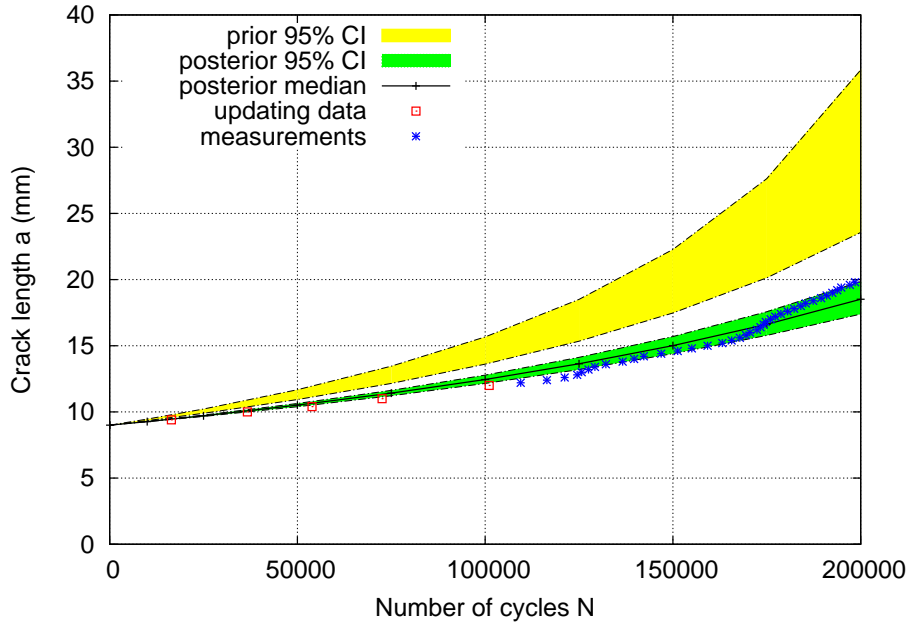


Figure 5.3: Fatigue crack growth – posterior 95% confidence interval obtained by Bayesian inverse FORM analysis

5.1.5 Conclusion

The Bayesian updating methods developed in Sections 2 and 3 have been illustrated on the example of fatigue crack growth. It has been shown that the use of data collected in the early stage of propagation allows the analyst to predict accurately the later evolution of the crack size. In particular, the introduction of the measurement/model error allows the analyst to account for phenomena that are not considered in a simple model (*e.g.* a constant crack propagation coefficients in the Paris-Erdogan law). It has been shown that both methods provide similar results, although their computational scheme is quite different. A detailed investigation of the approaches and parametric studies with respect to the number of observations, accuracy of the measurements, etc. can be found in Perrin (2008).

5.2 Stochastic identification of a Young's modulus

5.2.1 Problem statement

In order to illustrate the methods proposed in Section 4, an academic example is devised, namely the identification of the aleatoric uncertainty of the Young's modulus of identical simply supported beams is considered (Figure 5.6). The beams have a length $L = 2$ m and a rectangular cross section with width b and height h .

A pinpoint load is applied at midspan by the experimental device and the vertical displacement at midspan v_{max} is measured. A simple model of bending beam is considered. Assuming that the material constitutive law is linear (Young's modulus E), the maximal deflection reads:

$$v_{max} = \frac{F L^3}{48 E I} \quad (5.71)$$

where I is the inertia of the beam, which is equal to $I = b h^3/12$ in case of a rectangular cross section. Thus the model of the bending beams under consideration reads:

$$v_{max} = \mathcal{M}(L, b, h, F, E) \equiv \frac{F L^3}{4 E b h^3} \quad (5.72)$$

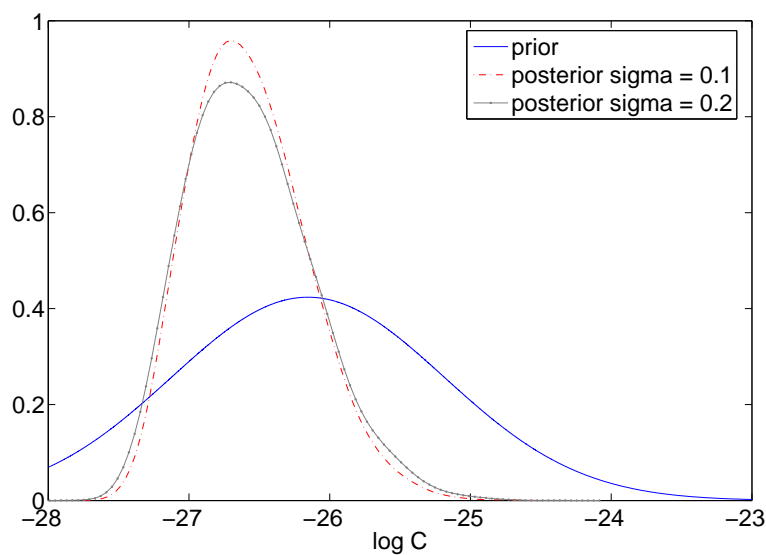
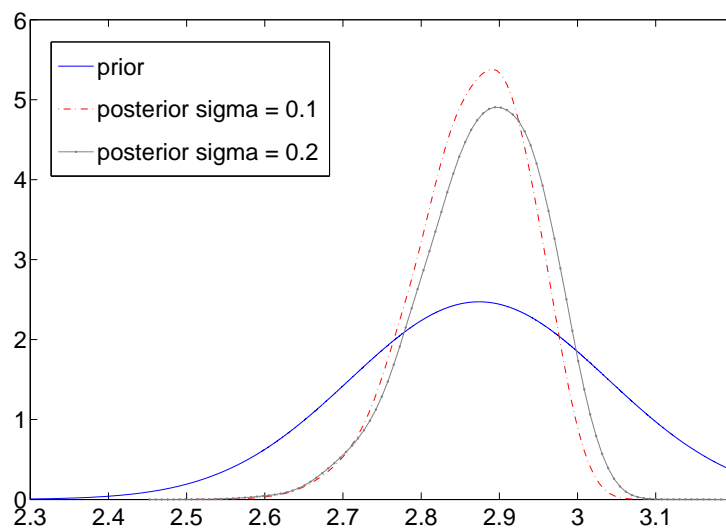
a - Parameter $\log C$ b - Parameter m

Figure 5.4: Fatigue crack growth – prior and posterior PDFs of $(\log C, m)$ obtained by Markov chain Monte Carlo simulation

The probabilistic description of the “known” parameters is given in Table 5.3 whereas the Young’s modulus is the single “unknown” parameter⁶. All the input variables are independent.

Table 5.3: Stochastic inverse problem – probabilistic description of the parameters

Parameter	Type of distribution	Mean value	Coef. of variation
Length L	deterministic	2 m	–
Width b	Gaussian	0.1 m	3%
Height h	Gaussian	0.1 m	3%
Load F	lognormal	10 kN	5%

⁶These terms have been defined in page 96.

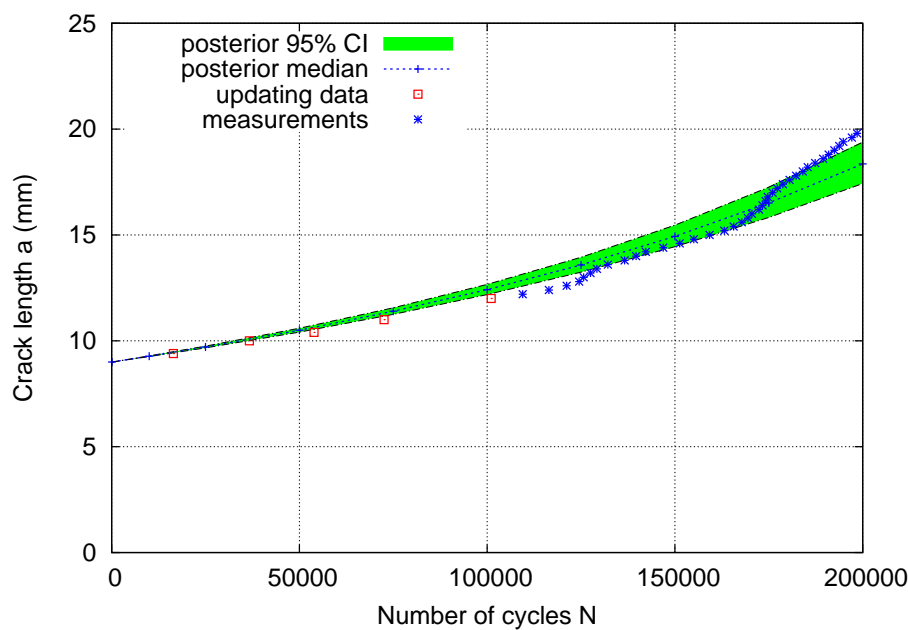
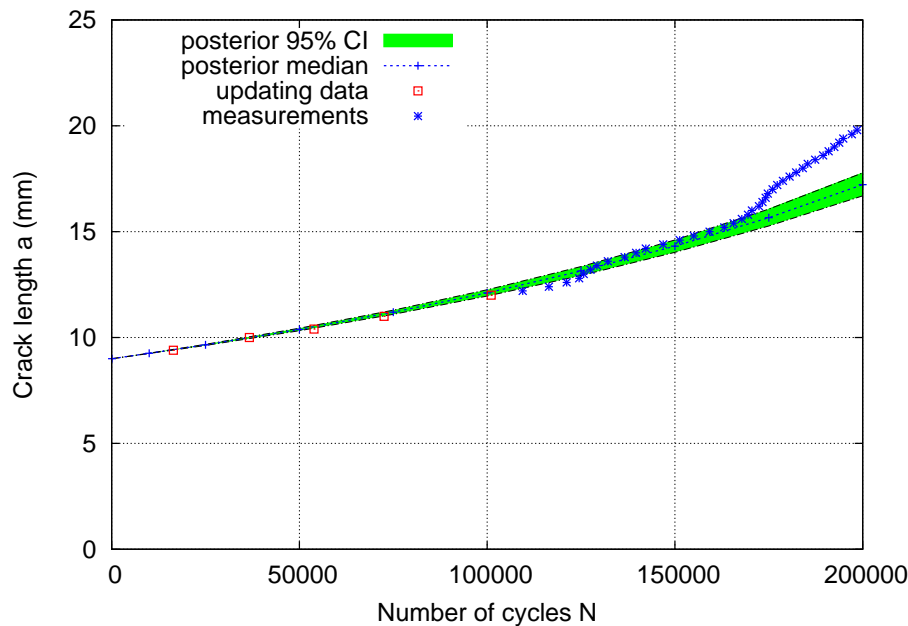


Figure 5.5: Fatigue crack growth - posterior 95% confidence interval obtained by Markov chain Monte Carlo simulation

5.2.2 Pseudo-measurement data

In a real-life situation, a set of identical beams would have been tested and the maximum deflection at midspan measured for each of them. In the present case, these “measurement data” are generated as follows. It is supposed that the Young’s modulus of the material follows a lognormal distribution with mean value $\mu_E = 10,000$ MPa and coefficient of variation $CV_E = 25\%$. A number $n = 50$ samples of the input parameters $\mathbf{X} = \{L, b, h, F, E\}$ are drawn according to their respective distributions and a sample maximal displacement is computed from Eq.(5.72) in each case.

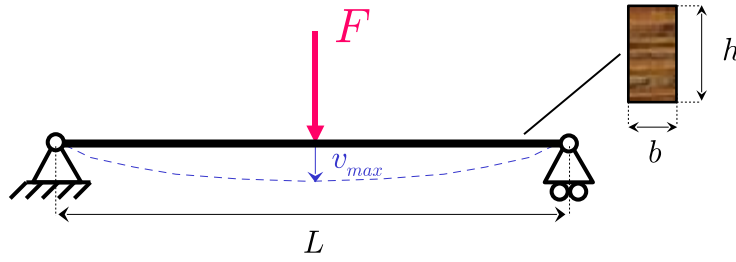


Figure 5.6: Stochastic inverse problem – experimental device

Two cases are then considered in the sequel:

- if the measurement procedure is supposed to be perfect, then the obtained 50 samples are supposed to be the observed values. These values are gathered in a set denoted by $\mathbf{y}_{obs}^{(1)}$;
- if measurement error is taken into account, then the values of maximal displacement obtained previously are perturbed by adding independent realizations of a centered Gaussian random variable with standard deviation σ_{meas} . The results are gathered in a set denoted by $\mathbf{y}_{obs}^{(2)}$;

5.2.3 Results in case of perfect measurements

The probability density function of the Young's modulus is identified using the PC-based parametric stochastic inverse method presented in Section 4.2.2. The sample set of vertical displacements v_{max} (in cm) is:

$$\mathbf{y}_{obs}^{(1)} = \begin{Bmatrix} 3.460 & 3.530 & 1.862 & 1.348 & 2.866 & 1.389 & 2.195 & 3.450 & 2.111 & 2.381 \\ 1.616 & 1.849 & 2.391 & 1.510 & 1.481 & 1.634 & 1.065 & 2.437 & 1.292 & 1.935 \\ 1.595 & 2.532 & 2.750 & 2.421 & 1.688 & 1.952 & 2.041 & 3.365 & 2.542 & 1.709 \\ 2.338 & 1.958 & 2.591 & 2.278 & 2.652 & 1.595 & 2.021 & 2.409 & 1.563 & 2.162 \\ 1.883 & 1.638 & 2.370 & 1.759 & 1.868 & 2.399 & 1.690 & 2.562 & 2.750 & 2.063 \end{Bmatrix} \quad (5.73)$$

A third order PC expansion of the Young's modulus is used with 4 unknown coefficients $\mathfrak{A} = \{a_0, a_1, a_2, a_3\}$. A number $n_K = 10,000$ samples is used in the kernel representation together with a Gaussian kernel. The PC coefficients obtained by the maximum likelihood estimator in Eq.(5.58) are reported in Table 5.4.

Table 5.4: Stochastic inverse problem – results (case of perfect measurements)

PC coefficients	$a_0 = 9,966.6$	$a_1 = 2,328.3$	$a_2 = 276.8$	$a_3 = -136.5$
Statistical moments	From PC coefficients	From samples	Discrepancy (%)	
Mean value	9,966.6	9,972.8	0.1	
Standard deviation	2,348.7	2,434.4	3.5	
Skewness coefficient	0.4306	0.5396	20.2	
Kurtosis coefficient	2.7929	2.9351	4.8	

The statistical moments obtained from the PC expansion coefficients are reported in Table 5.4, column #2. They compare very well with the statistical moments obtained from the sample set of Young's moduli (column #3) that have provided the pseudo-measurement data (note that these values would not be available in a real problem). Indeed, the error in the mean and standard deviation is 0.1% and 3.5% respectively.

It is worth noting that these values slightly differ from the parameters of the theoretical distribution of E that was used to generate the pseudo-measurement data ($\mu_E = 10,000$ MPa and $\sigma_E = 2,500$ MPa). This is due to statistical uncertainty. A closer fit is of course obtained when the size of the observation data set is increased.

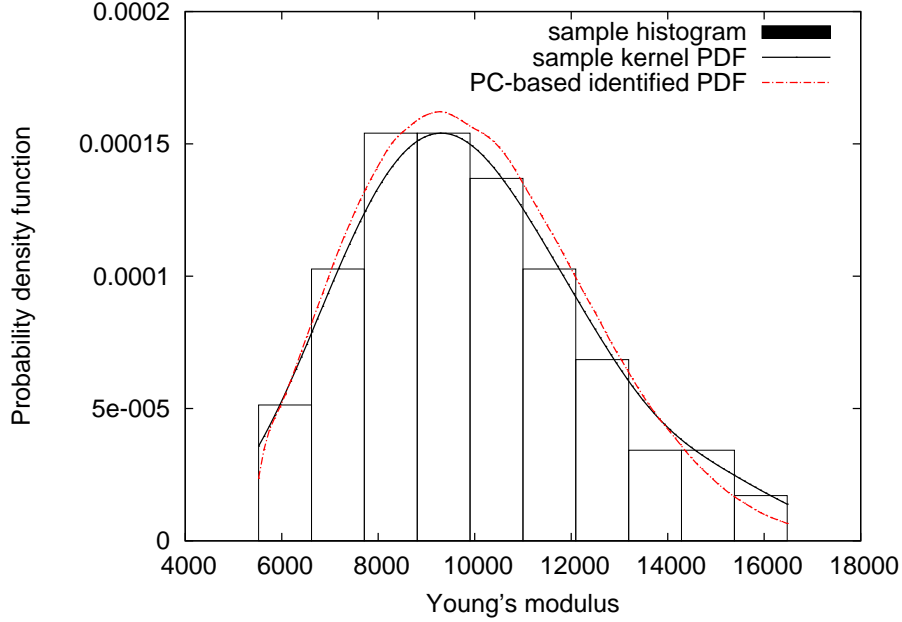


Figure 5.7: Stochastic inverse problem – PDF of the identified Young's modulus (case of perfect measurement)

These results are confirmed by graphical representation. The PDF of the identified Young's modulus is plotted in Figure 5.7 using a kernel smoothing technique onto the PC expansion (see details in Chapter 4, Section 5.1). It is compared to the histogram and kernel distribution of the sample set of Young's moduli used to generate the pseudo-measurement data. The curves fit reasonably well the data in the central part, whereas the result is less accurate in the tails. This is mainly due to the fact that $n = 50$ data points are not enough to describe the tails of the distribution. The convergence to the true underlying distribution when n is increased has been numerically assessed.

5.2.4 Results in case of measurement error

The stochastic inverse problem is now solved in presence of measurement uncertainty. It is supposed that the accuracy of the displacement measurement is ± 1 mm (which is intentionally rather gross for the sake of illustration). Accordingly, the set of observations $\mathbf{y}_{obs}^{(1)}$ has been perturbed by adding realizations of centered Gaussian variables with standard deviation $\sigma_{meas} = 0.5$ mm and rounding. This procedure yields the following sample set of measured vertical displacements v_{max} (in cm):

$$\mathbf{y}_{obs}^{(2)} = \begin{Bmatrix} 3.5 & 3.5 & 1.8 & 1.2 & 2.9 & 1.4 & 2.2 & 3.6 & 2.1 & 2.3 \\ 1.6 & 1.9 & 2.3 & 1.5 & 1.5 & 1.6 & 1.0 & 2.4 & 1.2 & 2.0 \\ 1.6 & 2.5 & 2.7 & 2.4 & 1.7 & 1.9 & 2.0 & 3.3 & 2.5 & 1.7 \\ 2.3 & 2.0 & 2.7 & 2.3 & 2.7 & 1.6 & 2.1 & 2.4 & 1.6 & 2.2 \\ 1.9 & 1.7 & 2.4 & 1.8 & 1.8 & 2.4 & 1.6 & 2.6 & 2.9 & 2.0 \end{Bmatrix} \quad (5.74)$$

The PC coefficients obtained by the maximum likelihood estimator in Eq.(5.66) are reported in Table 5.5. The integrals are evaluated using Monte Carlo simulation for the sake of simplicity (10,000 samples were

used). The statistical moments obtained from this PC expansion are compared to the sample statistical moments obtained from the sample set of Young's moduli (Table 5.5, columns #2 and 3 respectively).

Table 5.5: Stochastic inverse problem – results (case of measurement uncertainty)

PC coefficients	$a_0 = 10,072.0 \quad a_1 = 2,447.6 \quad a_2 = 626.3 \quad a_3 = 36.6$		
Statistical moments	From PC coefficients	From sample set	Discrepancy (%)
Mean value	10,072.0	9,972.8	1.0
Standard deviation	2,526.7	2,434.4	3.8
Skewness coefficient	1.0667	0.5396	97.6
Kurtosis coefficient	4.6690	2.9351	59.1

As in the case of perfect measurements, the mean value and standard deviation of the Young's modulus obtained from the PC expansion coefficients compare fairly well with the empirical moments computed from the sample set. The results for higher order moments is however less accurate than in that case.

The PDF of the identified Young's modulus is plotted in Figure 5.8 using a kernel smoothing technique onto the PC expansion. It is compared to the histogram and kernel distribution of the sample set of Young's moduli. The curves fit reasonably well the data in the central part, whereas the result is less good in the tails due to the rather small size of the sample set. Again it is emphasized that the measurement error is purposely far greater than what should be expected in real experiments, for the sake of illustration.

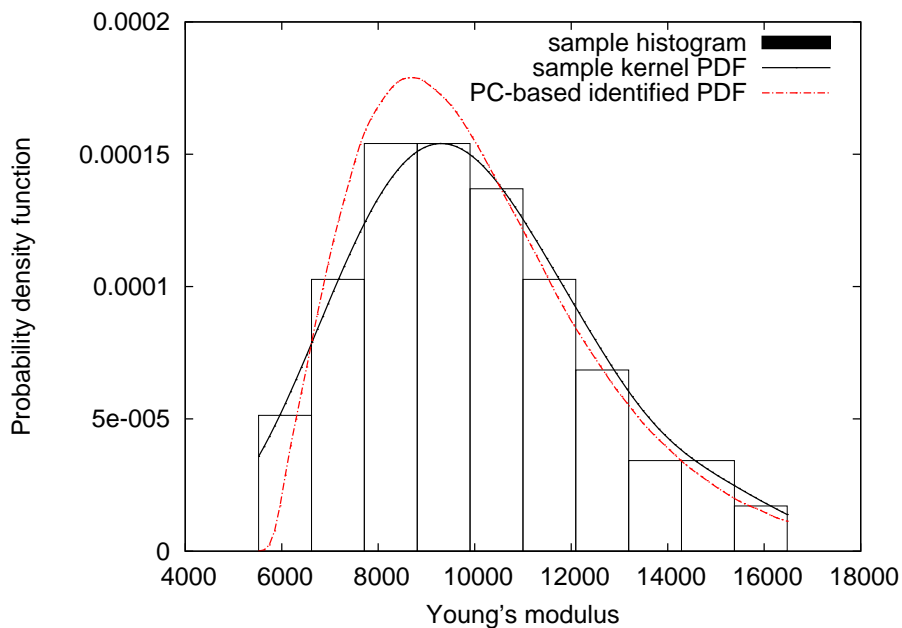


Figure 5.8: Stochastic inverse problem – PDF of the Young's modulus (case of measurement/model error $\sigma_{meas} = 0.5$ mm)

5.2.5 Conclusion

An academic application example of the stochastic inverse methods presented in Section 4 has been presented. The aleatoric uncertainty of a model input parameter (here, the material Young's modulus of a bending beam) is identified in a PC-based parametric context from observations of the model response (here, the deflection at midspan). A similar example was presented in Perrin et al. (2007) where the

randomness of the applied loading on identical beams was of interest. In that communication, various numerical methods for the computation of the integrals in Eq.(5.66) and their incidence onto the obtained PC coefficients are compared.

The framework for stochastic inverse problems may be applied to other identification problems, *e.g.* the identification of complex non linear constitutive laws, for which the deterministic algorithms that are usually used do not take into account the possible aleatoric uncertainty of these parameters. The identification of random fields may also be addressed using the same framework provided the fields are given a discretized spectral representation beforehand.

Numerous application examples and convergence studies have been carried out to assess the robustness of the proposed methods in Perrin (2008). In particular, it is shown that the limit case of the inverse method with measurement/model error (Section 4.3) when σ_{meas} tends to zero, is the inverse method with perfect measurement (Section 4.2).

6 Conclusions

In this chapter, methods for introducing experimental observations in the treatment of uncertainties in mathematical models of physical phenomena have been proposed. Two classes of problems have been distinguished, namely:

- single *real* systems that are monitored in time: the observations of the model response may be used to *update* in a Bayesian context either the joint PDF of the input parameters (Markov chain Monte Carlo approach) or directly the model response (Bayesian inverse FORM approach);
- the stochastic inverse problems, in which the aleatoric uncertainty of some input parameters is to be inferred from observations of response quantities.

In the latter case, various original methods have been proposed and illustrated on a simple application example. It is worth emphasizing that the field of stochastic inverse problems is not yet as mature as that of uncertainty propagation. In particular, significant efforts should be made in the future to alleviate the computational burden associated with these techniques. Note that original ideas are in progress in the domain of identification that may lead to consider the problem differently (Tarantola, 2007).

Chapter 6

Time and space-variant reliability methods

1 Introduction

1.1 Motivation

Although more or less ignored so far in this document, the time dimension is often present in structural reliability problems and has to be properly taken into account. Let us come back to the most basic reliability problem known as “R-S”, for which failure occurs when a demand S is greater than a capacity R . It is clear that for real structures both quantities may depend on time. Indeed:

- the resistance (or capacity) of the structure (*e.g.* material properties) may be degrading in time. The degradation mechanisms usually present an initiation phase and a propagation phase. Both the initiation duration and the propagation kinetics may be considered as random in the analyses. Examples of these mechanisms are crack initiation and propagation in fracture mechanics, corrosion in steel structures or in reinforced concrete rebars, concrete shrinkage and creep phenomena, etc. The specific feature of degradation models is that they are usually monotonic and irreversible;
- *loading* may be randomly varying in time. In this case, the fluctuations of the load intensity should be modelled by random processes. In practice, this modelling is required in order to describe properly environmental loads such as wind velocity, temperature, wave height, or service loading (traffic, occupancy loads, etc.).

The time dependency in the so-called *time-variant reliability problems* may come from one or both of these sources. As will be seen in the sequel, the unique characteristics of time-variant reliability problems urge to devise specific methods.

1.2 Outline

The probabilistic modelling of quantities randomly varying in time requires the introduction of *random processes*. In essence, random processes are the same mathematical objects as the random fields introduced in Chapter 2, Section 4. However, specific additional tools are required in time-variant reliability analysis. They will be briefly described in Section 2. Again, the purpose of this section is not to present

the mathematics of general random processes comprehensively. It is rather a short summary of useful notation and basic properties. Specific attention is devoted to random processes that are commonly used in time-variant structural reliability problems.

The formulation of time-variant reliability problems is then given in Section 3, where the important notion of *outcrossing rate* is introduced. Analytical results for outcrossing rates are given in Section 4 for Gaussian differentiable processes.

Two methods are then introduced to solve time-variant reliability problems based on the *outcrossing approach*:

- the so-called *asymptotic method* (AsM), which is based on a set of analytical results and related algorithms, has been developed through the 80's up to the mid 90's. There is a large number of contributions to this topic in the literature, which have been thoroughly reviewed in Rackwitz (1998, 2001). A comprehensive presentation can be found in Rackwitz (2004). The reader is also referred to well-known text books for complementary viewpoints, namely Ditlevsen and Madsen (1996, Chap. 15), Melchers (1999, Chap. 6), Faber (2003, Chap. 9). The main ingredients of the AsM are summarized in Section 5.
- the so-called *PHI2 method*, which is based on the computation of the outcrossing rate by solving a two-component parallel system reliability problem, is detailed in Section 6.

Application examples and a concluding discussion are presented in Section 7. Finally, space-variant reliability problems and their resolution are introduced in Section 8. Note that this chapter does not encompass methods of stochastic dynamics and random vibrations. Should the reader be interested in these topics, he or she should refer to specific publications, *e.g.* Kree and Soize (1983); Soize (1988); Roberts and Spanos (1990); Lutes and Sarkani (2003) among others.

2 Random processes

2.1 Definition

A scalar *random* (or stochastic) process $X(t, \omega)$ is a continuous set of random variables, such that for any time instant t_0 , $X(t_0, \omega) \equiv X_{t_0}(\omega)$ is a random variable with prescribed properties. In this notation, ω denotes the *outcome*, all the possible outcomes (or *realizations*) of the random variables being gathered in the sample space Ω . It will be omitted in the sequel unless necessary. Conversely, a realization (or *sample function* or *trajectory*) of the random process is obtained by fixing the outcome to ω_0 and will be denoted using small letters by $x(t, \omega_0)$, or simply $x(t)$ for the sake of simplicity. Examples of realizations are given in Figure 6.1.

The complete probabilistic description of a random process is given by assigning the set of all joint probability density functions (PDF) of finite sets of variables $\{X_{t_1}(\omega), \dots, X_{t_n}(\omega)\}$ for any values $\{t_1 < \dots < t_n \in \mathbb{R}^n\}$. In usual cases, this comprehensive assignment reduces to few clearly identified quantities, as described below.

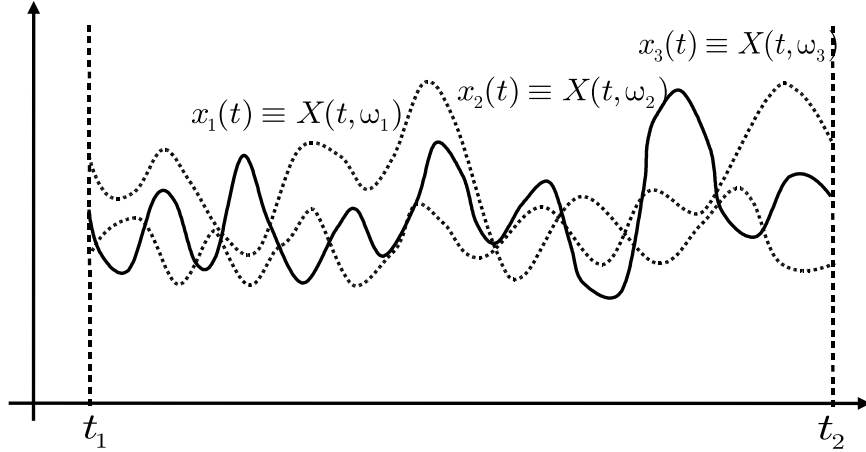


Figure 6.1: Realizations of a scalar random process

2.2 Statistics of scalar random processes

Let us denote by $f_X(x, t)$ the probability density function (PDF) of random variable X_t . The *mean value* and *variance* of the process are defined by:

$$\mu_X(t) = E[X_t] = \int_{-\infty}^{\infty} x f_X(x, t) dx \quad (6.1)$$

$$\sigma_X^2(t) = E[(X_t - \mu_X(t))^2] = \int_{-\infty}^{\infty} (x - \mu_X(t))^2 f_X(x, t) dx \quad (6.2)$$

where $E[\cdot]$ denotes the mathematical expectation. The *autocorrelation function* of the process is defined by:

$$R_{XX}(t_1, t_2) = E[X_{t_1} X_{t_2}] = \int_{-\infty}^{\infty} \int_{-\infty}^{\infty} x_1 x_2 f_{XX}(x_1, x_2; t_1, t_2) dx_1 dx_2 \quad (6.3)$$

where $f_{XX}(\cdot)$ is the joint probability density function of variables $\{X_{t_1}(\omega), X_{t_2}(\omega)\}$. The *autocovariance function* is defined as follows:

$$\begin{aligned} C_{XX}(t_1, t_2) &= \text{Cov}[X_{t_1}, X_{t_2}] = E[(X_{t_1} - \mu_X(t_1))(X_{t_2} - \mu_X(t_2))] \\ &= \int_{-\infty}^{\infty} \int_{-\infty}^{\infty} (x_1 - \mu_X(t_1))(x_2 - \mu_X(t_2)) f_{XX}(x_1, x_2; t_1, t_2) dx_1 dx_2 \\ &= R_{XX}(t_1, t_2) - \mu_X(t_1)\mu_X(t_2) \end{aligned} \quad (6.4)$$

As might be expected, if $t_2 = t_1 = t$, the autocovariance function reduces to the variance function $\sigma_X^2(t)$:

$$\sigma_X^2(t) = C_{XX}(t, t) = R_{XX}(t, t) - \mu_X^2(t) \quad (6.5)$$

Finally the *autocorrelation coefficient function* is defined by :

$$\rho(t_1, t_2) = \frac{\text{Cov}[X_{t_1}, X_{t_2}]}{\sigma_X(t_1)\sigma_X(t_2)} \quad (6.6)$$

2.3 Properties of random processes

2.3.1 Stationarity

A random process is said *stationary* when its probabilistic characteristics is independent of a shift in the parameter origin. Precisely, when all its statistical moments are independent of time, it is *strictly stationary*.

When the mean value μ_X does not depend on time, and the autocorrelation function $R_{XX}(t_1, t_2)$ only depends on the time shift $\tau = t_2 - t_1$, the process is said to be *weakly stationary*. In this case, the autocorrelation function may be rewritten as:

$$R_{XX}(\tau) = E[X_t X_{t+\tau}] \quad (6.7)$$

The following properties hold for stationary processes:

- $R_{XX}(0) = E[X_t^2]$ represents the *mean-square* value of X_t .
- $R_{XX}(\tau)$ is an even function in τ : $R_{XX}(\tau) = R_{XX}(-\tau)$
- $|R_{XX}(\tau)| \leq R_{XX}(0) = E[X_t^2]$: the maximum is reached for $\tau = 0$
- As a consequence, its derivatives, if they exist, have to satisfy¹:

$$\left. \frac{dR_{XX}(\tau)}{d\tau} \right|_{\tau=0} = \dot{R}_{XX}(0) = 0 \quad ; \quad \left. \frac{d^2 R_{XX}(\tau)}{d\tau^2} \right|_{\tau=0} = \ddot{R}_{XX}(0) \leq 0 \quad (6.8)$$

Random processes are *non stationary* when their statistical properties vary in time. Examples of realizations of non-stationary processes are given in Figure 6.2, which includes the special cases of (a) time varying mean value, (b) time varying standard deviation, and (c) a combination of both.

2.3.2 Differentiability

A series of random variables $\{X_n(\omega), n \geq 1\}$ having a finite variance is said to *converge in the mean square sense* to the random variable $X(\omega)$ if:

$$\lim_{n \rightarrow \infty} E[(X_n - X)^2] = 0 \quad (6.9)$$

which is written (l.i.m stands for *limit in the mean square sense*):

$$\text{l.i.m}_{n \rightarrow \infty} X_n = X \quad (6.10)$$

The derivative of a random process is defined by the following l.i.m (if it exists) and it is denoted by $\dot{X}(t)$:

$$\text{l.i.m}_{\Delta t \rightarrow 0} \frac{X(t + \Delta t, \omega) - X(t, \omega)}{\Delta t} = \frac{d}{dt} X(t, \omega) \equiv \dot{X}(t, \omega) \quad (6.11)$$

In this case, the process is said *differentiable*. By linearity, the mean of the derivative process is the derivative of the mean:

$$E[\dot{X}(t, \omega)] = \frac{d}{dt} \mu_X(t) \quad (6.12)$$

The *cross-correlation* between a process and its derivative can be computed as follows:

$$\begin{aligned} R_{X\dot{X}}(t_1, t_2) &= E[X_{t_1} \dot{X}_{t_2}] = \lim_{\Delta t_2 \rightarrow 0} E \left[X_{t_1} \frac{X(t_2 + \Delta t_2) - X_{t_2}}{\Delta t_2} \right] \\ &= \lim_{\Delta t_2 \rightarrow 0} \left[\frac{R_{XX}(t_1, t_2 + \Delta t_2) - R_{XX}(t_1, t_2)}{\Delta t_2} \right] \end{aligned} \quad (6.13)$$

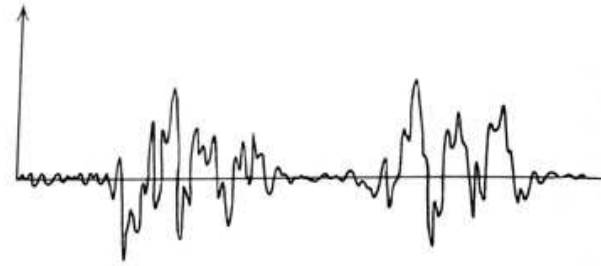
which turns out to be:

$$R_{X\dot{X}}(t_1, t_2) = \frac{\partial R_{XX}(t_1, t_2)}{\partial t_2} \quad (6.14)$$

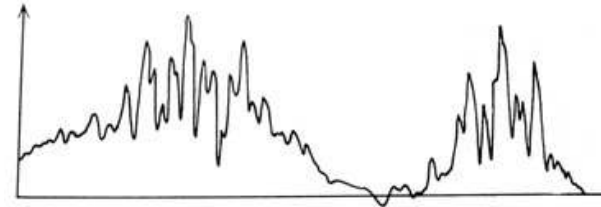
¹In the following the notation $\dot{Z}(\tau)$ denotes the first derivative of any differentiable function $Z(\tau)$ which depends on a single parameter τ . The notation $\ddot{Z}(\tau)$ denotes the second derivative, etc.



a - Time varying mean value



b - Time varying standard deviation



c - Time varying mean and standard deviation

Figure 6.2: Realizations of non stationary random processes

Similarly the autocorrelation function of the derivative process reads:

$$R_{\dot{X}\dot{X}}(t_1, t_2) = \frac{\partial^2 R_{XX}(t_1, t_2)}{\partial t_1 \partial t_2} \quad (6.15)$$

From the above equation, it can be shown that a necessary and sufficient condition for a process to be differentiable is that the autocorrelation function $R_{XX}(t_1, t_2)$ has a continuous mixed second derivative on the diagonal $t_1 = t_2$. If $X(t, \omega)$ is stationary, it follows from Eq.(6.12) that its derivative is a zero-mean process. Using $\tau = t_2 - t_1$, one gets:

$$R_{X\dot{X}}(\tau) = \dot{R}_{XX}(\tau), \quad R_{\dot{X}\dot{X}}(\tau) = -\ddot{R}_{XX}(\tau) \quad (6.16)$$

which shows that the process $\dot{X}(t)$ is weakly stationary if $X(t)$ is weakly stationary. From Eqs.(6.8),(6.16) one gets:

$$R_{X\dot{X}}(0) \equiv \mathbb{E} \left[X(t) \dot{X}(t) \right] = 0 \quad (6.17)$$

which means that *there is no correlation between a stationary process and its derivative process at any point in time t .*

2.3.3 Ergodic and mixing processes

Let us define the *time-average* of a trajectory as follows:

$$\langle x(t) \rangle = \lim_{T \rightarrow +\infty} \left[\frac{1}{T} \int_0^T x(t) dt \right] \quad (6.18)$$

A stationary random process is said *ergodic* in the mean if *its time-average is equal to its mean value*, say μ_X , for any trajectory:

$$\text{Ergodicity in the mean: } \langle x(t) \rangle = \mu_X = E[X(t, \omega)] \quad (6.19)$$

Ergodicity in correlation is defined as:

$$\langle x(t + \tau)x(t) \rangle = \lim_{T \rightarrow +\infty} \left[\frac{1}{T} \int_0^T x(t + \tau)x(t) dt \right] = R_{XX}(\tau) \quad (6.20)$$

In essence, ergodicity deals with determining the statistics of a process $X(t, \omega)$ from a single trajectory. It is of considerable practical use in estimating statistical parameters from one or a few sufficiently long records of the process. The obtained accuracy will depend on the duration T of available records. Ergodicity (which implies stationarity) is often assumed to hold in the analysis of stochastic records unless there is evidence of the contrary.

A random process is said to be *mixing* if random variables $X_{t_1}(\omega)$, $X_{t_2}(\omega)$ become independent when $\tau = t_2 - t_1 \rightarrow \infty$. As far as stationary processes are concerned, this implies that the autocovariance function tends to zero when $\tau \rightarrow \infty$.

2.3.4 Vector random processes

A *vector random process* $\mathbf{X}(t, \omega)$ is a vector whose components $\{X_1(t, \omega), X_2(t, \omega), \dots, X_n(t, \omega)\}$ are scalar random processes. The definitions in Section 2.2 for scalar processes may be generalized to vector processes. The *covariance matrix* \mathbf{C} is defined by the following entries:

$$\begin{aligned} \mathbf{C}_{i,j}(t_1, t_2) &= \text{Cov}[X_i(t_1), X_j(t_2)] \\ &= \int_{-\infty}^{\infty} \int_{-\infty}^{\infty} (x_i - \mu_{X_i}(t_1)) (x_j - \mu_{X_j}(t_2)) f_{X_i X_j}(x_i, x_j; t_1, t_2) dx_i dx_j \end{aligned} \quad (6.21)$$

When $i = j$, the entry is the *autocovariance* function of process $X_i(t, \omega)$; when $i \neq j$, $\mathbf{C}_{i,j}(t_1, t_2)$ is called the *cross-covariance* function. Finally, the *cross-correlation coefficient matrix* \mathbf{R} is defined by:

$$\mathbf{R}_{i,j}(t_1, t_2) = \rho[X_i(t_1), X_j(t_2)] = \frac{\text{Cov}[X_i(t_1), X_j(t_2)]}{\sigma_{X_i}(t_1) \cdot \sigma_{X_j}(t_2)} \quad (6.22)$$

2.4 Poisson processes

Point processes appear in numerous situations when similar events occur randomly in time (computer connections to a server, customers arriving at a booth, etc.). In structural reliability, they allow one to count crossings of a limit state surface.

Let us denote by $T_n(\omega)$, $n \geq 1$ the time of n -th occurrence of the event under consideration. It is assumed that:

$$0 < T_1(\omega) < \dots < T_n(\omega) \quad (6.23)$$

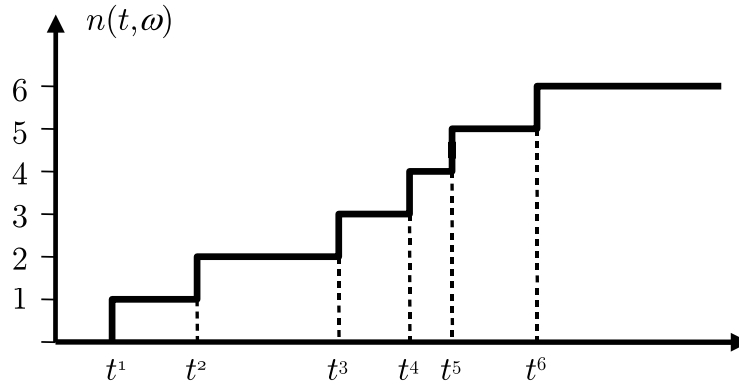


Figure 6.3: Realizations of a Poisson counting process

The counting function $N(t, \omega)$ of the point process is defined as the number of events occurring in the time interval $]0, t]$:

$$N(t, \omega) = \sup \{n : T_n(\omega) \leq t\} \quad (6.24)$$

A trajectory of such a process is given in Figure 6.3.

The point process is called *homogeneous Poisson process* if and only if the following conditions are satisfied:

- $\forall s < t$, $N_t(\omega) - N_s(\omega)$ is a Poisson random variable of parameter $\lambda(t - s)$. The positive real value λ is the intensity of the process;
- the random variables $N_{t_1}(\omega)$, $N_{t_2}(\omega) - N_{t_1}(\omega)$, \dots , $N_{t_k}(\omega) - N_{t_{k-1}}(\omega)$ are independent.

It follows that the probability function of $N_t(\omega)$ reads:

$$\mathbb{P}(N_t(\omega) = n) = e^{-\lambda t} \frac{(\lambda t)^n}{n!} \quad (6.25)$$

In other words, the probability of having one occurrence within $[t, t + \Delta t]$ is equal to $\lambda \Delta t$ (where Δt is a small time interval), and the probability of having more than one occurrence within this time interval is negligible with respect to Δt (the process is said *regular*).

The mean number of occurrences $\mathbb{E}[N(0, t)]$ is equal to λt . Thus λ may be interpreted as the mean rate of occurrence per unit time. It is easy to show that the time of first occurrence $T_1(\omega)$ as well as the subsequent inter-arrival times $T_k(\omega) - T_{k-1}(\omega)$, $k \geq 2$ have an exponential distribution with parameter $1/\lambda$:

$$\mathbb{P}(T_1 \leq t) = 1 - e^{-\lambda t} \quad (6.26)$$

As the sum of n such independent variables, the time elapsed before the n -th occurrence, $T_n(\omega)$, has a Gamma distribution with parameters n and $1/\lambda$ (mean value n/λ , variance n/λ^2). *Non homogeneous Poisson processes* can be defined by replacing λ by a function $\lambda(t)$. In this case, the term λt in Eqs.(6.25),(6.26) should be replaced by $\int_0^t \lambda(\tau) d\tau$.

2.5 Rectangular wave renewal processes

Rectangular wave renewal processes are defined as processes whose amplitude is stepwise constant and changing (*i.e.* making jumps) in a random way at random renewal points in time. They are characterized by:

- the probability distribution function of their amplitude, say $f_S(s)$,
- the probability distribution function of their inter-arrival times.

It is usually assumed that the renewals follow a Poisson process. Thus the specification of the inter-arrival time is limited to the *jump rate* λ , which is the mean rate of renewals. It follows that the renewals are supposed to occur *independently* of each other. For numerical computation, it is assumed that rectangular wave processes jump from a random value $S(t)$ to another value $S(t + \Delta t)$ *without returning to zero*. Rectangular wave renewal processes are regular processes. The probability of occurrence of any two or more renewals in a small time interval Δt is thus negligible.

Non stationary rectangular wave renewal processes can be defined either using time-dependent parameters of the amplitude distribution or time-dependent jump rates. *Vector* rectangular wave renewal processes are vectors whose components are rectangular wave renewal processes defined as above. It is usually assumed that all components are independent.

Rectangular wave renewal processes are used to model occupancy loads, traffic loads, etc. A typical example of a trajectory of such a process is sketched in Figure 6.4.

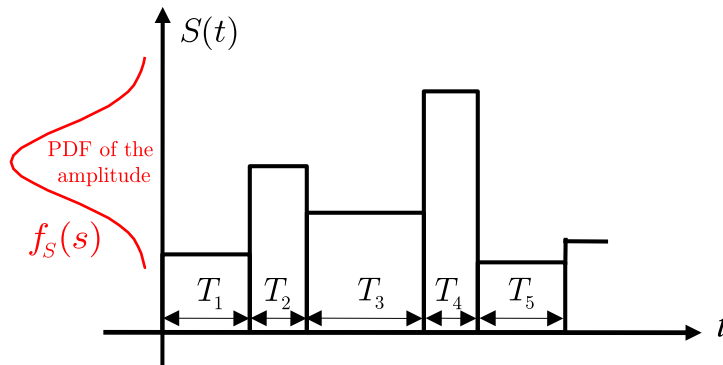


Figure 6.4: Example of a trajectory of a rectangular renewal wave process

2.6 Gaussian processes

A scalar process $X(t, \omega)$ is *Gaussian* if any random vector $\{X_{t_1}(\omega), \dots, X_{t_n}(\omega)\}$ is a Gaussian vector. Practically, it is defined by:

- its mean function $\mu_X(t)$,
- either its autocorrelation function $R_{XX}(t_1, t_2)$, its covariance function $C_{XX}(t_1, t_2)$ or both its variance function $\sigma_X^2(t)$ and its autocorrelation coefficient function $\rho(t_1, t_2)$.

The marginal probability density function is given by:

$$f_X(x, t) = \frac{1}{\sqrt{2\pi}\sigma_X(t)} \exp\left[-\frac{1}{2}\left(\frac{x - \mu_X(t)}{\sigma_X(t)}\right)^2\right] \quad (6.27)$$

Gaussian processes are *differentiable* if and only if their autocorrelation function is twice differentiable at $t_1 = t_2$. *Stationary* Gaussian processes are completely defined by their mean μ_X , variance σ_X^2 and autocorrelation coefficient function $\rho(\tau)$. The condition for differentiability reduces to the existence of $\rho''(0)$. The derivative process $\dot{X}(t, \omega)$ has zero mean, and its variance is:

$$\sigma_{\dot{X}}^2 = -\sigma_X^2 \rho''(0) \quad (6.28)$$

Standardized Gaussian processes are of interest in solving time-variant reliability problems. They are defined as:

$$U(t) = \frac{X(t) - \mu_X(t)}{\sigma_X(t)} \quad (6.29)$$

Obviously they have zero mean and unit standard deviation. The *cycle rate* of a Gaussian process is defined as:

$$\varpi_0^2(t) = \left. \frac{\partial^2 \rho(t_1, t_2)}{\partial t_1 \partial t_2} \right|_{t=t_1=t_2} \quad (6.30)$$

In the stationary case, the cycle rate becomes constant and reduces to:

$$\varpi_0^2 = -\rho''(0) \quad \varpi_0 = \sigma_{\dot{X}}/\sigma_X \quad (6.31)$$

Typical shapes for the autocorrelation coefficient function have been already shown in Chapter 2, Section 4 (see Figure 2.2). They respectively correspond to the following equations (ℓ is referred to as the *correlation length*):

- Type A:

$$\rho_A(\tau) = \exp\left(-\left|\frac{\tau}{\ell}\right|\right) \quad (6.32)$$

- Type B:

$$\rho_B(\tau) = \exp\left(-\left(\frac{\tau}{\ell}\right)^2\right) \quad (6.33)$$

- Type C:

$$\rho_C(\tau) = \frac{\sin(\tau/\ell)}{\tau/\ell} \quad (6.34)$$

A random process of type A is clearly *not* differentiable since the autocorrelation coefficient function is not differentiable in $\tau = 0$. In contrast, type B and C processes are differentiable, and their cycle rate respectively read $\omega_B = \sqrt{2}/\ell$ and $\omega_C = 1/\sqrt{3}\ell$. Typical trajectories of such Gaussian processes are given in Figure 6.5 for various autocorrelation coefficient functions (same correlation length $\ell = 1$, $t \in [0, 50]$). These trajectories have been obtained from the EOLE expansion of the related random processes (Chapter 2, Section 4.3.3). The “Type A” trajectory is clearly less smooth than the other ones. The cycle rate may be interpreted as a dominant frequency of the trajectories: this is visually confirmed by the fact that the “Type B” curve ($\omega_B = \sqrt{2}$) oscillates more than the “Type C” curve ($\omega_C = 1/\sqrt{3}$).

3 Time-variant reliability problems

3.1 Problem statement

Let us denote by $\mathbf{X}(t, \omega)$ the set of random variables $\mathbf{R} = \{R_j(\omega), j = 1, \dots, p\}$ and one-dimensional random processes $\mathbf{S} = \{S_j(t, \omega), j = p+1, \dots, p+q\}$ describing the randomness in the geometry, material properties and loading of the system under consideration. Let us denote by $g(t, \mathbf{X}(t, \omega))$ the time dependent limit state function associated with the reliability analysis. The failure domain (resp. safe domain) at time instant t is denoted by $\mathcal{D}_f(t)$ (resp. $\mathcal{D}_s(t)$), and the limit state surface by $\partial\mathcal{D}$. Denoting by $[t_1, t_2]$ the time interval of interest, the probability of failure of the structure within this time interval is defined as follows:

$$\begin{aligned} P_f(t_1, t_2) &= \mathbb{P}(\exists t \in [t_1, t_2] : \mathbf{X}(t, \omega) \in \mathcal{D}_f(t)) \\ &= \mathbb{P}(\exists t \in [t_1, t_2] : g(t, \mathbf{X}(t, \omega)) \leq 0) \end{aligned} \quad (6.35)$$

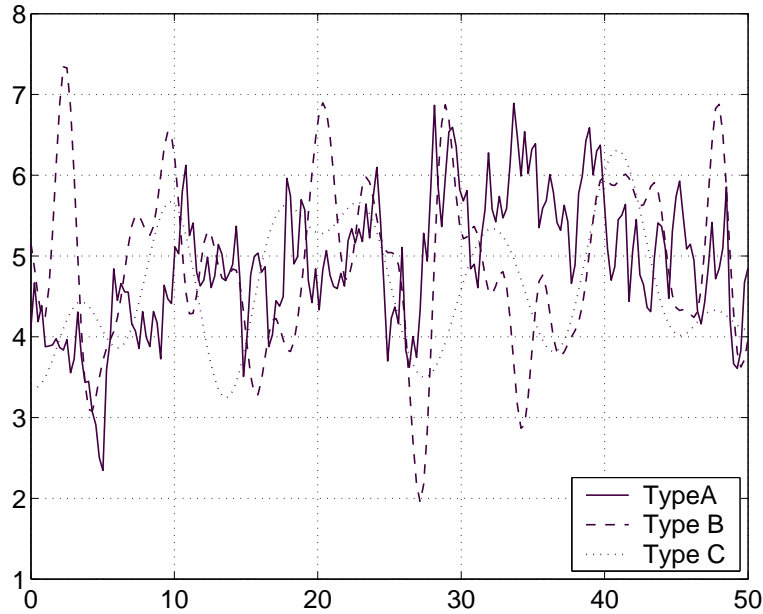


Figure 6.5: Trajectories of Gaussian random processes for various autocorrelation coefficient functions ($\mu_X = 5$, $\sigma_X = 1$, $\ell = 1$)

This definition corresponds to the probability of being in the failure domain at least at one point in time within the interval under consideration. It is also called *cumulative probability of failure* in the literature. Let us consider now a structure over a time interval $[0, \mathfrak{T}]$. Let us denote by $T_1(\omega)$ the *first passage time* to the failure domain $\mathcal{D}_f(t)$ (conventionnally set equal to zero if the structure already fails at $t = 0$). This quantity is sometimes referred to as the failure time. Let us denote by $F_{T_1}(t)$ its cumulative distribution function. It is clear from Eq.(6.35) that:

$$F_{T_1}(t) \equiv \mathbb{P}(T_1 \leq t) = P_f(0, t) \quad (6.36)$$

Thus the cumulative probability of failure is closely related to the distribution of the first passage time.

On the other hand, the so-called *point-in-time* (or instantaneous) probability of failure is defined as follows:

$$P_{f,i}(t) = \mathbb{P}(g(t, \mathbf{X}(t, \omega)) \leq 0) \quad (6.37)$$

In Eq.(6.37), time is treated as a dummy parameter. Thus the point-in-time probability of failure is computed by fixing time in all the functions appearing in the limit state function and by replacing the random processes by the corresponding random variables, which formally rewrites, using the above notation:

$$P_{f,i}(t) = \mathbb{P}(g(t, \mathbf{R}(\omega), \mathbf{S}_t(\omega)) \leq 0) \quad (6.38)$$

The standard time-invariant reliability methods described in Chapter 3, Section 3 may be used to evaluate Eq.(6.38). As may be expected from the above definitions, the cumulative probability of failure is much more complex to compute than the instantaneous probability of failure. There is a remarkable exception to this general situation, which is addressed in the next paragraph.

3.2 Right-boundary problems

A special class of time-variant problems is defined by the following assumptions:

- the limit state function does not depend explicitly on random processes (such as Gaussian, renewal wave, etc.), but only on random variables and deterministic functions of time. The limit state function is denoted by $g(t, \mathbf{X}(\omega))$ in this case.
- the limit state function is *monotonically decreasing in time* whatever the realizations of the random variables. For each realization, the minimum value of $g(t, \mathbf{X}(\omega_0))$ over a time interval $[t_1, t_2]$ is attained for $t = t_2$, thus the expression *right-boundary problems*.

From these assumptions it comes:

$$\begin{aligned}
 P_f(t_1, t_2) &= 1 - \mathbb{P}(g(t, \mathbf{X}(\omega)) > 0 \quad \forall t \in [t_1, t_2]) \\
 &= 1 - \mathbb{P}(g(t_2, \mathbf{X}(\omega)) > 0) \\
 &= P_{f,i}(t_2)
 \end{aligned}
 \tag{6.39}$$

It clearly appears that the time-variant problem reduces to a time-invariant analysis at the end of the time interval. This situation is of crucial importance in practice: in design and assessment of structures, static calculations are often carried out. In an uncertain context, the loading is then represented by random variables (whose PDF is for instance determined by the extreme value theory) instead of random processes. When degradation of material is taken into account, deterministic functions of time model the kinetics of the phenomenon. These functions are usually monotonically decreasing for physical reasons (*e.g.* the crack length, the size of corroded zones increases in time, etc.). Thus in numerous applications, Eq.(6.39) will apply.

3.3 The outcrossing approach

When random processes enter the definition of the limit state function, it is not possible anymore to compute the probability of failure $P_f(t_1, t_2)$ directly because the instant t for which the limit state function becomes negative (first passage time) is random. This point is illustrated in Figure 6.6, where failure corresponds to the outcrossing of a threshold a by a scalar random process $X(t, \omega)$ (the three realizations of the random process correspond to three different first-passage times denoted by $T_1^{(1)}$, $T_1^{(2)}$, $T_1^{(3)}$).

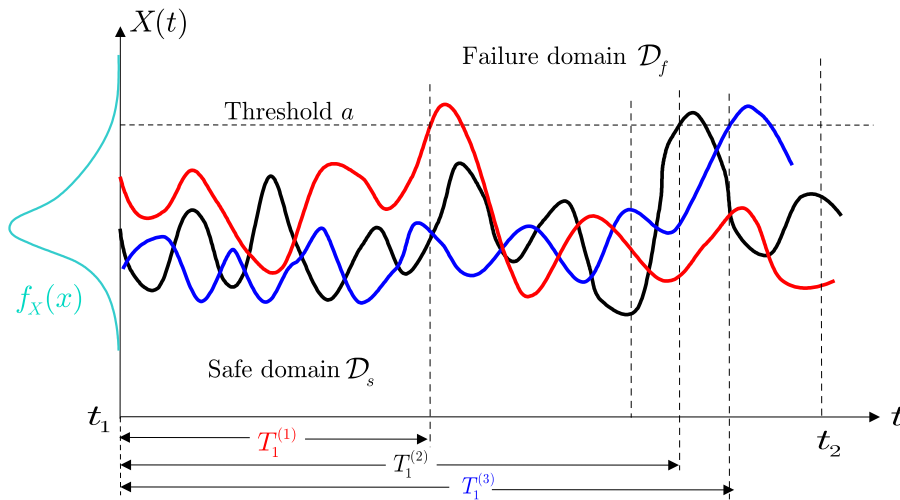


Figure 6.6: Examples of trajectories and outcrossing of a threshold by a scalar process $X(t, \omega)$

An alternative method called *outcrossing approach* has been proposed to bypass the difficulty.

3.3.1 Bounds to the probability of failure

A simple lower bound to the probability of failure has been derived by Shinozuka (1964). First remark that:

$$P_f(t_1, t_2) = 1 - \mathbb{P}(g(t, \mathbf{X}(t, \omega)) > 0 \quad \forall t \in [t_1, t_2]) \quad (6.40)$$

Note that:

$$\begin{aligned} \mathbb{P}(g(t, \mathbf{X}(t, \omega)) > 0 \quad \forall t \in [t_1, t_2]) &= \mathbb{P}\left(\bigcap_{t \in [t_1, t_2]} g(t, \mathbf{X}(t, \omega)) > 0\right) \\ &\leq \mathbb{P}(g(t_0, \mathbf{X}(t_0, \omega)) > 0) \equiv 1 - P_{f,i}(t_0) \end{aligned} \quad (6.41)$$

where the latter bound holds for any $t_0 \in [t_1, t_2]$. This rewrites:

$$1 - \mathbb{P}(g(t, \mathbf{X}(t, \omega)) > 0 \quad \forall t \in [t_1, t_2]) \geq P_{f,i}(t_0) \quad \forall t_0 \in [t_1, t_2] \quad (6.42)$$

From Eqs.(6.40),(6.42), it follows:

$$P_f(t_1, t_2) \geq \max_{t \in [t_1, t_2]} P_{f,i}(t) \quad (6.43)$$

This lower bound is however often crude in practice. Let us now consider the event $\mathcal{F} = \{\exists t \in [t_1, t_2] : \mathbf{X}(t) \in \mathcal{D}_f(t)\}$. Its complementary reads:

$$\bar{\mathcal{F}} = \{\forall t \in [t_1, t_2] : \mathbf{X}(t) \in \mathcal{D}_s(t)\} \quad (6.44)$$

which is equivalent to:

$$\bar{\mathcal{F}} = \{\mathbf{X}(t_1) \in \mathcal{D}_s(t_1)\} \cap \{N^+(t_1, t) = 0\} \quad (6.45)$$

where $N^+(t_1, t)$ is the number of outcrossings² from the safe domain through the limit state surface within the time interval $]t_1, t]$ (see Figure 6.7). Consequently, its complementary event reads:

$$\mathcal{F} = \{\mathbf{X}(t_1) \in \mathcal{D}_f(t_1)\} \cup \{N^+(t_1, t) > 0\} \quad (6.46)$$

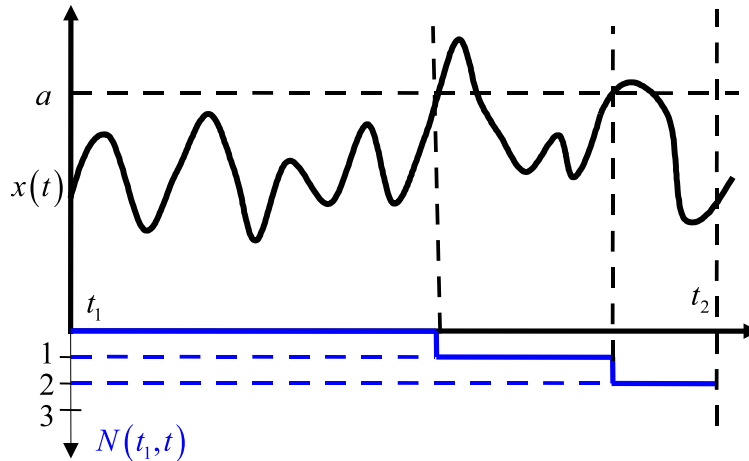


Figure 6.7: Evolution in time of the number of outcrossings

Using this notation, Eq.(6.35) rewrites:

$$P_f(t_1, t_2) = \mathbb{P}(\{g(t_1, \mathbf{X}(t_1)) \leq 0\} \cup \{N^+(t_1, t_2) > 0\}) \quad (6.47)$$

²The notation ω for describing the random dimension will be discarded from now on unless necessary.

As the events in the union are not necessarily disjoint, the probability of their union can be upper bounded by the sum of their respective probabilities. Hence:

$$P_f(t_1, t_2) \leq P_{f,i}(t_1) + \mathbb{P}(N^+(t_1, t_2) > 0) \quad (6.48)$$

Moreover:

$$\begin{aligned} \mathbb{P}(N^+(t_1, t_2) > 0) &= \sum_{k=1}^{\infty} \mathbb{P}(N^+(t_1, t_2) = k) \\ &\leq \sum_{k=0}^{\infty} k \mathbb{P}(N^+(t_1, t_2) = k) \\ &\leq \mathbb{E}[N^+(t_1, t_2)] \end{aligned} \quad (6.49)$$

where $\mathbb{E}[N^+(t_1, t_2)]$ is the *mean number of outcrossings* in $[t_1, t_2]$. Using Eqs.(6.40),(6.48), (6.49), one finally gets the following bounds to the probability of failure:

$$\max_{t \in [t_1, t_2]} P_{f,i}(t) \leq P_f(t_1, t_2) \leq P_{f,i}(t_1) + \mathbb{E}[N^+(t_1, t_2)] \quad (6.50)$$

3.3.2 Outcrossing rate

Let us consider the point process defined by the crossings of a surface \mathfrak{S} by a random process $\mathbf{S}(t)$, and the associated counting function $N^+(t_1, t)$, $t_1 < t$. The *outcrossing rate* is defined by:

$$\nu^+(t) = \lim_{\Delta t \rightarrow 0} \frac{\mathbb{P}(N^+(t, t + \Delta t) = 1)}{\Delta t} \quad (6.51)$$

This quantity is interpreted as the probability of having one crossing in an infinitesimal interval $]t, t + \Delta t]$ divided by Δt . This only makes sense if the counting process is *regular*, *i.e.* if the probability of having *more* than one outcrossing in $]t, t + \Delta t]$ is negligible:

$$\lim_{\Delta t \rightarrow 0} \frac{\mathbb{P}(N^+(t, t + \Delta t) > 1)}{\Delta t} = 0 \quad (6.52)$$

Due to this regularity, the quantity $\nu^+(t) \Delta t = \mathbb{P}(N^+(t, t + \Delta t) = 1)$ is also equal to $\mathbb{E}[N^+(t, t + \Delta t)]$. As the counting function is additive in time by definition, one finally gets the mean number of outcrossings within a time interval $[t_1, t_2]$:

$$\mathbb{E}[N^+(t_1, t_2)] = \int_{t_1}^{t_2} \nu^+(t) dt \quad (6.53)$$

In the context of reliability analysis, the process under consideration will be the limit state function itself, *i.e.* $g(t, \mathbf{X}(t, \omega))$ and the surface \mathfrak{S} will be the zero level. Having one outcrossing in $]t, t + \Delta t]$ corresponds to being in the safe domain at time t and in the failure domain at time $t + \Delta t$. Thus Eq.(6.51) may be also rewritten as:

$$\nu^+(t) = \lim_{\Delta t \rightarrow 0} \frac{\mathbb{P}(\{g(t, \mathbf{X}(t, \omega)) > 0\} \cap \{g(t + \Delta t, \mathbf{X}(t + \Delta t, \omega)) \leq 0\})}{\Delta t} \quad (6.54)$$

This expression will be taken advantage of in the sequel. As a conclusion, the evaluation of the upper bound to the probability of failure reduces to computing the outcrossing rate through the limit state surface and integrating it in time.

Stationary time-variant reliability problems deserve special attention. They correspond to the following assumptions:

- the random processes $\{S_j(t, \omega), j = p + 1, \dots, p + q\}$ are stationary processes;
- there is no direct time dependence in the limit state function, *i.e.* it can be formally written as $g(\mathbf{R}, \mathbf{S}(t, \omega))$

In this case, the point-in-time reliability problem and the outcrossing rate are independent of the time instant. Thus Eqs.(6.53),(6.50) reduce to:

$$\mathbb{E} [N^+(t_1, t_2)] = \nu^+ \cdot (t_2 - t_1) \quad (6.55)$$

$$P_{f,i}(t_1) \leq P_f(t_1, t_2) \leq P_{f,i}(t_1) + \nu^+ \cdot (t_2 - t_1) \quad (6.56)$$

4 Analytical results for outcrossing rates

As seen from the previous section, the computation of the outcrossing rate of random processes through thresholds (one refers to upcrossing rate in this particular case) or surfaces is of crucial importance. In this section, we review some important analytical results for the differentiable Gaussian processes. Note that in the context of reliability analysis, the results presented below only apply when the failure is defined by the crossing of a random process through a *deterministic* surface, *i.e.* when there are no \mathbf{R} -random variables in the problem.

4.1 Rice's formula

Let us consider a scalar differentiable (not necessarily Gaussian) random process $X(t, \omega)$ and a deterministic, possibly time varying threshold $a(t)$. The outcrossing rate of $X(t, \omega)$ has been defined in Eq.(6.51). According to Figure 6.8, an outcrossing occurring in $[t, t + \Delta t]$ requires that:

- the slope of the trajectory $\dot{x}(t)$ is greater than that of the threshold $\dot{a}(t)$;
- the trajectory at t is in the neighbourhood of the threshold, more precisely no further than the distance $\dot{x}(t)\Delta t$, to $a(t + \Delta t)$.

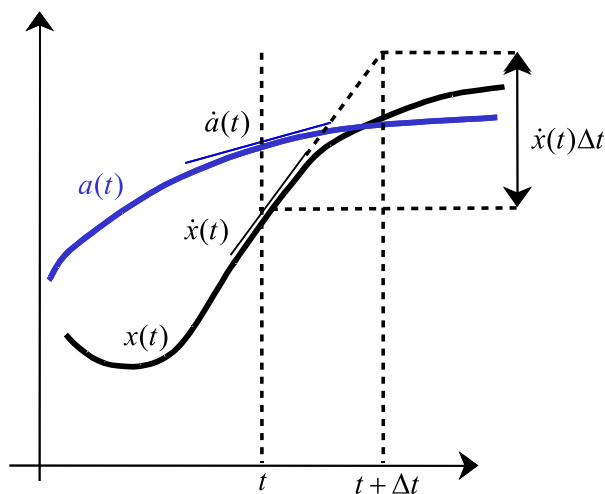


Figure 6.8: Outcrossing of a scalar differentiable process

Thus:

$$\begin{aligned}\nu^+(t) &= \lim_{\Delta t \rightarrow 0} \frac{\mathbb{P}(N^+(t, t + \Delta t) = 1)}{\Delta t} \\ &= \lim_{\Delta t \rightarrow 0} \frac{\mathbb{P}\left(\left\{\dot{X}(t) \geq \dot{a}(t)\right\} \cap \left\{a(t + \Delta t) - \Delta t \dot{X}(t) \leq X(t) \leq a(t)\right\}\right)}{\Delta t}\end{aligned}\quad (6.57)$$

Denoting by $f_{X\dot{X}}(x, \dot{x})$ the joint probability density function of the process and its derivative, Eq.(6.57) becomes:

$$\nu^+(t) = \lim_{\Delta t \rightarrow 0} \int_{\dot{a}(t)}^{\infty} \int_{a(t+\Delta t) - \Delta t \dot{x}}^{a(t)} \frac{1}{\Delta t} f_{X\dot{X}}(x, \dot{x}) dx d\dot{x}\quad (6.58)$$

The lower bound of the inner integral may be rewritten as $a(t) - \Delta t(\dot{x} - \dot{a}(t))$. Using the mean value theorem and the limit passage $\Delta t \rightarrow 0$, the inner integral becomes $(\dot{x} - \dot{a}(t)) f_{X\dot{X}}(a(t), \dot{x})$. This finally leads to the so-called *Rice's formula* (Rice, 1944, 1945):

$$\nu^+(t) = \int_{\dot{a}(t)}^{\infty} (\dot{x} - \dot{a}(t)) f_{X\dot{X}}(a(t), \dot{x}) d\dot{x}\quad (6.59)$$

4.2 Application of Rice's formula to Gaussian processes

In case of a stationary process $X(t, \omega)$ and constant threshold, Eq.(6.59) becomes:

$$\nu^+(a) = \int_0^{\infty} \dot{x} f_{X\dot{X}}(a, \dot{x}) d\dot{x}\quad (6.60)$$

If the process is furthermore Gaussian (mean value μ_X , standard deviation σ_X), its derivative process $\dot{X}(t, \omega)$ is also Gaussian (zero mean value, standard deviation $\sigma_{\dot{X}}$) and independent from $X(t, \omega)$. Thus the joint PDF:

$$f_{X\dot{X}}(x, \dot{x}) = \frac{1}{\sigma_X} \frac{1}{\sigma_{\dot{X}}} \varphi\left(\frac{x - \mu_X}{\sigma_X}\right) \varphi\left(\frac{\dot{x}}{\sigma_{\dot{X}}}\right)\quad (6.61)$$

By substituting Eq.(6.61) in Eq.(6.60), the outcrossing rate of $X(t, \omega)$ through threshold a eventually reads:

$$\nu^+(a) = \frac{1}{\sqrt{2\pi}} \frac{\sigma_{\dot{X}}}{\sigma_X} \varphi\left(\frac{a - \mu_X}{\sigma_X}\right)\quad (6.62)$$

Introducing the cycle rate $\varpi_0 = \sigma_{\dot{X}}/\sigma_X$ (see Eq.(6.31)), the latter also reads:

$$\nu^+(a) = \frac{\varpi_0}{\sqrt{2\pi}} \varphi\left(\frac{a - \mu_X}{\sigma_X}\right)\quad (6.63)$$

Hence the mean number of outcrossing in the time interval $[t_1, t_2]$:

$$\mathbb{E}[N^+(t_1, t_2)] = (t_2 - t_1) \frac{\varpi_0}{\sqrt{2\pi}} \varphi\left(\frac{a - \mu_X}{\sigma_X}\right)\quad (6.64)$$

Introducing the standardized threshold

$$b(t) = \frac{a(t) - \mu_X(t)}{\sigma_X(t)}\quad (6.65)$$

which reduces to a constant b in the stationary case, Eq.(6.64) may be rewritten as:

$$\mathbb{E}[N^+(t_1, t_2)] = (t_2 - t_1) \frac{\varpi_0}{\sqrt{2\pi}} \varphi(b)\quad (6.66)$$

If the threshold $a(t)$ varies in time, substituting Eq.(6.61) in Eq.(6.59) yields:

$$\nu^+(t) = \int_{\dot{a}(t)}^{\infty} (\dot{x} - \dot{a}(t)) \frac{1}{\sigma_X} \frac{1}{\sigma_{\dot{X}}} \varphi\left(\frac{a(t) - \mu_X}{\sigma_X}\right) \varphi\left(\frac{\dot{x}}{\sigma_{\dot{X}}}\right) d\dot{x} \quad (6.67)$$

Using results by Owen (1980) and $\varpi_0 = \sigma_{\dot{X}}/\sigma_X$, the latter integral reduces to:

$$\nu^+(t) = \varpi_0 \varphi\left(\frac{a(t) - \mu_X}{\sigma_X}\right) \Psi\left(\frac{\dot{a}(t)}{\sigma_{\dot{X}}}\right) \quad (6.68)$$

where $\Psi(x) = \varphi(x) - x\Phi(-x)$. Using the standardized notation, this result may also be written as:

$$\nu^+(t) = \varpi_0 \varphi(b(t)) \Psi\left(\frac{\dot{b}(t)}{\varpi_0}\right) \quad (6.69)$$

The mean number of outcrossing then reads:

$$\mathbb{E}[N^+(t_1, t_2)] = \int_{t_1}^{t_2} \varpi_0 \varphi(b(t)) \Psi\left(\frac{\dot{b}(t)}{\varpi_0}\right) dt \quad (6.70)$$

If the process is non stationary, the parameters $\mu_X, \sigma_X, \sigma_{\dot{X}}, \varpi_0$ becomes *time dependent*. However the derivations in the previous paragraph still hold and the mean number of outcrossings reads (Cramer and Leadbetter, 1967):

$$\mathbb{E}[N^+(t_1, t_2)] = \int_{t_1}^{t_2} \varpi_0(t) \varphi(b(t)) \Psi\left(\frac{\dot{b}(t)}{\varpi_0(t)}\right) dt \quad (6.71)$$

4.3 Belyev's formula

The determination of the outcrossing rate of a Gaussian differentiable vector process $\mathbf{X}(t, \omega)$ through a time varying limit state surface by means of Eq.(6.57) requires introducing some additional notation. Let $\mathfrak{S}(t)$ be the time-variant limit state surface under consideration, whose outwards normal at point \mathbf{x} is $\mathbf{n}(\mathbf{x}, t)$. Let $\mathbf{v}(\mathbf{x}, t)$ be the velocity of the limit state surface, and $v_{\perp}(\mathbf{x}, t) = \mathbf{v}(\mathbf{x}, t) \cdot \mathbf{n}(\mathbf{x}, t)$ its normal component. In analogy to Rice's formula, an outcrossing of the failure surface within time interval $[t, t + \Delta t]$ implies that:

- the derivative vector process has such a direction and intensity that it can cross a moving surface with velocity $\mathbf{v}(\mathbf{x}, t)$. By introducing the projection of the derivative process $\dot{\mathbf{X}}(t, \omega)$ onto the normal to $\mathfrak{S}(t)$:

$$\dot{X}_{\perp}(t) = \mathbf{n}(\mathbf{x}, t) \cdot \dot{\mathbf{X}}(t) \quad (6.72)$$

this condition writes for a given trajectory:

$$\dot{x}_{\perp}(t) > v_{\perp}(\mathbf{x}, t) \quad (6.73)$$

- the trajectory $\mathbf{x}(t)$ is in a layer $\mathbb{L}(\mathfrak{S}(t))$ defined around the failure surface $\mathfrak{S}(t)$, whose thickness is $(\dot{x}_{\perp}(t) - v_{\perp}(\mathbf{x}, t)) \cdot \Delta t$

These conditions are sketched in Figure 6.9. With the above notation, the outcrossing rate reads:

$$\nu^+(t) = \lim_{\Delta t \rightarrow 0} \frac{\mathbb{P}\left(\{\mathbf{X}(t) \in \mathbb{L}(\mathfrak{S}(t))\} \cap \left\{\dot{X}_{\perp}(t) > v_{\perp}(\mathbf{x}, t)\right\}\right)}{\Delta t} \quad (6.74)$$

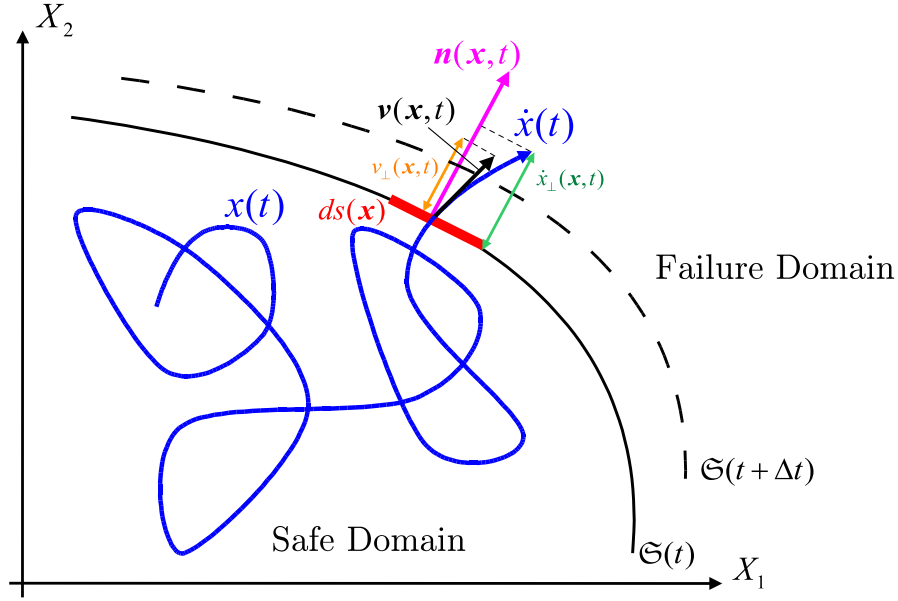


Figure 6.9: Outcrossing of a differentiable vector process

As $\mathbf{X}(t)$ is a Gaussian vector, its derivative as well as the projection of the latter onto $\mathbf{n}(\mathbf{x}, t)$ are also Gaussian. The above equation thus rewrites:

$$\begin{aligned} \nu^+ &= \lim_{\Delta t \rightarrow 0} \frac{1}{\Delta t} \left[\int_{\mathbb{L}(\mathfrak{S}(t))} \int_{\dot{x}_\perp(t) > v_\perp(\mathbf{x}, t)} \varphi_{n+1}(\mathbf{x}, \dot{x}_\perp) d\mathbf{x} d\dot{x}_\perp \right] \\ &= \lim_{\Delta t \rightarrow 0} \frac{1}{\Delta t} \left[\int_{\mathfrak{S}(t)} \int_{\dot{x}_\perp(t) > v_\perp(\mathbf{x}, t)} \Delta t (\dot{x}_\perp(t) - v_\perp(\mathbf{x}, t)) \varphi_{n+1}(\mathbf{x}, \dot{x}_\perp) ds(\mathbf{x}) d\dot{x}_\perp \right] \end{aligned} \quad (6.75)$$

where $ds(\mathbf{x})$ represents the infinitesimal surface element on $\mathfrak{S}(t)$. Thus the expression for the outcrossing rate:

$$\nu^+(t) = \int_{\mathfrak{S}(t)} \int_{\dot{x}_\perp(t) > v_\perp(\mathbf{x}, t)} (\dot{x}_\perp(t) - v_\perp(\mathbf{x}, t)) \varphi_{n+1}(\mathbf{x}, \dot{x}_\perp) ds(\mathbf{x}) d\dot{x}_\perp \quad (6.76)$$

The latter equation is the *Belayev's formula* (Belayev, 1968) for Gaussian vector processes (a general expression also exists when $\mathbf{X}(t)$ is not Gaussian). The practical computation of this integral requires determining the statistics of the projection $\dot{X}_\perp(t)$ and a so-called scalarization of the problem. The details of the computation are out of the scope of the present document (see Rackwitz (2004) for details).

In the *stationary case*, the failure surface is constant and its normal velocity $v_\perp(\mathbf{x})$ is equal to 0. Moreover, the normal derivative process \dot{X}_\perp is independent on the initial vector process \mathbf{X} . Thus the latter equation reduces to:

$$\begin{aligned} \nu^+ &= \int_{\mathfrak{S}(t)} \int_{\dot{x}_\perp(t) > 0} \dot{x}_\perp \varphi_{n+1}(\mathbf{x}, \dot{x}_\perp) ds(\mathbf{x}) d\dot{x}_\perp \\ &\equiv E_0^\infty [\dot{X}_\perp] \int_{\mathfrak{S}(t)} \varphi_n(\mathbf{x}) ds(\mathbf{x}) \end{aligned} \quad (6.77)$$

4.4 Another estimation of the probability of failure

In the various cases presented so far in this section, the randomness in the problem lies only in the scalar or vector random process \mathbf{S} under consideration. In this specific case, the occurrence of outcrossing of a deterministic surface may be considered as a Poisson process, provided the process \mathbf{S} is mixing. The

probability of failure associated to the outcrossing event, which is the CDF of the first passage time to the failure domain reads in this case:

$$F_T(t) = P_f(0, t) \approx 1 - e^{-\nu^+ t} \quad (6.78)$$

where the intensity of the Poisson process is nothing but the outcrossing rate ν^+ in this case. The latter equation can be slightly modified in order to take into account the fact that the system may fail at $t = 0$ (see Madsen and Tvedt (1990); Schall et al. (1991)):

$$P_f(0, t) \approx P_{f,i}(0) + (1 - P_{f,i}(0)) \left(1 - \exp \left[\frac{-\nu^+ t}{1 - P_{f,i}(0)} \right] \right) \quad (6.79)$$

This result does not apply anymore when \mathbf{R} -variables are present in the problem statement. Indeed, the compound process defined by $g(t, \mathbf{R}, \mathbf{S}(t))$ is no more mixing in this case, due to the non ergodicity of the \mathbf{R} -variables. Other arguments have to be devised to solve the problem in this general case. This is the aim of the next section.

5 Asymptotic method

5.1 Introduction

In the previous section, expressions for the outcrossing rate and related mean number of outcrossings have been derived in the case when the thresholds (or more generally the limit state surface) are *deterministic*, *i.e.* the unique source of randomness taken into account so far is that of the random processes. However, in real problems, other sources of randomness (including those related to the resistance of the structure) have to be dealt with in a common framework. Moreover, the problem of efficiently integrating the outcrossing rate with respect to time (Eqs.(6.70),(6.71)) has not been addressed so far.

The so-called *asymptotic method* (AsM) provides a framework that allows the analyst to solve both problems in an efficient manner. In order to make a link with the existing literature on the topic (*e.g.* Rackwitz (1998)), the following notation due to Schall et al. (1991) is introduced. The randomness in the problem is modelled by means of three types of random variables, namely:

- \mathbf{R} is a vector of random variables as in time-invariant reliability. Its distribution parameters may be deterministic functions of time. This vector is used to model resistance variables. These variables are said non-ergodic;
- \mathbf{Q} denotes stationary and ergodic vector sequences. Usually they are used to model long term variations in time (traffic states, sea states, wind velocity regimes, etc.). \mathbf{Q} -variables may also determine the fluctuating parameters of the random processes described next;
- \mathbf{S} is a vector random process whose parameters can depend on \mathbf{Q} and/or \mathbf{R} . Its components are not necessarily stationary. Usually they are used to describe short-term fluctuations of the loading³.

The closed-form formulæ derived in the previous section can be used to compute the *conditional outcrossing rate* $\nu^+(t | \mathbf{r}, \mathbf{q})$. The conditional mean number of outcrossings reads:

$$E [N^+(t_1, t_2) | \mathbf{r}, \mathbf{q}] = \int_{t_1}^{t_2} \nu^+(t | \mathbf{r}, \mathbf{q}) dt \quad (6.80)$$

³Apart from the \mathbf{Q} -variables, this notation is identical to what was already introduced in Section 3.1 of this report in page 123.

The upper bound to the probability of failure is obtained by taking the expectation of Eq.(6.50) with respect to the \mathbf{R}/\mathbf{Q} variables:

$$P_f(t_1, t_2) \leq \mathbb{P}(g(t_1, \mathbf{R}, \mathbf{Q}, \mathbf{S}(t_1)) \leq 0) + E_{\mathbf{R}, \mathbf{Q}} [E [N^+(t_1, t_2) | \mathbf{r}, \mathbf{q}]] \quad (6.81)$$

As a whole, three integrations are required with respect to \mathbf{R} and \mathbf{Q} - variables and time. The time integration is carried out approximately using Laplace integration. The expectation operation with respect to \mathbf{R} and \mathbf{Q} is also carried out using asymptotic results for multidimensional integrals (Breitung, 1988), see also Rackwitz (1998). In order to get a flavor of how asymptotic Laplace integration works, the principles are recalled for the one-dimensional case in the next paragraph.

5.2 Asymptotic Laplace integration

5.2.1 Introduction

The Laplace integration is an asymptotic method used to approximate integrals of the following type:

$$I = \int_a^b h(t) \exp(-\lambda f(t)) dt \quad (6.82)$$

under the following conditions:

- λ is a positive parameter and possibly a large number,
- $f(t)$ is twice differentiable, unimodal and strictly *positive* over $[a, b]$,
- $h(t)$ is differentiable and strictly *positive* over $[a, b]$.

The calculation of the integral is performed separately whether f is a monotonic function in $[a, b]$ (*boundary point case*) or f has a minimum in $]a, b[$ (*interior point case*).

5.2.2 “Boundary point” case

Suppose that f is monotonically increasing over $[a, b]$. Then the most important contribution to the integral corresponds to values of t close to a , which is the point where $f(t)$ attains its minimum within the interval. Consequently, $h(t)$ is replaced by $h(a)$ and $f(t)$ by its Taylor series expansion around a :

$$f(t) = f(a) + (t - a)\dot{f}(a) + o(t - a) \quad (6.83)$$

Substituting for Eq.(6.83) in Eq.(6.82) yields after basic algebra:

$$I \approx h(a) \exp(-\lambda f(a)) \frac{1 - \exp(-\lambda(b - a)\dot{f}(a))}{\lambda\dot{f}(a)} \quad (6.84)$$

A similar reasoning holds in case f is strictly decreasing by using a Taylor series expansion around b . Finally, denoting by t^* the critical point (*i.e.* a or b , wherever the integrand is maximal), the asymptotic integral reads in the boundary point case:

$$I \approx h(t^*) \exp(-\lambda f(t^*)) \frac{1 - \exp(-\lambda(b - a)|\dot{f}(t^*)|)}{\lambda|\dot{f}(t^*)|} \quad (6.85)$$

5.2.3 “Interior point” case

Suppose now that f has a minimum in a single point t^* in $]a, b[$, i.e. $\dot{f}(t^*) = 0$. Then the most important contribution to the integral corresponds to values of t close to t^* . Consequently, $h(t)$ is replaced by $h(t^*)$ and $f(t)$ by its Taylor series expansion around t^* :

$$f(t) \approx f(t^*) + \frac{1}{2}(t - t^*)^2 \ddot{f}(t^*) + o(t - t^*)^2 \quad (6.86)$$

After basic algebra, the integral in Eq.(6.82) reduces to:

$$I \approx h(t^*) \exp(-\lambda f(t^*)) \sqrt{\frac{2\pi}{\lambda \ddot{f}(t^*)}} \left[\Phi \left((b - t^*) \sqrt{\lambda \ddot{f}(t^*)} \right) - \Phi \left((a - t^*) \sqrt{\lambda \ddot{f}(t^*)} \right) \right] \quad (6.87)$$

where Φ is the standard normal CDF.

5.3 Application to scalar Gaussian differentiable processes

Eq.(6.71) rewrites in this case:

$$\mathbb{E} [N^+(t_1, t_2)] = \int_{t_1}^{t_2} \frac{\varpi_0(t)}{\sqrt{2\pi}} \Psi \left(\frac{\dot{b}(t)}{\varpi_0(t)} \right) \exp(-b^2(t)/2) dt \quad (6.88)$$

This is a Laplace integral of the form (6.82) provided:

- $\lambda=1$
- $f(t) = b^2(t)/2$
- $h(t) = \frac{\varpi_0(t)}{\sqrt{2\pi}} \Psi \left(\frac{\dot{b}(t)}{\varpi_0(t)} \right)$

Two formulæ can be obtained according to the position of the critical point t^* . In the “boundary point” case ($t^* = t_1, t_2$), the mean number of outcrossings reads:

$$\mathbb{E} [N^+(t_1, t_2)] \approx \varpi_0(t^*) \Psi \left(\frac{\dot{b}(t^*)}{\varpi_0(t^*)} \right) \varphi(b(t^*)) \left[\frac{1 - \exp \left(-b(t^*) \left| \frac{\dot{b}(t^*)}{\varpi_0(t^*)} \right| (t_2 - t_1) \right)}{b(t^*) \left| \frac{\dot{b}(t^*)}{\varpi_0(t^*)} \right|} \right] \quad (6.89)$$

In the “interior point” case ($t_1 < t^* < t_2$) the first order derivative of the threshold is zero at the critical point. Hence the expansions:

$$\begin{aligned} b^2(t) &\approx b^2(t^*) + b(t^*) \ddot{b}(t^*) (t - t^*)^2 + o(t - t^*)^2 \\ \dot{b}(t) &\approx \ddot{b}(t^*) (t - t^*) + o(t - t^*) \end{aligned} \quad (6.90)$$

and the mean number of outcrossings is approximated by:

$$\begin{aligned} \mathbb{E} [N^+(t_1, t_2)] &\approx \frac{\sqrt{2\pi} \varpi_0(t^*) \varphi(b(t^*))}{\sqrt{b(t^*) \ddot{b}(t^*)}} \\ &\times \left[\frac{\sqrt{1 + \gamma^2}}{\sqrt{2\pi}} \Phi \left(u \sqrt{1 + \gamma^2} \right) + \gamma \varphi(u) \Phi(-\gamma u) \right] \frac{\sqrt{b(t^*) \ddot{b}(t^*) (t_2 - t^*)}}{\sqrt{b(t^*) \ddot{b}(t^*) (t_1 - t^*)}} \end{aligned} \quad (6.91)$$

where $\gamma(t^*) = \frac{1}{\varpi_0(t^*)} \sqrt{\frac{\dot{b}(t^*)}{b(t^*)}}$.

5.4 Outcrossing for general surfaces defined in the R - Q - S -space

The results derived so far apply in the case when the randomness is limited to a vector process \mathbf{S} . In real problems, other \mathbf{R} and \mathbf{Q} random variables are usually present in the model. The above results may be used *conditionally* to the values of r and q . Thus the mean number of outcrossings reads:

$$E [N^+(t_1, t_2)] = E_{\mathbf{R}, \mathbf{Q}} [E [N^+(t_1, t_2 | \mathbf{r}, \mathbf{q})]] = \int_{t_1}^{t_2} E_{\mathbf{R}, \mathbf{Q}} [\nu^+(t | \mathbf{r}, \mathbf{q})] dt \quad (6.92)$$

As for time integration, the expectation operation, *i.e.* the integration over \mathbf{r}, \mathbf{q} in the above equation is performed by asymptotic (now multidimensional) formulæ. As explained in Rackwitz (1998), this reduces to computing the design point in the \mathbf{R} - \mathbf{Q} - \mathbf{S} -space by asymptotic SORM and the reliability index accordingly.

5.5 Conclusion

The asymptotic method (AsM) relies upon the use of Laplace integrals to carry out approximately the time integration of the outcrossing rate as well as the expectation operation with respect to \mathbf{R} - and \mathbf{Q} -variables.

The full package is implemented in a commercial software called COMREL-TV (RCP Consult, 1998). To the author's knowledge, there is no other comprehensive implementation of this asymptotic theory. This may explain why the time-variant reliability methods are not used much in industrial applications yet.

The PHI2 method presented in the next section is an interesting alternative since it allows to solve time-variant reliability problems using any *time-invariant* reliability software at hand without implementing specific algorithms.

6 System reliability approach: the PHI2 method

6.1 Introduction

The so-called PHI2 method has been developed by Andrieu-Renaud (2002); Andrieu-Renaud et al. (2004). The original idea can be found in an early paper by Hagen (1992) and has been subsequently used in various forms by Li and Der Kiureghian (1995); Der Kiureghian and Li (1996); Vijalapura et al. (2000); Der Kiureghian (2000) in the context of random vibrations.

The main idea is to compute directly the outcrossing rate from Eq.(6.54) by replacing the limit operation by a finite difference scheme:

$$\nu^+(t) \approx \frac{\mathbb{P}(\{g(t, \mathbf{X}(t, \omega)) > 0\} \cap \{g(t + \Delta t, \mathbf{X}(t + \Delta t, \omega)) \leq 0\})}{\Delta t} \quad (6.93)$$

The numerator of the above equation is nothing but the probability of failure of a two-component parallel system. Using FORM for systems (Ditlevsen and Madsen, 1996, chap. 14), it may be approximated by:

$$\nu^+(t) \approx \frac{\Phi_2(\beta(t), -\beta(t + \Delta t), \rho(t, t + \Delta t))}{\Delta t} \quad (6.94)$$

In this expression, Φ_2 stands for the binormal cumulative distribution function (thus the name "PHI2" for the method), $\beta(t)$ (resp. $\beta(t + \Delta t)$) is the point-in-time reliability index computed by FORM at time instant t (resp. $t + \Delta t$), and $\rho(t, t + \Delta t)$ is the dot product of the α -vectors computed in each FORM analysis.

As shown in Andrieu et al. (2002), the time increment Δt has to be selected carefully. Indeed, a too large time increment would lead to an inaccurate estimation of the limit value. In contrast, a too small time increment corresponds to a correlation coefficient $\rho(t, t + \Delta t)$ close to -1 , which leads to numerical instabilities.

The rigorous expression for the limit value in Eq.(6.54) has been recently derived in Sudret (2005a, 2007). It is based on a Taylor series expansion of the various terms appearing in that equation, which leads to a closed-form expression for the outcrossing rate. This derivation is summarized in Section 6.2. The “user’s manuel” to the PHI2 method is then presented in Section 6.3. The time-variant problem is cast as a set of two *time-invariant* FORM analyses, and the analytical expression for the outcrossing rate is given a computational practical counterpart.

6.2 Analytical derivation of the outcrossing rate

Let us introduce the following function:

$$f_t(h) = \mathbb{P} \left(\{g(t, \mathbf{X}(t, \omega)) > 0\} \cap \{g(t+h, \mathbf{X}(t+h, \omega)) \leq 0\} \right) \quad (6.95)$$

It is obvious that $f_t(0) = 0$ since the events in the intersection are disjoint. From this remark and Eq.(6.54) it comes:

$$\nu^+(t) = \lim_{h \rightarrow 0} \frac{f_t(h) - f_t(0)}{h} = \dot{f}_t(0) \quad (6.96)$$

where $\dot{f}_t(\cdot)$ is the derivative of $f_t(h)$ with respect to h . When interpreting Eq.(6.95) as a two-component parallel system, the use of the First Order Reliability Method (FORM) leads to:

$$f_t(h) = \Phi_2(\beta(t), -\beta(t+h), \rho(t, h)) \quad (6.97)$$

where $\Phi_2(x, y, \rho)$ is the binormal CDF, $\beta(t)$ is the *point-in-time* reliability index at time instant t , $\beta(t+h)$ is the *point-in-time* reliability index at time instant $t+h$. Moreover the “correlation coefficient” $\rho(t, h)$ between the limit state functions at t and $t+h$ is defined as:

$$\rho(t, h) = -\boldsymbol{\alpha}(t) \cdot \boldsymbol{\alpha}(t+h) \quad (6.98)$$

i.e., it is the obtained by the dot product between the design point directions $\boldsymbol{\alpha}(t) = \boldsymbol{\xi}^*(t)/\beta(t)$ and $\boldsymbol{\alpha}(t+h) = \boldsymbol{\xi}^*(t+h)/\beta(t+h)$, $\boldsymbol{\xi}^*$ being the coordinates of the design point in the standard normal space.

After some cumbersome derivations, whose details are given in Sudret (2007), the outcrossing rate finally reads in the general (*i.e.* non stationary) case:

$$\nu^+(t) = \|\dot{\boldsymbol{\alpha}}(t)\| \varphi(\beta(t)) \Psi \left(\frac{\dot{\beta}(t)}{\|\dot{\boldsymbol{\alpha}}(t)\|} \right) \quad (6.99)$$

If the problem is stationary (*i.e.* if β is independent of time), the above equation reduces to:

$$\nu^+ = \frac{\varphi(\beta)}{\sqrt{2\pi}} \|\dot{\boldsymbol{\alpha}}\| \quad (6.100)$$

One can remark the similarity between Eqs.(6.99) and (6.69) (resp. Eqs.(6.100) and (6.66)). There is a simple explanation for this: in the case when the upcrossing of a standard normal process $U(t)$ (with cycle rate ϖ_0) through a threshold $b(t)$ is considered, it is easy to show that $\beta(t) \equiv b(t)$ and $\|\dot{\boldsymbol{\alpha}}(t)\| \equiv \varpi_0$, thus the result. However, Eqs.(6.99),(6.100) are applicable to solve general problems involving **R-Q-S**-variables, whereas the use of (6.66),(6.69) in this general case requires on top the use of asymptotic integration, as presented in Section 5.2.

6.3 Implementation of the PHI2 method using a time-invariant reliability code

The practical implementation of the PHI2 method reads as follows:

- The point-in-time reliability index $\beta(t)$ associated with the limit state function $g(t, \mathbf{X}(t, \omega)) \leq 0$ is computed after freezing t in all functions of time and replacing the random processes $S_j(t, \omega)$ by random variables $S_j^{(1)}, j = p+1, \dots, p+q$. Classical FORM analysis corresponds to approximating the limit state surface by the hyperplane $\beta(t) - \boldsymbol{\alpha}(t) \cdot \boldsymbol{\xi} = 0$ in the standard normal space (see Eq.(3.48)). As a consequence, the reliability index associated with the limit state $g(t, \mathbf{X}(t, \omega)) > 0$ is $-\beta(t)$.
- The point-in-time reliability index $\beta(t + \Delta t)$ associated with the limit state function $g(t + \Delta t, \mathbf{X}(t + \Delta t, \omega)) \leq 0$ is computed by another FORM analysis. It is important to notice that the random processes $S_j(t, \omega)$ are now replaced by another set of random variables $S_j^{(2)}$ that are different from, although correlated with the $S_j^{(1)}$ variables. The correlation coefficient writes:

$$\rho(S_j^{(1)}, S_j^{(2)}) = \rho_{S_j}(t, t + \Delta t) \quad (6.101)$$

where $\rho_{S_j}(t_1, t_2)$ denotes the autocorrelation coefficient function of process S_j . The approximate limit state surface writes $\beta(t + \Delta t) - \boldsymbol{\alpha}(t + \Delta t) \cdot \boldsymbol{\xi} = 0$ in the standard normal space. The corresponding reliability index is $\beta(t + \Delta t)$.

- The outcrossing rate is evaluated by the "finite difference" version of Eq.(6.99) (resp.(6.100)). This yields, in the stationary case:

$$\nu_{\text{PHI2}}^+ = \frac{\varphi(\beta)}{\sqrt{2\pi}} \frac{\|\boldsymbol{\alpha}(t + \Delta t) - \boldsymbol{\alpha}(t)\|}{\Delta t} \quad (6.102)$$

and in the non stationary case:

$$\nu_{\text{PHI2}}^+(t) = \frac{\|\boldsymbol{\alpha}(t + \Delta t) - \boldsymbol{\alpha}(t)\|}{\Delta t} \varphi(\beta(t)) \Psi \left(\frac{\beta(t + \Delta t) - \beta(t)}{\|\boldsymbol{\alpha}(t + \Delta t) - \boldsymbol{\alpha}(t)\|} \right) \quad (6.103)$$

For an accurate evaluation of the outcrossing rate, it is necessary to select a sufficiently small time increment, *e.g.* $\Delta t \leq 1\%$ of the correlation length of the most rapidly varying component $\{S_j(t, \omega), j = p+1, \dots, p+q\}$. A parametric study with respect to the size of Δt can be found in Sudret (2007). Eqs.(6.102)-(6.103) reveal rather insensitive to Δt (provided it is small enough), whereas the original version of the method (Eq.(6.94)) revealed quite unstable.

7 Application examples

Various comparisons of the PHI2 method and the AsM can be found in the literature (Andrieu-Renaud, 2002). Sudret et al. (2002) consider two analytical examples, namely a Gaussian differentiable process crossing a random barrier that can be either constant in time or time-variant. The second case is reported in Section 7.1 in order to show the accuracy of the PHI2 method when an analytical solution exists. The problem of a corroded bending beam submitted to a midspan load is addressed in Andrieu-Renaud et al. (2004); Sudret (2007) and reported in Section 7.2. In Andrieu-Renaud et al. (2004), the authors propose an example involving a Gaussian differentiable vector process. The case of a concrete beam submitted to creep and a random pinpoint load randomly applied during the life time of the structure is

addressed in Andrieu et al. (2003); Andrieu-Renaud et al. (2004), where results are compared with Monte Carlo simulation. Recently, the PHI2 method has been applied to study the time-variant reliability of viscoplastic plates (Cazuguel et al., 2005, 2006). In naval engineering, it has been used to evaluate the reliability of a corroded plate with non linear constitutive law submitted to a random loading (Cazuguel and Cognard, 2006).

7.1 Analytical example

7.1.1 Problem statement

The first example under consideration is that of the outcrossing of a time-dependant random threshold by a Gaussian stationary random process $S(t, \omega)$ (mean value μ_S , standard deviation σ_S). The auto-correlation coefficient function of the process is denoted by $\rho_S(t_1, t_2)$. The limit state function under consideration in this section is:

$$g(\mathbf{X}(t, \omega)) = R(\omega) + at - S(t, \omega) \quad (6.104)$$

where $R(\omega)$ is a Gaussian random variable (mean μ_R , standard deviation σ_R) and $a < 0$ is a constant that can model a deterministic degradation of the random capacity R with time during the time interval $[0, T]$.

7.1.2 Closed-form solution

The starting point is a closed form solution to the outcrossing rate through a linear threshold $r + at$ (Leadbetter & Cramer, 1967).

$$\nu^+(r, t) = \varpi_0 \varphi\left(\frac{r + at - \mu_S}{\sigma_S}\right) \Psi\left(\frac{a}{\varpi_0 \sigma_S}\right) \quad ; \quad \Psi(x) = \varphi(x) - x \Phi(-x) \quad (6.105)$$

Using the total probability rule, it comes:

$$\nu^+(t) = \int_{\mathbf{R}} \nu^+(r, t) f_R(r) dr \quad (6.106)$$

where $f_R(r) = \frac{1}{\sigma_R} \varphi\left(\frac{r - \mu_R}{\sigma_R}\right)$. Thus:

$$\begin{aligned} \nu^+(t) &= \int_{\mathbf{R}} \varpi_0 \Psi\left(\frac{a}{\varpi_0 \sigma_S}\right) \varphi\left(\frac{r + at - \mu_S}{\sigma_S}\right) \frac{1}{\sigma_R} \varphi\left(\frac{r - \mu_R}{\sigma_R}\right) dr \\ &= \varpi_0 \Psi\left(\frac{a}{\varpi_0 \sigma_S}\right) \frac{\sigma_S}{\sqrt{\sigma_R^2 + \sigma_S^2}} \varphi\left(\frac{\mu_R + at - \mu_S}{\sqrt{\sigma_R^2 + \sigma_S^2}}\right) \end{aligned} \quad (6.107)$$

Due to non stationarity, this outcrossing rate varies in time and has to be integrated to give the upper bound to the mean number of outcrossings. This is done by substituting for (6.107) in Eq.(6.53):

$$\begin{aligned} \mathbb{E} [N^+(0, T)] &= \int_0^T \varpi_0 \Psi\left(\frac{a}{\varpi_0 \sigma_S}\right) \frac{\sigma_S}{\sqrt{\sigma_R^2 + \sigma_S^2}} \varphi\left(\frac{\mu_R + at - \mu_S}{\sqrt{\sigma_R^2 + \sigma_S^2}}\right) dt \\ &= \frac{\varpi_0 \sigma_S}{a} \Psi\left(\frac{a}{\varpi_0 \sigma_S}\right) \left[\Phi\left(\frac{\mu_R + aT - \mu_S}{\sqrt{\sigma_R^2 + \sigma_S^2}}\right) - \Phi\left(\frac{\mu_R - \mu_S}{\sqrt{\sigma_R^2 + \sigma_S^2}}\right) \right] \end{aligned} \quad (6.108)$$

7.1.3 Numerical results

A standard normal stationary process S is chosen. The autocorrelation coefficient function is:

$$\rho_S(t_1, t_2) = \exp\left(-\left(\frac{t_2 - t_1}{\ell}\right)^2\right) \quad (6.109)$$

The correlation length of the process is $\ell = 0.5$, the time interval under consideration is $[0, 20]$. The decaying kinetics is represented by $a = -0.15$.

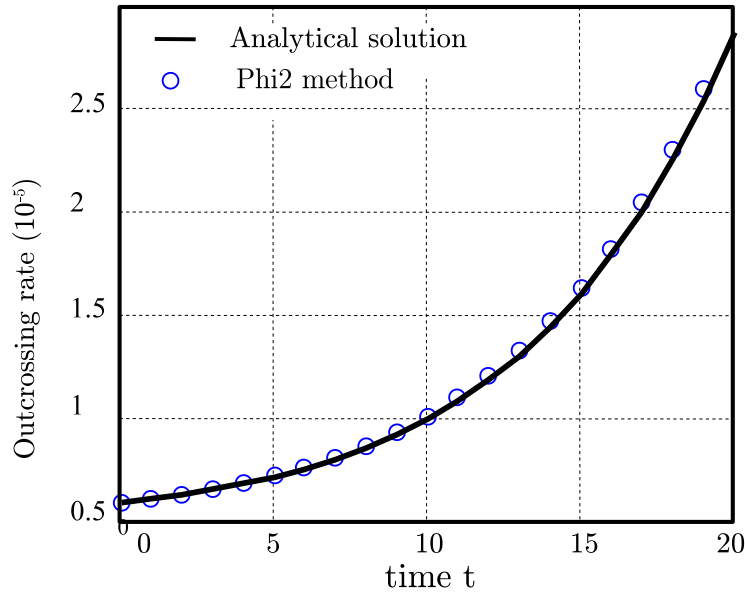


Figure 6.10: Non stationary analytical example: $g(\mathbf{X}(t, \omega)) = R(\omega) + at - S(t, \omega)$ - outcrossing rate $\nu^+(t)$ vs. time t

In a first run, the mean value of R is set equal to 20 and its standard deviation σ_R is set equal to 4. The evolution of the outcrossing rate $\nu^+(t)$ over the time interval is represented in Figure 6.10 using both the analytical solution (Eq.(6.107)) and the PHI2 method (Eq.(6.103)). It appears that PHI2 provides almost exact results all along the time interval. The asymptotic approach does not provide the outcrossing rate, but directly its integral over the time interval. Thus it is not represented in Figure 6.10.

The cumulative probability of failure $P_f(0, t)$ may then be evaluated from Eq.(6.50) and transformed into a generalized reliability index $\beta_{gen}(0, t) = -\Phi^{-1}(P_f(0, t))$. Accordingly, the lower bound $P_f^{LB}(0, t)$ (resp. upper bound $P_f^{UB}(0, t)$) in Eq.(6.50) may be transformed into bounds to the generalized reliability index as follows: $\beta^b(0, t) = -\Phi^{-1}(P_f^b(0, t))$, $b \in \{LB, UB\}$. Note that the upper bound to $P_f(0, t)$ corresponds to a lower bound of β and vice versa. One finally gets:

$$\beta^{UB}(0, t) \leq \beta_{gen}(0, t) \leq \beta^{LB}(0, t) \quad (6.110)$$

These generalized reliability indices associated with $P_f(0, t)$ are plotted in Figure 6.11 as a function of time $t \in [0, 20]$. Again, PHI2 provides almost exact results whatever the value of β , whereas the asymptotic method, which is quite accurate for large β 's (small values of time) is all the more conservative since β is small.

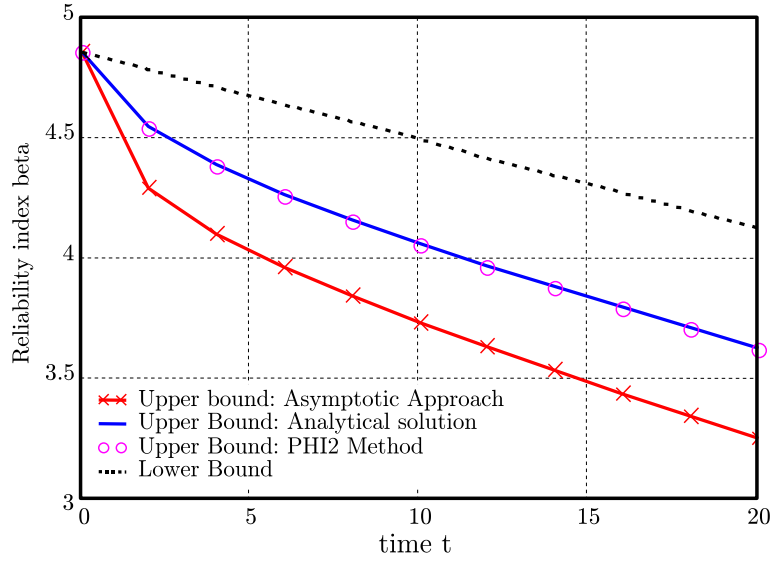


Figure 6.11: Non stationary analytical example - bounds to the reliability index

7.2 Durability of a corroded bending beam

7.2.1 Problem statement

Let us consider a steel bending beam. Its length is $L = 5$ m, its cross-section is rectangular (initial breadth b_0 and height h_0). This beam is submitted to dead loads (denoting by $\rho_{st} = 78.5$ kN/m³ the steel mass density, this load is equal to $p = \rho_{st} b_0 h_0$ (N/m)) as well as a pinpoint load F applied at midspan (see Figure 6.12).

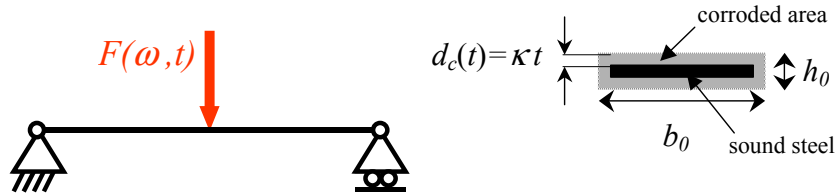


Figure 6.12: Corroded bending beam under midspan load

The bending moment is maximal in this point:

$$M = \frac{Fl}{4} + \frac{\rho_{st} b_0 h_0 L^2}{8} \quad (6.111)$$

Assuming the steel has an elastic perfectly plastic constitutive law, and denoting by σ_e the yield stress, the ultimate bending moment of the rectangular section is:

$$M_{ult} = \frac{b h^2 \sigma_e}{4} \quad (6.112)$$

It is now supposed that the steel beam corrodes in time. Precisely, the corrosion phenomenon is supposed to start at $t = 0$ and to be linear in time, meaning that the corrosion depth d_c all around the section increases linearly in time ($d_c = \kappa t$). Assuming that the corroded areas have lost all mechanical stiffness, the dimensions of the sound cross-section entering Eq.(6.112) at time t writes:

$$b(t) = b_0 - 2\kappa t \quad h(t) = h_0 - 2\kappa t \quad (6.113)$$

Using the above notation, the beam fails at a given point in time if $M(t) > M_{ult}(t)$ (appearance of a plastic hinge in the midspan). The limit state function associated with the failure reads:

$$g(t, \mathbf{X}) = M_{ult}(t) - M(t) = \frac{b(t)h(t)^2\sigma_e}{4} - \left(\frac{Fl}{4} + \frac{\rho_{st}b_0h_0L^2}{8} \right) \quad (6.114)$$

where the dependency of the cross section dimensions with respect to time have been specified in Eq.(6.113). The random input parameters are gathered in Table 6.1.

Table 6.1: Corroded bending beam - random variables and parameters

Parameter	Type of distribution	Mean	Coefficient of variation
Load F	Gaussian	3500 N	20 %
Steel yield stress σ_e	Lognormal	240 MPa	10 %
Initial beam breadth b_0	Lognormal	0.2 m	5 %
Initial beam height h_0	Lognormal	0.04 m	10 %

The time interval under consideration is $[0, 20 \text{ years}]$. The corrosion kinetics is controlled by $\kappa = 0,05 \text{ mm/year}$. The load is either modelled as a random variable (see Table 6.1) or as a Gaussian random process with the same statistics. In the latter case, the autocorrelation coefficient function is of exponential square type, with a correlation length $l = 1 \text{ day}$ (*i.e.* $2.74 \cdot 10^{-3} \text{ year}$). It is emphasized that the time scales corresponding to the loading and to the corrosion are completely different, without introducing any difficulty in the PHI2 solving strategy.

7.2.2 Numerical results

The initial probability of failure is computed by a time-invariant FORM analysis. It yields $\beta = 4.53$, *i.e.* $P_{f,0} = 2.86 \cdot 10^{-6}$. In the case when the load is modelled by a random variable F , the problem under consideration reduces to a *right-boundary* problem (see Section 3.2). The reliability index smoothly decreases in time due to the slow corrosion of the beam section. The reliability index is about 4 at the end of the time interval (Figure 6.13).

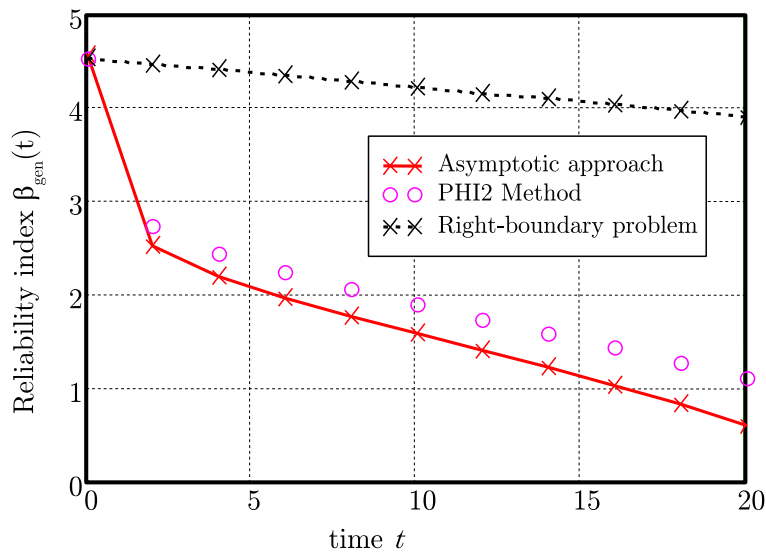


Figure 6.13: Reliability of a corroded beam - Generalized reliability index $\beta_{gen}(t) = -\Phi^{-1}(P_f(0, t))$ related to the upper bound of $P_f(0, t)$

When the loading is modelled by a Gaussian random process, the problem mixes a degradation phenomenon and a time-varying load. The outcrossing approach has to be used. The evolution in time of the outcrossing rate is plotted in Figure 6.14. Although the loading process is stationary, it appears that this outcrossing rate strongly evolves in time (due to the change in the size of the beam section), since its value at $t = 20$ years is about 13 times that at $t = 0$.

The evolution in time of the generalized reliability index $\beta_{gen}(t) = -\Phi^{-1}(P_f(0, t))$ is represented in Figure 6.13. The dashed curve corresponds to the lower bound to $P_f(0, t)$ obtained from Eq.(6.50). The curve marked with circles corresponds to values of the upper bound to $P_f(0, t)$ obtained from Eq.(6.50), where the outcrossing rate has been computed by PHI2 (Eq.(6.102)). The plain curve marked with crosses corresponds to values of the upper bound to $P_f(0, t)$ obtained by asymptotic Laplace integration in time domain. It appears that the reliability index decreases from 4.5 to 1.1. Again the asymptotic method provides slightly conservative results compared to PHI2.

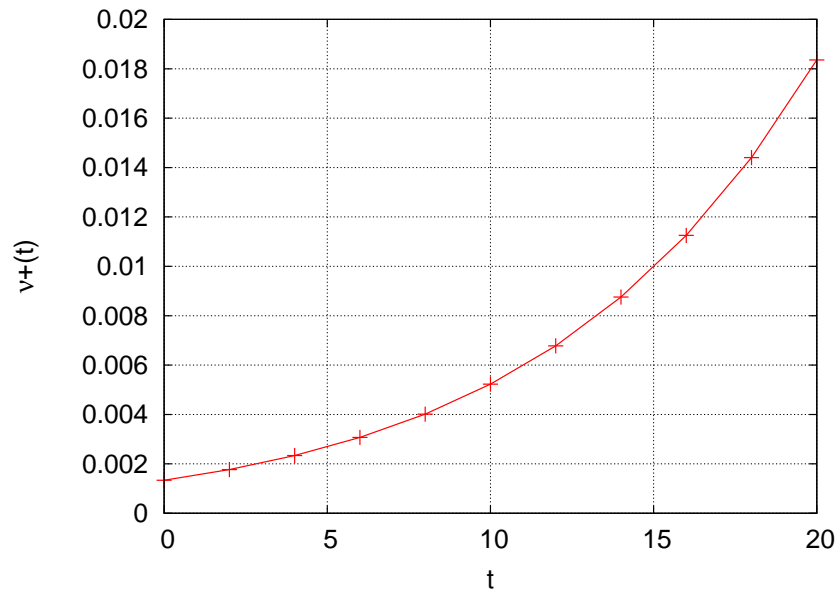


Figure 6.14: Reliability of a corroded beam - Outcrossing rate $\nu^+(t)$

It appears that the evolution in time of the reliability index is drastically different in the second analysis from that obtained for the right-boundary problem ($\beta \approx 1$ instead of $\beta \approx 4$ for $t = 20$ years). As the latter is related to the lower bound $P_f^{LB}(0, t)$ in Eq.(6.50), it is clear from this example that this lower bound is indeed crude.

7.3 General comparison between PHI2 and the asymptotic method

AsM makes use of analytical results for the outcrossing rate as well as asymptotic integration. It requires one *modified* time-invariant FORM analysis to get $P_f(t_1, t_2)$ in the stationary case (the design point is searched both in the standard normal space and in the time interval $[t_1, t_2]$ using a specific algorithm (Abdo and Rackwitz, 1990)). When there is non stationarity in the problem, the first and second order derivatives of the reliability index $\beta(t^*)$ have to be computed by finite difference, which requires additional FORM analyses around point t^* , thus additional computational cost. Globally speaking, the approach is efficient, however at the price of various approximations.

Comparatively, the main advantage of the PHI2 method is the fact that it involves only well-established *time-invariant* reliability tools to carry out the analysis. Any classical reliability software can thus be used, see Schuëller, G.I. (Editor) (2006) for a recent review of existing softwares. Computationally

speaking, obtaining the outcrossing rate $\nu_{\text{PHI2}}^+(t)$ requires two successive FORM analyses. Note that the second one is quite inexpensive, provided that the starting point is selected as the design point of the first FORM analysis.

In stationary cases, one single evaluation of $\nu_{\text{PHI2}}^+(t)$ is necessary. When non stationarity is present, several evaluations of $\nu_{\text{PHI2}}^+(t)$ at different instants are necessary when using PHI2, in order to be able to further carry out the time integration. However, if the non stationarity is not too strong, only few integration points are necessary for an accurate estimate, using *e.g.* a Gaussian quadrature rule. Accordingly, for one single calculation of $P_f(0, T)$, the PHI2 approach may be less efficient than the AsM, since the latter requires in contrast only one (modified) FORM analysis that directly provides the time-integrated result. Note that the asymptotic formulæ could also be used in conjunction with PHI2, provided that the critical point is selected manually: indeed, in contrast with AsM, the PHI2 method does *not* provide the most critical point in time, as defined above.

More generally, engineers are usually interested not only in a single value of the probability of failure, but in its evolution in time, *i.e.* $\{P_f(0, t_i), i = 1, \dots, N \text{ where } t_N = T\}$. In this case, the AsM would require N successive analyses in a parametric study, whereas PHI2 would require $2N$ FORM analyses. As it is possible to use the design point from the FORM analysis at t_i as a starting point for the FORM analysis at t_{i+1} , PHI2 appears in practice less computationally expensive than AsM for this kind of parametric studies, and provides a slightly better accuracy in all cases, as shown in Andrieu-Renaud et al. (2004).

7.4 Conclusion

As observed by Rackwitz (2001), time-variant reliability methods are not yet as mature as the methods used for solving time-invariant problems. One can observe that most of the theoretical results were developed in the 80's, at a time where computer science had not attained its current power. Roughly speaking, the asymptotic method as presented in Section 5 stems from the requirement of pushing the analytical derivations as far as possible, even at the cost of additional assumptions (*e.g.* those used in order to apply Laplace integration in time). It is the belief of the author that the alternative approach initiated by Hagen, Der Kiureghian, and presented in its most recent version under the acronym PHI2, has more potential to emerge in industrial applications, at least for three reasons:

- it is conceptually easier to understand, since it is essentially based on FORM. It practically avoids to refer to the complex formalism of asymptotic integration;
- it may be applied using classical softwares designed for time-invariant reliability analysis;
- it has revealed more accurate (*i.e.* less conservative) than the AsM in various application examples, whilst having a comparable cost.

The packaging of the PHI2 approach in commercial softwares would be of great help for propagating the concepts of time-variant reliability analysis.

8 Space-variant reliability problems

8.1 Introduction

As shown in the previous sections, time-variant reliability problems correspond to cases when the limit state function depends on time either directly or through random processes. Broadly speaking, the

cumulative probability of failure is the probability that there is failure of the system at some (unknown) time instant within a given time interval $[t_1, t_2]$.

Similarly, *space-variant* reliability problems correspond to cases when the limit state function depends on the spatial coordinates describing the geometry of the system, either directly or through random fields. Two kinds of problems may be more specifically addressed, namely:

- the computation of the *spatial cumulative probability of failure*, *i.e.* the probability that failure is attained at some (unknown) point \mathbf{x} of the system, which occupies a domain $\mathcal{B} \in \mathbb{R}^d$, $d = 1, 2, 3$. This problem is briefly reviewed in Section 8.2. It was originally addressed in a pioneering paper by Der Kiureghian and Zhang (1999), where a spatial counterpart of the now so-called PHI2 method (Section 6) was proposed. A direct solution to the space-variant problem using FORM and importance sampling is proposed in Sudret et al. (2005) with a specific application to the reliability of cooling towers.
- the characterization of the *extent of damage*, which is defined as a measure of the subdomain of \mathcal{B} in which the failure criterion is attained. The contribution of the author to this field (Sudret et al., 2007; Sudret, 2008b) is summarized in Section 8.3.

8.2 Space-variant probability of failure

Let us suppose that the system under consideration occupies a volume $\mathcal{B} \subset \mathbb{R}^d$, where $d = 1, 2$ or 3 . The case $d = 1$ corresponds to modelling beam or arch structures, the case $d = 2$ to plate or shell structures. Let us denote by $\mathbf{x} \in \mathcal{B}$ the vector of spatial coordinates. In order to avoid any confusion, the input parameters (resp. the input random vector) of the model and/or the limit state function are denoted by \mathbf{z} (resp. \mathbf{Z}) in this section.

Due to the introduction of spatial variability, the random vector describing the uncertainty in the input should be replaced by M multivariate scalar random fields gathered in a vector $\mathbf{Z}(\mathbf{x})$, the probabilistic description of these fields being yet to be specified. Note however that in practice the following assumptions usually apply:

- the spatial variability of certain components of \mathbf{Z} is negligible. They are accordingly modelled as random variables. As a consequence, only a small number of scalar random fields have to be specified in practice. However, for the sake of simplicity, the most general notation $\mathbf{Z}(\mathbf{x})$ is kept in this section.
- the random field components are often *homogeneous* fields at the scale of the system. For instance, when the degradation of structures is considered, the size of the structure is usually small compared to the scale of fluctuation of the parameters driving the degradation (*e.g.* environmental parameters such as surface chloride or carbon dioxide concentration, etc.).

The time-and-space variant limit state function $g(\mathbf{z}, \mathbf{x}, t)$ that represents mathematically the failure criterion defines in each point $\mathbf{x} \in \mathcal{B}$ at each time instant t a safe domain $\mathcal{D}_s(\mathbf{x}, t)$ and a failure domain $\mathcal{D}_f(\mathbf{x}, t)$:

$$\mathcal{D}_s(\mathbf{x}, t) = \{\mathbf{z} \in \mathbb{R}^M : g(\mathbf{z}, \mathbf{x}, t) > 0\} \quad (6.115)$$

$$\mathcal{D}_f(\mathbf{x}, t) = \{\mathbf{z} \in \mathbb{R}^M : g(\mathbf{z}, \mathbf{x}, t) \leq 0\} \quad (6.116)$$

The *point-in-space* probability of failure at time instant t is defined in each $\mathbf{x} \in \mathcal{B}$ by:

$$P_f(\mathbf{x}, t) = \int_{\mathcal{D}_f(\mathbf{x}, t)} f_{\mathbf{Z}(\mathbf{x})}(\mathbf{z}) d\mathbf{z} = \mathbb{E} [\mathbf{1}_{\mathcal{D}_f(\mathbf{x}, t)}(\mathbf{z})] \quad (6.117)$$

It is computed by freezing \mathbf{x} (*i.e.* replacing the random field $\mathbf{Z}(\mathbf{x})$ by the corresponding random vector) and t , and by applying standard time-invariant reliability methods (MCS, FORM/SORM, etc.). Note that if the random field $\mathbf{Z}(\mathbf{x})$ is *homogeneous* and if the limit state function does not depend directly on \mathbf{x} , then the same reliability problem is posed at whatever the position of the point \mathbf{x} under consideration. Thus the point-in-space probability of failure is *independent* of \mathbf{x} in this case.

The *space-variant* probability of failure is defined for any subdomain $\mathcal{B}' \subset \mathcal{B}$ by (Der Kiureghian and Zhang, 1999):

$$P_f(\mathcal{B}', t) = \mathbb{P}(\exists \mathbf{x} \in \mathcal{B}' \quad , \quad g(\mathbf{Z}(\mathbf{x}), \mathbf{x}, t) \leq 0) = \mathbb{P}\left(\bigcup_{\mathbf{x} \in \mathcal{B}'} \{g(\mathbf{Z}(\mathbf{x}), \mathbf{x}, t) \leq 0\}\right) \quad (6.118)$$

This quantity is the spatial counterpart of the so-called *cumulative* probability of failure in time-variant reliability problems. Note that, similarly to Eq.(6.50), the space variant probability of failure $P_f(\mathcal{B}', t)$ is always greater than the maximum over \mathcal{B}' of the point-in-space probability of failure. It may be in practice dramatically different, *e.g.* 2 or 3 orders of magnitude greater (Sudret et al., 2005).

Der Kiureghian and Zhang (1999) derived an upper bound to the space-variant probability of failure by introducing the mean density of visits to the failure domain (which is the spatial counterpart of the outcrossing rate defined in Eq.(6.51)) and its integration over the domain of interest \mathcal{B}' .

8.3 Extent of damage for degrading structures

8.3.1 A class of degradation models

The degradation of structures in time may be defined in a broad sense as the loss of certain properties as the result of chemical, physical or mechanical processes, or combinations thereof. For instance, concrete structures are submitted to many degradation mechanisms, including rebars corrosion due to chloride ingress or concrete carbonation.

The deterministic models for these degradation mechanisms are usually based on semi-empirical equations that yield a so-called *damage measure* D (considered here as a scalar quantity) as a function of parameters \mathbf{z} and time:

$$D(t) = \mathcal{M}(\mathbf{z}, t) \quad (6.119)$$

Examples of damages measures are:

- crack width, which may be modelled as a function of the corrosion rate of the rebars, the concrete cover, the rebars diameter, etc. (Li et al., 2004),
- loss of rebars diameter, which depends on the corrosion rate and the time for initiation of corrosion, the latter being modelled specifically in case of chloride or carbonation-induced corrosion (Sudret et al., 2006)
- fatigue damage due to repeated application of stress cycles onto the structure (Petryna and Krätzig, 2005).

In order to assess the durability of the structure with respect to a given category of damage, a limit value \bar{D} is usually prescribed (*e.g.* maximal acceptable crack width, etc.). Note that the damage measure in Eq.(6.119) is an *increasing* function of time. Indeed, the degradation phenomena are usually irreversible.

8.3.2 Space-variant reliability of damaged structures

The probabilistic degradation model in Eq.(6.119) is referred to as *zero-dimensional*, in the sense that it does not involve any coordinate system attached to the structure. Thus it implicitly assumes a complete homogeneity of the degradation all over the structure. In other words, for a given realization \mathbf{z}_0 of the input random vector, the *full* structure would be either in the safe state (undamaged) or in the failure state (fully damaged).

This is of course a coarse simplification of the real world. Moreover, it does clearly not allow the analyst to characterize the extent of damage, since the structure is considered either as fully undamaged or undamaged. To overcome this difficulty, the damage model has to be made space-variant, *i.e.* defined in each point $\mathbf{x} \in \mathcal{B}$. Then the limit state function associated to excessive damage reads:

$$g(\mathbf{Z}(\mathbf{x}), t) = \bar{D}(\mathbf{x}, t) - \mathcal{M}(\mathbf{Z}(\mathbf{x}), t) \quad (6.120)$$

where $\bar{D}(\mathbf{x}, t)$ is the maximal admissible damage at position \mathbf{x} and time instant t .

The space-variant probability of failure Eq.(6.118) associated to the limit state function in Eq.(6.120) is used when the structure is supposed to fail as soon as the local criterion is attained in a single point. This may be the case when, for instance, the equivalent stress should not be greater than the yield stress in any point of the structure (Der Kiureghian and Zhang, 1999).

8.3.3 Definition of the extent of damage

When considering the life cycle cost analysis of structures, the above quantity is not relevant. Indeed, the serviceability of degrading structures is rather related to the extent of damage, which appears suited to characterizing the global state of ageing of the structure. The cracked surface of the concrete deck of a bridge, the corroded surface of steel structures, etc. are examples of extent of damage that may be used for the optimization of maintenance policies (Li et al., 2004; Stewart, 2006).

In this report, the extent of damage is defined at each time instant t as the measure of the subdomain of \mathcal{B} in which the local failure criterion is attained:

$$\mathcal{E}(\mathcal{B}, t) = \int_{\mathcal{B}} \mathbf{1}_{\mathcal{D}_f(\mathbf{x}, t)}(\mathbf{x}) d\mathbf{x} = \int_{\mathcal{B}} \mathbf{1}_{g(\mathbf{Z}(\mathbf{x}), \mathbf{x}, t) \leq 0}(\mathbf{x}) d\mathbf{x} \quad (6.121)$$

Note that $\mathcal{E}(\mathcal{B}, t)$ is a scalar random variable since the integral over \mathcal{B} is defined for each realization of the input random field, say $\mathbf{z}(\mathbf{x})$. It is positive-valued, and by definition, it is bounded by the volume of the structure in \mathbb{R}^d denoted by $|\mathcal{B}|$. Moreover, due to the monotonicity of degradation phenomena, each realization of $\mathcal{E}(\mathcal{B}, t)$, say $\epsilon(\mathcal{B}, t)$ is a continuously increasing function of time.

8.3.4 Statistical moments of the extent of damage

Analytical expressions for the mean value and variance of the extent of damage have been derived in Sudret (2008b), based on ideas developed in Koo and Der Kiureghian (2003). The results are now summarized.

By taking the expectation of Eq.(6.121) (*i.e.* with respect to \mathbf{Z}), one gets the following expression for the mean value of the extent of damage:

$$\overline{\mathcal{E}(\mathcal{B}, t)} \equiv \mathbb{E}[\mathcal{E}(\mathcal{B}, t)] = \int_{\mathcal{B}} \mathbb{E}[\mathbf{1}_{g(\mathbf{Z}(\mathbf{x}), \mathbf{x}, t) \leq 0}(\mathbf{x})] d\mathbf{x} \quad (6.122)$$

By comparing the integrand of the above equation with Eq.(6.117), one gets:

$$\overline{\mathcal{E}(\mathcal{B}, t)} = \int_{\mathcal{B}} P_f(\mathbf{x}, t) d\mathbf{x} \quad (6.123)$$

In case of homogeneous input random fields, this integrand is independent of \mathbf{x} , as explained above. Thus:

$$\overline{\mathcal{E}(\mathcal{B}, t)} = P_f(\mathbf{x}_0, t) \cdot |\mathcal{B}| \quad (\text{Homogeneous case}) \quad (6.124)$$

where the point-in-space probability of failure is computed at any point $\mathbf{x}_0 \in \mathcal{B}$.

The above equation has the following interpretation: the proportion of the structure where the damage criterion is attained (*i.e.* $\overline{\mathcal{E}(\mathcal{B}, t)}/|\mathcal{B}|$) is, in the mean, equal to the point-in-space probability of failure. This remark has two important consequences:

- it is not necessary to introduce the complex formalism of random fields when one is interested only in the mean value of $\mathcal{E}(\mathcal{B}, t)$. Only the description of the input random *variables* gathered in vector \mathbf{Z} is required.
- the mean proportion of the structure that is damaged is independent of the correlation structure of the input random field $\mathbf{Z}(\mathbf{x})$, if the spatial variability is modelled. This is a valuable result, since the determination of the correlation structure is difficult and hardly done in practice, due to the lack of data (the auto-correlation functions and their parameters being often chosen from “expert judgment”, as in Li et al. (2004); Stewart (2006)).

The variance of the extent of damage can also be derived. By definition, this quantity reads:

$$\text{Var}[\mathcal{E}(\mathcal{B}, t)] = \text{E}[\mathcal{E}^2(\mathcal{B}, t)] - \overline{\mathcal{E}(\mathcal{B}, t)}^2 \quad (6.125)$$

From the definition in Eq.(6.121) one can write:

$$\begin{aligned} \mathcal{E}^2(\mathcal{B}, t) &= \left(\int_{\mathcal{B}} \mathbf{1}_{g(\mathbf{Z}(\mathbf{x}), t) \leq 0}(\mathbf{x}) d\mathbf{x} \right) \cdot \left(\int_{\mathcal{B}} \mathbf{1}_{g(\mathbf{Z}(\mathbf{x}), t) \leq 0}(\mathbf{x}) d\mathbf{x} \right) \\ &= \int_{\mathcal{B}} \int_{\mathcal{B}} \mathbf{1}_{g(\mathbf{Z}(\mathbf{x}_1), t) \leq 0}(\mathbf{x}_1) \cdot \mathbf{1}_{g(\mathbf{Z}(\mathbf{x}_2), t) \leq 0}(\mathbf{x}_2) d\mathbf{x}_1 d\mathbf{x}_2 \end{aligned} \quad (6.126)$$

The integrand is equal to one if and only if the limit state function takes negative values at both locations \mathbf{x}_1 and \mathbf{x}_2 . Thus (6.126) may be rewritten as:

$$\mathcal{E}^2(\mathcal{B}, t) = \int_{\mathcal{B}} \int_{\mathcal{B}} \mathbf{1}_{g(\mathbf{Z}(\mathbf{x}_1), t) \leq 0 \cap g(\mathbf{Z}(\mathbf{x}_2), t) \leq 0}(\mathbf{x}_1, \mathbf{x}_2) d\mathbf{x}_1 d\mathbf{x}_2 \quad (6.127)$$

Hence:

$$\text{E}[\mathcal{E}^2(\mathcal{B}, t)] = \int_{\mathcal{B}} \int_{\mathcal{B}} \mathbb{P}(g(\mathbf{Z}(\mathbf{x}_1), t) \leq 0 \cap g(\mathbf{Z}(\mathbf{x}_2), t) \leq 0) d\mathbf{x}_1 d\mathbf{x}_2 \quad (6.128)$$

Here again, the assumption of homogeneity allows to simplify the above equation. Indeed, the integrand in Eq.(6.128) depends only on $|\mathbf{x}_1 - \mathbf{x}_2|$ in this case, meaning that it is an even function of $(x_1^j - x_2^j)$, $j = 1, \dots, d$. One can prove that the above double integral may be reduced to a single integral (Sudret, 2008b). For the sake of clarity, results are reported here separately for $d = 1$ and $d = 2$.

- For a beam of length L ($d = 1$, $|\mathcal{B}| = L$), the variance of the extent of damage is:

$$\text{Var}[\mathcal{E}(\mathcal{B}, t)] = L^2 \int_0^1 \mathbb{P}(g(\mathbf{Z}(0), t) \leq 0 \cap g(\mathbf{Z}(Lu), t) \leq 0) (2 - 2u) du - \overline{\mathcal{E}(\mathcal{B}, t)}^2 \quad (6.129)$$

- For a rectangular plate of dimensions (L_1, L_2) , the variance of the extent of damage is:

$$\begin{aligned} \text{Var} [\mathcal{E}(\mathcal{B}, t)] = & L_1^2 L_2^2 \int_0^1 \int_0^1 \mathbb{P}(g(\mathbf{Z}(0, 0), t) \leq 0 \cap g(\mathbf{Z}(L_1 u, L_2 v), t) \leq 0) \dots \\ & \dots (2 - 2u)(2 - 2v) du dv - \overline{\mathcal{E}(\mathcal{B}, t)}^2 \end{aligned} \quad (6.130)$$

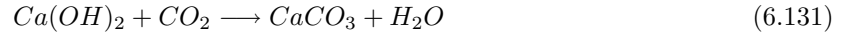
The integrals in Eqs.(6.129),(6.130) are rather easy to evaluate since both the integration domain and the integrands are bounded. A typical Gaussian quadrature rule (Abramowitz and Stegun, 1970) may be used for this purpose.

8.4 Application example

In this section, a RC beam submitted to carbonation-induced rebars corrosion is considered for the sake of illustration. A simple degradation model including the kinetics of concrete carbonation and rebars corrosion is first described. Then the mean and variance of the extent of damage are computed from Eqs.(6.124)-(6.129) and compared to Monte Carlo simulation results. These results are taken from Sudret (2008b).

8.4.1 Point-in-space model of concrete carbonation

Concrete carbonation is a complex physico-chemical process that includes the diffusion of CO_2 into the gas phase of the concrete pores and its reaction with the calcium hydroxyl $Ca(OH)_2$. The latter can be simplified into:



As the high pH of uncarbonated concrete is mainly due to the presence of $Ca(OH)_2$, it is clear that the consumption of this species will lead to a pH drop, which can attain a value of 9 when the reaction is completed. In this environment, the oxide layer that protected the reinforcement bars is attacked and corrosion starts. The corrosion products tend to expand into the pores of concrete, developing tensile stresses which eventually lead to cracking (Liu and Weyers, 1998; Thoft-Christensen, 2003; Bhargava et al., 2006).

In practice, CO_2 penetrates into the concrete mass by diffusion from the surface layer. Thus a carbonation front appears that moves into the structure. A model for computing the carbonation depth x_c is proposed by the CEB Task Group 5.1 & 5.2 (1997). The simplified version retained in the present paper reads:

$$x_c(t) = \sqrt{\frac{2 C_0 D_{CO_2} t}{a}} \quad (6.132)$$

where D_{CO_2} is the coefficient of diffusion of carbon dioxide in dry concrete, C_0 is the carbon dioxide concentration in the surrounding air and a is the binding capacity, *i.e.* the amount of carbon dioxide necessary for a complete carbonation of a concrete volume. It is supposed that corrosion immediately starts when carbonation has attained the rebars. Denoting by e the concrete cover, the time necessary for corrosion to start, called *initiation time*, reads:

$$T_{init} = \frac{a e^2}{2 C_0 D_{CO_2}} \quad (6.133)$$

If *generalized* corrosion is considered, the loss of metal due to corrosion is approximately uniform over the whole surface. In this case, Faraday's law indicates that a unit corrosion current density (or corrosion rate) corresponds to a uniform corrosion penetration of $\kappa = 11, 6 \mu\text{m}/\text{year}$. If a constant annual corrosion rate is supposed, the expression of the rebars diameter as a function of time eventually reads:

$$\phi(t) = \begin{cases} \phi_0 & \text{if } t \leq T_{init} \\ \max[\phi_0 - 2 i_{corr} \kappa (t - T_{init}), 0] & \text{if } t > T_{init} \end{cases} \quad (6.134)$$

This evolution of the rebars' diameter is sketched in Figure 6.15 together with the expected damage at each step.

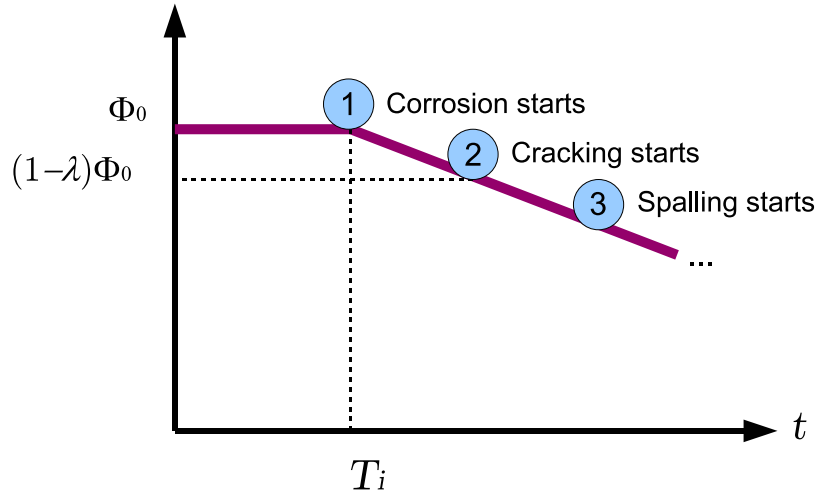


Figure 6.15: Evolution in time of the rebars diameter and associated state of damage

From experimental evidence (Alonso et al., 1998; Broomfield, 1997), it is possible to associate a value λ (representing the relative loss of rebar's diameter) to a given state of damage (*i.e.* crack initiation, severe cracking, spalling, etc.). For instance, a value of $\lambda = 0.5 - 1\%$ is consistent with the apparition of cracks.

8.4.2 Probabilistic problem statement

Point-in-space failure criterion The parameters appearing in Eqs.(6.133),(6.134) are uncertain in nature. Thus they are represented by random variables gathered in a random vector \mathbf{Z} :

$$\mathbf{Z} = \{D_{CO_2}, C_0, a, e, \phi_0, i_{corr}\}^T \quad (6.135)$$

The damage criterion is defined at a given time instant by the fact that the residual rebar's diameter (Eq.(6.134)) becomes smaller than a prescribed fraction $(1 - \lambda)$ of its initial value:

$$g(\mathbf{Z}, t) = \phi(t) - (1 - \lambda) \phi_0 \quad (6.136)$$

After some basic algebra, this reduces to:

$$g(\mathbf{Z}, t) = \lambda \phi_0 - 2 i_{corr} \kappa \left(t - \frac{a e^2}{2 C_0 D_{CO_2}} \right) \quad (6.137)$$

Probabilistic model of the input parameters The RC beam under consideration (of length $L = 10 \text{ m}$) is reinforced by a single longitudinal reinforcing bar whose initial diameter is modelled by a lognormal random variable ϕ_0 . The concrete cover $e(x)$ is a univariate homogeneous lognormal random field, obtained by exponentiation of a Gaussian random field, whose properties are given below. This allows to model the imperfections in placing the rebar into the falsework.

The parameters $\{C_0, a\}$ are modelled by lognormal random variables. The coefficient of diffusion D_{CO_2} is modelled as a homogeneous lognormal random field. The corrosion current density $i_{corr}(x)$ is supposed to be inversely proportional to the concrete cover (Vu and Stewart, 2005):

$$i_{corr}(x) = i_{corr}^0 \frac{e_0}{e(x)} \quad (6.138)$$

In this equation, $e_0 = 50$ mm is the mean concrete cover and i_{corr}^0 is a lognormal random variable. The above expression has the following interpretation: variable i_{corr}^0 models the overall uncertainty on the corrosion rate, whereas its spatial variability is perfectly correlated to that of the concrete cover. The mean value of the corrosion rate is $2.08 \mu A/cm^2$. The parameters describing these six input quantities (2 random fields and 4 random variables) are gathered in Table 6.2.

Table 6.2: Extent of damage in a RC beam - Probabilistic input data

Parameter	Type of PDF	Mean value	Coef. Var.	A.c.f. [†]
Rebars diameter ϕ_0	lognormal	10 mm	10 %	–
Diffusion coefficient D_{CO_2}	lognormal	$5 \cdot 10^{-8}$ m ² /s	30 %	$\rho_D(x_1, x_2)$
Surface concentration C_0	lognormal	$6.2 \cdot 10^{-4}$ kg/m ³	30 %	–
Binding capacity a	lognormal	80 kg/m ³	30 %	–
Nominal corrosion rate $i_{corr}^0(x)$	lognormal	1 $\mu A/cm^2$	25 %	–
Concrete cover $e(s)$	lognormal	50 mm	20 %	$\rho_e(x_1, x_2)$

[†] Autocorrelation coefficient function of the underlying Gaussian field

$$\rho_D(x_1, x_2) = e^{-\pi(x_1-x_2)^2/\theta_D^2}, \theta_D = 2 \text{ m}; \rho_e(x_1, x_2) = e^{-\pi(x_1-x_2)^2/\theta_e^2}, \theta_e = 2 \text{ m}$$

8.4.3 Mean value and standard deviation of the extent of damage

The mean value of the extent of damage is computed by three approaches and plotted in Figure 6.16, namely:

- Eq.(6.124), where the point-in-space probability of failure, obtained by freezing the spatial coordinate x (*i.e.* replacing the random fields $e(x)$ and $D_{CO_2}(x)$ by lognormal random variables) is computed by FORM analysis (∇ -curve);
- Eq.(6.124), where the point-in-space probability of failure is obtained by Monte Carlo simulation using 100,000 samples (Δ -curve);
- A Monte Carlo simulation method based on the discretization of the input random fields and used as a reference result, see Sudret (2008b) for details (continuous curve). The EOLE discretization of both input fields was carried out using a regular grid consisting in $N = 81$ points over $[0, 10]$ m]. A number $r = 16$ points was retained in the spectral decomposition (Eq.(2.83)). This allows one to get a maximal relative discretization error on the field variance of 0.1 %. A total number of 10,000 spatial realizations of the limit state function was used.

An excellent agreement between the various approaches is observed. The maximal discrepancy between FORM and the field discretization approach is less than 5%, and less than 2% for $t \geq 40$ years.

The standard deviation of the extent of damage is computed by three approaches as well:

- Eq.(6.129) where the system reliability problem under the integral is solved by FORM;
- Eq.(6.129) where this problem is solved by MCS (100,000 samples were used);
- a Monte Carlo approach based on random field discretizations.

The standard deviation of the extent of damage obtained by the three approaches is plotted in Figure 6.17. Here again, the agreement between the various approaches is excellent. The maximal discrepancy between the analytical and the field discretization approaches is less than 9%, and about 0.2% for $t \geq 40$ years. Note that the coefficient of variation of the extent of damage is rather large (more than 300% in the early ages down to about 120% for $t = 60$ years).

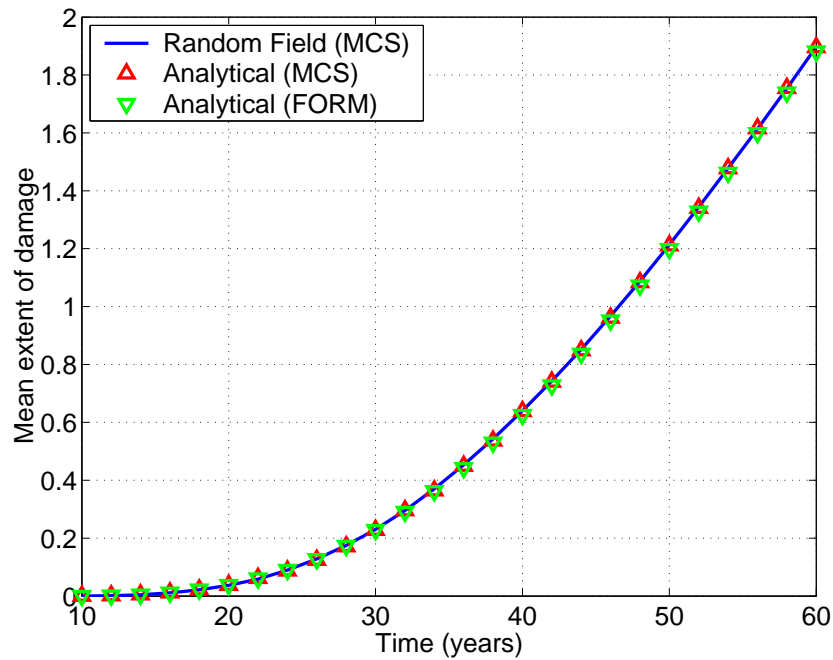


Figure 6.16: Evolution in time of the mean extent of damage

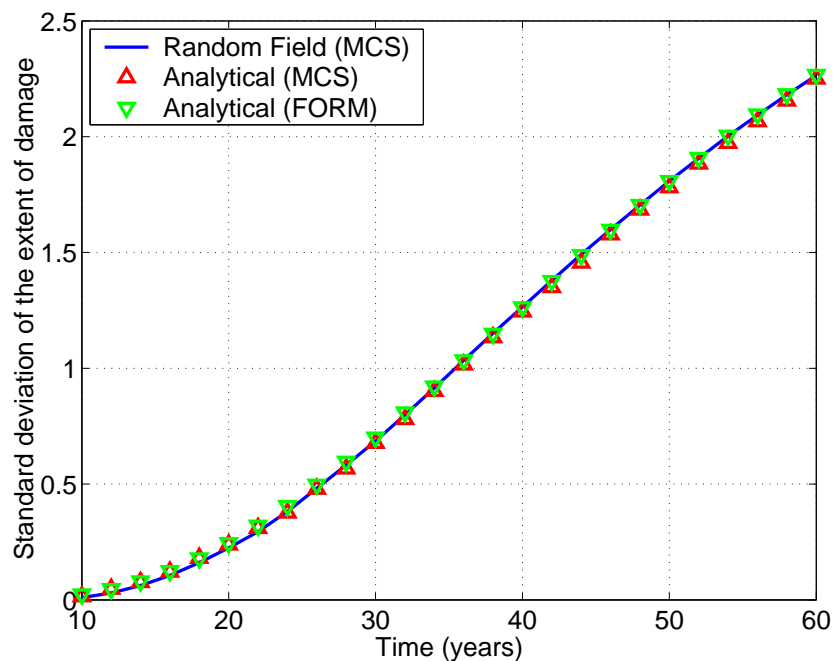


Figure 6.17: Evolution in time of the standard deviation of the extent of damage

The various algorithms to compute the mean and standard deviation of the extent of damage are implemented in MathCad. In terms of efficiency, the random field discretization approach requires about 5 hours on a standard PC (Pentium M processor at 1.6 GHz, 512MB RAM) to get the curves in Figures 6.16-6.17, whereas the analytical approach (FORM and MCS) requires less than 2 minutes.

8.4.4 Histogram of the extent of damage

From the Monte Carlo simulations of the extent of damage, it is possible to plot histograms of the extent of damage, see Figure 6.18. It is first observed that there is always a non zero number of spatial realizations of the limit state function that are strictly positive, meaning that the associated realization of the extent of damage $\epsilon([0, L], t)$ is exactly equal to zero. In other words, there is a probability spike on zero. This spike is all the greater since the time instant is small (the spikes in the figure are not on scale). Similarly, when time increases (*e.g.* $t = 60$ years), another spike appears for $\epsilon([0, L], t) = L$. This represents cases where the beam is fully damaged.

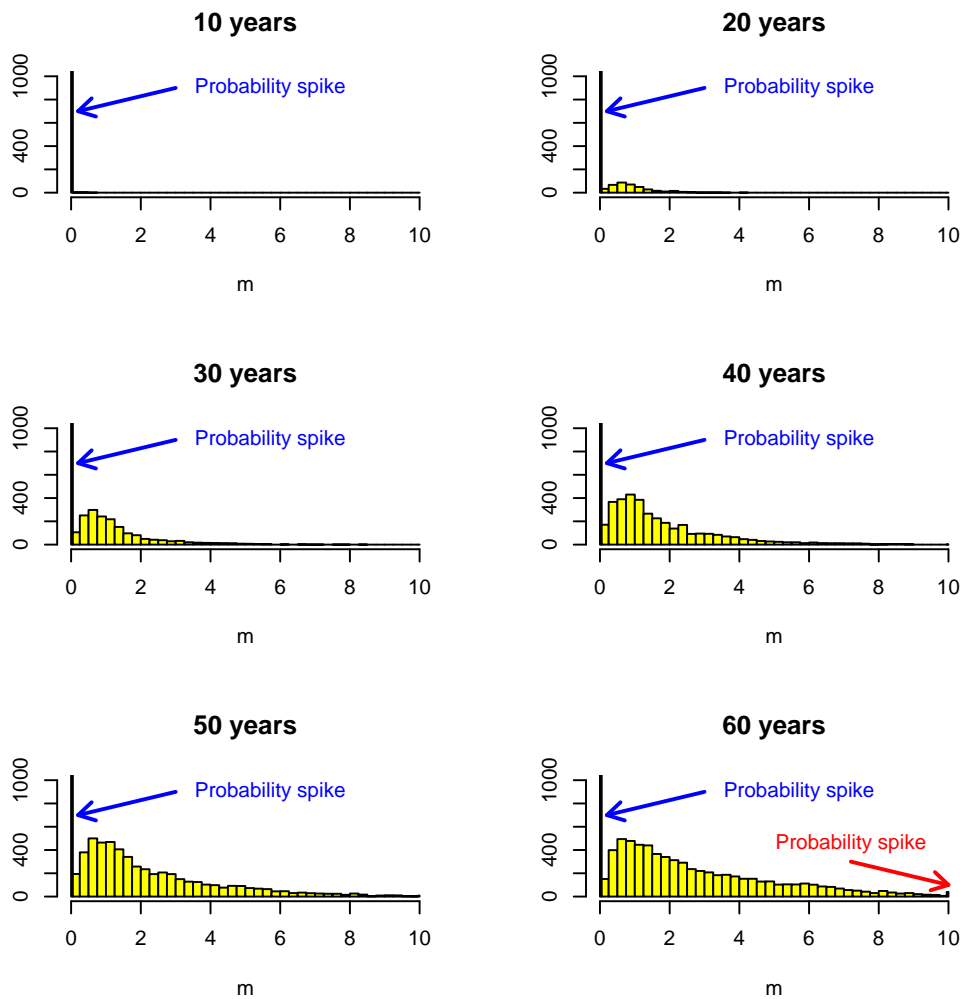


Figure 6.18: Histogram of the extent of damage (m) at various time instants (10,000 samples)

Additional results concerning the computation of the probability spikes at the left boundary (probability of no corrosion) and the influence of the autocorrelation coefficient function (*i.e.* type and correlation length) of the input random fields are given in Sudret (2008b). It is shown in particular that the standard deviation of the extent of damage is rather insensitive to the latter, which is a valuable result since the shape and scale parameters of the autocorrelation coefficient functions are difficult to infer in practice due to lack of data.

8.5 Conclusion

Space-variant reliability problems have emerged in the last few years in various domains of mechanical and civil engineering. Apart from a pioneering paper by Der Kiureghian and Zhang (1999), not much work has been devoted to the theoretical aspects of the computation of space-variant probabilities of failure.

From the viewpoint of applications, space-variant reliability has been recently considered in the concrete deterioration of structures by Li et al. (2004); Stewart (2004); Vu and Stewart (2005); Darmawan and Stewart (2007); Stewart and Al-Harthy (2008), where Monte-Carlo simulation is used for the practical computation. The use of the extent of damage to optimize maintenance policies has been more specifically addressed in Li (2004); Li et al. (2004); Stewart et al. (2006); Stewart and Mullard (2007).

As far as the extent of damage is considered, the analytical expressions presented above have been originally presented in Sudret et al. (2006, 2007) and more rigorously derived and extended in Sudret (2008b). Note that the distribution of the random variable $\mathcal{E}(\mathcal{B}, t)$ (Eq.(6.121)) cannot be described only by its mean and standard deviation. As shown in the application example, it is a *mixed* random variable obtained as the sum of two probability peaks at the bounds of its support, *e.g.* $\mathbf{e}(\mathcal{B}, t) = 0$ (resp. $\mathbf{e}(\mathcal{B}, t) = |\mathcal{B}|$), and a continuous distribution in between. This should be accounted for when the random variable $\mathcal{E}(\mathcal{B}, t)$ itself enters a reliability problem, for instance for maintenance issues.

9 Conclusion

This chapter has presented a short survey of methods for solving time and space-variant reliability problems. After introducing the basics of random processes, the general formulation of *time-variant* reliability problems has been given. The important case of so-called *right-boundary problems* was first addressed. It corresponds to applications where time enters the problem definition through deterioration of material properties, which is associated with a monotonic *decreasing* kinetics of the resistance quantities. This class of problems can be reduced to time-invariant problems if it is possible to show that the limit state function is monotonically decreasing in time whatever the realizations of the random variables.

In more general cases when loading is modelled using random processes, the *outcrossing approach* has to be used. The central quantity to be computed is the outcrossing rate $\nu^+(t)$, which gives by integration over $[t_1, t_2]$ the mean number of outcrossings $E[N^+(t_1, t_2)]$.

The computation of $\nu^+(t)$ and $E[N^+(t_1, t_2)]$ has been presented for Gaussian differentiable processes. Additional results for rectangular wave renewal processes can be found in Sudret (2006b). The case of problems involving random variables together with random processes is addressed using asymptotic integration, which is equivalent to applying SORM. In non stationary cases, the time integration is also carried out asymptotically using Laplace integration.

The PHI2 method is an alternative method that allows the analyst to use any time-invariant reliability software at hand. It is based on analytical derivations for the outcrossing rate. The numerical examples show that the evolution of the outcrossing rate obtained by PHI2 tends to be more accurate than that obtained by AsM (which is however often conservative).

Finally, space-variant reliability problems and the associated extent of damage have been introduced. It is observed that this field is not yet as mature as that of time-variant reliability. However, it may become more and more important in the future especially in the life cycle cost analysis of structures.

Chapter 7

Durability of industrial systems

1 Introduction

As mentioned in the first chapter, the research work reported in this thesis has been carried out in an industrial context at the Research and Development Division of EDF. For this reason, the author was constantly in contact with many applications in civil and mechanical engineering that were submitted by his colleagues. Interestingly, these practical problems have often raised challenging research problems that required advanced theoretical formulations.

Three application examples are reported in this chapter in order to illustrate this valuable interaction between practical uncertainty propagation problems and theoretical formulations.

The first example deals with fatigue analysis. The natural scatter that is observed in the fatigue behaviour of structures is recognized by the engineers but not often taken into account through probabilistic models. The probabilistic framework presented in Section 2 aims at giving a consistent model for the various uncertainties appearing in fatigue design.

The second example deals with the reliability of cooling towers, which are huge concrete structures used in nuclear power plants as heat exchangers. This example allows to illustrate some aspects of time- and space-variant reliability problems that were presented from a theoretical point of view in Chapter 6.

The third example deals with the crack propagation in a pipe structure submitted to internal pressure and axial tensile stress. It is a classical reliability problem which is solved here by means of polynomial chaos expansions. Various non intrusive methods presented in Chapter 4 are coupled with a non linear finite element model of the cracked pipe.

2 Thermal fatigue problems

2.1 Introduction

A number of components in nuclear power plants are subject to thermal and mechanical loading cycles. The assessment of these components with respect to low cycle and high cycle fatigue is of great importance for the global safety, efficiency and availability of the power plant. The French assessment rules, which are codified in a design code called RCC-M (AFCEN, 2000) are fully deterministic in nature. However, it is well known that various sources of uncertainty affect the behaviour of structures subject to fatigue, namely:

- the scatter of the results observed when fatigue tests are carried out onto a set of identical specimens (same material, same loading conditions, same environment, etc.), see Shen et al. (1996);
- the size, surface finish and environmental effects (temperature, oxygen content in the pressurized water reactor (PWR) environment), which globally reduce the fatigue life time of a real structure (Collectif, 1998; Chopra and Shack, 1998; Rosinski, 2001). In the codified design, the so-called margin factors are applied to the “best-fit” experimental curve in order to obtain the design fatigue curve, *i.e.* to compute the number-of-cycles-to-failure of a structure in its operating conditions from the number-of-cycles-to-failure of a specimen tested in the laboratory. These factors denoted hereinafter by γ^N, γ^S are respectively applied to reducing the number of cycles or increasing the applied stress, whichever is more conservative. They allow one to take into account inclusively the scatter of the specimen test data as well as the size, surface finish and environmental effects.
- the imperfection of the mechanical model that yields the stress cycles amplitudes. The model may be quite accurate *per se* while the input parameters (*e.g.* material properties) may not be well known. Furthermore, in the specific case of fatigue due to thermal fluctuations in PWR circuits, the loading itself may not be well known.
- the uncertainty in evaluating the cumulated damage, using for instance Miner’s rule of linear damage accumulation.

In this context, it appears interesting to introduce explicitly the uncertainties in fatigue analysis through a rigorous probabilistic modelling of all uncertain input quantities, and study their influence onto the output (*e.g.* the cumulated damage D). In the probabilistic context, this cumulated damage indeed becomes a random variable, which depends on all input random variables and can be characterized in terms of mean value, standard deviation, etc. The latter corresponds to the scattering of life time of identical components that could be observed in a fleet of identical pressurized water reactors.

From the point of view of reliability analysis, it will be possible to compute the probability of failure with respect to crack initiation, *i.e.* the probability that the cumulated damage is greater than 1 for a prescribed operating duration.

The deterministic framework used for fatigue assessment of nuclear components is first recalled in a simplified manner. The various sources of uncertainty that have been mentioned above are then listed and a suitable probabilistic model is proposed for each of them. Finally an application example concerning the probabilistic fatigue assessment of a pipe is presented. This section is much inspired from Sudret and Guédé (2005); Guédé et al. (2007), which are synthesis papers based on the Ph.D thesis of Guédé (2005).

2.2 Deterministic framework for fatigue assessment

The assessment of structural components such as pipes against thermal fatigue requires the following input, according to the French nuclear design code RCC-M (AFCEN, 2000):

- **Description of the loading applied to the component:** the temperature history applied onto the inner wall of the pipe is given *e.g.* from a thermo-hydraulic calculation, experimental data obtained from scaled models or *in situ* measurements.
- **Mechanical model:** it allows to compute the evolution in time of the stresses in each point of the component. The input parameters are the geometry (*e.g.* pipe radius and thickness), the material properties (*e.g.* Young’s modulus, Poisson’s ratio, coefficient of thermal expansion) and fluid/structure boundary conditions (*e.g.* heat transfer coefficient). Analytical or numerical (*e.g.* finite element) models can be used. An equivalent stress $\sigma_{eq}(t)$ is then obtained using for instance the Tresca criterion.

- **Extraction and counting of the cycles:** from the computed evolution $\sigma_{eq}(t)$, stress cycles are extracted using the Rainflow method (Amzallag et al., 1994). A sequence of stress amplitudes S_i , $i = 1, \dots, N_c$ can be determined on a time interval (each stress amplitude S_i corresponds to half of the difference between the consecutive peaks obtained by the Rainflow method).
- **Choice of a design curve:** as described in the introduction, the design curve $N_d(S)$ is obtained from experimental results that provide the best-fit specimen curve $N_{bf}(S)$, and from margin factors ($\gamma^N = 20$ on number of cycles, $\gamma^S = 2$ on stress, whichever is more conservative):

$$N_d(S) = \min(N_{bf}(S)/\gamma_N, N_{bf}(\gamma^S S)) \quad (7.1)$$

- **Computation of the cumulated damage:** the Miner's rule (linear damage accumulation) is used in order to estimate the fatigue damage. It postulates that the elementary damage d_i associated with one cycle of amplitude S_i is computed by $d_i = 1/N_d(S_i)$ (where $N_d(S)$ is the design curve) and that the total damage is obtained by summation. This leads to compute the cumulated damage (also called usage factor) D by:

$$D = \sum_{i=1}^N d_i = \sum_{i=1}^N 1/N_d(S_i) \quad (7.2)$$

This usage factor is then compared to 1: if it is smaller than 1, the component is supposed to be safely designed. If it is greater than 1, fatigue cracks may appear onto the component. Moreover, if D is the usage factor associated with a sequence of cycles which is repeated periodically, the fatigue life T_d of the component may be computed as $T_d = 1/D$ and is interpreted as the number of (periodic) sequences of cycles that the component may undergo before crack initiation. The flow chart summarizing the deterministic design procedure is given in Figure 7.1.

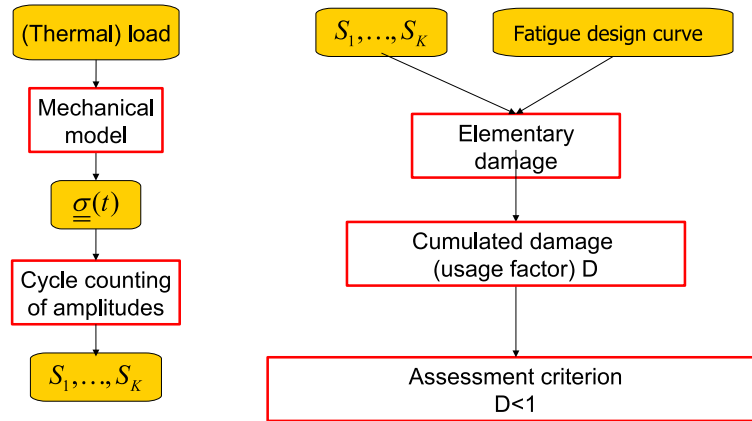


Figure 7.1: Fatigue – Flow chart of the deterministic assessment

2.3 Probabilistic representation of the input data and the cumulated damage

2.3.1 Thermal loading

The temperature of the fluid at the inner wall of the pipe may be represented either by:

- a deterministic signal obtained from measurements (*in situ* or from scale models) or a thermo-hydraulic computation (Benhamadouche et al., 2003);

- a random process, which is supposed Gaussian and stationary due to the periodicity in the circuit operating. Generally speaking, this process may be indexed on both time and space coordinates. In order to be handled in the calculation, the process has to be discretized either in the time domain (generation of trajectories) or in the frequency domain (using the power spectral density function).

2.3.2 Mechanical model

The mechanical model allows to compute the history of the stress tensor from the geometry, material properties and loading parameters. Its complexity can vary from low (*e.g.* analytical one-dimensional formulation) to high (*e.g.* three-dimensional non linear finite element analysis).

From the probabilistic point of view, all the input parameters of the code can be considered as random variables, including geometrical characteristics (*e.g.* pipe radius and thickness), material properties (*e.g.* Young's modulus, Poisson's ratio, thermal expansion coefficient) and fluid/structure boundary conditions (*e.g.* heat transfer coefficient). Each random variable is defined by its probability density function, which may be inferred using the methods developed in Chapters 2 and 5.

2.3.3 Scatter of the fatigue test results

Natural approach The number-of-cycles-to-failure observed in a set of specimens made of the same material tested in the same experimental conditions (same alternate stress, strain ratio, etc.) shows a significant scatter. This scatter is all the larger since the alternate stress S is close to the endurance limit. The number-of-cycles-to-failure at a given alternate stress S is thus represented by a random variable $N_S(\omega)$. The statistical analysis used in order to characterize properly this random variable has been originally presented in Sudret et al. (2003) under three different assumptions. The statistical model which revealed the most accurate is summarized in the sequel.

For each stress amplitude S , the number-of-cycles-to-failure $N_S(\omega)$ is supposed to follow a *lognormal* distribution, whose mean and standard deviation are dependent on S . Moreover, it is assumed that these random variables $N_S(\omega)$ are perfectly correlated whatever the stress level S . This corresponds to the heuristic assumption that a given sample (which is a *realization* of the material in the probabilistic vocabulary) is globally "well" or "poorly" resisting to fatigue crack initiation whatever the applied stress. Unfortunately this assumption cannot be verified since only one test at a given stress level can be carried out (then the sample is broken and cannot be tested at another stress level). These assumptions lead to write:

$$\log N_S(\omega) = \lambda(S) + \sigma(S) \xi(\omega) \quad (7.3)$$

where $\lambda(S)$ and $\sigma(S)$ are the mean and standard deviation of $\log N_S$ and ξ is a standard normal random variable. The model for the median curve is based on the work by Langer (1962). The observation of data leads to consider the standard deviation $\sigma(S)$ as proportional to the median curve (heteroscedastic assumption). Thus:

$$\lambda(S) = A \log(S - S_D) + B \quad \sigma(S) = \delta \lambda(S) \quad (7.4)$$

The probabilistic S - N curve is thus fully characterized by four parameters, namely A, B, S_D, δ , which are estimated using the maximum likelihood method. Due to Eqs.(7.3),(7.4), the median S - N curve, denoted by $N_{50\%}(S)$ has the following expression:

$$N_{50\%}(S) = e^B (S - S_D)^A \quad (7.5)$$

ESOPE approach The above approach has been slightly modified by Perrin et al. (2005) in order to take into account the censored data, *i.e.* the samples that have not failed before the maximum number-of-cycles under consideration. In the same communication, it is also compared to the so-called ESOPE method, which is a French codified approach for establishing probabilistic S - N curves (AFNOR, 1990).

In the ESOPE method, the CDF of the number-of-cycles-to-failure, say $F_{N_S}(S, N)$, is supposed to vary as the Gaussian CDF as follows:

$$F_{N_S}(S, N) = \Phi\left(\frac{S - \mu(N)}{\sigma}\right) \quad (7.6)$$

where σ is a scattering parameter and $\mu(N)$ has to be given a parametric expression. It is seen that, in this approach, iso-probabilistic S - N curve (*i.e.* the curves $N_p(S)$ corresponding to a given quantile p such that $\mathbb{P}(N_S(\omega) \leq N_p(S)) = p$) are implicitly defined by:

$$p = \Phi\left(\frac{S - \mu(N)}{\sigma}\right) \quad (7.7)$$

Hence the relationship between the median curve ($p = 0$) and the (yet-to-be-defined) expression for $\mu(\cdot)$ in the ESOPE approach:

$$N_{50\%}(S) \quad : \quad S = \mu(N_{50\%}(S)) \quad (7.8)$$

In order to be consistent with Eq.(7.5), the expression for $\mu(N)$ is chosen by solving for S in this very equation:

$$\mu(N) \equiv S_D + e^{-B/A} N^{1/A} \quad (7.9)$$

Again, the parameters A, B, S_D, σ are obtained by the maximum likelihood method.

The two approaches have been compared using a private data base comprising 153 specimens of austenitic stainless steel tested at room temperature. As far as the median S - N curves are compared, the approach by Guédé *et al.* and the ESOPE approach provide very similar results. However, goodness-of-fit tests applied to each estimation show that the formulation in Eqs.(7.3)-(7.4) provides the best fit of the aleatoric uncertainty of N_S , the assumptions in the ESOPE formulation being rejected by the various tests. Note that the comparison has been carried out on a specific type of material and that the conclusion on the efficiency of the ESOPE method may not be general. It would be interesting to apply both approaches to other types of material in further investigations.

Complementary results The above approach by Guédé *et al.* may be improved by considering that S_D is not only a parameter of the statistical model, but also a physically meaningful quantity, *i.e.* the endurance limit of the material. In this respect, S_D can be thought as dependent on the sample under consideration and thus be modelled as a random variable. Following the assumptions in Pascual and Meeker (1997), it is supposed that this variable has a lognormal distribution, whose mean and standard deviation have to be estimated from the sample set:

$$S_D = e^V \quad ; \quad V \sim \mathcal{N}(m_V, \sigma_V) \quad (7.10)$$

The probabilistic model for the S - N curve thus depends on the five parameters $A, B, \delta, m_V, \sigma_V$. This approach is investigated in details by Perrin et al. (2007b) and compared to the previous results by Guédé *et al.* on the same data set. As expected, the incidence of the randomness of the endurance limit appears negligible in the Low Cycle Fatigue (LCF) domain (large amplitude S) but may be significant in the High Cycle Fatigue (HCF) domain.

2.3.4 Specimen-to-structure passage factors

As described above, each of the design margin factors ($\gamma^N = 20$; $\gamma^S = 2$) can be decomposed into a product of two sub-factors.

$$\begin{aligned}\gamma^N &= \gamma_{scat}^N \cdot \gamma_{passage}^N \\ \gamma^S &= \gamma_{scat}^S \cdot \gamma_{passage}^S\end{aligned}\quad (7.11)$$

In this expression, γ_{scat}^N and $\gamma_{passage}^N$ respectively denote:

- a subfactor taking into account the scatter of the test results, *e.g.* $\gamma_{scat}^N = 2$ on $\gamma^N = 20$ and $\gamma_{scat}^S = 1.19$ on $\gamma^S = 2$ (Collectif, 1998);
- a specimen-to-structure passage factor taking into account the reduction of fatigue life of a real component in its environment compared to a specimen made of the same material tested in the laboratory. This global passage factor is the product of the size effect, the surface finish and the environment- subfactors.

In the present probabilistic framework, the scatter of the number-of-cycles-to-failure of the specimens is already described by the very definition of the random variable $N_S(\omega)$. Passage factors are also considered as random variables, whose parameters are yet to be defined, *e.g.* from experiments carried out both on specimen and scaled structures and comparisons thereof. This work is currently in progress, see Perrin et al. (2007).

When only empirical results are available from the literature, it is possible to take loose assumptions on the PDF of these passage factors, such as positiveness and upper bounds.

2.3.5 Random fatigue damage

Introduction According to the above assumptions, the elementary damage $d(S, \omega)$ undergone by a structure submitted to a cycle S is a random variable defined by:

$$d(S, \omega) = 1 / \min [N(S, \omega) / \gamma_{passage}^N, N(\gamma_{passage}^S S, \omega)] \quad (7.12)$$

where the notation $N(S, \omega) \equiv N_S(\omega)$ is used in the sequel for the sake of clarity. Using Miner's rule, the cumulated damage is also a random variable depending on all the input random variables described above:

$$D(\omega) = \sum_{i=1}^{N_c} d(S_i, \omega) \quad (7.13)$$

where N_c is the number of applied stress cycles. If the model that computes the stress cycles depends itself on random variables, this randomness also propagates into the final expression of damage. The aim of this section is to define more clearly what is the random fatigue damage. Two alternatives are presented, namely a *continuous* and a *discrete* formulation. In the sequel, this random variable is characterized in terms of statistics (mean value, standard deviation) or extreme values (*e.g.* probability of exceeding the threshold value of 1.)

For the sake of clarity, the following notation is used in this paragraph: the randomness in the fatigue strength of the material is denoted by ω_m , *i.e.* the number-of-cycles-to-failure is $N(S, \omega_m)$. Conversely, the randomness associated to the loading is denoted by ω_S , *e.g.* the thermal loading is $T(t, \omega_S)$. Suppose also that the other input variables may be considered as deterministic for the time being.

The thermal loading $T(t, \omega_S)$ is supposed to be Gaussian stationary process throughout the component service life. It is also assumed that the mechanical model relating the loading to the equivalent scalar

stress $S(t, \omega_S)$ keeps the normality and the stationarity of the random process. This is the case when elastic material behaviour is imposed. Under this hypothesis, $S(t, \omega_S)$ is likewise a Gaussian stationary process. Let us consider $\{S_i(\omega_S)\}_{i=1}^{N_c}$ the set of stress amplitudes extracted from the equivalent stress by the Rainflow counting, where N_c , which is presumably random, denotes the total number of cycles throughout the actual component service life. Under the assumption of stationarity of $S(t, \omega_S)$ and for a large number of cycles, N_c can be regarded as a constant (Tovo, 2001). Finally, $\{S_i(\omega_S)\}_{i=1}^{N_c}$ is assumed to be a set of independent and identically distributed random variables with probability density function $f_S(S)$. The resulting random fatigue damage is expressed in two ways, namely by a continuous formulation and a discrete formulation.

Discrete formulation According to Miner's rule, the cumulative damage also reads:

$$D(N_c, \omega_S, \omega_m) = \sum_{i=1}^{N_c} Y_i(\omega_S, \omega_m) \quad \text{where} \quad Y_i(\omega_S, \omega_m) = \frac{1}{N(S_i(\omega_S), \omega_m)} \quad (7.14)$$

Having noted that $\{S_i(\omega_S)\}_{i=1}^{N_c}$ is a set of independent and identically distributed random variables, it is clear that $\{Y_i(\omega_S, \omega_m)\}_{i=1}^{N_c}$ is, likewise, a set of independent and identically distributed random variables. Let $\mu_Y(\omega_m) = \text{E}_S [Y_i(\omega_S, \omega_m)]$ and $\sigma_Y^2(\omega_m) = \text{Var}_S [Y_i(\omega_S, \omega_m)]$ be the mean and the variance of the Y_i 's with respect to ω_S . Since N_c is large enough, the central limit theorem states that the cumulative damage tends to be normally distributed with mean value $N_c \mu_Y(\omega_m)$ and standard deviation $\sigma_Y(\omega_m) \sqrt{N_c}$. Thus, for a sufficiently large value of N_c , the cumulative random damage is approximated by:

$$D(N_c, \omega_S, \omega_m) \approx N_c \mu_Y(\omega_m) \left[1 + \frac{\sigma_Y(\omega_m)}{\mu_Y(\omega_m) \sqrt{N_c}} \xi(\omega_S) \right] \quad (7.15)$$

where $\xi(\omega_S)$ is a standard Gaussian variable. When N_c tends to infinity, the factor $\sigma_Y(\omega_m) / \mu_Y(\omega_m) \sqrt{N_c}$ vanishes, and the damage becomes:

$$D(N_c, \omega_S, \omega_m) \approx N_c \mu_Y(\omega_m) = N_c \text{E}_S \left[\frac{1}{N(S, \omega_m)} \right] \quad (7.16)$$

Continuous formulation Let $n(S, \omega_S) dS$ be the number of cycles of stress amplitudes in the elementary interval $[S; S + dS]$ throughout the component service life. Since N_c takes large values, the law of large numbers states that $n(S, \omega_S) dS$ is given by:

$$n(S, \omega_S) dS = N_c f_S(S) dS \quad (7.17)$$

Based on Miner's rule, the elementary damage associated to the cycles of stress amplitudes between S and $S + dS$ is given by:

$$dD(N_c, S, \omega_S, \omega_m) = \frac{N_c f_S(S) dS}{N(S, \omega_m)} \quad (7.18)$$

The total damage is written as:

$$D(N_c, S, \omega_m) = \int_0^{\infty} \frac{N_c f_S(S) dS}{N(S, \omega_m)} = N_c \text{E}_S \left[\frac{1}{N(S, \omega_m)} \right] \quad (7.19)$$

where $\text{E}_S [\cdot]$ is the mathematical expectation operator with respect to ω_S . This is exactly what comes out of the discrete formulation when N_c tends to infinity.

Note that in this formulation, the random damage contains no uncertainty related to the stress variations, since ω_S is removed by application of the expectation operator $\text{E}_S [\cdot]$. This can be interpreted as follows: provided the rule for damage accumulation is linear, and provided the Rainflow stress amplitudes are independent random variables, the cumulative damage for a large number of cycles is independent of the randomness in the loading.

2.4 Application example to a pipe

2.4.1 Problem statement

Let us consider a pipe typically encountered in a circuit of a pressurized water reactor (inner radius R_{int} , thickness t). Due to the shape of the circuit, the load temperature in a given section of the pipe is close to periodical. Of course, thermal fluctuations may appear in the real operating procedure. However, the thermal loading will be considered here as deterministic for the sake of simplicity. The fluid temperature history at the inner wall of the pipe is plotted in Figure 7.2 for one sequence of operating.

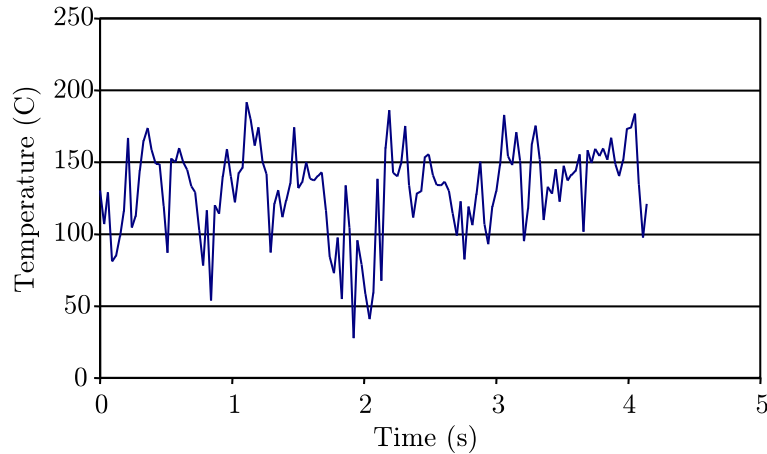


Figure 7.2: Fatigue analysis of a pipe: fluid temperature history

2.4.2 Mechanical model

Let us consider a typical section of a straight portion of the circuit. Due to symmetry, the one-dimensional axisymmetric model is relevant to compute the stress history. The simulation assumes generalized plane strain conditions (strain component ε_{zz} is supposed constant throughout the pipe thickness and is an unknown of the problem). Geometry and material properties are gathered in Table 7.1.

Table 7.1: Fatigue analysis of a pipe: input random variables

Parameter	Type of law	Mean value	CV
Internal radius R_{int}	lognormal	0.12728 m	5 %
Thickness t	lognormal	0.00927 m	5 %
Heat capacity ρC_p	lognormal	4,024,000 J/kg	10 %
Thermal conductivity λ	lognormal	16.345 W.m ⁻¹ .K ⁻¹	15 %
Heat transfer coefficient H	lognormal	20,000 W.K ⁻¹ .m ⁻²	30 %
Young's modulus E	lognormal	189,080 MPa	15 %
Poisson's ratio ν	Beta [0 ; 0,5]	0.3	10 %
Thermal expansion coefficient α	lognormal	16.95 10 ⁻⁶	10 %
Passage factor $\gamma_{passage}^N$	Beta [0 ; 20]	10	20 %
Passage factor $\gamma_{passage}^S$	Beta [0 ; 2]	1.68	20 %
Fatigue strength scatter ξ (Eq.(5))	normal	0	Std. Dev.: 1

Due to the peculiar geometry of the problem, the stress tensor is diagonal in the cylindrical coordinate system (r, θ, z) . The stress component σ_{rr} due to thermal loading is zero at the inner wall, whereas the two other components are equal ($\sigma_{\theta\theta} = \sigma_{zz}$). This means that the three-dimensional stress state is

completely described by a scalar stress history $\sigma_{\theta\theta}(t)$, from which the stress cycles can be easily obtained using the Rainflow counting method.

2.4.3 Deterministic fatigue analysis

The fatigue behavior of the material of the pipe under consideration is assumed to be described by Eqs.(7.3)-(7.4), where the parameters have been identified on a set of 304L austenitic stainless steel samples (Sudret *et al.* , 2003). The best-fit curve (median value) of the number-of-cycles-to-failure is $N_{bf}(S) = \exp [(-2, 28 \log(S - 185, 9) + 24, 06)]$. A thermo-mechanical analysis together with the *mean values* of the parameters (See Table 7.1, column #3) is first carried out.

The Rainflow counting provides 33 cycles, from which 2 are leading to elementary damage, namely $S_1 = 102.1$ MPa, $S_2 = 190.6$ MPa. Accordingly, the cumulated damage associated with one sequence of loading is $5.98 \cdot 10^{-6}$. Thus the codified design gives a life time of $N_{seq}^{det} = 1/5.98 \cdot 10^{-6} = 167,200$ sequences.

2.4.4 Probabilistic analysis

The parameters of the thermo-mechanical analysis are now described in terms of random variables. The choice of the probability density functions is dictated by common practice. The mean value and coefficient of variation of each parameter are given in Table 7.1.

The number-of-cycles-to-failure of the specimen is represented by a lognormal random variable (Eq.(7.3)) where the parameters in Eq.(7.4) read: $A = -2.28$, $B = 24.06$, $S_D = 185.9$, $\delta = 0.09$. This corresponds to:

$$N_S(\omega) = \exp [(-2, 28 \log(S - 185, 9) + 24, 06) (1 + 0, 09 \xi (\omega))] \quad (7.20)$$

where $\xi(\omega)$ is a standard normal random variable. The passage factors yielding the number-of-cycles-to-failure of the structure are represented by random variables following a Beta distribution whose mean values are respectively $20/2 = 10$ (low cycle domain) and $2/1.19 = 1.68$ (high cycle domain) and whose coefficient of variation is 20 %. The lower bound of the distributions is zero and the upper bounds are 20 and 2 respectively.

Using this probabilistic input, it is possible to characterize the randomness of the cumulated damage for a given life time, say 100,000 sequences of operating. The Latin Hypercube sampling technique was applied using 1,000 samples. The mean value and standard deviation of the cumulated damage are 0.921 and 2.00 respectively, hence a coefficient of variation of 217 %. It is clear from this analysis that the large scatter of the fatigue strength in the limited endurance domain yields a large scatter in the fatigue life time of the structure. The approach allows to quantify the latter properly.

The reliability of the structure under consideration may now be studied as a function of the number of sequences of operating N_{seq} . The limit state function is defined by:

$$g(N_{seq}, \mathbf{X}) = 1 - N_{seq} d_{seq}(\mathbf{X}) \quad (7.21)$$

In this expression, vector \mathbf{X} gathers all the input random variables as reported in Table 7.1. FORM is used to compute the reliability index and the probability of failure. For $N_{seq} = 100,000$ sequences, the results are: $\beta = 0.68$; $P_f = 0.249$. The coordinates of the design point (back-transformed into the physical space) as well as the sensitivity factors are reported in Table 7.2 .

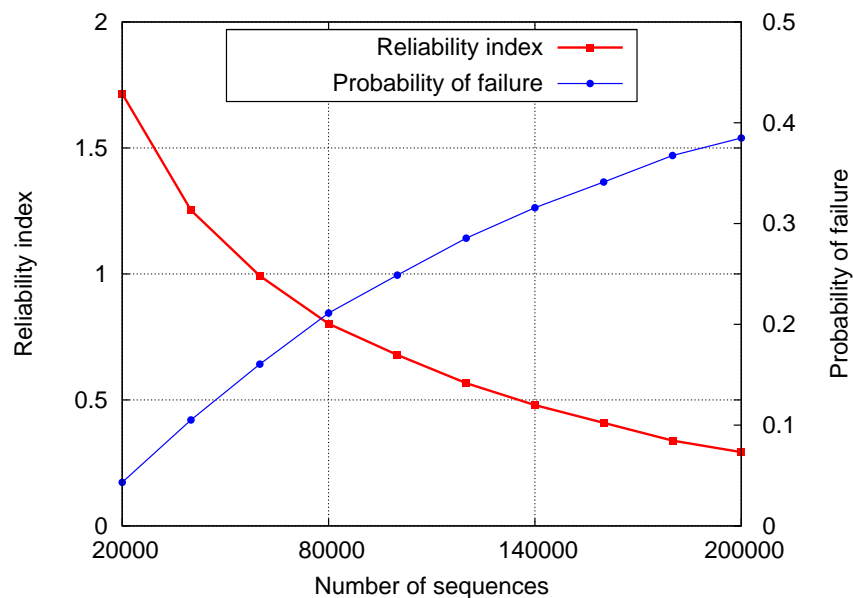
It is observed that the uncertainty related to the fatigue strength of the material is the most important factor driving the reliability of the structure. Variable ξ is of course a *resistance* variable since its design point value is below the median value. Then there are the Young's modulus and the coefficient of thermal expansion (which transform cycles of temperature in the pipe into stress cycles), the heat

Table 7.2: Fatigue analysis of a pipe: probabilistic results for $N_{seq} = 100,000$ sequences

Parameter	Mean value	Design point	Importance factors α_i^2 (%)
Fatigue strength scatter ξ	0	-0.433	41.3
Young' modulus E (MPa)	189,080	194,381	15.2
Thermal expansion coefficient α (K^{-1})	$16.95 \cdot 10^{-6}$	$17.42 \cdot 10^{-6}$	15.2
Heat transfer coefficient ($W.K^{-1}.m^{-2}$)	20,000	20,676	15.0
Passage factor $\gamma_{passage}^S$	1.68	1.863	11.1
Poisson's ratio ν	0.3	0.302	1.3
Thermal conductivity λ ($W.m^{-1}.K^{-1}$)	16.345	16.182	0.6
Heat capacity ρC_p (J/kg)	4 024,000	3,989,040	0.3
Inner radius R_{int} (m)	0.12728	0.12712	0.0
Thickness t (m)	0.00927	0.00926	0.0
Passage factor $\gamma_{passage}^N$	10	10	0.0

transfer coefficient (which transforms the peaks of temperature in the fluid into the peaks of temperature at the pipe inner wall) and finally the passage factor $\gamma_{passage}^S$.

These four variables are *demand* variables since their value at the design point is above the median value. All other random variables have negligible importance factors: this means that they could be considered as *deterministic* in this kind of analysis. Note that the passage factor $\gamma_{passage}^N$ has zero importance in the present example because it does not enter the analysis at all: the obtained stress cycles are sufficiently small so that only the “high cycle passage factor” $\gamma_{passage}^S$ is used.

Figure 7.3: Fatigue analysis of a pipe: reliability index (resp. the probability of failure) vs. life time N_{seq}

Finally a parametric study is carried out with respect to the required life time N_{seq} . The evolution of both the reliability index and the probability of failure as a function of N_{seq} is plotted in Figure 7.3. This figure would allow to regulate the use of the portion of pipe under consideration, if a target reliability index was prescribed.

2.5 Conclusions

Fatigue analysis of structural components in nuclear power plants is of crucial importance. The fatigue phenomenon is random in nature due to the mechanisms responsible for crack initiation at the microscopic scale. The present section proposes a probabilistic framework of analysis which aims at incorporating in a rigorous manner all kinds of uncertainties appearing in the fatigue assessment.

In order to be easily understood by practitioners, the usual assessment rules codified in the French regulatory guide have been taken as a baseline. In each step, sources of uncertainty have been identified and a probabilistic model has been proposed. As a consequence, the cumulated damage (which is an indicator of fatigue crack initiation) becomes random. Its randomness can be characterized a) in terms of mean value and standard deviation b) in terms of probability of exceeding the threshold 1. Note that this threshold could be modelled as a random variable as well in order to take into account model uncertainty associated with Miner's rule.

The pipe application example provides additional useful insight on the fatigue design. The first analysis shows that the coefficient of variation of the cumulated damage is rather high (217 % in the application example). Hence the well-known randomness on the fatigue life time of a structure in the high cycle domain is quantified.

The reliability analysis allows to compute the probability of failure corresponding to crack initiation. Sensitivity factors related to the use of FORM analysis may also be computed. They allow to rank the input random variables according to their importance with respect to failure. Five important variables have been identified, namely the fatigue strength of the material, the Young's modulus and the coefficient of thermal expansion, the heat transfer coefficient at the pipe inner wall and finally the passage factor $\gamma_{passage}^S$. The other random variables (termed as "unimportant" from a probabilistic point of view) may be considered as deterministic in subsequent analyses. Note that the very values of the sensitivity factors should be taken with caution since they truly depend on the choice of the PDF of the input parameters and their respective coefficients of variation.

Simple models have been retained in all steps of the analysis for the application example (deterministic loading, thermo-mechanical 1D calculation, linear damage accumulation). More complex models can be easily integrated in the framework, including non linear two- or three-dimensional finite element models). The case of a random loading represented by a Gaussian random process has been dealt with in Guédé et al. (2004). The computation takes place in the frequency domain in this case. Due to linearity, it is possible to derive an analytical transfer function that yields the stress components as a function of the temperature at each frequency. This transfer function used together with the power spectral density of the fluid temperature provides the power spectral density of the stress. The latter is then transform into the probability density function of the stress amplitudes, which directly enters the probabilistic analysis. Details on this work can be found in Guédé (2005); Guédé et al. (2007).

Recently, a multiaxial fatigue model has been used by Schwob (2007) together with the probabilistic fatigue framework developed above. A modified Papadopoulos criterion (Papadopoulos et al., 1997) has been used in order to take into account stress gradients in complex sample structures such as bored or notched plates. The parameters of the criterion have been identified by a stochastic inverse approach such as those presented in Chapter 5.

3 Cooling towers

3.1 Introduction

Natural-draught cooling towers are used in nuclear power plants as heat exchangers. These shell structures are submitted to environmental loads such as wind and thermal gradients that are stochastic in nature. Due to the complexity of the building procedure, uncertainties in the material properties as well as differences between the theoretical and the real geometry also exist.

Structural reliability is well suited to the evaluation of the safety of these structures all along their life time. A first application of structural reliability to cooling towers was presented by Liao and Lu (1996). The first order second moment method was used together with an axisymmetric finite element model. More recently, Mohamed et al. (2002) applied FORM together with a three-dimensional shell finite element model.

Based on this preliminary work, the durability of cooling towers submitted to rebars corrosion induced by concrete carbonation has been studied in Sudret and Pendola (2002); Sudret et al. (2002). The problem is cast in the framework of *time-variant finite element reliability analysis*. A more efficient response surface-based approach has been later developed in Sudret et al. (2005) by taking advantage of the linearity of the peculiar model of the structure. This section summarizes these results.

3.2 Exact response surface for linear structures

The basic idea of response surfaces is to replace the exact limit state function $g(\mathbf{x})$, which is known implicitly through a finite element procedure, with an approximate, usually polynomial function $\tilde{g}(\mathbf{x})$, the coefficients of the expansion being determined by means of a least-square minimization procedure.

In this section, a response surface is derived from mechanical considerations. Precisely, let us consider a linear elastic finite element model of the structure with homogeneous material properties (mass density ρ , Young's modulus E , Poisson's ratio ν , thermal dilatation coefficient α). Let us consider q different mechanical load cases (*e.g.* self weight, applied pressure, etc.) defined by a load intensity λ_i and a load pattern \mathbf{F}_i , $i = 1, \dots, q$ (vector \mathbf{F}_i is the vector of nodal forces corresponding to a unit value of the load intensity). Let λ_T be the intensity of the thermal load, *e.g.* the temperature increment with respect to some reference state.

Furthermore, let us denote by \mathbf{U}_i , $i = 1, \dots, q$ the displacement vector resulting from the load pattern \mathbf{F}_i and unit load intensity $\lambda_i = 1$ (resp. \mathbf{U}_T the displacement vector resulting from a unit temperature increment) applied to a structure with unit Young's modulus and thermal dilatation coefficient. The total displacement vector may be cast as (Sudret et al., 2005):

$$\mathbf{U} = \alpha \lambda_T \mathbf{U}_T + \frac{1}{E} \sum_{i=1}^q \lambda_i \mathbf{U}_i \quad (7.22)$$

A similar expression can be derived for the internal forces (membrane forces and bending moments).

Suppose now that all unit response quantities ($\mathbf{U}_T, \{\mathbf{U}_i\}_{i=1}^q$) are computed from a finite element analysis. Note that this requires a single assembling of the unit stiffness matrix \mathbf{K}_1 , the computation of the unit vectors of nodal forces ($\mathbf{F}_T, \{\mathbf{F}_i\}_{i=1}^q$), a single inversion of the unit stiffness matrix \mathbf{K}_1^{-1} and $(q+1)$ matrix-vector products ($\mathbf{K}_1^{-1} \cdot \mathbf{F}_T$; $\mathbf{K}_1^{-1} \cdot \mathbf{F}_i$, $i = 1, \dots, q$). Then Eq.(7.22) gives the displacement vector *analytically* for any set of parameter $(\alpha, E, \lambda_T, \{\lambda_i\}_{i=1}^q)$, and the same holds for the internal forces gathered in a vector $\mathbf{S}(\mathbf{U}(\mathbf{X}))$.

This implies that any limit state function based on these response quantities is defined *analytically* in terms of the model parameters $\alpha, E, \lambda_T, \{\lambda_i\}_{i=1}^q$:

$$g(t, \mathbf{X}, \mathbf{U}(\mathbf{X}), \mathbf{S}(\mathbf{U}(\mathbf{X}))) \equiv \tilde{g}(t, \alpha, E, \lambda_T, \{\lambda_i\}_{i=1}^q) \quad (7.23)$$

Thus the finite element reliability analysis is decoupled into a single *multi-load case* elastic finite element analysis providing unit response quantities, then a reliability analysis using an *analytical* limit state function

3.3 Deterministic model of the cooling tower

The cooling tower under consideration is a shell structure with axisymmetric geometry depicted in Figure 7.4. The height of the tower is 165 m, the meridian line is described by the shell radius $R_m(z)$ as a function of the altitude z :

$$R_m(z) = -0.00263z + 0.2986\sqrt{(z - 126.74)^2 + 2694.5} + 23.333 \quad (7.24)$$

The shell is supported by 52 pairs of V-shaped circular columns with radius 0.5 m. The shell thickness is varying with z from 21 cm to 120 cm. The structure is modelled by means of EDF's finite element code Code_Aster. The mesh comprises 12,376 9-node isoparametric shell elements. The reinforced concrete is modelled as an homogeneous isotropic elastic material.

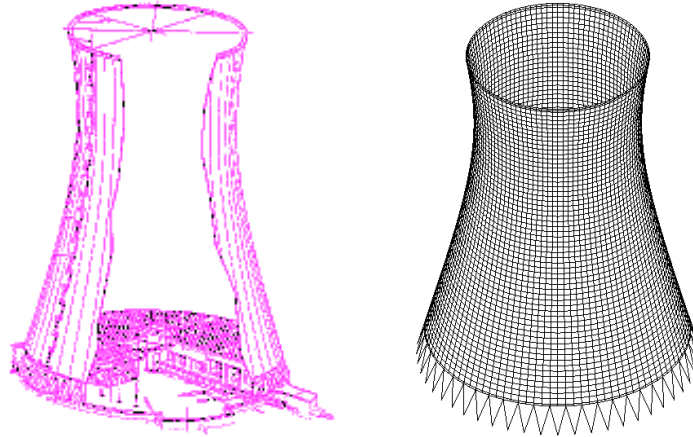


Figure 7.4: Cooling tower – scheme and mesh used in the finite element analysis

When the power plant is in service, the cooling tower is submitted to a combination of loads, namely the self-weight (corresponding to a mass density ρ), the wind pressure $q_w(z, \theta)$ (which is codified in French Standard NV65 and depends both on the altitude z and azimuth θ), the internal depression P_{int} due to air circulation in service (which is supposed to be constant all over the tower and is equal to $-0.4 P_{max}$, P_{max} being the maximal wind pressure at the top of the cooling tower), and finally the thermal gradient ΔT within the shell thickness (see detailed expressions in Sudret et al. (2005)).

3.4 Limit state function and probabilistic model

3.4.1 Deterministic assessment of the structure

The serviceability of the cooling tower as a reinforced concrete structure is assessed according to the French concrete design code BAEL (2000). In each node of the mesh, the membrane forces and bending moments in each direction are compared to the strength of a one-meter wide concrete section.

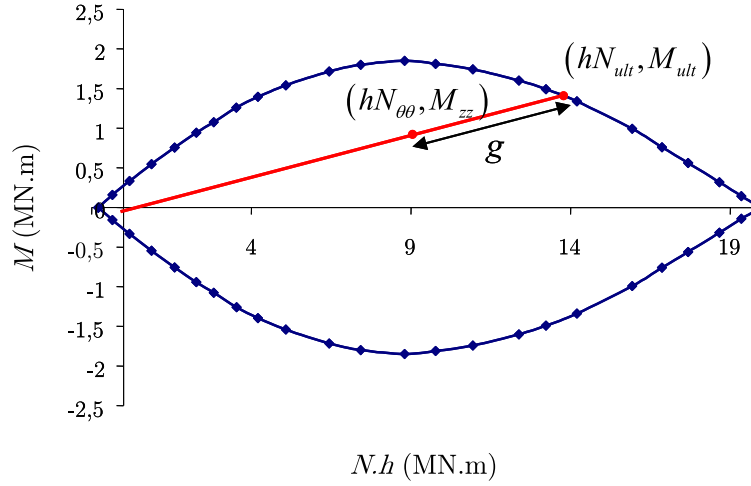


Figure 7.5: Cooling tower – Load carrying capacity diagram for a concrete section and associated limit state function

Practically speaking, the membrane and bending forces ($N_{\theta\theta}$, M_{zz}) used to assess the circumferential reinforcement are reported in the *load carrying capacity diagram* (Figure 7.5), which shows the combinations of the internal forces that can be taken by the concrete section. This diagram depends on the following parameters: geometry of the concrete section (width of 1 m, height equal to the shell thickness), rebars diameter and density, concrete cover, concrete compressive strength and steel yield stress. If the representative point lies inside the diagram, the design criterion is satisfied for the section under consideration. This assessment is carried out at each node of the structure. The same procedure is applied using the internal forces (N_{zz} , $M_{\theta\theta}$) for assessing the longitudinal reinforcement.

3.4.2 Limit state function

The limit state function is defined as the algebraic distance from the point representing the internal forces to the boundary of the load carrying capacity diagram, this distance being measured along the radial line, as shown in Figure 7.5. This leads to the following expression:

$$g(\mathbf{X}) = (h^2 N_{ult}^2(\mathbf{X}) + M_{ult}^2(\mathbf{X})) - (h^2 N_{\theta\theta}^2(\mathbf{X}) + M_{zz}^2(\mathbf{X})) \quad (7.25)$$

where h is the shell thickness, ($N_{\theta\theta}$, M_{zz}) are the internal forces resulting from the finite element computation at the node and (N_{ult} , M_{ult}) is obtained as the intersection between the radial line $[(0, 0); (hN_{\theta\theta}, M_{zz})]$ and the diagram boundary.

3.4.3 Probabilistic model of the input parameters

The type and parameters of the random variables used in the analysis are listed in Table 7.3. Two variables are defined as functions of others, namely the concrete Young's modulus and the internal depression in service.

As a consequence, eight independent random variables are used. These random variables appear implicitly in Eq.(7.25) as follows:

- $E, \rho, \alpha, P_c, P_{int}, \Delta T$ appear in the finite element computation, hence in ($N_{\theta\theta}$, M_{zz}).
- f_y, f_{c_j}, d_0, e appear in the initial load carrying capacity diagram.

Table 7.3: Cooling tower – Definition of the random variables

Random variable	Type	Mean value	CV
Concrete mass density ρ	lognormal	2,500 kg/m ³	10 %
Concrete thermal dilatation coefficient α	lognormal	10 ⁻⁵ /K	10 %
Wind pressure P_c	Gaussian	350 Pa	30 %
Internal depression P_{int}		-0.813 P_c	
Difference between the inside and outside concrete temperatures ΔT	Gaussian	12 °C	20 %
Steel yield stress f_y	lognormal	420 MPa	5 %
Concrete compressive strength f_{c_j}	lognormal	40 MPa	15 %
Concrete Young's modulus E		11,000 $\sqrt[3]{f_{c_j}}$	
Rebars initial diameter d_0	Beta([0.009, 0.011m])	0.01 m	5 %
Concrete cover e	Beta([0, 0.1m])	0.025 m	30%

The internal forces ($N_{\theta\theta}$, M_{zz}) associated with each unit load case are computed in each node once and for all and stored in a database. The reliability problem is then solved using the general purpose reliability code PhimecaSoft (Phimeca Engineering SA, 2004; Lemaire and Pendola, 2006). The FORM method is used. In each iteration of the optimization leading to the design point, a realization of the random variables is provided by PhimecaSoft to a routine that computes the value of the limit state function from the finite element results stored in the database. The coordinates of the design point, the reliability index and the importance factors are provided as end results.

3.5 Point-in-space reliability analysis

3.5.1 Initial time-invariant analysis

In a first analysis, a point-in-space reliability problem is considered. A deterministic finite element run with *mean values* of the parameters is carried out. The limit state function Eq.(7.25) is evaluated at each node of the mesh. The *critical point* is defined as the node where $g(\mu_{\mathbf{X}})$ takes its minimal value. Then the reliability analysis is carried out by evaluating the limit state function in this critical point all along the analysis.

The initial reliability index at time $t = 0$, *i.e.* when corrosion of the rebars has not started, is $\beta = 4.36$, corresponding to a probability of failure $P_{f,FORM}^0 = 6.56 \times 10^{-6}$. The coordinates of the design point are reported in Table 7.4.

Table 7.4: Cooling tower – Point-in-space reliability analysis at initial time instant – Coordinates of the design point and importance factors

Random variable	Design point	Importance factor (%)
Difference between the inside- and outside concrete temperatures ΔT	19.10°C	46.0
Concrete thermal dilatation coefficient α	1.26E-05/°C	29.0
Rebars initial diameter d_0	9.23 mm	12.3
Steel yield stress f_y	396.7 MPa	6.6
Concrete compressive strength f_{c_j}	46.4 MPa	6.1

As expected, d_0 and f_y are *resistance* variables since the design point is below the median value. Variables ΔT and α are *demand* variables since the design point is above the median value. The concrete compressive strength f_{c_j} should be physically a resistance variable. However, it is linked to the concrete Young's

modulus, which is an important demand variable due to the thermal loading. The addition of these two opposite effects globally makes f_{c_j} a demand variable. The most important variables are the temperature gradient (46.0%), the concrete thermal dilatation coefficient (29.0%), the concrete cover (12.3%), the steel yield stress (6.6%) and the concrete compressive strength (6.1%). Note that the concrete cover and the wind pressure have zero importance in this initial reliability analysis.

3.5.2 Time-variant analysis

The concrete carbonation and associated corrosion of the rebars in the shell is now considered. The carbonation model presented in Chapter 6, Section 8.4.1 is used. The parameters of the model, namely the coefficient of diffusion of carbon dioxide in dry concrete D_{CO_2} , the carbon dioxide concentration in the surrounding air C_0 , the binding capacity a and the corrosion rate i_{corr} are modelled by random variables.

The time-variant reliability problem under consideration is a *right-boundary problem* as defined in Chapter 6, Section 2.3. Indeed the limit state function is a distance between a point representing the internal forces and the boundary of the load carrying capacity diagram (see Eq .7.25). The point representing the internal forces does not change in time, since it results from a finite element analysis whose parameters are realisations of the random variables $E, \rho, \alpha, P_c, P_{int}, \Delta T$. In contrast, the load carrying capacity diagram monotonically shrinks due to the reduction of the rebars diameter. Thus the distance keeps decreasing in time and the limit state function fulfills the criterion for right-boundary problems. As a consequence, the evolution in time of the time-variant probability of failure is identical to the instantaneous probability of failure: $P_f(0, t) = P_{f,i}(t)$ (see Chapter 6, Section 3.2).

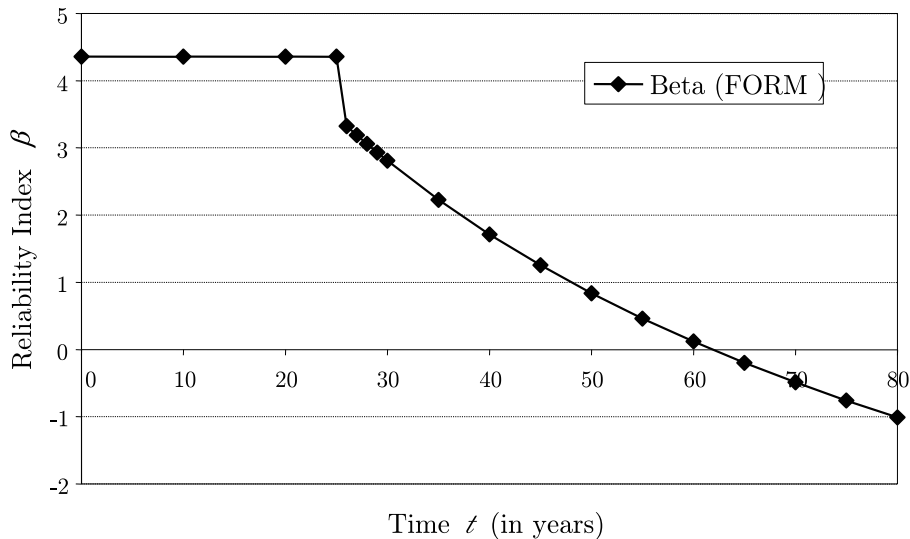


Figure 7.6: Cooling tower – Point-in-space reliability problem – evolution in time of the reliability index

The initiation time for corrosion $T_{init} = \frac{a e^2}{2 C_0 D_{CO_2}}$ has been simulated by MCS. Its mean value is 26.5 years and its standard deviation 7.1 years (CV= 26.8%). It may be well approximated by a lognormal distribution.

The evolution in time of the reliability index is plotted in Figure 7.6. The curve presents a plateau for the first 25 years which corresponds to the initiation of corrosion. The reliability index sharply decreases around 25 years. Then it further decreases smoothly and monotonically.

The evolution in time of the importance factors has been investigated as well. Results are reported in Figure 7.7. During the initiation phase, the important variables are basically those obtained at $t = 0$, *i.e.*

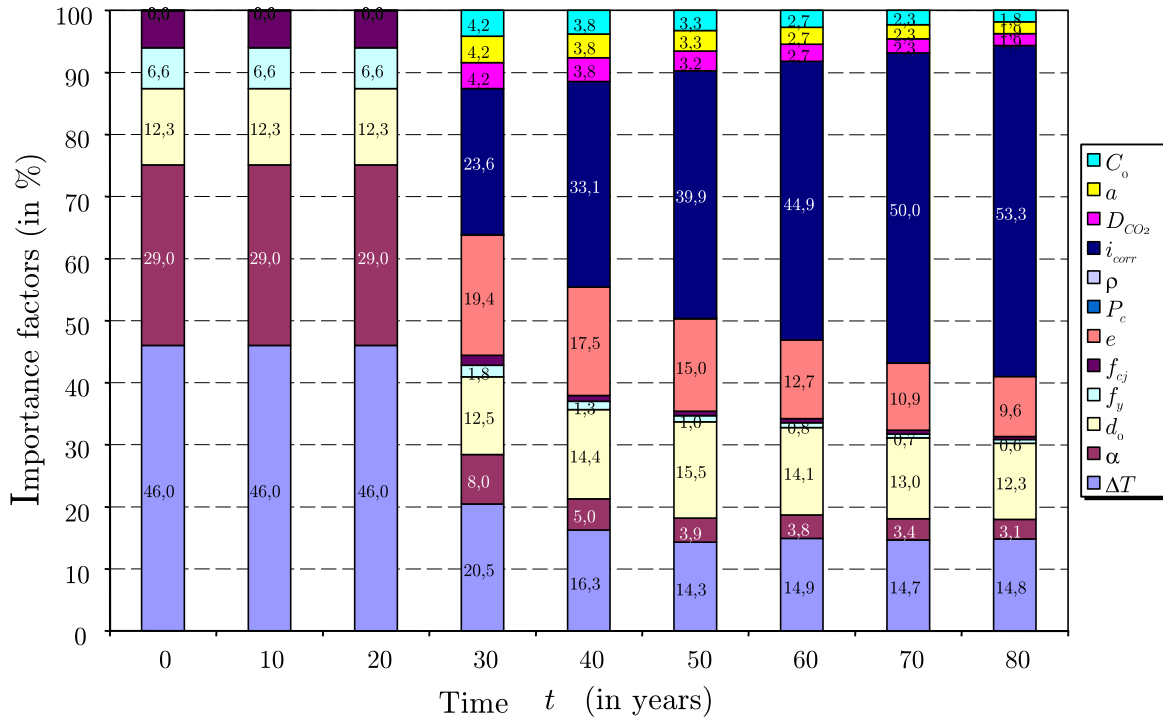


Figure 7.7: Cooling tower – Point-in-space reliability problem – evolution in time of the importance factors

$\Delta T, \alpha, d_0, f_y, f_{c_j}$. After corrosion has started, the cumulated importance of these variables reduces to 40%. Then the most important variables are the corrosion current density and the concrete cover. The importance of the corrosion current density keeps increasing in time up to a value of 50% at $t = 70$ years while the importance of all other variables decreases accordingly.

3.6 Space-variant reliability analysis

3.6.1 Problem statement

The above analysis pertains to the class of *point-in-space* reliability analysis. Indeed the node where the limit state function is evaluated (critical point) is fixed, being determined once and for all from a prior deterministic analysis using the mean values of the parameters. However it is expected that the critical point changes when the parameters vary.

Accordingly, another failure criterion can be defined as follows: failure occurs if the limit state function takes a negative value in *any* point of the shell (in practice, any node of the mesh). The limit state function then reads:

$$g_2(\mathbf{X}) = \min_{\text{all nodes}} \{ (h^2 N_{ult}^2(\mathbf{X}) + M_{ult}^2(\mathbf{X})) - (h^2 N_{\theta\theta}^2(\mathbf{X}) + M_{zz}^2(\mathbf{X})) \} \quad (7.26)$$

In this case, in each iteration of the optimization leading to the design point, a routine computes the value of the g -function from the finite element results stored in the database *in each node* and takes the minimal value over the whole set. Thus the critical node may change from one iteration to another.

Due to the “min” function in Eq.(7.26), the limit state function is not continuously differentiable in all points. In order to obtain reliable results, importance sampling (IS) is used. A FORM analysis is carried

out first. The obtained design point (which may not be reliable due to the differentiability issue) is used as the center of the sampling density. Note that even if the design point is wrong or if there are several design points, the IS results may be taken confidently provided the coefficient of variation of the simulation is sufficiently small.

3.6.2 Results

The space-variant reliability analysis has been carried out first at the initial instant $t=0$ using FORM. The reliability index obtained from this analysis is equal to 1.89 corresponding to a probability of failure of 2.92×10^{-2} . The result is confirmed by importance sampling using 500 realizations (the c.o.v. of the simulation being 7.5 %). The probability of failure is $P_{f,IS} = 2.17 \times 10^{-2}$. The equivalent reliability index $\beta_{IS} = -\Phi^{-1}(P_{f,IS})$ is equal to 2.02, which is slightly greater than the value obtained by FORM.

This result is about 4 decades greater than the result obtained in the point-in-space reliability analysis. This phenomenon has been already pointed out in the context of the space-variant reliability analysis of a damaged plate by Der Kiureghian and Zhang (1999). However, the importance factors obtained from this space-variant analysis are rather close to those obtained in the former analysis.

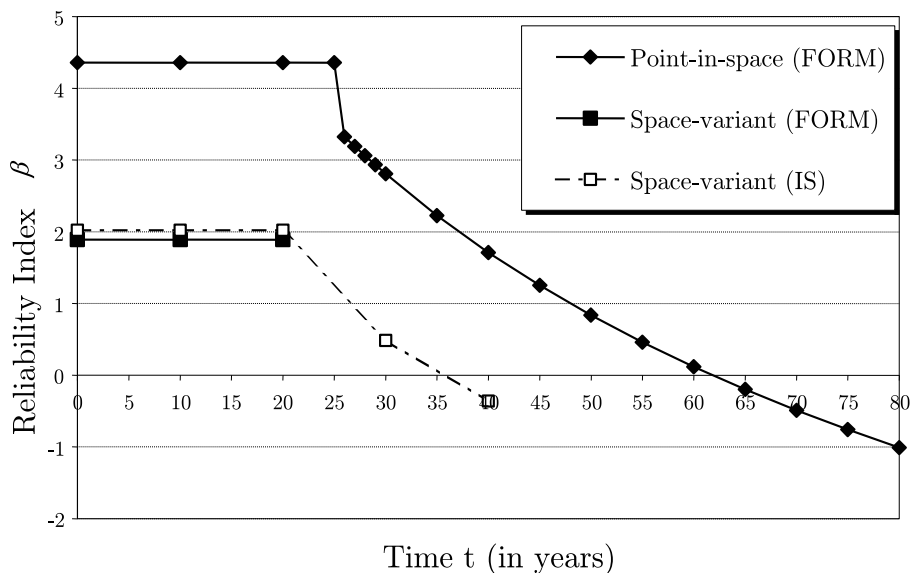


Figure 7.8: Cooling tower – Space-variant reliability problem – evolution in time of the reliability index

The time-variant space-variant reliability analysis has been carried out by importance sampling (Figure 7.8). The sampling density is the one used at the initial instant $t=0$. The decrease of the reliability index in time is similar to that obtained in the point-in-space analysis.

3.7 Conclusion

The durability of cooling towers submitted to concrete carbonation and induced rebar corrosion has been investigated using the framework of finite element reliability analysis. In the linear domain, mechanical considerations allow one to derive an exact (non linear) response surface in terms of model parameters under certain conditions which are sufficiently versatile for applications in basic design. A *single* finite element analysis using unit values of material properties and load parameters provides unit- displacement vectors and internal forces that are stored in a database. Then the limit state function is given an analytical form, which allows a fast computation of the probability of failure.

The point-in-space and space-variant probabilities of failure revealed significantly different. This shows the importance of selecting properly the failure criterion. In practice, the extent of damage would probably be the most relevant quantity to consider for the long-term assessment of cooling towers. The methods developed in Chapter 6, Section 8 may be applied to this aim.

4 Non linear fracture mechanics

4.1 Introduction and deterministic problem statement

Pipes in nuclear power plants are subject to thermal and mechanical loads which can lead to the initiation and the propagation of cracks. When a crack is observed, it is important to know whether the structure has to be repaired or if it can be proven that this crack will not propagate. In this section, various stochastic finite element methods are compared for solving the associated structural reliability problem. The results are reported from the Ph.D thesis of Berveiller (2005) and were originally published in (Berveiller et al., 2005a).

Consider an axisymmetrically cracked pipe subject to internal pressure and axial tension (Figure 7.9). The inner radius of the pipe is $R_i = 393.5$ mm, its thickness is $t = 62.5$ mm. The length of pipe under consideration in the model is $L = 1000$ mm and the crack length is $a = 15$ mm.

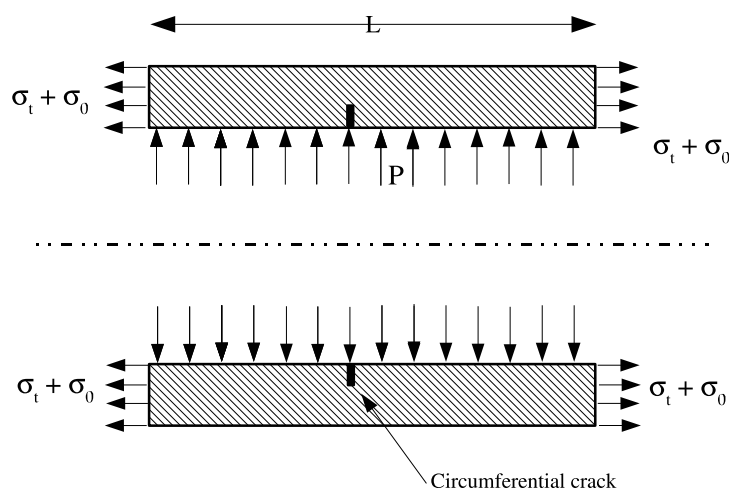


Figure 7.9: Non linear fracture mechanics – sketch of the axisymmetrically cracked pipe

The applied internal pressure is $P = 15.5$ MPa. An axial tensile load $\sigma_0 = P \frac{R_i^2}{(R_i + t)^2 - R_i^2}$ due to end effects of the pressure is superimposed. An additional tensile stress σ_t , whose intensity varies from 0 up to 200 MPa, is also applied. It is considered as a deterministic parameter in the analysis. Indeed, the evolution of the probability of failure (where failure means crack propagation, see below) with respect to this loading parameter is of interest. The mesh of half of the structure (due to symmetry) is given in Figure 7.10.

The pipe is made of steel, whose constitutive behavior is described by the Ramberg-Osgood law (Lemaitre and Chaboche, 1990). The one-dimensional relationship between strain ε and stress σ reads:

$$\varepsilon = \frac{\sigma}{E} + \alpha \frac{\sigma_y}{E} \left(\frac{\sigma}{\sigma_y} \right)^n \quad (7.27)$$

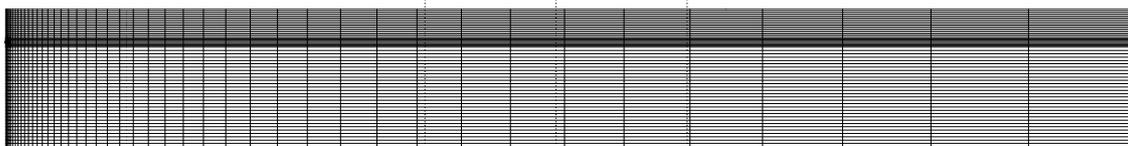


Figure 7.10: Non linear fracture mechanics – mesh of the axisymmetrically cracked pipe

In this expression, E denotes the Young's modulus of steel, σ_y is the yield strength, n is the strain hardening exponent and α is the Ramberg-Osgood coefficient (Figure 7.11).

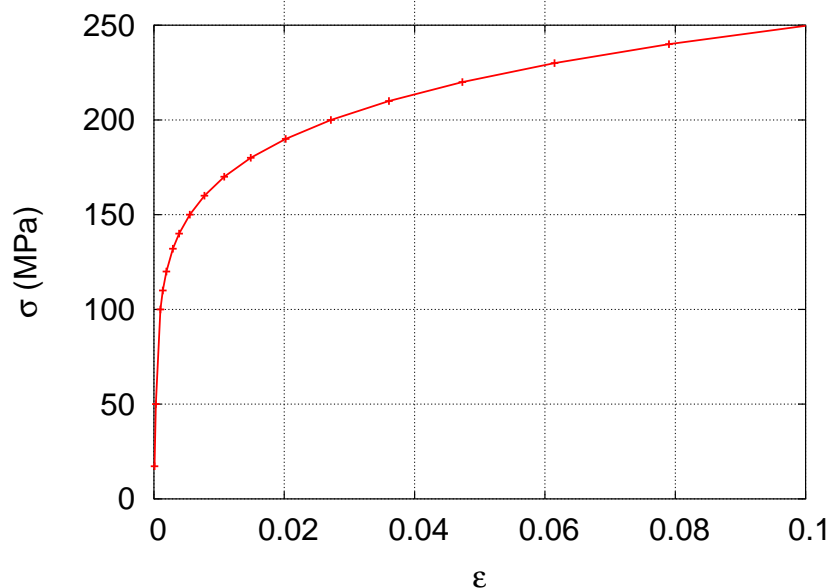


Figure 7.11: Non linear fracture mechanics – strain/stress curve of the steel under consideration

Of interest in the analysis is the so-called *crack driving force* J , which allows to check whether an existing crack is likely to propagate under a given loading. This quantity (which is obtained by the Rice integral in fracture mechanics) is directly computed by the finite element code:

$$J(\sigma_t) = \mathcal{M}(E, \sigma_y, n, \alpha, \sigma_t) \quad (7.28)$$

4.2 Probabilistic description of the input parameters

In this example, the constitutive law of the material is supposed to be uncertain. As a consequence, $M = 4$ mutually independent random variables are considered (see Eq.(7.27)). The probabilistic description of these random variables is given in Table 7.5.

Table 7.5: Non linear fracture mechanics – description of the input random variables

Parameter	Notation	Distribution	Mean	Coef. of Var.
Young's modulus	E	lognormal	175,500 MPa	5%
Ramberg-Osgood coefficient	α	Gaussian	1.15	13%
Strain hardening exponent	n	Gaussian	3.5	3%
Yield strength	σ_y	lognormal	259.5 MPa	3.8%

Due to the randomness in the input parameters, the crack driving force J becomes random. A third order Hermite polynomial chaos expansion is considered ($p = 3$). For this purpose, the input random vector $\mathbf{X} = \{E, \alpha, n, \sigma_y\}^T$ is first transformed into a standard normal random vector $\mathbf{\Xi}$.

The third order PC expansion of the crack driving force denoted by J_{PC} reads, for each value of the applied tensile stress σ_t :

$$J_{PC}(\boldsymbol{\xi}, \sigma_t) = \sum_{j=0}^{P-1} J_j(\sigma_t) \Psi_j(\boldsymbol{\xi}) \quad (7.29)$$

where $\{J_j(\sigma_t), j = 0, \dots, P-1\}$ are the unknown PC coefficients and $P = \binom{3+4}{3} = 35$ is the number of those unknown coefficients.

4.3 Statistical moments of the crack driving force

The statistical moments of the response are first computed for $\sigma_t = 200$ MPa using various non intrusive methods. Table 7.6 gathers the moments of J up to order 4 obtained by projection methods. A reference result is obtained by crude Monte Carlo simulation of the deterministic problem (1,000 samples were used). Latin Hypercube sampling is first applied to compute the PCE coefficients using 500, 1,000 and 1,500 samples respectively. A full quadrature scheme of third and fourth order is then applied.

Table 7.6: Non linear fracture mechanics – statistical moments of J for $\sigma_t = 200$ MPa (Latin Hypercube sampling)

	MC Sampling	Latin Hypercube			Quadrature	
# FE Runs	1000	500	1000	1500	3 ⁴	4 ⁴
Mean	71.38	71.63	71.65	71.65	71.64	71.65
Std. dev.	7.93	10.11	9.82	10.74	7.84	7.84
Skewness	0.40	2.41	-0.49	2.26	1.23	1.23
Kurtosis	3.18	39.28	9.67	22.09	6.86	6.85

Then regression is applied using a deterministic experimental design based on the roots of the Hermite polynomials for various numbers of collocation points in the range 35 to 256. Results are reported in Table 7.7.

Table 7.7: Statistical moments of J for $\sigma_t = 200$ MPa

	Regression				
# FE Runs	35	70	105	140	256
Mean	51.20	66.48	71.64	71.64	71.64
Std. dev.	48.20	26.39	7.81	7.81	7.81
Skewness	-2.90	-4.86	0.32	0.32	0.32
Kurtosis	18.99	45.92	3.20	3.21	3.21

When considering the projection method, Latin Hypercube sampling does not give accurate results whatever the size of the sample set used here (even the standard deviation is poorly estimated). A larger number of samples would probably improve the results. The results obtained by the full quadrature schemes are almost identical. This means that the PCE expansion of the response has a number of higher order terms close to zero that do not influence the computation of the moments when they are computed using a low order quadrature scheme $\boldsymbol{\nu} = (3, 3, 3, 3)$.

As far as the regression method is concerned, the convergence is achieved when 105 collocation points are used. This confirms the thumb rule by Berveiller (2005), which says that the size of the experimental design should be $(M - 1) \times P$. The results are rather accurate compared to the reference Monte Carlo results.

4.4 Reliability analysis of the cracked pipe

In order to evaluate the structural integrity of the pipe, the probability that the crack driving force J exceeds the ductile tearing resistance $J_{0.2}$ is to be computed:

$$P_f(\sigma_t) = \text{Prob}(J(\sigma_t) \geq J_{0.2}) \quad (7.30)$$

The associated limit state function reads:

$$g(J_{0.2}, \mathbf{X}, \sigma_t) = J_{0.2} - J(E, \sigma_y, n, \alpha, \sigma_t) \quad (7.31)$$

The ductile tearing resistance $J_{0.2}$ is modelled by a lognormal random variable (mean value 52 MPa.mm and coefficient of variation 18%). A reference solution of (7.30) is obtained using FORM and a direct coupling between the finite element code Code_Aster and the reliability code Proban (Det Norske Veritas, 2000).

On the other hand, the stochastic finite element approximation $J_{\text{PC}} = \sum_{j=0}^{34} J_k(\sigma_t) \Psi_k(\boldsymbol{\xi})$ is post-processed in order to evaluate the probability of failure associated with the PC-based limit state function:

$$g_{\text{PC}}(J_{0.2}, \boldsymbol{\xi}, \sigma_t) = J_{0.2} - \sum J_k(\sigma_t) \Psi_k(\boldsymbol{\xi}) \quad (7.32)$$

FORM is first applied: indeed, the approximate limit state function in this case is polynomial in standard normal variables making this computation inexpensive. Then importance sampling around the design point is used in order to get accurate values of P_f (a coefficient of variation of about 5% is obtained using 1,000 simulations).

Figure 7.12 shows the evolution of the logarithm of the probability of failure as a function of the applied tensile stress for PC expansion obtained by quadrature or LHS¹. Each curve corresponds to a particular projection scheme.

Latin Hypercube sampling is applied using 500, 1,000 and 1,500 samples respectively. It seems that even the largest sample size considered here (*i.e.* 1,500 sample) is not large enough to compute accurate values of the PC coefficients that would lead to an accurate estimation of the failure probability (except for relatively high values, say $P_f \geq 0.1$). As far as the quadrature method is concerned, selecting 3 or 4 integration points in each dimension provides the same results, which compare very well with the reference solution.

Figure 7.13 shows the evolution of the logarithm of the probability of failure as a function of the applied tensile stress σ_t using the regression method. Each curve corresponds to a particular regression scheme. Here again, using 105 points (*i.e.* 3 times the size of the polynomial chaos expansion) allows us to get accurate results in the range $P_f \in [10^{-8}, 1]$. The curves obtained using more than 105 points are one and the same whatever the load parameter σ_t .

In terms of computational cost, the direct coupling requires 542 calls to the finite element code to compute the “reference” curve plotted in Figures 7.12 and 7.13 (each call means a full non linear finite element analysis under increasing tensile stress σ_t). This is more than 5 times the CPT required by the regression method using 105 points. The quadrature method is more than 6 times faster than the reference solution since only 81 finite element runs are sufficient to get accurate results.

¹For the sake of clarity, remark that LHS is used here as a means to evaluate the PC coefficients, and not as a means to directly compute the probability of failure.

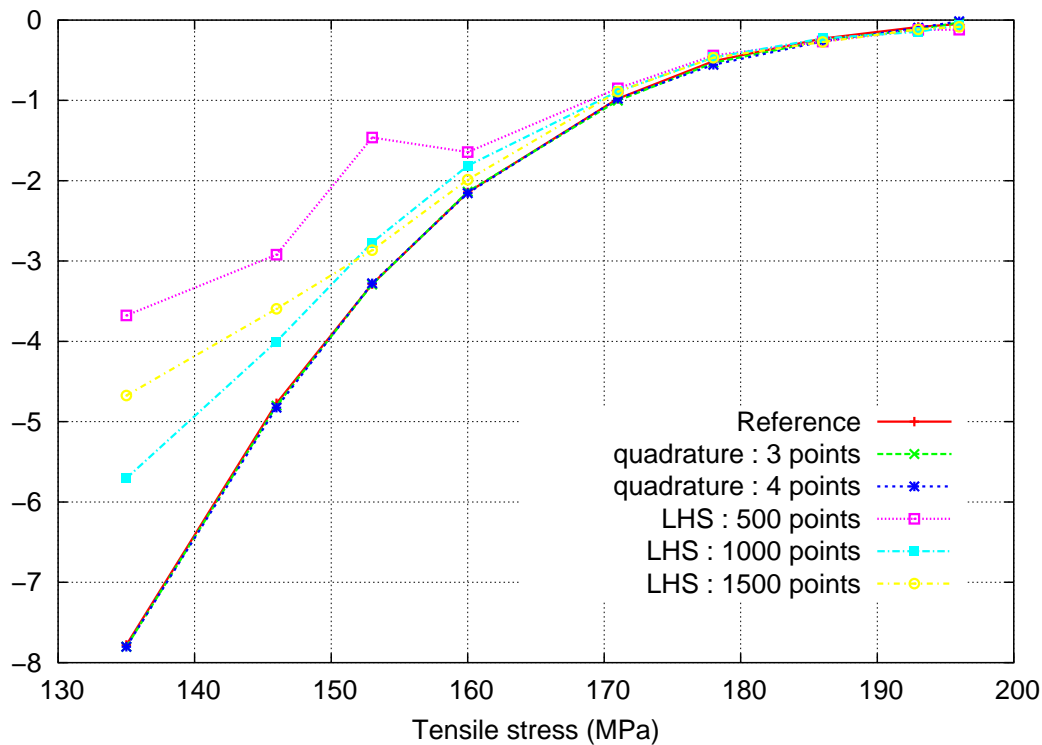


Figure 7.12: Logarithm of the failure probability vs. tensile stress using the projection method

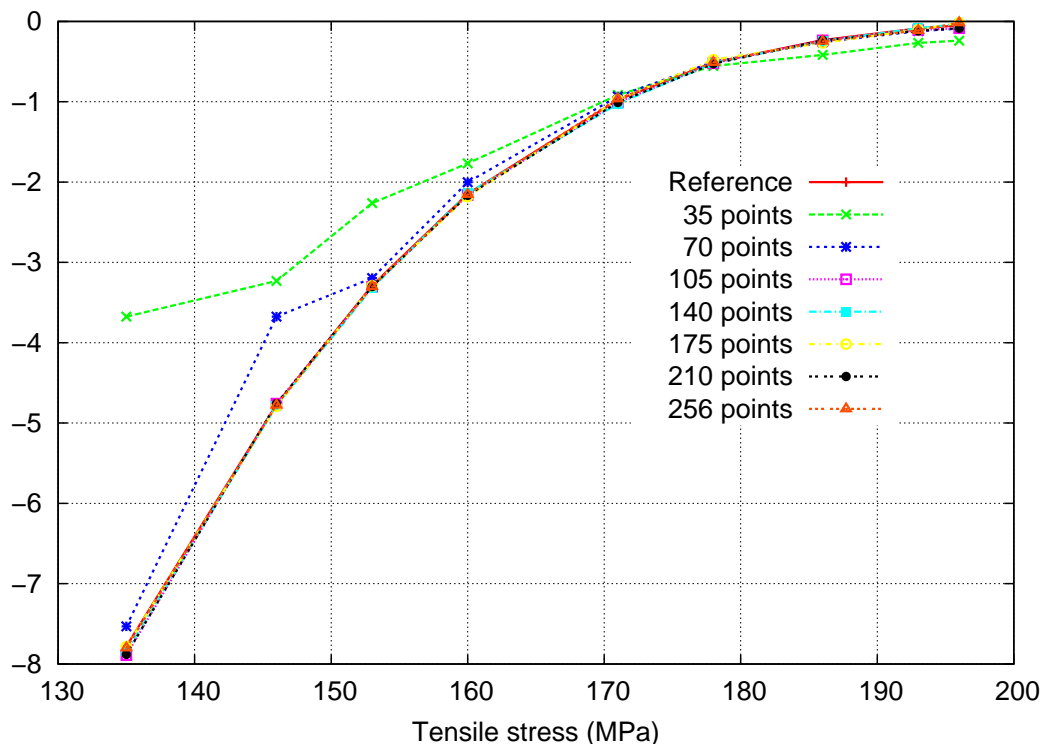


Figure 7.13: Logarithm of the failure probability vs. tensile stress using the regression method

The main difference between the direct coupling and the stochastic finite element approach should be emphasized here: the direct coupling analysis is started from scratch for each new value of σ_t , since the runs used by the iterative algorithm in FORM analysis at a lower value of σ_t cannot be reused in a

subsequent analysis at another σ_t (although the current design point at σ_t is used as a starting point for the next FORM analysis). In contrast, the deterministic runs of the finite element model that are used in the SFE approaches are carried out for all values of the loading parameter σ_t at once, and the regression or quadrature post-processing is applied afterwards.

Table 7.8: Reliability of a cracked pipe – Importance factors (%) ($\sigma_t = 200$ MPa)

Variable	Direct Coupling	Regression (105 points)
$J_{0.2}$	74.2	74.2
E	5.6	5.6
α	13.6	13.6
n	0.2	0.2
σ_y	6.4	6.4

To conclude this section, a sensitivity analysis was performed by FORM using either the finite element model \mathcal{M} or its PC expansion (regression approach). The importance factors obtained from both models are reported in Table 7.8. The obtained values are identical within less than 0.1%. This means that the SFE approach clearly represents the limit state function in a very accurate manner around the design point.

4.5 Conclusion

This third application example has shown the application of non intrusive stochastic finite element methods to an industrial non linear finite element model. In this example, both the regression and the full quadrature approaches yielded accurate results. It is likely that the Smolyak quadrature would lead to accurate results as well. Unfortunately it was not available to the author at the time when this application example was originally published.

Recently, the non intrusive methods have been applied to other industrial problems as a routine tool for uncertainty propagation and sensitivity analysis. Berveiller et al. (2007) makes use of polynomial chaos expansions together with Bayesian updating (see Chapter 5, Section 3) in order to predict the long-term creep deformation in concrete containment vessels of a nuclear power plant.

Berveiller et al. (2007) considers the sensitivity (*i.e.* the PC-based Sobol' indices, see Chapter 4, Section 5.4) of the creep deformations to the parameters of the concrete drying model.

Yameogo et al. (2007) considers PC-based Sobol' indices in the simulation of the thermo-mechanical behavior of fuel rods in nuclear reactors.

5 Conclusion

The various application examples reported in this chapter have shown all the potential of the methods described in the previous chapters.

The probabilistic framework for fatigue analysis is promising, provided new models are incorporated, such as other damage variables (*e.g.* based on cumulated plastic strains obtained from a non linear finite element analysis). The specific statistical work which was required to derive probabilistic $S-N$ curves could be fruitfully applied to other types of materials. However, since it is based on a statistical model which is rather different from (and sometimes not compatible with) the current French standard for the analysis of fatigue data, additional work is required to make it accepted by the community.

The study of cooling towers has shown that as complex a limit state function as that derived from a three-dimensional finite element analysis coupled with load carrying capacity diagrams is affordable using nowadays' power of computers. The great difference between point-in-space and space-variant probabilities of failure has been also illustrated on this example.

Finally, the use of spectral methods in industrial applications using non linear models has proven accurate and efficient. It is the opinion of the author that the polynomial chaos representation will become an everyday tool of the engineer in the near future. Indeed, it offers a cost-efficient smooth representation of complex models that could not be directly dealt with when using traditional uncertainty propagation methods that require a large number of model runs.

Chapter 8

Conclusion

Methods for modelling uncertainties in physical systems and propagating them through the associated mathematical models have been reviewed in this thesis. A general framework has been proposed, which consists in three main steps, namely the deterministic modelling, the uncertainty quantification and the uncertainty propagation, the latter being possibly linked with sensitivity analysis. Classical methods in probabilistic engineering mechanics and structural reliability have been reviewed in Chapters 2 and 3 respectively. The original contributions of the author to the field have been mainly presented in Chapters 4–7.

Spectral methods Chapter 4 has presented a state-of-the-art on spectral stochastic finite element methods, with an emphasis on non intrusive methods. The power of the spectral methods for moment, reliability and sensitivity analysis has been demonstrated. The advantage of the non intrusive approach lies in the fact that generic tools are developed that are independent from the physical system under consideration. Moreover, legacy codes can be used in conjunction with these methods without any complex implementation.

As mentioned in the presentation of regression methods, the polynomial chaos expansions may be viewed as particular metamodels. Other classes of metamodels such as wavelet decompositions or support vector machines should be investigated in the future, especially when non smooth models are considered. Techniques for assessing the accuracy of such metamodels with respect to their use are required.

The computational cost of polynomial chaos expansions remains an issue for large-scale industrial systems involving a large number of random variables, even if parallel computing on clusters of processors may be envisaged. The adaptive schemes investigated recently in the literature (either for regression or quadrature approaches) should help solve the curse of dimensionality.

It is the belief of the author that spectral methods will soon be a daily tool of the engineer in all industrial sectors where robust design is a key issue. In this sense it may become some day as popular as the finite element methods pioneered in the early 60's by Clough, Argyris and Zienkiewicz, which are nowadays inescapable in the design of complex mechanical systems.

Bayesian updating and stochastic inverse problems The Bayesian updating techniques addressed in Chapter 5 are promising for improving the predictions of the behaviour of complex systems, especially when monitoring data is gathered in time. The Markov chain Monte Carlo simulation is a versatile tool, which reveals however computationally expensive. Efforts to reduce this cost by using metamodels are necessary in this matter.

From another viewpoint, the stochastic inverse methods aim at characterizing the aleatoric uncertainty of some input quantity from the measurements of the response of a collection of real systems. A lot of

work remains to make the proposed methods computationally more efficient and more stable. In practice their coupling with metamodels is necessary to make them applicable to complex systems. They will be of utmost interest in the identification of constitutive laws (including elasto-plastic laws, fatigue criteria, damage laws, etc.) in cases when experimental scattering is not negligible.

Time and space-variant reliability methods Chapter 6 has reviewed some techniques for solving time-variant reliability problems. The PHI2 method is a refreshed presentation of a system reliability approach developed in the mid 90's. It is believed that this presentation, which clearly casts the problem in terms of time-invariant problems, may be more attractive than the asymptotic method.

Space-variant reliability is not yet as mature as time-variant reliability. It should be an important research topic in the near future. It has been observed that it should be incorporated in the analysis of deteriorating systems for the sake of efficient maintenance policies. Such problems require that the spatial variability of the input parameters is characterized. Experimental programs focusing on this aspect shall be devised in the future to feed these models.

Diffusion in the industrial applications Finally the application examples presented in Chapter 7 have shown that the methods presented all along this report are not limited to academic examples and that they are sufficiently mature to deal with complex industrial systems.

The interest in the proper treatment of uncertainties has grown up dramatically in the last five years in France, both in the academia and in the industry. This trend will amplify if the education of young engineers and scientists is fostered in this direction. This is not an easy task since the field is at the boundary of mechanics, statistics and probability theory, and may be repulsive to some people for this reason. Hopefully this report will help go beyond these prejudices and spread these fertile ideas.

Appendix A

Classical distributions and Monte Carlo simulation

1 Classical probability density functions

1.1 Normal distribution

A Gaussian random variable $X \sim \mathcal{N}(\mu, \sigma)$ is defined by two parameters, namely its mean value μ and its standard deviation σ ($\sigma > 0$). Its support is $\mathcal{D}_X = \mathbb{R}$ and its probability density function (PDF) reads:

$$f_X(x) = \frac{1}{\sigma} \varphi\left(\frac{x - \mu}{\sigma}\right) \quad (\text{A.1})$$

where the so-called standard normal PDF $\varphi(x)$ associated with $X \sim \mathcal{N}(0, 1)$ reads:

$$\varphi(x) = \frac{1}{\sqrt{2\pi}} e^{-x^2/2} \quad (\text{A.2})$$

Accordingly, the cumulative distribution function (CDF) of $X \sim \mathcal{N}(\mu, \sigma)$ reads:

$$F_X(x) = \Phi\left(\frac{x - \mu}{\sigma}\right) \quad (\text{A.3})$$

where $\Phi(x)$ denotes the standard normal CDF defined by:

$$\Phi(x) = \int_{-\infty}^x \frac{1}{\sqrt{2\pi}} e^{-x^2/2} dx \quad (\text{A.4})$$

The skewness coefficient of a Gaussian random variable is $\delta = 0$ (symmetrical PDF) and its kurtosis coefficient is $\kappa = 3$.

1.2 Lognormal distribution

A lognormal random variable $X \sim \mathcal{LN}(\lambda, \zeta)$ is such that its logarithm is a Gaussian random variable: $\log X \sim \mathcal{N}(\lambda, \zeta)$. In other words, denoting by ξ a standard normal variable, one gets:

$$X = \exp(\lambda + \zeta \xi) \quad (\text{A.5})$$

The support of a lognormal distribution is $]0, +\infty[$ and its PDF reads:

$$f_X(x) = \frac{1}{\zeta x} \varphi\left(\frac{\log x - \lambda}{\zeta}\right) \quad (\text{A.6})$$

Its CDF reads:

$$F_X(x) = \Phi\left(\frac{\log x - \lambda}{\zeta}\right) \quad (\text{A.7})$$

Its mean value μ and standard deviation σ respectively read:

$$\begin{aligned} \mu &= \exp(\lambda + \zeta^2/2) \\ \sigma &= \mu \sqrt{e^{\zeta^2} - 1} \end{aligned} \quad (\text{A.8})$$

Conversely, if the mean value and the standard deviation are known, the parameters of the distribution read:

$$\begin{aligned} \lambda &= \log \frac{\mu}{\sqrt{1 + CV^2}} \\ \zeta &= \sqrt{\log(CV^2 + 1)} \end{aligned} \quad (\text{A.9})$$

where $CV = \sigma/\mu$ is the coefficient of variation of X .

1.3 Uniform distribution

A uniform random variable $X \sim \mathcal{U}(a, b)$ is defined by the following PDF ($b > a$):

$$f_X(x) = 1/(b - a) \quad \text{for } x \in [a, b], \quad 0 \text{ otherwise} \quad (\text{A.10})$$

Its CDF reads:

$$F_X(x) = \frac{x - a}{b - a} \quad \text{for } x \in [a, b], \quad 0 \text{ otherwise} \quad (\text{A.11})$$

Its mean value and standard deviation read:

$$\begin{aligned} \mu &= \frac{a + b}{2} \\ \sigma &= \frac{b - a}{2\sqrt{3}} \end{aligned} \quad (\text{A.12})$$

Its skewness coefficient is $\delta = 0$ and its kurtosis coefficient is $\kappa = 1.8$.

1.4 Gamma distribution

A random variable follows a Gamma distribution $\mathcal{G}(\kappa, \lambda)$ if its PDF reads:

$$f_X(x) = \frac{\lambda^\kappa}{\Gamma(\kappa)} x^{\kappa-1} e^{-\lambda x} \quad \text{for } x \geq 0, \quad 0 \text{ otherwise} \quad (\text{A.13})$$

where $\Gamma(k)$ is the Gamma function defined by:

$$\Gamma(k) = \int_0^\infty t^{k-1} e^{-t} dt \quad (\text{A.14})$$

Its CDF reads:

$$F_X(x) = \gamma(k, \lambda x) / \Gamma(k) \quad \text{for } x \geq 0, \quad 0 \text{ otherwise} \quad (\text{A.15})$$

where $\gamma(k, x)$ is the incomplete Gamma function defined by:

$$\gamma(k, x) = \int_0^x t^{k-1} e^{-t} dt \quad (\text{A.16})$$

Its mean value and standard deviation read:

$$\begin{aligned} \mu &= k/\lambda \\ \sigma &= \sqrt{k}/\lambda \end{aligned} \quad (\text{A.17})$$

Its skewness and kurtosis coefficients read:

$$\begin{aligned} \delta &= 2/\sqrt{k} \\ \kappa &= 3 + 6/k \end{aligned} \quad (\text{A.18})$$

Note that the case $k = 1$ corresponds to the so-called exponential distribution whose PDF and CDF respectively read:

$$f_X(x) = \lambda e^{-\lambda x} \quad , \quad F_X(x) = 1 - e^{-\lambda x} \quad \text{for } x \geq 0, \quad 0 \text{ otherwise} \quad (\text{A.19})$$

1.5 Beta distribution

A random variable follows a Beta distribution $\mathcal{B}(r, s, a, b)$ if its PDF reads:

$$f_X(x) = \frac{(x-a)^{r-1}(b-x)^{s-1}}{(b-a)^{r+s-1}B(r, s)} \quad \text{for } x \in [a, b], \quad 0 \text{ otherwise} \quad (\text{A.20})$$

where $B(r, s)$ is the Beta function defined by:

$$B(r, s) = \int_0^1 t^{r-1}(1-t)^{s-1} dt = \frac{\Gamma(r)\Gamma(s)}{\Gamma(r+s)} \quad (\text{A.21})$$

Its CDF reads:

$$f_X(x) = \frac{1}{(b-a)^{r+s-1}B(r, s)} \int_a^x (t-a)^{r-1}(b-t)^{s-1} dt \quad \text{for } x \in [a, b], \quad 0 \text{ otherwise} \quad (\text{A.22})$$

Its mean value and standard deviation respectively read:

$$\begin{aligned} \mu &= a + (b-a) \frac{r}{r+s} \\ \sigma &= \frac{b-a}{r+s} \sqrt{\frac{rs}{r+s+1}} \end{aligned} \quad (\text{A.23})$$

1.6 Weibull distribution

A random variable follows a Weibull distribution $\mathcal{W}(\alpha, \beta)$ if its CDF reads:

$$F_X(x) = 1 - \exp\left(-\left(\frac{x}{\alpha}\right)^\beta\right) \quad \text{for } x \geq 0, \quad 0 \text{ otherwise} \quad (\text{A.24})$$

Consequently, its PDF reads:

$$f_X(x) = \frac{\beta}{\alpha} \left(\frac{x}{\alpha}\right)^{\beta-1} \exp\left(-\left(\frac{x}{\alpha}\right)^\beta\right) \quad \text{for } x \geq 0, \quad 0 \text{ otherwise} \quad (\text{A.25})$$

Its mean value and standard deviation respectively read:

$$\begin{aligned} \mu &= \alpha \Gamma(1 + 1/\beta) \\ \sigma &= \alpha \left[\Gamma(1 + 2/\beta) - \Gamma(1 + 1/\beta)^2 \right]^{1/2} \end{aligned} \quad (\text{A.26})$$

2 Monte Carlo simulation

2.1 Introduction

Monte Carlo simulation has emerged at the end of World War II as a means for solving the problem of neutronic diffusion in fissible materials (Metropolis and Ulam, 1949; Metropolis, 1987). The dramatic growth of computer capabilities in the last two decades, and especially the techniques of parallel and distributed computation have renewed the interest in this topic. It has become a generic tool that is now used in many domains of science and engineering. For a comprehensive approach of the method, the reader is referred to Rubinstein (1981).

Monte Carlo simulation consists first in producing an artificial sample set of numbers that “look like” they were random. They are generated by a purely deterministic algorithm. Once the series of numbers is available, the model is run for each and any sample. The obtained results form a pseudo-random set of outcomes of the response quantity of interest Y . This set is then used to compute estimators of the statistics of interest : mean value, standard deviation, quantiles, PDF, CDF, etc.

The generation of uniform random numbers is first described. Then the transforms that allow to simulate according to a prescribed PDF are presented.

2.2 Random number generators

The classical algorithms for simulating random numbers produce sequences of numbers that are asymptotically *uniformly distributed* over the interval $[0, 1]$ (Saporta, 2006, Chap. 15). The algorithm is usually initialized by a *seed* and produces then a periodic sequence. The efficiency of such a simulator is evaluated with respect to the period of the sequence (which has to be as large as possible), the uniformity of the samples and their respective independency.

The *linear congruential generators* (Press et al., 2002, Chap. 7) are easy-to-implement algorithms that have been used a lot in the early ages of computer science. Starting from a seed I_0 , the algorithm provides a periodic sequence of integers:

$$I_{i+1} = a I_i + b \text{ mod } (m) \quad (\text{A.27})$$

from which real numbers in the range $[0, 1]$ are obtained

$$u_i = \frac{I_i}{m - 1} \quad (\text{A.28})$$

The period is at most equal to m , but may be far smaller, depending on the choice of the constants a and b . Usually m is selected according to the type of processor of the computer at hand, *i.e.* $m = 2^p$ for a p -bit processor, since the “mod” operation in (A.27) is free in this case. This type of random number generator is implemented in the built-in `rand` function on Unix systems. The values $a = 1,664,525$, $b = 1,013,904,223$ are widely used, as reported in Press et al. (2002). Note that the linear congruential generators are known to produce sample points that lie on hyperplanes, when used in high dimensional sampling, which implies that there is some unwanted correlation between the points.

Recently, the so-called *Mersenne-Twister* algorithm has been proposed by Matsumoto and Nishimura (1998). It is based on bit manipulation in the binary representation of numbers. Its period is proven to be as large as $2^{19937} - 1$. It has a high order of dimensional equidistribution (up to $M = 623$ dimensions) as opposed to linear congruential generator. Finally it is as fast as the other common random number generators. Recent versions of the algorithm including a 64-bit implementation can be found at <http://www.math.sci.hiroshima-u.ac.jp/m-mat/MT/emt.html>.

2.3 Non uniform sampling

In practice, the input random variables to be simulated have a prescribed PDF which is not uniform over $[0, 1]$. The acceptance / rejection method is a powerful approach that can be used in general cases. The transformation method, which is based on the following lemma, is efficient when a closed-form expression of the inverse cumulative distribution function exists.

Lemma A.1. *Let X be a continuous random variable with prescribed CDF $F_X(x)$. The random variable $U = F_X(X)$ has a uniform distribution over $[0, 1]$.*

Proof : By definition of the CDF, U is defined on the range $[0, 1]$. The PDF of $U = F_X(X)$ satisfies $f_U(u) = f_X(x) J_{x,u}$ where $J_{x,u}$ is the Jacobian of the transform $u \mapsto x = F_X^{-1}(u)$ which is equal to $1/f_X(x)$. Thus $f_U(u) = 1$. \diamond

The following algorithm for generating a sample set $\{x^{(1)}, \dots, x^{(n)}\}$ according to a sampling density $f_X(x)$ straightforwardly follows:

1. generate a sample set $\{u^{(1)}, \dots, u^{(n)}\}$ according to the uniform distribution over $[0, 1]$.
2. back-transform the sample points one-by-one:

$$x^{(i)} = F_X^{-1}(u^{(i)}) \quad i = 1, \dots, n \quad (\text{A.29})$$

The algorithm is illustrated in Figure A.1, where a uniform sample set of 1,000 points has been used.

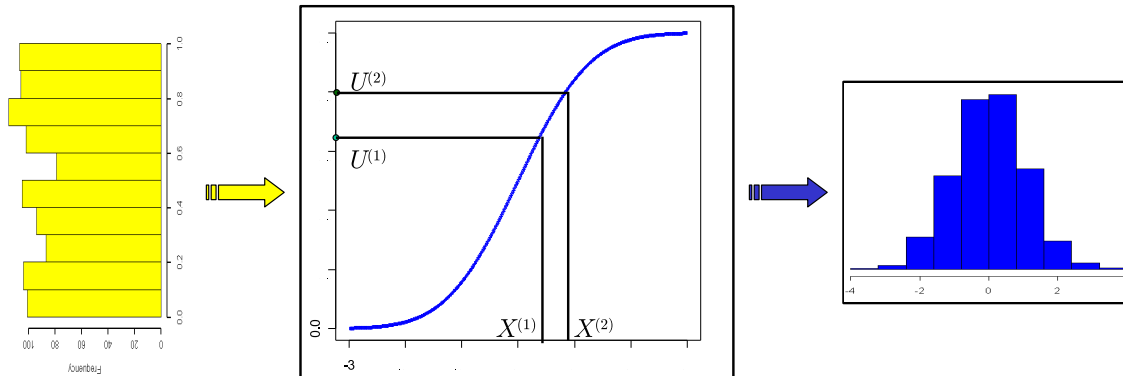


Figure A.1: Simulation of a Weibull random variable by the inverse CDF method

A particular algorithm may be used in order to generate standard normal Gaussian random variables, due to a result by Box and Muller (1958).

Lemma A.2. *Let U_1, U_2 be two independent random variables uniformly distributed over $]0, 1[$. The variables ξ_1, ξ_2 defined in Eq.(A.30) are independent standard normal random variables.*

$$\begin{aligned} \xi_1 &= \sqrt{-2 \log U_1} \sin(2\pi U_2) \\ \xi_2 &= \sqrt{-2 \log U_1} \cos(2\pi U_2) \end{aligned} \quad (\text{A.30})$$

Proof : Let us denote by $f_U(u_1, u_2)$ the joint probability density function of $U = \{U_1, U_2\}^T$:

$$f_U(u_1, u_2) = \mathbf{1}_{[0,1]}(u_1) \mathbf{1}_{[0,1]}(u_2) \quad (\text{A.31})$$

The joint probability density function of $\Xi = \{\xi_1, \xi_2\}^T$ reads:

$$f_\Xi(\xi_1, \xi_2) = f_U(u_1, u_2) |\det \mathcal{J}_{U, \Xi}| \quad (\text{A.32})$$

where $\mathcal{J}_{\mathbf{U}, \Xi}$ is the Jacobian of the mapping $\mathbf{U} \mapsto \Xi$ from $[0, 1] \times [0, 1] \mapsto \mathbb{R}^2$. From (A.30) this mapping reads:

$$\begin{aligned} U_1 &= \exp [-(\xi_1^2 + \xi_2^2)/2] \\ U_2 &= \frac{1}{2\pi} \arctan \xi_1/\xi_2 \end{aligned} \quad (\text{A.33})$$

Thus:

$$\mathcal{J}_{\mathbf{U}, \Xi} = \begin{pmatrix} -\xi_1 U_1 & \xi_2 U_1 \\ \frac{1}{2\pi} \frac{1/\xi_2}{1 + (\xi_1/\xi_2)^2} & \frac{1}{2\pi} \frac{-\xi_1/\xi_2^2}{1 + (\xi_1/\xi_2)^2} \end{pmatrix} \quad (\text{A.34})$$

from which one gets:

$$f_{\Xi}(\xi_1, \xi_2) = \exp [-(\xi_1^2 + \xi_2^2)/2] / 2\pi \quad (\text{A.35})$$

thus the lemma. \diamond

This result allows one to generate a standard normal sample set without using the inverse standard normal CDF (which has indeed no closed-form expression):

$$\begin{aligned} \xi^{(2i-1)} &= \sqrt{-2 \log u^{(2i-1)}} \sin (2\pi u^{(2i)}) \\ \xi^{(2i)} &= \sqrt{-2 \log u^{(2i-1)}} \cos (2\pi u^{(2i)}) \end{aligned} \quad i = 1, \dots, [n/2] + 1 \quad (\text{A.36})$$

It is then straightforward to simulate Gaussian variates $X \sim \mathcal{N}(\mu, \sigma)$ by a linear transform $X = \mu + \sigma \xi$:

$$x^{(i)} = \mu + \sigma \xi^{(i)} \quad i = 1, \dots, n \quad (\text{A.37})$$

Similarly, a lognormal random variable $X \sim \mathcal{LN}(\lambda, \zeta)$ can be obtained by $X = \exp(\lambda + \zeta \xi)$. Thus the lognormally-distributed sample:

$$x^{(i)} = \exp(\lambda + \zeta \xi^{(i)}) \quad i = 1, \dots, n \quad (\text{A.38})$$

When a random vector \mathbf{X} with independent components is to be simulated, the above methods can be applied component by component. When the complete joint PDF $f_{\mathbf{X}}(\mathbf{x})$ is prescribed, specific methods have to be used.

Approximate transformations such as the Nataf transform may be used in order to approximate \mathbf{X} as a function of a standard normal vector Ξ . The latter is then simulated and the transform is applied to the standard normal sample set.

3 Nataf transform

The Nataf transform (Nataf, 1962) has been introduced in the field of structural engineering by Der Kiureghian and Liu (1986). It allows to build a multidimensional PDF that fits some prescribed marginal distributions and some correlation matrix.

Suppose a random vector \mathbf{X} has prescribed marginal distributions, say $F_{X_i}(x_i)$, $i = 1, \dots, M$ and correlation matrix \mathbf{R} . It is possible to transform the components of \mathbf{X} into standard normal random variables ξ_i , $i = 1, \dots, M$:

$$\xi_i = \Phi^{-1}(F_{X_i}(x_i)) \quad (\text{A.39})$$

The Nataf transform assumes that $\Xi = \{\xi_1, \dots, \xi_M\}^T$ is a standard normal *correlated* random vector whose joint PDF reads:

$$f_{\Xi}(\xi) = \varphi_M(\xi; \tilde{\mathbf{R}}) \quad (\text{A.40})$$

where $\varphi_M(\xi; \tilde{\mathbf{R}})$ is the multidimensional normal PDF:

$$\varphi_M(\xi; \tilde{\mathbf{R}}) = (2\pi)^{-M/2} \exp \left[-\frac{1}{2} \xi^T \cdot \tilde{\mathbf{R}}^{-1} \cdot \xi \right] \quad (\text{A.41})$$

and $\tilde{\mathbf{R}}$ is a *pseudo-correlation matrix* that should be compatible with the prescribed correlation matrix \mathbf{R} . From the above equations, one can write:

$$f_{\mathbf{X}}(\mathbf{x}) = f_{\Xi}(\boldsymbol{\xi}) |\det \mathcal{J}_{\Xi, \mathbf{X}}| \quad (\text{A.42})$$

where the Jacobian of the transform is a diagonal matrix:

$$\mathcal{J}_{\Xi, \mathbf{X}} = \text{diag} \left(\frac{f_{X_1}(x_1)}{\varphi(\xi_1)}, \dots, \frac{f_{X_M}(x_M)}{\varphi(\xi_M)} \right) \quad (\text{A.43})$$

This leads to the Nataf transform (1962):

$$f_{\mathbf{X}}(\mathbf{x}) = \frac{f_{X_1}(x_1) \cdots f_{X_M}(x_M)}{\varphi(\xi_1) \cdots \varphi(\xi_M)} \varphi_M(\boldsymbol{\xi}, \tilde{\mathbf{R}}) \quad (\text{A.44})$$

The pseudo-correlation matrix $\tilde{\mathbf{R}}$ is computed term by term by solving the following consistency equation for $\tilde{\mathbf{R}}_{ij}$:

$$\mathbf{R}_{ij} = \int_{\mathbb{R}^2} \left(\frac{x_i - \mu_{X_i}}{\sigma_{X_i}} \right) \left(\frac{x_j - \mu_{X_j}}{\sigma_{X_j}} \right) \varphi_2(\xi_i, \xi_j, \tilde{\mathbf{R}}_{ij}) d\xi_i d\xi_j \quad (\text{A.45})$$

Due to the burden of such a computation in the general case, values of $\tilde{\mathbf{R}}_{ij}/\mathbf{R}_{ij}$ have been tabulated for various couples of distributions $(f_{X_i}(x_i), f_{X_j}(x_j))$ in Der Kiureghian and Liu (1986); Liu and Der Kiureghian (1986), see also Melchers (1999, Appendix B).

It is important to mention that the above equations do not always have a solution, depending on the input marginal distributions. Moreover, the obtained pseudo-correlation matrix $\tilde{\mathbf{R}}$ may not be a correlation matrix in the sense that it may not be positive definite.

It is interesting to note that the introduction of the copula theory briefly mentioned in Chapter 4 should be of great help in this matter. Indeed, assuming a Nataf distribution for a random vector with prescribed margins is equivalent to considering a Gaussian copula.

Appendix B

Orthogonal polynomials and quadrature schemes

1 Orthogonal polynomials

1.1 Definition

Let us consider a weight function $w : \mathcal{B} \subset \mathbb{R} \mapsto \mathbb{R}$ such that $w(x) \geq 0 \forall x \in \mathcal{B}$ and $\int_{\mathcal{B}} w(x) dx = 1$. Let us consider the space of square integrable functions with respect to this weight function. This is a Hilbert space denoted by \mathcal{H} when equipped with the following inner product:

$$\langle f, g \rangle_{\mathcal{H}} \equiv \int_{\mathcal{B}} f(x) g(x) w(x) dx \quad (\text{B.1})$$

A set of orthogonal polynomials with respect to w may be obtained by a Gram-Schmidt orthogonalization of the monomials $\{x^k, k \in \mathbb{N}\}$. This leads to the following recurrence relationship:

$$\begin{aligned} P_{-1}(x) &\equiv P_0(x) = 1 \\ P_{k+1}(x) &= (x - a_k) P_k(x) - b_k P_{k-1}(x) \quad \forall k \in \mathbb{N}^* \end{aligned} \quad (\text{B.2})$$

where the coefficients (a_k, b_k) read:

$$a_k = \frac{\langle x P_k, P_k \rangle_{\mathcal{H}}}{\langle P_k, P_k \rangle_{\mathcal{H}}} \quad (\text{B.3})$$

$$b_k = \frac{\langle P_k, P_k \rangle_{\mathcal{H}}}{\langle P_{k-1}, P_{k-1} \rangle_{\mathcal{H}}} \quad (\text{B.4})$$

1.2 Classical orthogonal polynomials

The well-known families of orthogonal polynomials that correspond to classical probability density functions are reported in Table B.1 (Abramowitz and Stegun, 1970). The associated orthonormal Hilbertian basis of \mathcal{H} denoted by $\{\psi_k(x) = P_k(x)/\sqrt{\langle P_k, P_k \rangle_{\mathcal{H}}}, k \in \mathbb{N}\}$ is also given.

Links between the various families and the so-called hypergeometric functions have been shown in Askey and Wilson (1985), see also Xiu and Karniadakis (2002) for their use in stochastic finite element analysis. The properties of the Legendre and Hermite polynomials that have been more specifically used in this thesis are then reviewed for the sake of completeness.

Table B.1: Orthogonal polynomials associated with classical probability density functions

Type of variable	Weight functions	Orthogonal polynomials	Hilbertian basis $\psi_k(x)$
Uniform	$\mathbf{1}_{]-1,1[}(x)/2$	Legendre $P_k(x)$	$P_k(x)/\sqrt{\frac{1}{2k+1}}$
Gaussian	$\frac{1}{\sqrt{2\pi}}e^{-x^2/2}$	Hermite $H_{e_k}(x)$	$H_{e_k}(x)/\sqrt{k!}$
Gamma	$x^a e^{-x} \mathbf{1}_{\mathbb{R}^+}(x)$	Laguerre $L_k^a(x)$	$L_k^a(x)/\sqrt{\frac{\Gamma(k+a+1)}{k!}}$
Beta	$\mathbf{1}_{]-1,1[}(x) \frac{(1-x)^a(1+x)^b}{B(a)B(b)}$	Jacobi $J_k^{a,b}(x)$	$J_k^{a,b}(x)/\tilde{\mathfrak{J}}_{a,b,k}$
		$\tilde{\mathfrak{J}}_{a,b,k}^2 = \frac{2^{a+b+1}}{2k+a+b+1} \frac{\Gamma(k+a+1)\Gamma(k+b+1)}{\Gamma(k+a+b+1)\Gamma(k+1)}$	

1.3 Hermite polynomials

The Hermite polynomials $He_n(x)$ are solution of the following differential equation:

$$y'' - xy' + ny = 0 \quad , \quad n \in \mathbb{N} \quad (\text{B.5})$$

They may be generated in practice by the following recurrence relationship:

$$He_{-1}(x) \equiv He_0(x) = 1 \quad (\text{B.6})$$

$$He_{n+1}(x) = xHe_n(x) - nHe_{n-1}(x) \quad , \quad n \in \mathbb{N} \quad (\text{B.7})$$

They are orthogonal with respect to the Gaussian probability measure:

$$\int_{-\infty}^{\infty} He_m(x) He_n(x) \varphi(x) dx = n! \delta_{mn} \quad (\text{B.8})$$

where δ_{mn} is the Kronecker symbol: $\delta_{mn} = 1$ if $m = n$ and 0 otherwise. If ξ is a standard normal random variable, the following relationship holds:

$$\mathbb{E}[He_m(\xi) He_n(\xi)] = n! \delta_{mn} \quad (\text{B.9})$$

The first three Hermite polynomials are:

$$He_1(x) = x \quad He_2(x) = x^2 - 1 \quad He_3(x) = x^3 - 3x \quad (\text{B.10})$$

1.4 Legendre polynomials

The Legendre polynomials $P_n(x)$ are solution of the following differential equation:

$$(1-x^2)y'' - 2xy' + n(n+1)y = 0 \quad , \quad n \in \mathbb{N} \quad (\text{B.11})$$

They may be generated in practice by the following recurrence relationship:

$$P_{-1}(x) \equiv P_0(x) = 1 \quad (\text{B.12})$$

$$(n+1)P_{n+1}(x) = (2n+1)xP_n(x) - nP_{n-1}(x) \quad , \quad n \in \mathbb{N} \quad (\text{B.13})$$

They are orthogonal with respect to the uniform probability measure over $[-1, 1]$:

$$\int_{-1}^1 P_m(x) P_n(x) dx = \frac{2}{2n+1} \delta_{mn} \quad (\text{B.14})$$

If U is a random variable with uniform PDF over $[-1, 1]$, the following relationship holds:

$$\mathbb{E}[P_m(U) P_n(U)] = \frac{1}{2n+1} \delta_{mn} \quad (\text{B.15})$$

The first three Legendre polynomials are:

$$P_1(x) = x \quad P_2(x) = \frac{1}{2}(3x^2 - 1) \quad P_3(x) = \frac{1}{2}(5x^3 - 3x) \quad (\text{B.16})$$

2 Gaussian quadrature rules

Let us consider the following one-dimensional integral :

$$I = \int_{\mathcal{B}} f(x)w(x) dx \quad (\text{B.17})$$

A quadrature rule consists in approximating I by a weighted sum of evaluations of the integrand:

$$I \approx \mathcal{Q}^K(f) \equiv \sum_{k=1}^K w_k f(x_k) \quad (\text{B.18})$$

In this equation, K is the order of the quadrature rule and $\{w_k, k = 1, \dots, K\}$ (resp. $\{x_k, k = 1, \dots, K\}$) are the integration weights (resp. points).

The so-called *Gaussian quadrature scheme* ensures the optimal accuracy for the integration of polynomial functions. Precisely, the integration weights and points are selected so that the K -th order quadrature rule exactly integrates the polynomials up to order $2K - 1$. It can be proven that the corresponding integration points are the roots of polynomial P_K . The associated weights read:

$$w_k = \frac{\langle P_{K-1}, P_{K-1} \rangle_{\mathcal{H}}}{P'_K(x_k)P_{K-1}(x_k)} \quad (\text{B.19})$$

The Gaussian quadrature schemes are the most efficient in terms of degree of exactness for polynomial integration. However, it is worth emphasizing that the integration points are completely different when moving from a K -th order to a $(K+1)$ -th order scheme. This means that evaluations of f used to compute $\mathcal{Q}^K(f)$ cannot be used to compute $\mathcal{Q}^{K+1}(f)$. This may be a drawback when adaptive integration schemes are considered. Note that nested schemes, for which the set of points used in \mathcal{Q}^{K+1} contains the set of points use in \mathcal{Q}^K exist, *e.g.* the Clenshaw-Curtis scheme (Clenshaw and Curtis, 1960).

Appendix C

Academic achievements

1 Academic distinctions

1.1 Awards

- 2000 *Best Ph.D thesis of Year 1999* at the Ecole Nationale des Ponts et Chaussées, awarded by the *Fondation de l'Ecole Nationale des Ponts et Chaussées*, Paris, France.
- 2003 *SMIRT Junior Award* by the *International Association for Structural Mechanics in Reactor Technology* (IASMIRT) to the best paper of the SMIRT17 Conference by a young researcher: “Reliability of the repairing of double wall containment vessels in the context of leak tightness assessment”.
- 2005 *Jean Mandel Prize*. National distinction awarded by the *Association Française de Mécanique* (AFM) every second year to a young researcher under 35 in mechanics.

1.2 Honors

- Since 2004 Member of the Advisory Council of the *International Forum on Engineering Decision Making* (IFED).
- Since 2004 Member of the *Joint Committee on Structural Safety* (JCSS).
- Since 2005 Member of the Working Group on *Reliability and Optimization of Structural Systems*, International Federation for Information Processing (IFIP WG 7.5).
- Since 2007 Member of the Board of Directors of the *International Civil Engineering Risk and Reliability Association*, (CERRA), which organizes the International Conferences on Applications of Statistics and Probability in Civil Engineering (ICASP).

1.3 Participation in Ph.D jury

1.3.1 Co-supervisor of the Ph.D

- Céline Andrieu-Renaud, *Fiabilité mécanique des structures soumises à des phénomènes physiques dépendant du temps*, Université Blaise Pascal, Clermont-Ferrand, 13 décembre 2002.
- Zakoua Guédé, *Approche probabiliste de la durée de vie des structures soumises à la fatigue thermique*, Université Blaise Pascal, Clermont-Ferrand, 7 juin 2005.

- Marc Berveiller, *Eléments finis stochastiques – Analyse de sensibilité, analyse de fiabilité*, Université Blaise Pascal, Clermont-Ferrand, 18 octobre 2005.

1.3.2 External examiner

- Franck Alexandre, *Aspects probabilistes et microstructuraux de l'amorçage des fissures de fatigue dans l'alliage Inco 718*, Ecole Nationale Supérieure des Mines de Paris, 12 Mars 2004.
- Cyrille Schwob, *Approche non locale probabiliste pour l'analyse en fatigue des zones à gradient de contraintes*, Université Paul Sabatier, Toulouse, 21 Mai 2007.
- Xuan Son Nguyen, *Algorithmes probabilistes pour la durabilité et la mécanique des ouvrages de Génie Civil*, Université Paul Sabatier, Toulouse, 15 Octobre 2007.

1.4 Invited lectures and seminars

- *Eléments finis stochastiques : historique et nouvelles perspectives*, Keynote lecture, 16^e Congrès Français de Mécanique, Nice (4 Septembre 2003).
- *Eléments finis stochastiques : historique et nouvelles perspectives*, Université Technologique de Compiègne (26 Septembre 2003).
- *Fiabilité des structures et mécanique probabiliste – Théorie et applications*, Académie des Technologies, as a part of the *Enquête sur les frontières de la simulation numérique*, Paris (4 Décembre 2003).
- *Fiabilité des structures et mécanique probabiliste*, Ecole Supérieure d'ingénieurs Léonard de Vinci, Paris La Défense (9 et 16 Janvier 2004).
- *Eléments finis stochastiques : approches Galerkin et non intrusives*, Séminaire EDF R&D/ SINET-ICS, Clamart (24 Novembre 2004).
- *Approches non intrusives des éléments finis stochastiques*, The Computational Stochastic Mechanics Association (CSMA), Ecole Centrale de Paris (19 Janvier 2005).
- *Mécanique probabiliste et fiabilité des structures*, Centre des Matériaux P.M. Fourt, Ecole des Mines de Paris (21 Novembre 2005).
- *Propagation d'incertitudes par éléments finis stochastiques – Méthodes intrusives et non intrusives*, Institut de Recherche en Génie Civil et Mécanique, Université de Nantes (8 Mars 2007).

1.5 Organization of scientific events

- | | |
|------|---|
| 2003 | Member of the Scientific Committee of the 9th International Conference on Applications of Statistics and Probability in Civil Engineering (ICASP9), San Francisco, USA. |
| 2007 | Co-organizer of the mini-symposium on <i>probabilistic approaches</i> in the 18 ^e Congrès Français de Mécanique, Grenoble. |
| 2007 | Member of the International Scientific Committee of the 10th International Conference on Applications of Statistics and Probability in Civil Engineering (ICASP10), Tokyo, Japan. |

1.6 Peer reviewing

Since 2004, I reviewed numerous papers for the following journals:

- Canadian Geotechnical Journal;
- Civil Engineering and Environmental Systems;
- Computer Methods in Applied Mechanics and Engineering;
- European Journal of Computational Mechanics (formerly Revue Européenne des Eléments Finis);
- International Journal of Fatigue;
- Journal of Computational Physics;
- Journal of Geotechnical and Geoenvironmental Engineering (ASCE);
- Mécanique & Industries;
- Reliability Engineering & System Safety;
- SIAM Journal on Scientific Computing;
- Structure and Infrastructure Engineering.

2 Teaching

I have been teaching classes of *structural mechanics* at the Ecole Nationale des Ponts et Chaussées (Marne-la-Vallée) since 1998 under Prs. Yves Bamberger (1998-1999), Adnan Ibrahimbegovic (2001), Philippe Bisch (since 2002) (30 hours/year).

I have designed a new course on *probabilistic mechanics and structural reliability* at the Ecole Supérieure d'ingénieurs Léonard de Vinci (Paris La Défense). I have been teaching this course since 2004 (21 hours/year).

I have been giving a seminar entitled “*Introduction to structural reliability and stochastic finite element methods*” within the short course on “*Physics and mechanics of random media*” supervised by Pr. Dominique Jeulin at the Ecole des Mines de Paris (March 2006 and March 2007, 3 hours).

I have taught two classes entitled *time-variant reliability* and *industrial applications of structural reliability* in the short course on “*probabilistic approach of design in uncertain environment*” supervised by Pr. Maurice Lemaire (Institut pour la Promotion des Sciences de l'Ingénieur, 14-16 November, 2006).

3 Supervising students

3.1 Ph.D students

The Ph.D students listed below were co-supervised by Pr. Maurice Lemaire, *Laboratoire de Mécanique et Ingénieries*, Institut Français de Mécanique Avancée et Université Blaise Pascal, Clermont-Ferrand.

- 2006- Gérard Blatman, *Eléments finis stochastiques adaptatifs et méta-modèles pour la propagation d'incertitudes* (Adaptive stochastic finite element methods and metamodels for uncertainty propagation).
- 2004-2007 Frédéric Perrin, *Intégration des données expérimentales dans les modèles probabilistes de prédiction de la durée de vie des structures* (Experimental data integration in probabilistic models for the lifetime assessment of structures).
- 2002-2005 Marc Berveiller, *Eléments finis stochastiques – Analyse de sensibilité, analyse de fiabilité* (Stochastic finite element methods for sensitivity and reliability analyses).
- 2001-2005 Zakoua Guédé, *Approche probabiliste de la durée de vie des structures soumises à la fatigue thermique* (Probabilistic framework for the assessment of structures submitted to thermal fatigue).
- 2001-2002 Céline Andrieu-Renaud, *Fiabilité mécanique des structures soumises à des phénomènes physiques dépendant du temps* (Time-variant reliability analysis of structural systems).

Additionally, I co-supervised the Ph.D thesis of Roman Gaignaire (2004-2007) at the *Laboratoire d'Électrotechnique et d'Électronique de Puissance de Lille*, Université de Lille, with Pr. Stéphane Clénet.

3.2 MS students

- 2006 Gérard Blatman, *Méthodes non intrusives pour les analyses de sensibilité en modélisation probabiliste*.
- 2003 Thomas Sgarbi, *Couplages mécano-probabiliste pour des problèmes statiques ou dépendant du temps*.
- 2002 Imane Cherradi, *Méthodes de quadrature pour la fiabilité des structures*.
- 2002 Marc Berveiller, *Etude mécano-fiabiliste de la réparation par revêtement des enceintes de confinement*.
- 2001 Sonia Blayac, *Utilisation des réseaux de neurones pour la maintenance des tuyauteries de centrale nucléaire*.
- 2001 Sébastien Dron, *Etude fiabiliste d'un aéro-réfrigérant avec prise en compte de la corrosion des armatures*.
- 1998 Stefan Lenz, *Modélisation multiphasique de matériaux renforcés*.

4 List of publications

4.1 Thesis and monography

1. Sudret, B. (1999). *Modélisation multiphasique des ouvrages renforcés par inclusions*. Ph.D. thesis, Ecole Nationale des Ponts et Chaussées, Paris, France, 364 pages.
2. Sudret, B. and Der Kiureghian, A. (2000). *Stochastic finite elements and reliability: a state-of-the-art report*. Technical Report UCB/SEMM-2000/08, University of California, Berkeley, 173 pages.

4.2 Book chapters

1. Sudret, B. (2006). Time-variant reliability methods. In M. Lemaire (Ed.), *Approche probabiliste de la conception et du dimensionnement en contexte incertain*, chapter 11. Institut pour la Promotion des Sciences de l'Ingénieur (IPSI).

2. Sudret, B. (2006). Industrial applications. In M. Lemaire (Ed.), *Approche probabiliste de la conception et du dimensionnement en contexte incertain*, chapter 12. Institut pour la Promotion des Sciences de l'Ingénieur (IPSI).
3. Sudret, B. and Berveiller, M. (2007). Stochastic finite element methods in geotechnical engineering. In K.K. Phoon (Ed.), *Reliability-based design in geotechnical engineering: computations and applications*, chapter 7. Taylor and Francis. To appear.
4. Sudret, B. (2007). Approche probabiliste de la résistance à la fatigue des structures. In C. Bathias and A.-G. Pineau (Eds.), *Fatigue des matériaux et des structures*, Vol. 2, chapter 5. Editions Hermès (3^e édition). In preparation.

4.3 Peer-reviewed journal papers

1. Lieb, M. and Sudret, B. (1998). A fast algorithm for soil dynamics calculations by wavelet decomposition. *Arch. App. Mech.*, **68**, pp. 147–157.
2. Sudret, B., Maghous, S., de Buhan, P. and Bernaud, D. (1998). Elastoplastic analysis of inclusion reinforced structures. *Metals and materials*, **4**(3), pp. 252–255.
3. Sudret, B. and de Buhan, P. (1999). Modélisation multiphasique de matériaux renforcés par inclusions linéaires. *C. R. Acad. Sci. Paris*, **327**(Série IIb), pp. 7–12.
4. de Buhan, P. and Sudret, B. (1999). A two-phase elastoplastic model for unidirectionally-reinforced materials and its numerical implementation. *Eur. J. Mech. A/Solids*, **18**(6), pp. 995–1012.
5. de Buhan, P. and Sudret, B. (2000). Micropolar multiphase model for materials reinforced by linear inclusions. *Eur. J. Mech. A/Solids*, **19**(6), pp. 669–687.
6. de Buhan, P. and Sudret, B. (2000). Un modèle de comportement macroscopique des matériaux renforcés par inclusions linéaires, avec prise en compte des effets de flexion. *C. R. Acad. Sci. Paris*, **328**(Série IIb), pp. 555–560.
7. Sudret, B. and de Buhan, P. (2001). Multiphase model for reinforced geomaterials – application to piled raft foundations and rock-bolted tunnels. *Int. J. Num. Anal. Meth. Geomech.*, **25**, pp. 155–182.
8. Bourgeois, E., Garnier, D., Semblat, J.-F., Sudret, B. and Al Hallak, R. (2001). Un modèle homogénéisé pour le boulonnage du front de taille des tunnels : simulation d'essais en centrifugeuse. *Revue Française de Génie Civil*, **5**(1), pp. 8–38.
9. Sudret, B. and Der Kiureghian, A. (2002). Comparison of finite element reliability methods. *Prob. Eng. Mech.*, **17**, pp. 337–348.
10. Garnier, D., Sudret, B., Bourgeois, E. and Semblat, J.-F. (2003). Ouvrages renforcés : approche par superposition de milieux continus et traitement numérique. *Revue Française de Géotechnique*, **102**, pp. 43–52.
11. Andrieu-Renaud, C., Sudret, B. and Lemaire, M. (2004). The PHI2 method: a way to compute time-variant reliability. *Rel. Eng. Sys. Safety*, **84**, pp. 75–86.
12. Sudret, B., Berveiller, M. and Lemaire, M. (2004). A stochastic finite element method in linear mechanics. *Comptes Rendus Mécanique*, **332**, pp. 531–537.
13. Sudret, B., Defaux, G. and Pendola, M. (2005). Time-variant finite element reliability analysis – application to the durability of cooling towers. *Structural Safety*, **27**, pp. 93–112.

14. Sudret, B. and Guédé, Z. (2005). Probabilistic assessment of thermal fatigue in nuclear components. *Nuc. Eng. Des.*, **235**, pp. 1819–1835.
15. Berveiller, M., Sudret, B. and Lemaire, M. (2006). Stochastic finite elements: a non intrusive approach by regression. *Eur. J. Comput. Mech.*, **15**(1-3), pp. 81–92.
16. Sudret, B., Berveiller, M. and Lemaire, M. (2006). A stochastic finite element procedure for moment and reliability analysis. *Eur. J. Comput. Mech.*, **15**(7-8), pp. 825–866.
17. Guédé, Z., Sudret, B. and Lemaire, M. (2007). Life-time reliability based assessment of structures submitted to thermal fatigue. *Int. J. Fatigue*, **29**(7), pp. 1359–1373.
18. Gaignaire, R., Clénet, S., Sudret, B. and Moreau, O. (2007). 3-D spectral stochastic finite element method in electromagnetism. *IEEE Trans. Electromagnetism*, **43**(4), pp. 1209–1212.
19. Sudret, B., Defaux, G. and Pendola, M. (2007). Stochastic evaluation of the damage length in RC beams submitted to corrosion of reinforcing steel. *Civ. Eng. Envir. Sys.*, **24**(2), pp. 165–178.
20. Blatman, G., Sudret, B. and Berveiller, M. (2007). Quasi random numbers in stochastic finite element analysis. *Mécanique & Industries*, **8**, pp. 289–297.
21. Sudret, B. (2007). Probabilistic models for the extent of damage in degrading reinforced concrete structures. *Rel. Eng. Sys. Safety*, **93**, pp. 410–422.
22. Sudret, B. (2008). Analytical derivation of the outcrossing rate in time-variant reliability problems. *Struc. Infra. Eng.* In press.
23. Sudret, B. (2008). Global sensitivity analysis using polynomial chaos expansions. *Rel. Eng. Sys. Safety*. In press.

4.4 International conference papers

1. Sudret, B. and de Buhan, P. (1998). Multiphase model of reinforced materials. In *Proc. 2nd Int. PhD Symposium in Civil Engineering, Budapest, Hungary*, pp. 516–523.
2. Sudret, B. and de Buhan, P. (1999). Reinforced geomaterials: computational model and applications. In R.C. Picu and E. Krempl (Eds.), *Proc. 4th Int. Conf. on Constitutive Laws for Engineering Materials (CLEM'99), Troy, USA*, pp. 339–342.
3. Sudret, B., Lenz, S. and de Buhan, P. (1999). A multiphase constitutive model for inclusion-reinforced materials: theory and numerical implementation. In *Proc. 1st Eur. Conf. Comput. Mech. (ECCM'99), Munich, Germany*.
4. Sudret, B. and de Buhan, P. (2000). Multiphase model for piled raft foundations: the Messeturm case history. In *Proc. Eur. Congress Comput. Meth. Applied Sci. Eng. (ECCOMAS'2000), Barcelona, Spain*.
5. Bourgeois, E., Semblat, J.-F., Garnier, D. and Sudret, B. (2001). Multiphase model for the 2D and 3D numerical analysis of pile foundations. In *Proc. 10th Conf. of the Int. Assoc. Comput. Meth. Adv. Geomech. (IACMAG), Tucson, Arizona, USA*. Balkema, Rotterdam.
6. Garnier, D., Sudret, B., Bourgeois, E. and Semblat, J.-F. (2001). Analyse d'ouvrages renforcés par une approche de modèle multiphasique. In *Proc. 15th Int. Congress Soil Mech. Geotech. Eng. (ICSMGE), Istanbul, Turkey*.
7. Sudret, B., Dron, S. and Pendola, M. (2002). Time-variant reliability analysis of cooling towers including corrosion of steel in reinforced concrete. In *Proc. $\lambda\mu 13$ – ESREL'2002 Safety and Reliability Conf., Lyon, France*, pp. 571–575.

8. Andrieu, C., Lemaire, M. and Sudret, B. (2002). The PHI2 method: a way to assess time-variant reliability using classical reliability tools. In *Proc. $\lambda\mu 13$ – ESREL'2002 Safety and Reliability Conf., Lyon, France*, pp. 472–475.
9. Sudret, B. and Pendola, M. (2002). Reliability analysis of cooling towers: influence of rebars corrosion on failure. In *Proc. 10th Int. Conf. on Nucl. Eng. (ICONE10), Washington, USA*, pp. 571–575. Paper #22136.
10. Sudret, B., Defaux, G., Andrieu, C. and Lemaire, M. (2002). Comparison of methods for computing the probability of failure in time-variant reliability using the outcrossing approach. In P. Spanos and G. Deodatis (Eds.), *Proc. 4th Int. Conf. on Comput. Stoch. Mech (CSM4), Corfu, Greece*.
11. Sudret, B. (2002). Comparison of the spectral stochastic finite element method with the perturbation method for second moment analysis. In *Proc. 1st Int. ASRANet Colloquium, Glasgow, United Kingdom*.
12. Sudret, B., Berveiller, M. and Heinfling, G. (2003). Reliability of the repairing of double wall containment vessels in the context of leak tightness assessment. In *Trans. 17th Int. Conf. on Struct. Mech. in Reactor Tech. (SMiRT 17), Prague, Czech Republic*. Paper M-264.
13. Sudret, B., Guédé, Z., Hornet, P., Stéphan, J.-M. and Lemaire, M. (2003). Probabilistic assessment of fatigue life including statistical uncertainties in the S-N curve. In *Trans. 17th Int. Conf. on Struct. Mech. in Reactor Tech. (SMiRT 17), Prague, Czech Republic*. Paper M-232.
14. Sudret, B. and Heinfling, G. (2003). Methodology for the reliability evaluation of containment vessels repair through the coupling of finite elements and probabilistic analyses. In *Proc. 2nd Int. Workshop on Aging Management of Concrete Structures, Paris, France*.
15. Sudret, B. and Cherradi, I. (2003). Quadrature method for finite element reliability analysis. In A. Der Kiureghian, S. Madanat and J. Pestana (Eds.), *Proc. 9th Int. Conf. on Applications of Stat. and Prob. in Civil Engineering (ICASP9), San Francisco, USA*. Millpress, Rotterdam.
16. Andrieu, C., Lemaire, M. and Sudret, B. (2003). Time-variant reliability using the PHI2 method: principles and validation by Monte Carlo simulation. In A. Der Kiureghian, S. Madanat and J. Pestana (Eds.), *Proc. 9th Int. Conf. on Applications of Stat. and Prob. in Civil Engineering (ICASP9), San Francisco, USA*, pp. 27–34. Millpress, Rotterdam.
17. Sudret, B., Berveiller, M. and Lemaire, M. (2003). Application of a stochastic finite element procedure to reliability analysis. In M. Maes and L. Huyse (Eds.), *Proc 11th IFIP WG7.5 Conference on Reliability and Optimization of Structural Systems, Banff, Canada*, pp. 319–327. Balkema, Rotterdam.
18. Sudret, B., Guédé, Z. and Lemaire, M. (2003). Probabilistic framework for fatigue analysis. In M. Maes and L. Huyse (Eds.), *Proc. 11th IFIP WG7.5 Conference on Reliability and Optimization of Structural Systems, Banff, Canada*, pp. 251–257. Balkema.
19. Berveiller, M., Sudret, B. and Lemaire, M. (2004). Presentation of two methods for computing the response coefficients in stochastic finite element analysis. In *Proc. 9th ASCE Specialty Conference on Probabilistic Mechanics and Structural Reliability, Albuquerque, USA*.
20. Sudret, B., Defaux, G. and Pendola, M. (2004). Finite element reliability analysis of cooling towers submitted to degradation. In *Proc. 2nd Int. ASRANet Colloquium, Barcelona, Spain*.
21. Berveiller, M., Sudret, B. and Lemaire, M. (2004). Comparison of methods for computing the response coefficients in stochastic finite element analysis. In *Proc. 2nd Int. ASRANet Colloquium, Barcelona, Spain*.

22. Missoum, S., Benchaabane, S. and Sudret, B. (2004). Handling bifurcations in the optimal design of transient dynamic problems. In *Proc. 45th AIAA/ASME/ASCE Conf. on Structures, Dynamics and Materials, Palm Springs, California, USA*. Paper #2035.
23. Berveiller, M., Sudret, B. and Lemaire, M. (2005). Non linear non intrusive stochastic finite element method - application to a fracture mechanics problem. In G. Augusti, G. Schuëller and M. Ciampoli (Eds.), *Proc. 9th Int. Conf. Struct. Safety and Reliability (ICOSSAR'2005), Roma, Italy*. Millpress, Rotterdam.
24. Sudret, B. (2005). Analytical derivation of the outcrossing rate in time-variant reliability problems. In J. Sorensen and D. Frangopol (Eds.), *Proc. 12th IFIP WG7.5 Conference on Reliability and Optimization of Structural Systems, Aalborg, Denmark*, pp. 125–133. Taylor & Francis.
25. Berveiller, M., Sudret, B. and Lemaire, M. (2005). Structural reliability using non-intrusive stochastic finite elements. In J. Sorensen and D. Frangopol (Eds.), *Proc. 12th IFIP WG7.5 Conference on Reliability and Optimization of Structural Systems, Aalborg, Denmark*. Taylor & Francis.
26. Sudret, B. (2005). Probabilistic framework for the assessment of structures submitted to thermal fatigue. In *Trans. 18th Int. Conf. on Struct. Mech. in Reactor Tech. (SMiRT 18), Beijing, China*.
27. Guédé, Z., Sudret, B. and Lemaire, M. (2005). Life-time reliability-based assessment of structures submitted to random thermal loading. In *Proc. Fatigue Design 2005, Senlis, France*.
28. Perrin, F., Sudret, B., Pendola, M. and Lemaire, M. (2005). Comparison of two statistical treatments of fatigue test data. In *Proc. Fatigue Design 2005, Senlis, France*.
29. Petre-Lazar, I., Sudret, B., Foct, F., Granger, L. and Dechaux, L. (2006). Service life estimation of the secondary containment with respect to rebars corrosion. In *Proc. NucPerf 2006 "Corrosion and long term performance of concrete in NPP and waste facilities", Cadarache, France*.
30. Defaux, G., Pendola, M. and Sudret, B. (2006). Using spatial reliability in the probabilistic study of concrete structures: the example of a RC beam subjected to carbonation inducing corrosion. In *Proc. NucPerf 2006 "Corrosion and long term performance of concrete in NPP and waste facilities", Cadarache, France*.
31. Sudret, B., Perrin, F., Berveiller, M. and Pendola, M. (2006). Bayesian updating of the long-term creep deformations in concrete containment vessels. In *Proc. 3rd Int. ASRANet Colloquium, Glasgow, United Kingdom*.
32. Sudret, B., Defaux, G. and Pendola, M. (2006). Introducing spatial variability in the lifetime assessment of a concrete beam submitted to rebars corrosion. In *Proc. 2nd Int. Forum on Engineering Decision Making (IFED), Lake Louise, Canada*.
33. Sudret, B. (2006). Global sensitivity analysis using polynomial chaos expansions. In P. Spanos and G. Deodatis (Eds.), *Proc. 5th Int. Conf. on Comput. Stoch. Mech (CSM5), Rhodes, Greece*.
34. Gaignaire, R., Clénet, S., Sudret, B. and Moreau, O. (2006). 3D spectral stochastic finite element method in electromagnetism. In *Proc. 20th Conf. on Electromagnetic Field Computation (CEFC 2006), Miami, Florida, USA*.
35. Gaignaire, R., Clénet, S., Moreau, O. and Sudret, B. (2006). Influence of the order of input expansions in the spectral stochastic finite element method. *Proc. 7th International Symposium on Electric and Magnetic Fields (EMF2006), Aussois, France*.
36. Sudret, B., Blatman, G. and Berveiller, M. (2007). Quasi random numbers in stochastic finite element analysis – Application to global sensitivity analysis. In *Proc. 10th Int. Conf. on Applications of Stat. and Prob. in Civil Engineering (ICASP10), Tokyo, Japan*.

37. Perrin, F., Sudret, B., Pendola, M. and de Rocquigny, E. (2007). Comparison of Markov chain Monte-Carlo simulation and a FORM-based approach for Bayesian updating of mechanical models. In *Proc. 10th Int. Conf. on Applications of Stat. and Prob. in Civil Engineering (ICASP10)*, Tokyo, Japan.
38. Berveiller, M., Le Pape, Y., Sudret, B. and Perrin, F. (2007). Bayesian updating of the long-term creep deformations in concrete containment vessels using a non intrusive method. In *Proc. 10th Int. Conf. on Applications of Stat. and Prob. in Civil Engineering (ICASP10)*, Tokyo, Japan.
39. Berveiller, M., Le Pape, Y. and Sudret, B. (2007). Sensitivity analysis of the drying model on the delayed strain of concrete in containment vessels with a non intrusive method. In *Proc. 10th Int. Conf. on Applications of Stat. and Prob. in Civil Engineering (ICASP10)*, Tokyo, Japan.
40. Andrianov, G., Burriel, S., Cambier, S., Dutfoy, A., Dutka-Malen, I., de Rocquigny, E., Sudret, B., Benjamin, P., Lebrun, R., Mangeant, F. and Pendola, M. (2007). Open TURNS, an open source initiative to Treat Uncertainties, Risks'N Statistics in a structured industrial approach. In *Proc. ESREL'2007 Safety and Reliability Conference, Stavanger, Norway*.
41. Perrin, F., Sudret, B., Curtit, F., Stéphan, J.-M. and Pendola, M. (2007). Efficient Bayesian updating of structural fatigue design curve using experimental thermal fatigue data. In *Proc. Fatigue Design 2007, Senlis, France*.
42. Pendola, M. and Sudret, B. (2007). The various kinds of uncertainties in fatigue assessment of structures. In *Proc. Fatigue Design 2007, Senlis, France*.
43. Yaméogo, A., Sudret, B. and Cambier, S. (2007). Uncertainties in the no lift-off criterion used in fuel rod assessment. In *Trans. 19th Int. Conf. on Struct. Mech. In Reactor Tech. (SMiRT 19)*, Toronto, Canada.
44. Gaignaire, R., Clénet, S., Moreau, O. and Sudret, B. (2007). Current calculation in electrokinetics using a spectral stochastic finite element method. In *Proc. 16th Int. Conf. Comput. Electromagnetic Fields (COMPUMAG2007)*, Aachen, Germany.

4.5 National conference papers

1. de Buhan, P. and Sudret, B. (1999). Micropolar continuum description of materials reinforced by linear inclusions. In *Proc. Conf. to the memory of Pr. J.-P. Boehler, "Mechanics of heterogeneous materials"*, Grenoble.
2. de Buhan, P. and Sudret, B. (1999). Un modèle biphasique de matériau renforcé par inclusions linéaires. In *Proc. 14^e Congrès Français de Mécanique (CFM14)*, Toulouse.
3. Sudret, B. (2001). Eléments finis stochastiques spectraux et fiabilité. In *Proc. 15^e Congrès Français de Mécanique (CFM15)*, Nancy.
4. Dridi, W., Sudret, B. and Lassabatère, T. (2002). Experimental and numerical analysis of transport in a containment vessel. In *Proc. 2nd Biot Conference, Grenoble, France*.
5. Sudret, B., Berveiller, M. and Lemaire, M. (2003). Eléments finis stochastiques spectraux : nouvelles perspectives. In *Proc. 16^e Congrès Français de Mécanique (CFM16)*, Nice.
6. Andrieu, C., Lemaire, M. and Sudret, B. (2003). La méthode PHI2 ou comment prendre en compte la dépendance du temps dans une analyse en fiabilité mécanique. In *Proc. 6^e Colloque National en Calcul des Structures, Giens*.

7. Sudret, B. (2004). Cadre d'analyse probabiliste global des tuyauteries en fatigue thermique. In *Proc. 23^e Journées de Printemps - Commission Fatigue, "Méthodes fiabilistes en fatigue pour conception et essais", Paris.*
8. Guédé, Z., Sudret, B. and Lemaire, M. (2004). Analyse fiabiliste en fatigue thermique. In *Proc. 23^e Journées de Printemps - Commission Fatigue, "Méthodes fiabilistes en fatigue pour conception et essais", Paris.*
9. Raphael, W., Seif El Dine, B., Mohamed, A., Sudret, B. and Calgaro, J.-A. (2004). Correction bayésienne et étude fiabiliste des modèles de calcul du fluage du béton. In *Proc. $\lambda\mu 14$, Bourges.*
10. Berveiller, M., Sudret, B. and Lemaire, M. Construction de la réponse paramétrique déterministe d'un système mécanique par éléments finis stochastiques. In *Proc. 7^e Colloque National en Calcul des Structures, Giens.*
11. Berveiller, M., Sudret, B. and Lemaire, M. (2005). Eléments finis stochastiques non linéaires en mécanique de la rupture. In *Proc. 17^e Congrès Français de Mécanique (CFM17), Troyes.* Paper #159.
12. Sudret, B. (2005). Des éléments finis stochastiques spectraux aux surfaces de réponses stochastiques : une approche unifiée. In *Proc. 17^e Congrès Français de Mécanique (CFM17), Troyes.* Paper #864.
13. Gaignaire, R., Moreau, O., Sudret, B. and Clénet, S. (2006). Propagation d'incertitudes en électromagnétisme statique par chaos polynomial et résolution non intrusive. In *Proc. 5^e Conf. Eur. sur les Méthodes Numériques en Electromagnétisme (NUMELEC'2006), Lille.*
14. Perrin, F., Sudret, B., Blatman, G. and Pendola, M. (2007). Use of polynomial chaos expansion and maximum likelihood estimation for probabilistic inverse problems. In *Proc. 18^e Congrès Français de Mécanique, (CFM'2007), Grenoble.*
15. Perrin, F., Sudret, B. and Pendola, M. (2007). Bayesian updating of mechanical models – Application in fracture mechanics. In *Proc. 18^e Congrès Français de Mécanique (CFM'2007), Grenoble.*
16. Blatman, G., Sudret, B. and Berveiller, M. (2007). Quasi-random numbers in stochastic finite element analysis – Application to reliability analysis. In *Proc. 18^e Congrès Français de Mécanique, (CFM'2007), Grenoble.*

Bibliography

- Abdo, T. and R. Rackwitz (1990). A new β -point algorithm for large time invariant and time-variant reliability problems. In A. Der Kiureghian and P. Thoft-Christensen (Eds.), *Proc. 3rd WG 7.5 IFIP Conference on Reliability and Optimization of Structural Systems, Berkeley, California, USA – Lecture notes in Engineering, Vol. 61*. Springer Verlag.
- Abramowitz, M. and I. Stegun (1970). *Handbook of mathematical functions*. Dover Publications, Inc.
- Acharjee, S. and N. Zabaras (2006). Uncertainty propagation in finite deformations – A spectral stochastic Lagrangian approach. *Comput. Methods Appl. Mech. Engrg.* 195, 2289–2312.
- AFCEN (2000, juin). *Règles de Conception et de Construction des Matériels des Îlots Nucléaires, (RCCM)*. Paris.
- AFNOR (1990). Produits métalliques – Pratique des essais de fatigue oligocyclique. Technical Report A03-403, AFNOR.
- Alonso, C., A. Andrade, J. Rodriguez, and J. Diez (1998). Factors controlling cracking of concrete affected by reinforcement corrosion. *Materials and Structures* 31, 435–441.
- Amzallag, C., J.-P. Gerey, J.-L. Robert, and J. Bahuaud (1994). Standardization of the Rainflow counting method for fatigue analysis. *Int. J. Fatigue* 16, 287–293.
- Anders, M. and M. Hori (2001). Three-dimensional stochastic finite element method for elasto-plastic body. *Int. J. Numer. Meth. Engrg.* 51, 449–478.
- Andrieu, C., M. Lemaire, and B. Sudret (2002). The PHI2 method: a way to assess time-variant reliability using classical reliability tools. In *Proc. $\lambda\mu 13$ – ESREL’2002 Safety and Reliability Conf., Lyon, France*, pp. 472–475.
- Andrieu, C., M. Lemaire, and B. Sudret (2003). Time-variant reliability using the PHI2 method: principles and validation by Monte Carlo simulation. In A. Der Kiureghian, S. Madanat, and J. Pestana (Eds.), *Proc. 9th Int. Conf. on Applications of Stat. and Prob. in Civil Engineering (ICASP9), San Francisco, USA*, pp. 27–34. Millpress, Rotterdam.
- Andrieu-Renaud, C. (2002). *Fiabilité mécanique des structures soumises à des phénomènes physiques dépendant du temps*. Ph. D. thesis, Université Blaise Pascal, Clermont-Ferrand, France.
- Andrieu-Renaud, C., B. Sudret, and M. Lemaire (2004). The PHI2 method: a way to compute time-variant reliability. *Reliab. Eng. Sys. Safety* 84, 75–86.
- Archer, G., A. Saltelli, and I. Sobol’ (1997). Sensitivity measures, ANOVA-like techniques and the use of bootstrap. *J. Stat. Comput. Simul.* 58, 99–120.
- Arnst, M. (2007). *Inversion de modèles probabilistes de structures à partir de fonctions de transfert mesurées*. Ph. D. thesis, Ecole Centrale Paris.

- Arnst, M., D. Clouteau, H. Chebli, R. Othman, and G. Degrande (2006). A non-parametric probabilistic model for ground-borne vibrations in buildings. *Prob. Eng. Mech.* 21, 18–34.
- Askey, R. and J. Wilson (1985). Some basic hypergeometric polynomials that generalize Jacobi polynomials. *Mem. Amer. Math. Soc.* 319.
- Atkinson, A. and A. Donev (1992). *Optimum experimental design*. Oxford Science Publications.
- Au, S. and J. Beck (1999). A new adaptive importance sampling scheme for reliability calculations. *Structural Safety* 21(2), 135–158.
- Au, S. and J. Beck (2001a). Estimation of small failure probabilities in high dimensions by subset simulation. *Prob. Eng. Mech.* 16(4), 263–277.
- Au, S. and J. Beck (2001b). First excursion probabilities for linear systems by very efficient importance sampling. *Prob. Eng. Mech.* 16(3), 193–207.
- Au, S. and J. Beck (2003a). Important sampling in high dimensions. *Structural Safety* 25, 139–163.
- Au, S. and J. Beck (2003b). Subset simulation and its application to seismic risk based on dynamic analysis. *J. Eng. Mech.* 129(8), 901–917.
- Au, S., J. Ching, and J. Beck (2007). Application of subset simulation methods to reliability benchmark problems. *Structural Safety* 29(3), 183–193.
- Ayala-Uraga, E. and T. Moan (2002). System reliability issues of offshore structures considering fatigue failure and updating based on inspection. In *Proc. 1st Int. ASRANet Colloquium, Glasgow, United Kingdom*.
- Babuska, I. and P. Chatzipantelidis (2002). On solving elliptic stochastic partial differential equations. *Comput. Methods Appl. Mech. Engrg.* 191(37-38), 4093–4122.
- Babuska, I., F. Nobile, and R. Tempone (2007). A stochastic collocation method for elliptic partial differential equations with random input data. *SIAM J. Num. Anal.* 45(3), 1005–1034.
- Babuska, I., R. Tempone, and G. Zouraris (2004). Galerkin finite element approximations of stochastic elliptic differential equations. *SIAM J. Num. Anal.* 42, 800–825.
- Baecher, G. and T. Ingra (1981). Stochastic finite element method in settlement predictions. *J. Geotech. Eng. Div.* 107(4), 449–463.
- BAEL (2000). *Règles BAEL 91 modifiées 99 (Règles techniques de conception et de calcul des ouvrages et constructions en béton armé suivant la méthode des états-limites)*. Eyrolles, France.
- Baker, M. and I. Stanley (2002). An evaluation of reliability updating techniques for fatigue crack growth using experimental data. In *Proc. 1st Int. ASRANet Colloquium, Glasgow, United Kingdom*, pp. 1–15.
- Baldeweck, H. (1999). *Méthodes des éléments finis stochastiques - Applications à la géotechnique et à la mécanique de la rupture*. Ph. D. thesis, Université d'Evry-Val d'Essonne, France. 195 pages.
- Beck, J. and S. Au (2002). Bayesian updating of structural models and reliability using Markov chain Monte Carlo simulation. *J. Eng. Mech.* 128(4), 380–391.
- Beck, J. and L. Katafygiotis (2001). Updating models and their uncertainties. I: Bayesian statistical framework. *J. Eng. Mech.* 124(4), 455–461.
- Benhamadouche, S., M. Sakiz, C. Péniguel, and J.-M. Stéphan (2003). Presentation of a new methodology of chained computations using instationary 3D approaches for the determination of thermal fatigue in a T-junction of a PWR nuclear plant. In *Trans. 17th Int. Conf. On Struct. Mech. in Reactor Tech. (SMiRT 17), Prague, Czech Republic*.

- Bennett, A. (1992). *Inverse methods in physical oceanography*. Cambridge University Press.
- Berveiller, M. (2005). *Stochastic finite elements : intrusive and non intrusive methods for reliability analysis*. Ph. D. thesis, Université Blaise Pascal, Clermont-Ferrand.
- Berveiller, M., Y. Le Pape, and B. Sudret (2007). Sensitivity analysis of the drying model on the delayed strain of concrete in containment vessels with a non intrusive method. In *Proc. 10th Int. Conf. on Applications of Stat. and Prob. in Civil Engineering (ICASP10), Tokyo, Japan*.
- Berveiller, M., Y. Le Pape, B. Sudret, and F. Perrin (2007). Bayesian updating of the long-term creep deformations in concrete containment vessels using a non intrusive method. In *Proc. 10th Int. Conf. on Applications of Stat. and Prob. in Civil Engineering (ICASP10), Tokyo, Japan*.
- Berveiller, M., B. Sudret, and M. Lemaire (2004a). Comparison of methods for computing the response coefficients in stochastic finite element analysis. In *Proc. 2nd Int. ASRANet Colloquium, Barcelona, Spain*.
- Berveiller, M., B. Sudret, and M. Lemaire (2004b). Presentation of two methods for computing the response coefficients in stochastic finite element analysis. In *Proc. 9th ASCE Specialty Conference on Probabilistic Mechanics and Structural Reliability, Albuquerque, USA*.
- Berveiller, M., B. Sudret, and M. Lemaire (2005a). Non linear non intrusive stochastic finite element method – Application to a fracture mechanics problem. In G. Augusti, G. Schuëller, and M. Ciampoli (Eds.), *Proc. 9th Int. Conf. Struct. Safety and Reliability (ICOSSAR'2005), Roma, Italy*. Millpress, Rotterdam.
- Berveiller, M., B. Sudret, and M. Lemaire (2005b). Structural reliability using non-intrusive stochastic finite elements. In J. Sorensen and D. Frangopol (Eds.), *Proc. 12th IFIP WG7.5 Conference on Reliability and Optimization of Structural Systems, Aalborg, Denmark*. Taylor & Francis.
- Berveiller, M., B. Sudret, and M. Lemaire (2006). Stochastic finite elements: a non intrusive approach by regression. *Eur. J. Comput. Mech.* 15(1-3), 81–92.
- Bhargava, K., A. Ghosh, Y. Mori, and S. Ramanujam (2006). Model for cover cracking due to rebar corrosion in RC structures. *Eng. Struct.* 28(8), 1093–1109.
- Bjerager, P. (1988). Probability integration by directional simulation. *J. Eng. Mech.* 114(8), 1285–1302.
- Blatman, G. (2007). *Adaptive stochastic finite element methods and metamodels for uncertainty propagation*. Ph. D. thesis, Université Blaise Pascal, Clermont-Ferrand. in preparation.
- Blatman, G., B. Sudret, and M. Berveiller (2007a). Quasi-random numbers in stochastic finite element analysis. *Mécanique & Industries* 8, 289–297.
- Blatman, G., B. Sudret, and M. Berveiller (2007b). Quasi random numbers in stochastic finite element analysis – Application to reliability analysis. In *Proc. 18^e Congrès Français de Mécanique, (CFM'2007), Grenoble*.
- Bocquet, M. (2006). Introduction aux principes et méthodes de l'assimilation de données en géophysique – Notes de cours de l'école nationale supérieure des techniques avancées. Technical report, Centre d'Enseignement et de Recherche en Environnement Atmosphérique, Ecole Nationale des Ponts et Chaussées.
- Box, G. and M. Muller (1958). A note on the generation of random normal deviates. *Ann. Math. Stat.* 29, 610–611.
- Breitung, K. (1984). Asymptotic approximation for multinormal integrals. *J. Eng. Mech.* 110(3), 357–366.

- Breitung, K. (1988). Asymptotic crossing rates for stationary Gaussian vector processes. *Stochastic processes and their applications* 29, 195–207.
- Breitung, K. (1989). Asymptotic approximations for probability integrals. *Prob. Eng. Mech.* 4(4), 187–190.
- Brooks, S. and G. Roberts (1998). Convergence assessment techniques for Markov chain Monte Carlo algorithms. *Stat. Comput.* 8(4), 319–335.
- Broomfield, P. (1997). *Corrosion of steel in concrete. Understanding, investigation and repair*. E&FN Spon.
- Bucher, C. (1988). Adaptive sampling – An iterative fast Monte Carlo procedure. *Structural Safety* 5, 119–126.
- Cacuci, D. (2003). *Sensitivity and uncertainty analysis: theory*, Volume 1. Chapman & Hall/CRC, Boca Raton.
- Cambier, S., P. Guihot, and G. Coffignal (2002). Computational methods for accounting of structural uncertainties, applications to dynamic behavior prediction of piping systems. *Structural Safety* 24(1), 29–50.
- Cameron, R. and W. Martin (1947). The orthogonal development of nonlinear functionals in series of Fourier-Hermite functionals. *Ann. Math.*, 385–392.
- Cazuguel, M., C. Andrieu-Renaud, and J.-Y. Cognard (2005). Time-variant reliability on visco-plastic behavior of a plate. In G. Augusti, G. Schuëller, and M. Ciampoli (Eds.), *Proc. 9th Int. Conf. Struct. Safety and Reliability (ICOSSAR'2005), Roma, Italy*, pp. 1939–1946. Millpress, Rotterdam.
- Cazuguel, M. and J.-Y. Cognard (2006). Development of a time-variant reliability approach for marine structures subjected to corrosion. In *Proc. 3rd Int. ASRANet Colloquium, Glasgow, United Kingdom*.
- Cazuguel, M., C. Renaud, and J.-Y. Cognard (2006). Time-variant reliability of nonlinear structures: application to a representative part of a plate floor. *Quality and Reliability Engineering International* 22(1), 101–118.
- CEB Task Group 5.1 & 5.2 (1997). New approach to durability design – An example for carbonation induced corrosion. Technical Report 238, Comité Euro-international du béton.
- Celeux, G., D. Chauveau, and J. Diebolt (1996). Stochastic versions of the EM algorithm: an experimental study in the mixture case. *J. Stat. Comput.* 55, 287–314.
- Celeux, G. and J. Diebolt (1992). A stochastic approximation type EM algorithm for the mixture problem. *Stoch. Stoch. Rep.* 41(119-134).
- Ching, J., S. Au, and J. Beck (2005). Reliability estimation for dynamical systems subject to stochastic excitation using subset simulation with splitting. *Comput. Methods Appl. Mech. Engrg.* 194(12-16), 1557–1579.
- Ching, J. and J. Beck (2004). Bayesian analysis of the phase II IASC-ASCE structural health monitoring experimental benchmark data. *J. Eng. Mech.* 130(10), 1233–1244.
- Ching, J., J. Beck, and S. Au (2005). Hybrid subset simulation method for reliability estimation of dynamical systems subject to stochastic excitation. *Prob. Eng. Mech.* 20(3), 199–214.
- Ching, J., J. Beck, and K. Porter (2006). Bayesian state and parameter estimation of uncertain dynamical systems. *Prob. Eng. Mech.* 21(1), 81–96.

- Ching, J., J. Beck, K. Porter, and R. Shaikhutdinov (2006). Bayesian state estimation method for nonlinear systems and its application to recorded seismic response. *J. Eng. Mech.* 132(4), 396–410.
- Choi, S., R. Grandhi, and R. Canfield (2004). Structural reliability under non-Gaussian stochastic behavior. *Computers & Structures* 82, 1113–1121.
- Choi, S., R. Grandhi, R. Canfield, and C. Pettit (2004). Polynomial chaos expansion with Latin Hypercube sampling for estimating response variability. *AIAA Journal* 45, 1191–1198.
- Choi, S.-K., R. Grandhi, and R. Canfield (2006). Robust design of mechanical systems via stochastic expansion. *Int. J. Mat. Product Tech.* 25(1-2-3), 127–143.
- Chopra, O. and W. Shack (1998). Low-cycle fatigue of piping and pressure vessel steels in LWR environments. *Nuc. Eng. Des.* 184(1), 49–76.
- Chung, D., M. Gutiérrez, L. Graham-Brady, and F. Lingen (2005). Efficient numerical strategies for spectral stochastic finite element models. *Int. J. Numer. Meth. Engng.* 64, 1334–1349.
- Clément, A., A. Nouy, F. Schoefs, B. Bigourdan, and N. Moës (2007). Méthode X-SFEM pour le calcul de structure à géométrie aléatoire : application au calcul d’un joint de soudure. In *Proc. 18ème Congrès Français de Mécanique (CFM18), Grenoble*. Paper #228.
- Clenshaw, C. and A. Curtis (1960). A method for numerical integration on an automatic computer. *Num. Math.* 2, 197–205.
- Collectif (1998). Re-evaluation of fatigue analysis criteria. Technical Report EE/S 98.317, Framatome. (Final report to CEC-DG XI contract B4-3070/95/000876/MAR/C2).
- Cooke, R., M. Nauta, A. Havelaar, and I. van der Fels (2006). Probabilistic inversion for chicken processing lines. *Reliab. Eng. Sys. Safety* 91(10-11), 1364–1372.
- Cottareau, R. (2007). *Probabilistic models of impedance matrices – Application to dynamic soil-structure interaction*. Ph. D. thesis, Ecole Centrale Paris.
- Cottareau, R., D. Clouteau, and C. Soize (2007). Construction of a probabilistic model for impedance matrices. *Comput. Methods Appl. Mech. Engrg.* 196, 2252–2268.
- Cottareau, R., D. Clouteau, C. Soize, and S. Cambier (2005). Construction d’un modèle probabiliste de la matrice d’impédance d’un domaine non-borné par une méthode non paramétrique – Application au dimensionnement sismique d’un ouvrage. In *Proc. 7^e Colloque National en Calcul des Structures, Giens*.
- Cowles, M. and B. Carlin (1996). Markov chain Monte Carlo convergence diagnostics: a comparative review. *J. Amer. Stat. Assoc.* 91, 883–904.
- Cramer, H. and M. Leadbetter (1967). *Stationary and related processes*. Wiley & Sons.
- Cukier, H., R. Levine, and K. Shuler (1978). Nonlinear sensitivity analysis of multiparameter model systems. *J. Comput. Phys.* 26, 1–42.
- Darmawan, M. and M. Stewart (2007). Spatial time-dependent reliability analysis of corroding pretensioned prestressed concrete bridge girders. *Structural Safety* 29, 16–31.
- de Rocquigny, E. (2006a). La maîtrise des incertitudes dans un contexte industriel : 1^e partie – Une approche méthodologique globale basée sur des exemples. *J. Soc. Française Stat.* 147(3), 33–71.
- de Rocquigny, E. (2006b). La maîtrise des incertitudes dans un contexte industriel : 2^e partie – Revue des méthodes de modélisation statistique, physique et numérique. *J. Soc. Française Stat.* 147(3), 73–106.

- Deb, M., I. Babuska, and J. Oden (2001). Solution of stochastic partial differential equations using Galerkin finite element techniques. *Comput. Methods Appl. Mech. Engrg.* 190(48), 6359–6372.
- Debusschere, B., H. Najm, A. Matta, O. Knio, R. Ghanem, and O. Le Maître (2003). Protein labeling reactions in electrochemical microchannel flow: numerical simulation and uncertainty propagation. *Physics of Fluids* 15(8), 2238–2250.
- Delyon, B., M. Lavielle, and E. Moulines (1999). Convergence of a stochastic approximation version of the EM algorithm. *Ann. Stat.* 27(1), 94–128.
- Dempster, A., N. Laird, and D. Rubin (1977). Maximum likelihood from incomplete data via the EM algorithm. *J. Royal Stat. Soc. Series B* 39(1), 1–38.
- Dempster, A. P. (1968). A generalization of Bayesian inference. *J. Royal Stat. Soc., Series B* (30), 205–247.
- Deodatis, G. (1990). Bounds on response variability of stochastic finite element systems. *J. Eng. Mech.* 116(3), 565–585.
- Deodatis, G. (1991). The weighted integral method, I : stochastic stiffness matrix. *J. Eng. Mech.* 117(8), 1851–1864.
- Deodatis, G. and R. Micaletti (2001). Simulation of highly skewed non-Gaussian stochastic processes. *J. Eng. Mech.* 127(12), 1284–1295.
- Deodatis, G. and M. Shinozuka (1991). The weighted integral method, II : response variability and reliability. *J. Eng. Mech.* 117(8), 1865–1877.
- Der Kiureghian, A. (1999). Introduction to structural reliability. Handouts for course CE229, University of California, Berkeley.
- Der Kiureghian, A. (2000). The geometry of random vibrations and solutions by FORM and SORM. *Prob. Eng. Mech.* 15(1), 81–90.
- Der Kiureghian, A. and T. Dakessian (1998). Multiple design points in first and second-order reliability. *Structural Safety* 20(1), 37–49.
- Der Kiureghian, A. and M. de Stefano (1991). Efficient algorithms for second order reliability analysis. *J. Eng. Mech.* 117(12), 2906–2923.
- Der Kiureghian, A. and J. Ke (1988). The stochastic finite element method in structural reliability. *Prob. Eng. Mech.* 3(2), 83–91.
- Der Kiureghian, A. and C. Li (1996). Nonlinear random vibration analysis through optimization. In D. Frangopol, R. Corotis, and R. Rackwitz (Eds.), *Proc. 7th IFIP WG7.5 Conference on Reliability and Optimization of Structural Systems, Boulder, CO, USA*. Pergamon Press.
- Der Kiureghian, A., H. Lin, and S. Hwang (1987). Second order reliability approximations. *J. Eng. Mech.* 113(8), 1208–1225.
- Der Kiureghian, A. and P. Liu (1986). Structural reliability under incomplete probability information. *J. Eng. Mech.* 112(1), 85–104.
- Der Kiureghian, A. and R. Taylor (1983). Numerical methods in structural reliability. In *Proc. 4th Int. Conf. on Appl. of Statistics and Probability in Soil and Structural Engineering (ICASP4), Firenze, Italy*, pp. 769–784. Pitagora Editrice.
- Der Kiureghian, A. and Y. Zhang (1999). Space-variant finite element reliability analysis. *Comput. Methods Appl. Mech. Engrg.* 168, 173–183.

- Der Kiureghian, A., Y. Zhang, and C. Li (1994). Inverse reliability problem. *J. Eng. Mech.* 120, 1154–1159.
- Desceliers, C., R. Ghanem, and C. Soize (2006). Maximum likelihood estimation of stochastic chaos representations from experimental data. *Int. J. Numer. Meth. Engng.* 66, 978–1001.
- Desceliers, C., C. Soize, and S. Cambier (2003). Nonparametric-parametric model for random uncertainties in nonlinear structural dynamics: application to earthquake engineering. *Earthquake Eng. Struct. Dyn.* 33(3), 315–327.
- Desceliers, C., C. Soize, and R. Ghanem (2007). Identification of chaos representations of elastic properties of random media using experimental vibration tests. *Comput. Mech* 39(6), 831–838.
- Det Norske Veritas (2000). *PROBAN user's manual, V.4.3*.
- Ditlevsen, O. (1996). Dimension reduction and discretization in stochastic problems by regression method. In F. Casciati and B. Roberts (Eds.), *Mathematical models for structural reliability analysis, CRC Mathematical Modelling Series*, Chapter 2, pp. 51–138.
- Ditlevsen, O. and H. Madsen (1996). *Structural reliability methods*. J. Wiley and Sons, Chichester.
- Ditlevsen, O. and R. Olesen (1986). Statistical analysis of the Virkler data on fatigue crack growth. *Eng. Fract. Mech.* 25, 177–195.
- Ditlevsen, O., R. Olesen, and G. Mohr (1987). Solution of a class of load combination problems by directional simulation. *Structural Safety* 4, 95–109.
- Doostan, A. and R. Ghanem (2005). Characterization of stochastic system parameters from experimental data: a Bayesian inference approach. In G. Augusti, G. Schuëller, and M. Ciampoli (Eds.), *Proc. 9th Int. Conf. Struct. Safe. Reliab. (ICOSSAR'2005), Roma, Italy*, pp. 2147–2152.
- Du, C., D. Kurowicka, and R. Cooke (2006). Techniques for generic probabilistic inversion. *Comput. Stat. Data Anal.* 50(5), 1164–1187.
- eDF, R&D Division (2006). *Code_Aster : Analyse des structures et thermo-mécanique pour des études et des recherches, V.7*. <http://www.code-aster.org>.
- El Adlouni, S., A. Favre, and B. Bobée (2006). Comparison of methodologies to assess the convergence of Markov chain Monte Carlo methods. *Comput. Stat. Data Anal.* 50(10), 2685–2701.
- Er, G. (1998). A method for multi-parameter pdf estimation of random variables. *Structural Safety* 20, 25–36.
- Faber, M. H. (2003). Risk and safety in civil, surveying and environmental engineering. Lecture notes, Eidgenössische Technische Hochschule Zürich (ETHZ).
- Fedorov, V. (1972). *Theory of optimal experiments*. Academic Press, New York.
- Field, R. (2002). Numerical methods to estimate the coefficients of the polynomial chaos expansion. In *Proc. 15th ASCE Engineering Mechanics Division Conference, Columbia University, New York, USA*.
- Field, R., J. Red-Horse, and T. Paez (2000). A non deterministic shock and vibration application using polynomial chaos expansion. In *Proc. 8th ASCE Specialty Conference on Probabilistic Mechanics and Structural Reliability, University of Notre Dame, Indiana, USA*.
- Flores Macias, O. and M. Lemaire (1997). Eléments finis stochastiques et fiabilité : application en mécanique de la rupture. *Revue Française de Génie Civil* 1(2), 247–284.
- Flores Macias, O.-A. (1994). *Modèles fiabilistes et mécaniques : éléments finis stochastiques. Méthodes de couplage et applications*. Ph. D. thesis, Institut Français de Mécanique avancée.

- Frauenfelder, P., C. Schwab, and R. Todor (2005). Finite elements for elliptic problems with stochastic coefficient. *Comput. Methods Appl. Mech. Engrg.* 194, 205–228.
- Freudenthal, A. (1947). The safety of structures. *ASCE Trans.* 112, 125–180.
- Gaignaire, R., S. Clénet, O. Moreau, and B. Sudret (2006). Influence of the order of input expansions in the spectral stochastic finite element method. In *Proc. 7th International Symposium on Electric and Magnetic Fields (EMF2006), Aussois, France*.
- Gaignaire, R., S. Clénet, O. Moreau, and B. Sudret (2007). Current calculation using a spectral stochastic finite element method applied to an electrokinetic problem. In *Proc. 16th Int. Conf. Comput. Electromagnetic Fields (COMPUMAG2007), Aachen, Germany*.
- Gaignaire, R., S. Clénet, B. Sudret, and O. Moreau (2006). 3D spectral stochastic finite element method in electromagnetism. In *Proc. 20th Conf. on Electromagnetic Field Computation (CEFC 2006), Miami, Florida, USA*.
- Gaignaire, R., S. Clénet, B. Sudret, and O. Moreau (2007). 3-D spectral stochastic finite element method in electromagnetism. *IEEE Trans. Electromagnetism* 43(4), 1209–1212.
- Gaignaire, R., O. Moreau, B. Sudret, and S. Clénet (2006). Propagation d’incertitudes en électromagnétisme statique par chaos polynomial et résolution non intrusive. In *Proc. 5^e Conf. Eur. sur les Méthodes Numériques en Electromagnétisme (NUMELEC’2006), Lille*.
- Gardoni, P. (2002). *Probabilistic models and fragility estimates for bridge components and systems*. Ph. D. thesis, University of California at Berkeley.
- Gardoni, P., A. Der Kiureghian, and K. Mosalam (2002). Probabilistic capacity models and fragility estimates for reinforced concrete columns based on experimental observations. *J. Eng. Mech.* 128(10), 1024–1038.
- Gauchi, J.-P. (1997). Plans d’expériences optimaux pour modèles linéaires. In J.-J. Dreesbeke, J. Fine, and G. Saporta (Eds.), *Plans d’expérience, Applications à l’entreprise*, Chapter 7. Editions Technip.
- Gerstner, T. and M. Griebel (1998). Numerical integration using sparse grids. *Numerical Algorithms* 18(3-4), 209–232.
- Geyskens, P., A. Der Kiureghian, and P. Monteiro (1993). BUMP: Bayesian updating of models parameters. Technical Report Report UCB/SEMM-93/06, University of California at Berkeley.
- Geyskens, P., A. D. Kiureghian, and P. Monteiro (1998). Bayesian prediction of elastic modulus of concrete. *J. Struct. Eng.* 124 (1), 89–95.
- Ghanem, R. (1998). Probabilistic characterization of transport in heterogeneous media. *Comput. Methods Appl. Mech. Engrg.* 158, 199–220.
- Ghanem, R. (1999a). Ingredients for a general purpose stochastic finite elements implementation. *Comput. Methods Appl. Mech. Engrg.* 168, 19–34.
- Ghanem, R. (1999b). The nonlinear Gaussian spectrum of log-normal stochastic processes and variables. *J. Applied Mech.* 66, 964–973.
- Ghanem, R. (1999c). Stochastic finite elements with multiple random non-Gaussian properties. *J. Eng. Mech.* 125(1), 26–40.
- Ghanem, R. and V. Brzkala (1996). Stochastic finite element analysis of randomly layered media. *J. Eng. Mech.* 122(4), 361–369.

- Ghanem, R. and D. Dham (1998). Stochastic finite element analysis for multiphase flow in heterogeneous porous media. *Transp. Porous Media* 32, 239–262.
- Ghanem, R. and A. Doostan (2006). Characterization of stochastic system parameters from experimental data: a Bayesian inference approach. *J. Comp. Phys.* (217), 63–81.
- Ghanem, R. and D. Ghiocel (1998). Stochastic seismic soil-structure interaction using the homogeneous chaos expansion. In *Proc. 12th ASCE Engineering Mechanics Division Conference, La Jolla, California, USA*.
- Ghanem, R. and R. Kruger (1996). Numerical solution of spectral stochastic finite element systems. *Comput. Methods Appl. Mech. Engrg.* 129(3), 289–303.
- Ghanem, R., J. Red-Horse, and A. Sarkar (2000). Modal properties of a space-frame with localized system uncertainties. In *Proc. 8th ASCE Specialty Conference on Probabilistic Mechanics and Structural Reliability, Notre Dame, Indiana, USA*.
- Ghanem, R. and P. Spanos (1991a). *Stochastic finite elements – A spectral approach*. Springer Verlag. (Reedited by Dover Publications, 2003).
- Ghanem, R. and P.-D. Spanos (1990). Polynomial chaos in stochastic finite elements. *J. Applied Mech.* 57, 197–202.
- Ghanem, R. and P.-D. Spanos (1991b). Spectral stochastic finite-element formulation for reliability analysis. *J. Eng. Mech.* 117(10), 2351–2372.
- Ghiocel, D. and R. Ghanem (2002). Stochastic finite element analysis of seismic soil-structure interaction. *J. Eng. Mech.* 128, 66–77.
- Graham, L. and G. Deodatis (1998). Variability response functions for stochastic plate bending problems. *Structural Safety* 20(2), 167–188.
- Graham, L. and G. Deodatis (2001). Response and eigenvalue analysis of stochastic finite element systems with multiple correlated material and geometric properties. *Prob. Eng. Mech.* 16(1), 11–29.
- Grigoriu, M. (1998). Simulation of non-Gaussian translation processes. *J. Eng. Mech.* 124(2), 121–126.
- Guédé, Z. (2005). *Approche probabiliste de la durée de vie des structures soumises à la fatigue thermique*. Ph. D. thesis, Université Blaise Pascal, Clermont-Ferrand.
- Guédé, Z., B. Sudret, and M. Lemaire (2004). Analyse fiabiliste en fatigue thermique. In *Proc. 23^e Journées de Printemps – Commission Fatigue, "Méthodes fiabilistes en fatigue pour conception et essais"*, Paris.
- Guédé, Z., B. Sudret, and M. Lemaire (2007). Life-time reliability based assessment of structures submitted to thermal fatigue. *Int. J. Fatigue* 29(7), 1359–1373.
- Hagen, O. (1992). Threshold up-crossing by second order methods. *Prob. Eng. Mech.* 7, 235–241.
- Handa, K. and K. Andersson (1981). Application of finite element methods in the statistical analysis of structures. In T. Moan and M. Shinozuka (Eds.), *Proc. 3rd Int. Conf. Struct. Safety and Reliability (ICOSSAR'81), Trondheim, Norway*, pp. 409–420.
- Harbitz, A. (1983). Efficient and accurate probability of failure calculation by use of the importance sampling technique. In *Proc. 4th Int. Conf. on Appl. of Statistics and Probability in Soil and Structural Engineering (ICASP4), Firenze, Italy*, pp. 825–836. Pitagora Editrice.
- Hastings, W. (1970). Monte Carlo sampling methods using Markov chains and their application. *Biometrika* 57(1), 97–109.

- Haukaas, T. and A. Der Kiureghian (2005). Parameter sensitivity and importance measures in nonlinear finite element reliability analysis. *J. Eng. Mech.* 131(10), 1013–1026.
- Haukaas, T. and A. Der Kiureghian (2006). Strategies for finding the design point in non-linear finite element reliability analysis. *Prob. Eng. Mech.* 21(2), 133–147.
- Hisada, T. and S. Nakagiri (1981). Stochastic finite element method developed for structural safety and reliability. In T. Moan and M. Shinozuka (Eds.), *Proc. 3rd Int. Conf. Struct. Safety and Reliability (ICOSSAR'81), Trondheim, Norway*, pp. 395–408.
- Hisada, T. and S. Nakagiri (1985). Role of stochastic finite element method in structural safety and reliability. In I. Konishi, A.-S. Ang, and M. Shinozuka (Eds.), *Proc. 4th Int. Conf. Struct. Safety and Reliability (ICOSSAR'85), New York*, pp. 385–395.
- Hohenbichler, M. and R. Rackwitz (1981). Non normal dependent vectors in structural safety. *J. Eng. Mech.* 107(6), 1227–1238.
- Hohenbichler, M. and R. Rackwitz (1988). Improvement of second-order reliability estimates by importance sampling. *J. Eng. Mech.* 114(12), 2195–2199.
- Homma, T. and A. Saltelli (1996). Importance measures in global sensitivity analysis of non linear models. *Reliab. Eng. Sys. Safety* 52, 1–17.
- Huang, S., S. Mahadevan, and R. Rebba (2007). Collocation-based stochastic finite element analysis for random field problems. *Prob. Eng. Mech.* 22, 194–205.
- Huang, S., S. Quek, and K. Phoon (2001). Convergence study of the truncated Karhunen-Loève expansion for simulation of stochastic processes. *Int. J. Numer. Meth. Engng.* 52(9), 1029–1043.
- Isukapalli, S. S. (1999). *Uncertainty Analysis of Transport-Transformation Models*. Ph. D. thesis, The State University of New Jersey.
- Jaynes, E. (1957). Information theory and statistical mechanics. *Phys. Review* 106, 620–630.
- Johnson, E., H. Lam, L. Katafygiotis, and J. Beck (2004). Phase I IASC-ASCE structural health monitoring benchmark problem using simulated data. *J. Eng. Mech.* 130(1), 3–15.
- Joint Committee on Structural Safety (2002). *JCSS probabilistic model code*. <http://www.jcss.ethz.ch>.
- Kamiński, M. (2001). Stochastic second-order perturbation approach to the stress-based finite element method. *Int. J. Solids Struct.* 38(21), 3831–3852.
- Kamiński, M. (2007). Generalized perturbation-based stochastic finite element method in elastostatics. *Computers & Structures* 85(10), 586–594.
- Kamiński, M. and T. Hien (1999). Stochastic finite element modeling of transient heat transfer in layered composites. *Int. Comm. Heat Mass Transf.* 26(6), 801–810.
- Kapur, J. and H. Kesavan (1992). *Entropy optimization principles with application*. Academic Press, New York.
- Katafygiotis, L. and J. Beck (1998). Updating models and their uncertainties. II: model identifiability. *J. Eng. Mech.* 124(4), 463–467.
- Katafygiotis, L. and S. Cheung (2007). Application of spherical subset simulation method and auxiliary domain method on a benchmark reliability study. *Structural Safety* 29(3), 194–207.
- Katafygiotis, L., C. Papadimitriou, and H. Lam (1998). A probabilistic approach to structural model updating. *Soil Dynamics and Earthquake Engineering* 17(7-8), 495–507.

- Keese, A. (2004). *A general purpose framework for stochastic finite elements*. Ph. D. thesis, Technische Universität Braunschweig, Germany.
- Keese, A. and H.-G. Matthies (2005). Hierarchical parallelisation for the solution of stochastic finite element equations. *Computers & Structures* 83, 1033–1047.
- Kleiber, M. and T. Hien (1992). *The stochastic finite element methods - Basic perturbation technique and computational implementation*. J. Wiley and sons, Chichester.
- Knio, O. and O. Le Maître (2006). Uncertainty propagation in CFD using polynomial chaos decomposition. *Fluid Dyn. Res.* 38(9), 616–640.
- Koo, H. and A. Der Kiureghian (2003). FORM, SORM and simulation techniques for nonlinear random vibrations. Technical Report UCB/SEMM-2003/01, University of California at Berkeley.
- Kotulski, Z. A. (1998). On efficiency of identification of a stochastic crack propagation model based on virkler experimental data. *Arch. Mech.* 50(5), 829–847.
- Koutsourelakis, P., H. Pradlwarter, and G. Schuëller (2004). Reliability of structures in high dimensions, part I: algorithms and applications. *Prob. Eng. Mech.* 19, 409–417.
- Kree, P. and C. Soize (1983). *Mécanique aléatoire*. Dunod.
- Kuhn, E. (2003). *Estimation par maximum de vraisemblance dans des problèmes inverses non linéaires*. Ph. D. thesis, Université Paris Sud – Paris XI.
- Lacaze, B., C. Mailhes, M. Maubourguet, and J.-Y. Tournier (1997). *Probabilités et statistique appliquées*. Cépaduès Editions.
- Lam, H., L. Katafygiotis, and N. Mickleborough (2004). Application of a statistical model updating approach on phase I of the IASC-ASCE structural health monitoring benchmark study. *J. Eng. Mech.* 130(1), 34–48.
- Le Maître, O., O. Knio, H. Najm, and R. Ghanem (2001). A stochastic projection method for fluid flow – I. Basic formulation. *J. Comput. Phys.* 173, 481–511.
- Le Maître, O., O. Knio, H. Najm, and R. Ghanem (2004). Uncertainty propagation using Wiener-Haar expansions. *J. Comput. Phys.* 197, 28–57.
- Le Maître, O., H. Najm, R. Ghanem, and O. Knio (2004). Multi-resolution analysis of Wiener-type uncertainty propagation. *J. Comput. Phys.* 197, 502–531.
- Le Maître, O., M. Reagan, H. Najm, R. Ghanem, and O. Knio (2002). A stochastic projection method for fluid flow – II. Random process. *J. Comput. Phys.* 181, 9–44.
- Lemaire, M. (1998). Finite element and reliability : combined methods by response surfaces. In G. Frantziskonis (Ed.), *Probamat-21st Century, Probabilities and Materials : Tests, Models and Applications for the 21st century*, pp. 317–331. Kluwer Academic Publishers.
- Lemaire, M. (2005). *Fiabilité des structures – Couplage mécano-fiabiliste statique*. Hermès.
- Lemaire, M. and A. Mohamed (2000). Finite element and reliability: a happy marriage? In A. Nowak and M. Szerszen (Eds.), *Proc. 9th IFIP WG 7.5 Working Conference on Reliability and Optimization of Structural Systems (Keynote lecture)*, pp. 3–14. University of Michigan, Ann Arbor, USA.
- Lemaire, M. and M. Pendola (2006). Phimeca-Soft. *Structural Safety* 28(1-2), 130–149.
- Lemaitre, J. and J. Chaboche (1990). *Mechanics of solid materials*. Cambridge University Press.
- Lévi, R. (1949). Calculs probabilistes de la sécurité des constructions. *Annales des Ponts et Chaussées* 26.

- Li, C. and A. Der Kiureghian (1993). Optimal discretization of random fields. *J. Eng. Mech.* 119(6), 1136–1154.
- Li, C. and A. Der Kiureghian (1995). Mean out-crossing rate of nonlinear response to stochastic input. In M. Lemaire, J. Favre, and A. Mebarki (Eds.), *Proc. 7th Int. Conf. on Applications of Stat. and Prob. in Civil Engineering (ICASP7), Paris, France*, pp. 1135–1141. Balkema, Rotterdam.
- Li, H. and R. Foschi (1998). An inverse reliability method and its application. *Structural Safety* 20(3), 257–270.
- Li, L., K. Phoon, and S. Quek (2007). Comparison between Karhunen-Loève expansion and translation-based simulation of non-Gaussian processes. *Computers & Structures* 85(5-6), 263–276.
- Li, R. and R. Ghanem (1998). Adaptive polynomial chaos expansions applied to statistics of extremes in nonlinear random vibration. *Prob. Eng. Mech.* 13(2), 125–136.
- Li, Y. (2004). *Effect of spatial variability on maintenance and repair decisions for concrete structures*. Ph. D. thesis, Delft University of Technology.
- Li, Y., T. Vrouwenvelder, T. Wijnants, and J. Walraven (2004). Spatial variability of concrete deterioration and repair strategies. *Struct. Concrete* 5, 121–130.
- Liao, W. and W. Lu (1996). Reliability of natural-draught hyperbolic cooling towers. In U. Wittek and W. Krätzig (Eds.), *Proc. 4th International Symposium on Natural Draught Cooling Towers*, pp. 389–394. Balkema, Rotterdam.
- Lin, Y.-K. (1967). *Probabilistic theory of structural dynamics*. McGraw-Hill.
- Liu, P.-L. and A. Der Kiureghian (1986). Multivariate distribution models with prescribed marginals and covariances. *Prob. Eng. Mech.* 1(2), 105–112.
- Liu, P.-L. and A. Der Kiureghian (1991). Optimization algorithms for structural reliability. *Structural Safety* 9, 161–177.
- Liu, W., T. Belytschko, and A. Mani (1986a). Probabilistic finite elements for non linear structural dynamics. *Comput. Methods Appl. Mech. Engrg.* 56, 61–86.
- Liu, W., T. Belytschko, and A. Mani (1986b). Random field finite elements. *Int. J. Numer. Meth. Engrg.* 23(10), 1831–1845.
- Liu, Y. and R. Weyers (1998). Modelling the time-to-corrosion cracking in chloride contaminated reinforced concrete structures. *ACI Mater. J.* 95, 675–681.
- Loève, M. (1978). *Probability theory – Graduate texts in mathematics* (4th ed.), Volume 2. Springer Verlag, New-York.
- López de Lacalle, L., F. Viadero, and J. Hernández (1996). Applications of dynamic measurements to structural reliability updating. *Prob. Eng. Mech.* 11(2), 97–105.
- Lutes, L. and S. Sarkani (2003). *Random vibrations: analysis of structural and mechanical systems*. Butterworth-Heinemann.
- Madsen, H. (1987). Model updating in reliability theory. In N. Lind (Ed.), *Proc. 5th Int. Conf. on Applications of Stat. and Prob. in Civil Engineering (ICASP5), Vancouver, Canada*, Volume 1, pp. 564–577.
- Madsen, H. and L. Tvedt (1990). Methods for time-dependent reliability and sensitivity analysis. *J. Eng. Mech.* 116(10), 2118–2135.

- Maes, M., K. Breitung, and D. Dupuis (1993). Asymptotic importance sampling. *Structural Safety* 12, 167–183.
- Marzouk, Y., H. Najm, and L. Rahn (2007). Stochastic spectral methods for efficient Bayesian solution of inverse problems. *J. Comput. Phys.* 224, 560–586.
- Matheron, G. (1962). *Traité de Géostatistique appliquée*. Editions Technip.
- Matheron, G. (1967). Kriging or polynomial interpolation procedures. *Canadian Inst. Mining Bull.* 60, 1041.
- Matsumoto, M. and T. Nishimura (1998). Mersenne twister: A 623-dimensionally equidistributed uniform pseudorandom number generator. *ACM Trans. Mod. Comp. Sim.* 8(1), 3–30.
- Matthies, G., C. Brenner, C. Bucher, and C. Guedes Soares (1997). Uncertainties in probabilistic numerical analysis of structures and solids – Stochastic finite elements. *Structural Safety* 19(3), 283–336.
- Matthies, H. and A. Keese (2005). Galerkin methods for linear and nonlinear elliptic stochastic partial differential equations. *Comput. Methods Appl. Mech. Engrg.* 194, 1295–1331.
- Mayer, M. (1926). *Die Sicherheit der Bauwerke*. Springer Verlag.
- McKay, M. (1995). Evaluating prediction uncertainty. Technical report, Los Alamos National Laboratory. NUREG/CR-6311.
- McKay, M. D., R. J. Beckman, and W. J. Conover (1979). A comparison of three methods for selecting values of input variables in the analysis of output from a computer code. *Technometrics* 2, 239–245.
- Melchers, R. (1990). Radial importance sampling for structural reliability. *J. Eng. Mech.* 116, 189–203.
- Melchers, R.-E. (1999). *Structural reliability analysis and prediction*. John Wiley & Sons.
- Metropolis, N. (1987). The beginning of the Monte Carlo method. *Los Alamos Science, Special Issue*.
- Metropolis, N., A. W. Rosenbluth, M. N. Rosenbluth, and A. H. Teller (1953). Equations of state calculations by fast computing machines. *J. Chem. Phys.* 21(6), 1087–1092.
- Metropolis, N. and S. Ulam (1949). The Monte Carlo method. *J. Amer. Stat. Assoc.* 44(247), 335–341.
- Minguez, R., E. Castillo, and A. Hadi (2005). Solving the inverse reliability problem using decomposition techniques. *Structural Safety* 27(1), 1–23.
- Mohamed, A., M. Pendola, G. Heinfling, and G. Defaux (2002). Etude des aéro-réfrigérants par couplage éléments finis et fiabilité. *Revue Européenne des Eléments Finis* 1, 101–126.
- Morokoff, W. and R. Caflisch (1995). Quasi-monte carlo integration. *J. Comput. Phys.* 122, 218–230.
- Myers, R. and D. Montgomery (2002). *Response surface methodology: process and product optimization using designed experiments* (2nd ed.). J. Wiley & Sons.
- Nataf, A. (1962). Détermination des distributions dont les marges sont données. *C. R. Acad. Sci. Paris* 225, 42–43.
- Nelsen, R. (1999). *An introduction to copulas*, Volume 139 of *Lecture Notes in Statistics*. Springer.
- Niederreiter, H. (1992). *Random number generation and quasi-Monte Carlo methods*. Society for Industrial and Applied Mathematics, Philadelphia, PA, USA.
- Nouy, A. (2005). Technique de décomposition spectrale optimale pour la résolution d'équations aux dérivées partielles stochastiques. In *Proc. 17ème Congrès Français de Mécanique (CFM17)*, Troyes, Number Paper #697.

- Nouy, A. (2007). A generalized spectral decomposition technique to solve stochastic partial differential equations. *Comput. Methods Appl. Mech. Engrg.* Submitted for publication.
- Novak, E. and K. Ritter (1996). High dimensional integration of smooth functions over cubes. *Numer. Math.* 75(79-97).
- Oakley, J. and A. O'Hagan (2004). Probabilistic sensitivity analysis of complex models: a Bayesian approach. *J. Royal Stat. Soc., Series B* 66, 751–769.
- O'Hagan, A. and J. Forster (2004). *Kendall's advanced theory of statistics, Vol. 2B Bayesian inference.* Arnold.
- Olsson, A., G. Sandberg, and O. Dahlblom (2003). On Latin Hypercube sampling for structural reliability analysis. *Structural Safety* 25, 47–68.
- Owen, D. (1980). A table of normal integrals. *Comm. Stat. Simul. Comp.* B9(4), 389–419.
- Pacific Earthquake Engineering and Research Center (2004). *OpenSees: The Open System for Earthquake Engineering Simulation.*
- Pan, W., M. Tatang, G. McRae, and R. Prinn (1997). Uncertainty analysis of direct radiative forcing by anthropogenic sulfate aerosols. *J. Geophys. Research* 102(D18), 21915–21924.
- Papadimitriou, C., J. L. Beck, and L. S. Katafygiotis (2001). Updating robust reliability using structural test data. *Prob. Eng. Mech.* 16(2), 103–113.
- Papadopoulos, I., P. Davoli, C. Gorla, M. Filippini, and A. Bernasconi (1997). A comparative study of multiaxial high-cycle fatigue criteria for metals. *Int. J. Fatigue* 19(3), 219–235.
- Paris, P. and F. Erdogan (1963). A critical analysis of crack propagation laws. *Trans. the ASME, J. of Basic Eng.*, 528–534.
- Pascual, F. and W. Meeker (1997). Analysis of fatigue data with runouts based on a model with non constant standard deviation and a fatigue limit parameter. *J. Testing. Eval.* 25, 292–301.
- Pellisetti, M.-F. and R. Ghanem (2000). Iterative solution of systems of linear equations arising in the context of stochastic finite elements. *Adv. Eng. Soft.* 31, 607–616.
- Perrin, F. (2008). *Experimental data integration in probabilistic models for the lifetime assessment of structures.* Ph. D. thesis, Université Blaise Pascal, Clermont-Ferrand, France.
- Perrin, F., B. Sudret, G. Blatman, and M. Pendola (2007). Use of polynomial chaos expansion and maximum likelihood estimation for probabilistic inverse problems. In *Proc. 18^e Congrès Français de Mécanique, (CFM'2007), Grenoble.*
- Perrin, F., B. Sudret, F. Curtit, J.-M. Stéphan, and M. Pendola (2007). Efficient Bayesian updating of structural fatigue design curve using experimental thermal fatigue data. In *Proc. Fatigue Design 2007, Senlis, France.*
- Perrin, F., B. Sudret, and M. Pendola (2007a). Bayesian updating of mechanical models – Application in fracture mechanics. In *Proc. 18^e Congrès Français de Mécanique (CFM'2007), Grenoble.*
- Perrin, F., B. Sudret, and M. Pendola (2007b). Comparison of statistical methods for estimating probabilistic s - n curves. *Int. J. Fatigue.* In preparation.
- Perrin, F., B. Sudret, M. Pendola, and M. Lemaire (2005). Comparison of two statistical treatments of fatigue test data. In *Proc. Fatigue Design 2005, Senlis, France.*
- Petryna, Y. and W. Krätzig (2005). Computational framework for long-term reliability analysis of RC structures. *Comput. Methods Appl. Mech. Engrg.* 194, 1619–1639.

- Phimeca Engineering SA (2004). *PHIMECA-Software user's manual*.
- Phoon, K., H. Huang, and S. Quek (2005). Simulation of strongly non Gaussian processes using Karhunen-Loève expansion. *Prob. Eng. Mech.* 20(2), 188–198.
- Phoon, K., S. Huang, and S. Quek (2002a). Implementation of Karhunen-Loève expansion for simulation using a wavelet-Galerkin scheme. *Prob. Eng. Mech.* 17(3), 293–303.
- Phoon, K., S. Huang, and S. Quek (2002b). Simulation of second-order processes using Karhunen-Loève expansion. *Computers & Structures* 80(12), 1049–1060.
- Phoon, K., S. Quek, Y. Chow, and S. Lee (1990). Reliability analysis of pile settlements. *J. Geotech. Eng.* 116(11), 1717–1735.
- Pillet, E., N. Bouhaddi, and S. Cogan (2006). Bayesian experimental design for parametric identification of dynamical structures. In B. Topping, G. Montero, and R. Montenegro (Eds.), *Proc. 8th Int. Conf. Comput. Struct. Tech., Las Palmas de Gran Canaria*, Number 45. Civil-Comp Press.
- Pradlwarter, H., M. Pellissetti, C. Schenk, G. Schuëller, A. Kreis, S. Fransen, A. Calvi, and M. Klein (2005). Realistic and efficient reliability estimation for aerospace structures. *Comput. Methods Appl. Mech. Engrg.* 194, 1597–1617.
- Pradlwarter, H., G. Schuëller, P. Koutsourelakis, and D. Charmpis (2007). Application of line sampling simulation method to reliability benchmark problems. *Structural Safety* 29(3), 208–221.
- Press, W., , B. Flannery, S. Teukolsky, and W. Vetterling (2002). *Numerical recipes in C: the art of scientific computing*. Cambridge University Press.
- Puig, B. and J.-L. Akian (2004). Non-Gaussian simulation using Hermite polynomials expansion and maximum entropy principle. *Prob. Eng. Mech.* 19(4), 293–305.
- Rackwitz, R. (1998). Computational techniques in stationary and non stationary load combination – A review and some extensions. *J. Struct. Eng., India* 25(1), 1–20.
- Rackwitz, R. (2001). Reliability analysis – A review and some perspectives. *Structural Safety* 23, 365–395.
- Rackwitz, R. (2004). Zuverlässigkeit und Lasten im konstruktiven Ingenieurbau. Lecture notes, Technical University of Munich.
- Rackwitz, R. and B. Fiessler (1978). Structural reliability under combined load sequences. *Computers & Structures* 9, 489–494.
- Rafiq, M., M. Chryssanthopoulos, and T. Onoufriou (2004). Performance updating of concrete bridges using proactive health monitoring methods. *Reliab. Eng. Sys. Safety* 86(3), 247–256.
- Raftery, A. and S. Lewis (1992). The number of iterations, convergence diagnostics, and generic Metropolis algorithms. Technical report, Dpt. of Statistics, University of Washington, Seattle.
- Rajansankar, J., N. Iyer, and T. Appa Rao (2003). Structural integrity assessment of offshore tubular joints based on reliability analysis. *Int. J. Fat.* 25(7), 609–619.
- Ratier, L., S. Cambier, and L. Berthe (2005). Analyse probabiliste du désaccordement d'une roue de turbine. In *Proc. 7^e Colloque National en Calcul des Structures, Giens*.
- RCP Consult (1998). *COMREL user's manual*. RCP Consult.
- Reagan, M., H. Njam, R. Ghanem, and O. Knio (2003). Uncertainty quantification in reacting-flow simulations through non-intrusive spectral projection. *Combustion and Flame* 132, 545–555.
- Rice, S. (1944). Mathematical analysis of random noise. *Bell System Tech. J.* 23, 282–332.

- Rice, S. (1945). Mathematical analysis of random noise. *Bell System Tech. J.* 25, 46–156.
- Robert, C. (1992). *L'analyse statistique bayésienne*. Economica.
- Roberts, J. and P. Spanos (1990). *Random Vibration and Statistical Linearization*. Dover publications.
- Rosenblatt, M. (1952). Remarks on a multivariate transformation. *Ann. Math. Stat.* 23, 470–472.
- Rosinski, S. (2001). Evaluation of fatigue data including reactor water environmental effects – Materials reliability project (MRP-54). Technical Report 1003079, EPRI.
- Rubinstein, R.-Y. (1981). *Simulation and the Monte Carlo methods*. John Wiley & Sons.
- Sachdeva, S., P. Nair, and A. Keane (2006). Comparative study of projection schemes for stochastic finite element analysis. *Comput. Methods Appl. Mech. Engrg.* 195(19-22), 2371–2392.
- Sacks, J., W. Welch, T. Mitchell, and H. Wynn (1989). Design and analysis of computer experiments. *Stat. Sci.* 4, 409–435.
- Saltelli, A. (2002). Making best use of model evaluations to compute sensitivity indices. *Comput. Phys. Comm.* 145, 280–297.
- Saltelli, A. and R. Bolado (1998). An alternative way to compute Fourier amplitude sensitivity test (FAST). *Comput. Stat. Data Anal.* 26, 445–460.
- Saltelli, A., K. Chan, and E. Scott (Eds.) (2000). *Sensitivity analysis*. J. Wiley & Sons.
- Saltelli, A. and I. Sobol' (1995). About the use of rank transformation in sensitivity of model output. *Reliab. Eng. Sys. Safety* 50, 225–239.
- Saltelli, A., S. Tarantola, and K. Chan (1999). A quantitative, model independent method for global sensitivity analysis of model output. *Technometrics* 41(1), 39–56.
- Saporta, G. (2006). *Probabilités, analyse des données et statistique* (2nd ed.). Editions Technip.
- Schall, G., M. Faber, and R. Rackwitz (1991). The ergodicity assumption for sea states in the reliability assessment of offshore structures. *J. Offshore Mech. Arctic Eng., ASME* 113(3), 241–246.
- Schölkopf, B. and A. Smola (2002). *Learning with kernels*. MIT Press.
- Schuëller, G. and H. Pradlwarter (2007). Benchmark study on reliability estimation in higher dimensions of structural systems – An overview. *Structural Safety* 29, 167–182.
- Schuëller, G., H. Pradlwarter, and P. Koutsourelakis (2004). A critical appraisal of reliability estimation procedures for high dimensions. *Prob. Eng. Mech.* 19(4), 463–474.
- Schuëller, G.I. (Editor) (2006). General-purpose softwares for structural reliability analysis. *Structural Safety* 28(1-2).
- Schwob, C. (2007). *Approche non locale probabiliste pour l'analyse en fatigue des zones à gradient de contrainte*. Ph. D. thesis, Ecole des Mines d'Albi Carmaux.
- Shafer, G. (1976). *A mathematical theory of evidence*. Princeton University Press.
- Shen, C., P. Wirsching, and G. Cashman (1996). Design curve to characterize fatigue strength. *J. Eng. Mat. Tech., Trans. ASME* (118), 514–535.
- Shinozuka, M. (1964). Probability of failure under random loading. *J. Eng. Mech.* 90(5), 147–170.
- Shinozuka, M. (1983). Basic analysis of structural safety. *J. Struct. Eng.* 109(3), 721–740.

- Sklar, A. (1959). Fonctions de répartition à n dimensions et leurs marges. *Publications de l'Institut de Statistique de L'Université de Paris* 8 (229-231).
- Smola, A. and B. Schölkopf (2006). A tutorial on support vector regression. *Stat. Comput.* 14, 199–222.
- Smolyak, S. (1963). Quadrature and interpolation formulas for tensor products of certain classes of functions. *Soviet. Math. Dokl.* 4, 240–243.
- Sobol', I. (1993). Sensitivity estimates for nonlinear mathematical models. *Math. Modeling & Comp. Exp.* 1, 407–414.
- Sobol', I. and S. Kucherenko (2005). Global sensitivity indices for nonlinear mathematical models. Review. *Wilmott magazine* 1, 56–61.
- Soize, C. (1988). Problèmes classiques de dynamique stochastique : méthodes d'études. Technical report, Techniques de l'Ingénieur.
- Soize, C. (2000). A nonparametric model of random uncertainties for reduced matrix models in structural dynamics. *Prob. Eng. Mech.* 15, 277–294.
- Soize, C. (2005). A comprehensive overview of a non-parametric probabilistic approach of model uncertainties for predictive models in structural dynamics. *J. Sound Vibr.* 288, 623–652.
- Soize, C. (2006). Non-Gaussian positive-definite matrix-valued random fields for elliptic stochastic partial differential operators. *Comput. Methods Appl. Mech. Engrg.* 195, 26–64.
- Soize, C. and R. Ghanem (2004). Physical systems with random uncertainties: chaos representations with arbitrary probability measure. *SIAM J. Sci. Comput.* 26(2), 395–410.
- Sportisse, B. (2004). Assimilation de données – 1ère partie : éléments théoriques. Technical Report 2004-24, Centre d'Enseignement et de Recherche en Environnement Atmosphérique – Ecole Nationale des Ponts et Chaussées, Paris.
- Stewart, M. (2004). Effect of spatial variability of pitting corrosion and its influence on structural fragility and reliability of RC beams in flexure. *Structural Safety* 26(4), 453–470.
- Stewart, M. (2006). Spatial variability of damage and expected maintenance costs for deteriorating RC structures. *Struct. Infrastruct. Eng.* 2(2), 79–90.
- Stewart, M. and A. Al-Harthy (2008). Pitting corrosion and structural reliability of corroding RC structures: experimental data and probabilistic analysis. *Reliab. Eng. Sys. Safety* 93, 373–382.
- Stewart, M. and J. Mullard (2007). Spatial time-dependent reliability analysis of corrosion damage and the timing of first repair for RC structures. *Eng. Struct.* 29(7), 1457–1464.
- Stewart, M., J. Mullard, and B. Drake (2006). Utility of spatially variable damage performance indicators for improved safety and maintenance decisions of deteriorating infrastructure. In *Proc. 2nd Int. Forum Eng. Dec. Making (IFED)*. Lake Louise.
- Sudret, B. (2001). Eléments finis stochastiques spectraux et fiabilité. In *Proc. 15^e Congrès Français de Mécanique (CFM15)*, Nancy.
- Sudret, B. (2002). Comparison of the spectral stochastic finite element method with the perturbation method for second moment analysis. In *Proc. 1st Int. ASRANet Colloquium, Glasgow, United Kingdom*.
- Sudret, B. (2005a). Analytical derivation of the outcrossing rate in time-variant reliability problems. In J. Sorensen and D. Frangopol (Eds.), *Proc. 12th IFIP WG7.5 Conference on Reliability and Optimization of Structural Systems, Aalborg, Denmark*, pp. 125–133. Taylor & Francis.

- Sudret, B. (2005b). Des éléments finis stochastiques spectraux aux surfaces de réponses stochastiques : une approche unifiée. In *Proc. 17^e Congrès Français de Mécanique (CFM17)*, Troyes. Paper #864.
- Sudret, B. (2006a). Global sensitivity analysis using polynomial chaos expansions. In P. Spanos and G. Deodatis (Eds.), *Proc. 5th Int. Conf. on Comp. Stoch. Mech (CSM5)*, Rhodos, Greece.
- Sudret, B. (2006b). Time-variant reliability methods. In M. Lemaire (Ed.), *Approche probabiliste de la conception et du dimensionnement en contexte incertain*, Chapter 11. Institut pour la Promotion des Sciences de l'Ingénieur (IPSI).
- Sudret, B. (2007). Analytical derivation of the outcrossing rate in time-variant reliability problems. *Struct. Infrastruct. Eng.* In press.
- Sudret, B. (2008a). Global sensitivity analysis using polynomial chaos expansions. *Reliab. Eng. Sys. Safety*. In press.
- Sudret, B. (2008b). Probabilistic models for the extent of damage in degrading reinforced concrete structures. *Reliab. Eng. Sys. Safety* 93, 410–422.
- Sudret, B. and M. Berveiller (2007). Stochastic finite element methods in geotechnical engineering. In K. Phoon (Ed.), *Reliability-based design in geotechnical engineering: computations and applications*, Chapter 7. Taylor and Francis. To appear.
- Sudret, B., M. Berveiller, and M. Lemaire (2003a). Application of a stochastic finite element procedure to reliability analysis. In M. Maes and L. Huyse (Eds.), *Proc 11th IFIP WG7.5 Conference on Reliability and Optimization of Structural Systems, Banff, Canada*, pp. 319–327. Balkema, Rotterdam.
- Sudret, B., M. Berveiller, and M. Lemaire (2003b). Éléments finis stochastiques spectraux : nouvelles perspectives. In *Proc. 16^e Congrès Français de Mécanique (CFM16)*, Nice.
- Sudret, B., M. Berveiller, and M. Lemaire (2004). A stochastic finite element method in linear mechanics. *Comptes Rendus Mécanique* 332, 531–537.
- Sudret, B., M. Berveiller, and M. Lemaire (2006). A stochastic finite element procedure for moment and reliability analysis. *Eur. J. Comput. Mech.* 15(7-8), 825–866.
- Sudret, B., G. Blatman, and M. Berveiller (2007). Quasi random numbers in stochastic finite element analysis – Application to global sensitivity analysis. In *Proc. 10th Int. Conf. on Applications of Stat. and Prob. in Civil Engineering (ICASP10)*, Tokyo, Japan.
- Sudret, B. and I. Cherradi (2003). Quadrature method for finite element reliability analysis. In A. Der Kiureghian, S. Madanat, and J. Pestana (Eds.), *Proc. 9th Int. Conf. on Applications of Stat. and Prob. in Civil Engineering (ICASP9)*, San Francisco, USA. Millpress, Rotterdam.
- Sudret, B., G. Defaux, C. Andrieu, and M. Lemaire (2002). Comparison of methods for computing the probability of failure in time-variant reliability using the outcrossing approach. In P. Spanos and G. Deodatis (Eds.), *Proc. 4th Int. Conf. on Comput. Stoch. Mech (CSM4)*, Corfu, Greece.
- Sudret, B., G. Defaux, and M. Pendola (2005). Time-variant finite element reliability analysis – Application to the durability of cooling towers. *Structural Safety* 27, 93–112.
- Sudret, B., G. Defaux, and M. Pendola (2006). Introducing spatial variability in the lifetime assessment of a concrete beam submitted to rebars corrosion. In *Proc. 2nd Int. Forum on Engineering Decision Making (IFED)*, Lake Louise, Canada.
- Sudret, B., G. Defaux, and M. Pendola (2007). Stochastic evaluation of the damage length in RC beams submitted to corrosion of reinforcing steel. *Civ. Eng. Envir. Sys.* 24(2), 165–178.

- Sudret, B. and A. Der Kiureghian (2000). Stochastic finite elements and reliability: a state-of-the-art report. Technical Report UCB/SEMM-2000/08, University of California, Berkeley. 173 pages.
- Sudret, B. and A. Der Kiureghian (2002). Comparison of finite element reliability methods. *Prob. Eng. Mech.* 17, 337–348.
- Sudret, B., S. Dron, and M. Pendola (2002). Time-variant reliability analysis of cooling towers including corrosion of steel in reinforced concrete. In *Proc. $\lambda\mu 13$ – ESREL’2002 Safety and Reliability Conf., Lyon, France*, pp. 571–575.
- Sudret, B. and Z. Gu  d   (2005). Probabilistic assessment of thermal fatigue in nuclear components. *Nuc. Eng. Des.* 235, 1819–1835.
- Sudret, B., Z. Gu  d  , P. Hornet, J.-M. St  phan, and M. Lemaire (2003). Probabilistic assessment of fatigue life including statistical uncertainties in the S-N curve. In *Trans. 17th Int. Conf. on Struct. Mech. in Reactor Tech. (SMiRT 17), Prague, Czech Republic*. Paper M-232.
- Sudret, B. and M. Pendola (2002). Reliability analysis of cooling towers: influence of rebars corrosion on failure. In *Proc. 10th Int. Conf. on Nucl. Eng. (ICONE10), Washington, USA*, pp. 571–575. Paper #22136.
- Sudret, B., F. Perrin, M. Berveiller, and M. Pendola (2006). Bayesian updating of the long-term creep deformations in concrete containment vessels. In *Proc. 3rd Int. ASRANet Colloquium, Glasgow, United Kingdom*.
- Takada, T. (1990a). Weighted integral method in multidimensional stochastic finite element analysis. *Prob. Eng. Mech.* 5(4), 158–166.
- Takada, T. (1990b). Weighted integral method in stochastic finite element analysis. *Prob. Eng. Mech.* 5(3), 146–156.
- Talagrand, O. (1997). Assimilation of observations, an introduction. *J. Meteor. Soc. Japan* 75, 191–209.
- Tarantola, A. (1987). *Inverse problem theory – Methods for data fitting and model parameter estimation*. Elsevier.
- Tarantola, A. (2005). *Inverse problem theory and methods for model parameter estimation*. Society for Industrial and Applied Mathematics (SIAM).
- Tarantola, A. (2007). *Mapping of probabilities – Theory for the interpretation of uncertain physical measurements*. Submitted to Cambridge University Press.
- Tatang, M. (1995). *Direct incorporation of uncertainty in chemical and environmental engineering systems*. Ph. D. thesis, Massachusetts Institute of Technology.
- Tatang, M., W. Pan, R. Prinn, and G. McRae (1997). An efficient method for parametric uncertainty analysis of numerical geophysical models. *J. Geophys. Research* 102(D18), 21925–21932.
- Thoft-Christensen, P. (2003). FEM modelling of the evolution of corrosion cracks in reinforced concrete structures. In M. Maes and L. Huyse (Eds.), *Proc. 11th IFIP WG7.5 Conference on Reliability and Optimization of Structural Systems, Banff, Canada*, pp. 221–228. Balkema, Rotterdam.
- Tovo, R. (2001). On the fatigue reliability evaluation of structural components underservice loading. *Int. J. Fatigue* 23, 587–598.
- Tvedt, L. (1990). Distribution of quadratic forms in normal space – Applications to structural reliability. *J. Eng. Mech.* 116(6), 1183–1197.

- Vanden Berghen, F. (2004). *CONDOR: a constrained, non-linear, derivative-free parallel optimizer for continuous, high computing load, noisy objective functions*. Ph. D. thesis, Université libre de Bruxelles.
- Vanden Berghen, F. and H. Bersini (2004). CONDOR, a new parallel, constrained extension of Powell's UOBYQA algorithm: experimental results and comparison with the DFO algorithm. *J. Comput. Appl. Math.* 181, 157–175.
- Vanmarcke, E. (1983). *Random fields : analysis and synthesis*. The MIT Press, Cambridge, Massachusetts.
- Vanmarcke, E.-H. and M. Grigoriu (1983). Stochastic finite element analysis of simple beams. *J. Eng. Mech.* 109(5), 1203–1214.
- Vazquez, E. (2005). *Modélisation comportementale de systèmes non-linéaires multivariables par méthodes à noyaux reproduisants*. Ph. D. thesis, Université Paris XI.
- Vijalapura, P., J. Conte, and M. Meghella (2000). Time-variant reliability analysis of hysteretic SDOF systems with uncertain parameters and subjected to stochastic loading. In R. Melchers and M. Stewart (Eds.), *Proc. 8th Int. Conf. on Applications of Stat. and Prob. in Civil Engineering (ICASP8), Sydney, Australia*, Volume 1, pp. 827–834. Balkema, Rotterdam.
- Villadsen, J. and M. Michelsen (1978). *Solution of differential equation models by polynomial approximations*. Prentice-Hall.
- Virkler, D., B. M. Hillberry, and P. Goel (1979). The statistical nature of fatigue crack propagation. *Trans. ASME, J. Eng. Mat. Tech.* 101(2), 148–153.
- Vrouwenvelder, T. (1997). The JCSS probabilistic model code. *Structural Safety* 19(3), 245–251.
- Vu, K. and M. Stewart (2005). Predicting the likelihood and extent of reinforced concrete corrosion-induced cracking. *J. Struct. Eng.* 131(11), 1681–1689.
- Waarts, P.-H. (2000). *Structural reliability using finite element methods: an appraisal of DARS: Directional Adaptive Response Surface Sampling*. Ph. D. thesis, Technical University of Delft, The Netherlands.
- Wall, F. and G. Deodatis (1994). Variability response functions of stochastic plane stress/strain problems. *J. Eng. Mech.* 120(9), 1963–1982.
- Wan, X. and G. E. Karniadakis (2005). An adaptive multi-element generalized polynomial chaos method for stochastic differential equations. *J. Comput. Phys.* 209, 617–642.
- Wand, M. and M. Jones (1995). *Kernel smoothing*. Chapman and Hall.
- Wiener, N. (1938). The homogeneous chaos. *Amer. J. Math.* 60, 897–936.
- Xiu, D. (2007). Efficient collocational approach for parametric uncertainty analysis. *Comm. Comput. Phys.* 2(2), 293–309.
- Xiu, D. and G. Karniadakis (2002). The Wiener-Askey polynomial chaos for stochastic differential equations. *J. Sci. Comput.* 24(2), 619–644.
- Xiu, D. and G. Karniadakis (2003a). Modelling uncertainty in steady state diffusion problems via generalized polynomial chaos. *Comput. Methods Appl. Mech. Engrg.* 191(43), 4927–4948.
- Xiu, D. and G. Karniadakis (2003b). A new stochastic approach to transient heat conduction modeling with uncertainty. *Int. J. Heat Mass Transfer* 46, 4681–4693.

- Yameogo, A., B. Sudret, and S. Cambier (2007). Uncertainties in the no lift-off criterion used in fuel rod assessment. In *Trans. 19th Int. Conf. on Struct. Mech. In Reactor Tech. (SMiRT 19), Vancouver, Canada*.
- Yuen, K., S. Au, and J. Beck (2004). Two-stage structural health monitoring approach for Phase I benchmark studies. *J. Eng. Mech.* 130, 16–33.
- Yuen, K. and L. Katafygiotis (2001). Bayesian time-domain approach for modal updating using ambient data. *Prob. Eng. Mech.* 16(3), 219–231.
- Yuen, K. and L. Katafygiotis (2002). Bayesian modal updating using complete input and incomplete response noisy measurements. *J. Eng. Mech.* 128(3), 340–350.
- Zadeh, L. (1978). Fuzzy sets as the basis for a theory of possibility. *Fuzzy Sets and Systems* 1, 3–28.
- Zhang, J. and B. Ellingwood (1994). Orthogonal series expansions of random fields in reliability analysis. *J. Eng. Mech.* 120(12), 2660–2677.
- Zhang, R. and S. Mahadevan (2000). Model uncertainty and Bayesian updating. *Structural Safety* 22, 145–160.
- Zhang, Y. and A. Der Kiureghian (1995). Two improved algorithms for reliability analysis. In R. Rackwitz, G. Augusti, and A. Bori (Eds.), *Proc. 6th IFIP WG7.5 on Reliability and Optimization of Structural systems, Assisi, Italy*. Chapman & Hall, London.
- Zhang, Y. and A. Der Kiureghian (1997). Finite element reliability methods for inelastic structures. Technical Report UCB/SEMM-97/05, University of California, Berkeley.
- Zhao, Z. and A. Haldar (1996). Bridge fatigue damage evaluation and updating using non-destructive inspections. *Eng. Fract. Mech.* 53, 775–788.
- Zienkiewicz, O.-C. and R.-L. Taylor (2000). *The finite element method*. Butterworth Heinemann, 5th edition.

Index

- aleatoric, *see* uncertainty, aleatoric
- autocorrelation coefficient function, 18, 117
 - exponential, 18
 - Gaussian, 19
 - sinc, 19
- autocorrelation function, 117
- autocovariance function, 18, 117
- average method, *see* random field
- Bayes
 - theorem, 11, 17, 93
- Bayesian updating
 - application example, 104
 - input parameters, 92
 - model response, 89
 - probability of failure, 90
- coefficient of variation, 12
- collocation, *see* non intrusive methods, regression
- concrete carbonation, 148
- CONDOR algorithm, 98
- confidence interval
 - response, 91
 - updated response, 91
- cooling towers, 166
- copula
 - density, 50
 - function, 50
- correlation
 - coefficient, 13
 - matrix, 14
- covariance, 12
 - matrix, 14
- cumulative distribution function, 11
- design point, *see* FORM
- directional simulation, 40
- distribution
 - Beta, 185
 - Gamma, 184
 - joint, 13
 - lognormal, 183
 - marginal, 13
 - normal, 183
 - posterior, 17
 - predictive, 17
 - prior, 17
 - uniform, 184
 - Weibull, 185
- elliptic boundary value problem
 - deterministic, 55
 - stochastic, 56
- entropy
 - principle of maximum, 15
- EOLE, *see* random field
- epistemic, *see* uncertainty, epistemic
- event, 9
 - mutually exclusive, 10
 - independent, 11
- expectation, 12
- experimental design, 63
 - random, 65
 - roots of orthogonal polynomials, 65
- expert judgment, 14
- extent of damage, *see* space-variant reliability
- fatigue, 155
 - application example, 162
 - deterministic assessment, 156
 - endurance limit, 159
 - ESOPE method, 159
 - Miner's rule, 157
 - probabilistic $S-N$ curves, 158
 - random damage, 160
- fatigue crack growth, 104
- first passage time, 124
- FORM, 36
 - algorithms, 37
 - Bayesian inverse, 92
 - design point, 37
 - inverse, 91
- Galerkin method
 - deterministic, 55
 - stochastic, 56
- Hilbert space, 13, 49
- Hilbertian basis, 49

- importance
 - factors, *see* measures
 - measures
 - FORM, 42
 - perturbation, 42
 - sampling, 38
- inner product, 13
- intrusive method, *see* Galerkin method, stochastic
- isoprobabilistic transform, 36, 188

- Karhunen-Loève expansion, 20
- kernel density approximation, 67, 97, 99
- kurtosis, 12

- Latin Hypercube Sampling, 60
- likelihood function, 93
- limit state
 - function, 35
 - surface, 35
- low discrepancy sequences, 61

- maximum likelihood estimation, 16, 98, 100
- MCMC, *see* Monte Carlo simulation, Markov chain
- measurement uncertainty, 87
- Metropolis-Hastings algorithm, 94
 - cascade, 95
- midpoint method, *see* random field
- model, 1
 - calibration, 87
 - error, 88
 - mathematical, 3
- moments
 - method of, 16
 - statistical, 12, 68
- Monte Carlo simulation
 - coefficient of variation, 36
 - confidence interval, 28
 - Markov chain, 94
 - moments, 28
 - non intrusive methods, 60
 - principle, 186
 - probability of failure, 35
 - Sobol' indices, 44

- Nataf transform, 36, 188
- non intrusive methods, 59
 - projection, 60
 - quadrature, 62
 - simulation, 60
 - regression, 63
- non parametric
 - approach, 5
 - statistics, 16

- orthogonal polynomials, 51, 191
 - Hermite, 192
 - Legendre, 192
- orthogonal series expansion, *see* random field
- outcrossing rate, 127
 - Belayev's formula, 131
 - PHI2, 136, 137
 - Rice's formula, 129

- perturbation method, 29
 - finite element model, 31
 - mean value, 29
 - random field, 32
 - variance, 30
- PHI2 method, *see* time-variant reliability
- polynomial chaos
 - expansion, 51
 - finite dimensional, 53
 - generalized, 52
- probability
 - conditional, 11
 - density function, 11
 - joint, 13
 - response, 67
 - measure, 10
 - rule of total, 11
 - space, 10
- probability of failure, 35
 - cumulative, 124
 - bounds, 127
 - point-in-time, 124
 - space-variant, 144

- quadrature
 - 1D scheme, 32, 193
 - moments, 32
 - Smolyak, 63
 - sparse, *see* Smolyak
 - tensorized scheme, 33, 62
- quasi-random numbers, 61

- random field, 18
 - discretization, 19
 - average method, 20
 - midpoint method, 20
 - OLE/EOLE, 22
 - orthogonal series expansion, 21
 - shape function method, 20
 - weighted integral method, 34
 - Gaussian, 18
 - non Gaussian, 25
- random number generator, 186

- random process, 116
 - differentiable, 118
 - ergodic, 120
 - Gaussian, 122
 - Poisson, 121
 - rectangular wave renewal, 122
 - stationary, 117
- random variable, 11
 - Gaussian, 13
- random vector, 13
 - Gaussian, 14
 - standard normal, 14
- regression, *see* non intrusive methods
- reliability analysis, 5, 35, 68
 - space-variant, 143
 - time-variant, 123
- scale of fluctuation, 19
- second moment methods, 5, 28
- sensitivity analysis, 2, 6, 41
- shape function method, *see* random field
- skewness, 12
- Sobol'
 - decomposition, 42
 - indices, 44
 - polynomial chaos-based, 68
 - sequence, 61
- SORM, 38
- space-variant reliability, 143
 - cooling towers, 171
 - extent of damage, 145
 - application example, 148
 - moments, 146
- spectral methods, 5, 48
 - reliability, 68
 - response PDF, 67
 - Sobol' indices, 68
 - statistical moments, 68
- spectral stochastic finite element method, 54
- SSFEM, 54
- standard deviation, 12
- statistical inference, 15
 - polynomial chaos-based, 100
- stochastic identification, *see* stochastic inverse methods
- stochastic inverse methods, 86, 96
 - application example, 107
 - parametric, 97
 - polynomial chaos-based, 99
- structural reliability, *see* reliability analysis
- subset simulation, 40
- system
 - designed, 4
 - real, 4, 85
- Taylor series expansion, 29
- time-variant reliability, 123
 - application example, 140
 - asymptotic method, 132
 - cooling towers, 170
 - Laplace integration, 133
 - outcrossing rate, 127
 - PHI2 method, 135
 - right-boundary problems, 125
- uncertainty
 - aleatoric, 4
 - epistemic, 4
 - measurement, 4
 - model, *see* model, error
- uncertainty analysis, 2
 - Step A, 3
 - Step B, 4, 14
 - Step C, 5, 27
 - Step C', 6, 41
- uncertainty propagation, 2, 5, 27
 - reliability analysis, 35
 - second moment methods, 28
 - spectral methods, 47
- variance, 12
- weighted integral method, 33

